# Molecular analyses of candidate carotenoid biosynthetic genes in *Vitis vinifera* L.

by

**Philip Richard Young**

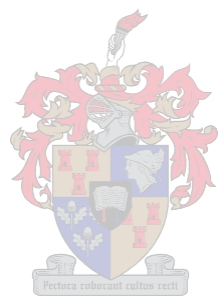


*Dissertation presented for the Degree of Doctor of Philosophy at Stellenbosch University.*

April 2004

*Promoter:*
Prof MA Vivier

*Co-promoter:*
Prof IS Pretorius

# DECLARATION

I, the undersigned, hereby declare that the work contained in this dissertation is my own original work and that I have not previously in its entirety or in part submitted it at any university for a degree.

**Philip R. Young**

# SUMMARY

Plants cannot avoid stress and must therefore be capable of rapidly responding to extreme environmental changes. An inability to control and regulate the photosynthetic process during stress conditions will lead to the formation of highly reactive oxygen species that concomitantly causes photo-oxidative damage to the pigments and proteins of the photosynthetic apparatus. Since light is the primary source of energy for the photosynthetic process, it is clear that plants are continuously required to balance the light energy absorbed for the photochemical reactions against photoprotection in a dynamic way in order to survive. Carotenoids are precursors of abscisic acid, but more importantly structural components of the photosynthetic apparatus. During photosynthesis carotenoids function as accessory light-harvesting pigments, and also fulfil a photoprotective function by quenching the reactive molecules formed during conditions that saturate the photosynthetic process.

Due to the importance of carotenoids to plant fitness and human health (as Vitamin A precursors) this study has attempted to isolate and characterise genes that are directly, or indirectly involved in carotenoid biosynthesis in *Vitis vinifera*. In total eleven full-length- and eight partial genes have been isolated, cloned and sequenced. These genes can be grouped into the following pathways: (i) the 1-deoxy-D-xylulose 5-phosphate (DOXP)/2-C-methyl-D-erythritol 4-phosphate (MEP) pathway (i.e. the plastidic isopentenyl diphosphate biosynthetic pathway); (ii) the mevalonate pathway (i.e. the cytosolic/mitochondrial IPP biosynthetic pathway); (iii) the carotenoid biosynthetic pathway; (iv) the abscisic acid biosynthetic pathway (as a degradation product of carotenoids); and general isoprenoid biosynthetic pathways (as precursors of carotenoids).

The full-length genes (i.e. from the putative ATG to the STOP codon) of DOXP synthase (DXS), 4-hydroxy-3-methylbut-2-enyl diphosphate reductase (lytB), IPP isomerase (IPI), 3-hydroxy-3-methylglutaryl coenzyme A synthase (HMGS), phytoene synthase (PSY), lycopene β-cyclase (LBCY), β-carotene hydroxylase (BCH), zeaxanthin epoxidase (ZEP), 9-*cis*-epoxy carotenoid dioxygenase (NCED), farnesyl diphosphate synthase (FPS) and geranylgeranyl diphosphate synthase (GGPS) have been isolated from cDNA. In addition, the full-length genomic copy and putative promoters of DXS, PSY, LBCY, BCH, NCED and ZEP have also been isolated from genomic DNA by the construction and screening of sub-genomic libraries. Alignments of the genomic copies of these genes to the corresponding cDNA sequences have provided useful information regarding the genomic organisation of these genes, including the intron-exon junction sites in *V. vinifera*. The copy number of the DXS, PSY, LBCY, BCH, NCED and ZEP encoding genes in the *Vitis* genome have been determined. DXS, PSY, BCH and ZEP are single copy genes, whereas LBCY and NCED have two and three copies, respectively.

The transcriptional activity of the putative promoters of six of the isolated genes (i.e. DXS, PSY, LBCY, BCH, ZEP and NCED) were tested with a transient reporter gene assay. None of the putative promoters tested showed any transcriptional activity of the reporter gene. The transcription of these genes, has however been shown using northern blot analysis and/or RT-PCR. Preliminary expression profiles for PSY, LBCY, BCH, and ZEP were determined in different plant organs and the expression of these genes was generally higher in photosynthetically active tissues. The expression of these genes following different treatments (abscisic acid, NaCl and wounding) was also assayed. The functionality of five of the isolated full-length

genes (IPI, GGPS, PSY, LBCY and BCH) has been shown in a bacterial colour complementation assay.

*In silico* analysis of the predicted protein sequences of all eleven isolated genes revealed that they are conserved and share a high degree of homology to the corresponding proteins in other plant species. The sequences were further analysed for conserved domains in the protein sequences, and these proteins typically demonstrated similar domain profiles to homologues in other species (plant, bacteria and algae). The predicted protein sequences were further analysed for transit peptides, the presence of which would provide evidence for the sub-cellular localisation of the mature peptides. Since these genes are involved in biosynthetic pathways that are active in discrete organelles, the sub-cellular localisation of most of these proteins is known. The carotenoid biosynthetic genes (PSY, LBCY, BCH and ZEP), the abscisic acid biosynthetic gene, NCED, as well as the DOXP/MEP pathway genes (DXS, lytB and IPI) were all localised to the chloroplast. The mevalonate pathway gene, HMGS, was localised to both the cytosol and the mitochondria, and the general isoprenoid precursor genes, FPS and GGPS, were localised to the cytosol and the chloroplast, respectively. All these results are in agreement with the localisation of the respective pathways.

In order to increase our understanding of carotenoid biosynthesis and functions in plants, we constitutively overexpressed one of the isolated genes (BCH) in the model plant, *Nicotiana tabacum.* Plants expressing the BCH gene in the sense orientation maintained a healthy photosynthetic rate under stress conditions that typically caused photoinhibition and photodamage in the untransformed control plants. This result was inferred using chlorophyll fluorescence and confirmed using $CO_2$ assimilation rates and stomatal conductance. Chlorophyll fluorescence measurements indicated that the photoprotective non-photochemical quenching ability of the BCH-expressing plants increased, enabling the plants to maintain photosynthesis under conditions that elicited a stress response in the untransformed control plants. An integral photosynthetic protein component, the D1 protein, was specifically protected by the additional zeaxanthin in the BCH sense plants. Plants expressing an antisense BCH proved the converse, i.e. lower levels of BCH resulted in decreased zeaxanthin levels and made the transgenic plants more susceptible to high-light induced stress. These results have shown the crucial role of carotenoids (specifically the xanthophylls) in the photoprotective mechanism in plants. The increased photoprotection provided by the BCH expressing plants suggests that the scenario in plants is not optimal and can be improved. Any improvement in the photoprotective ability of a plant will affect both the fitness and productivity of the plant as a whole and will therefore find application in a number of crop plants on a global scale. This study has resulted in the successful isolation and characterisation of genes involved in the direct, or indirect, carotenoid biosynthetic pathways. The further study and manipulation of these genes in model plants will provide useful insights into the physiological role of specific carotenoids in photosynthesis and in plants as a whole.

# OPSOMMING

Plante het nie die vermoë om stres te ontwyk nie en moet dus vinnig op veranderinge in hul omgewingstoestande kan reageer. Indien hulle nie die fotosinteseproses kan kontroleer en reguleer tydens streskondisies nie, sal dit tot die vorming van hoogs reaktiewe suurstofspesies lei, wat beide die pigmente en proteiene van die fotosintetiese apparaat sal beskadig. Lig is die primêre energiebron vir fotosintese en daarom is dit noodsaaklik dat plante deurgaans 'n dinamiese balans tussen fotosintese en fotobeskerming moet handhaaf. Karotenoiëde is voorlopers vir die vorming van absisiensuur, maar meer belangrik vir die plant, ook integrale komponente van die fotosintetiese apparaat. Tydens fotosintese word karotenoiëde vir die opneem van lig benodig, terwyl dit ook die fotosintetiese apparaat beskerm wanneer lig 'n versadigingspunt bereik vir fotosintese.

Weens die belang van karotenoiëde vir plant- en menslike gesondheid (as Vitamiene A voorlopers), het hierdie studie beoog om gene te isoleer en karakteriseer wat direk of indirek 'n rol in karoteenbiosintese in *Vitis vinifera* speel. Elf vollengte- en agt gedeeltelike gene is geïsoleer, gekloneer, en gekarakteriseer. Hierdie gene kan in die volgende biosintetiese paaie gegroepeer word: (i) die 1-deoksi-D-xilulose 5-fosfaat (DOXP)/2-C-metiel-D-eritritol-4-fosfaat (MEP) pad (d.w.s. die plastiediese isopenteniel difosfaat biosintetiese pad); (ii) die mevalonaat pad (d.w.s. the sitosoliese/mitokondriale IPP biosintetiese pad); (iii) die karotenoiëd biosintetiese pad; (iv) die absisiensuur biosintetiese pad (as 'n afbraak produk van karotenoiëde) en die algemene isoprenoïed bisintetiese paaie (as voorlopers van karotenoiëde).

Die vollengte gene (d.w.s. vanaf die geskatte ATG tot die STOP kodon) van DOXP-sintase (DXS), 4-hidroksi-3-metielbut-2-eniel difosfaatreduktase (lytB), IPP-isomerase (IPI), 3-hidroksi-3-metielglutariel koensiem A sintase (HMGS), fitoeën sintase (PSY), likopeen β-siklase (LBCY), β-karoteen hidroksilase (BCH), zeaxantien oksidase (ZEP), 9-*cis*-epoksi karotenoiëd dioksigenase (NCED), farnesiel difosfaat sintase (FPS)en geranielgeraniel difosfaat sintase (GGPS) is met behulp van. RT-PKR vanaf cDNA geïsoleer. Die vollengte genomiese kopieë en die verwagte promotors van die DXS, PSY, LBCY, BCH, NCED and ZEP gene is ook geïsoleer d.m.v. die opstel en sifting van subgenomiese biblioteke. Vergelykende analises van die genoom- en cDNA kopieë het insiggewende data oor die genomiese rangskikking van die gene, insluitende die intron-ekson setels in *V. vinifera* gelewer. Die kopiegetalle van DXS, PSY, LBCY, BCH, NCED en ZEP is bepaal. DXS, PSY, BCH en ZEP is in die *Vitis*-genoom as enkel kopieë teenwoordig, terwyl LBCY en NCED twee en drie kopieë, repektiewelik, beslaan.

Die transkipsionele aktiwiteit van die verwagte promotors van ses van die geïsoleerde gene (naamlik DXS, PSY, LBCY, BCH, ZEP en NCED) is d.m.v. 'n tydelike verklikkergeentoets ondersoek. Geeneen van die promotors het die transkripsie van die verklikkergeen bemiddel nie. Die transkripsie van die gene is egter wel bewys deur van northernhibridisasies en/of RT-PKR gebruik te maak. Die promotors van hierdie gene kan dus as transkipsioneel aktief beskou word. Voorlopige uitdrukkingsprofiele van PSY, LBCY, BCH, en ZEP is in verskillende plantorgane bepaal; die profiele was deurgaans hoër in fotosinteties aktiewe weefsels. Die uitdrukkingsprofiele van die gene is verder ook in reaksie op verskillende induktiewe behandelings (absisiensuur, NaCl en beskadiging) bepaal.

Vyf van die vollengte gene (IPI, GGPS, PSY, LBCY en BCH) is funksioneel bewys in 'n bakteriese funksionele kleurkomplementasiesisteem.

*In silico* analises van die afgeleide proteïene van al elf geïsoleerde gene het 'n hoë vlak van homologie met ooreenstemende proteiene van ander plantspesies getoon. Gekonserveerde domeine is ook in die proteïensekwense van die geïsoleerde gene teenwoordig. Hierdie proteïene het deurgaans dieselfde domeinprofiele vertoontoon as homoloë in ander spesies (bakterieë, alge en plante). Die sub-sellulêre teikening van die gene kon voorspel word deur die seinpeptiede in die proteiensekwense te eien. Aangesien hierdie gene betrokke is by biosintetiese paaie wat in diskrete kompartemente plaasvind; is die sub-sellulêre lokalisering van hierdie proteïene voorspelbaar. Die karotenoïed biosintetiese gene (PSY, LBCY, BCH en ZEP), die absisiensuur biosintetiese geen, NCED, sowel as die DOXP/MEP pad se gene (DXS, lytB en IPI) kom almal in die chloroplast voor. Die mevalonaatpadgeen, HMGS, word na beide die sitosol en die mitokondria geteiken, terwyl die algemene isoprenoïed voorlopergene, FPS en GGPS, onderskeidelik na die sitosol en die chloroplast geteiken word. Die verkreë voorspellings stem met die lokalisering van die biosintetiese paaie in die sel ooreen.

Om ons kennis rakende karotenoïed biosintese en veral hulle funksie(s) in plante te verbreed, het ons een van die geïsoleerde gene, BCH, in die modelplant, *Nicotiana tabacum*, konstitutief ooruitgedruk. Plante wat die BCH geen in die "sense" orientasie uitgedruk het, kon normale fotosintetiese aktiwiteit handhaaf onder kondisies wat foto-inhibisie en foto-osidatiewe skade in die ongetransformeerde kontrole plante veroorsaak het. Hierdie resultaat is met chlorofil fluoresensie analises aangetoon terwyl dit met $CO_2$ assimilasie- en huidmondjie geleidingseksperimente bevestig is. Chlorofil fluoresensie metings het aangetoon dat die beskermingsvermoë van die transgeniese plante verhoog is, en dit dan die plante in staat stel om fotosintetese te handhaaf onder streskondisies van hoë lig. Proteïen analises het aangetoon dat 'n integrale fotosintetiese proteien, die D1 proteïen, word veral deur die verhoogde zeaxantien vlakke in die BCH transgeniese plante beskerm. Plante wat verminderde zeaxantien vlakke gehad het, weens die konstitutiewe ooruitdrukking van die BCH geen in die anti-"sense" orientasie, het die teenoorgestelde bewys. Met ander woorde. laer BCH vlakke (en dus laer zeaxantien vlakke) het tot plante wat meer vatbaar was vir hoë lig geïnduseerde stress gelei. Hierdie resultate het die essensiële beskermende rol wat karotenoiede tydens fotosintese speel, uitgelig. Die vermoë om hierdie beskermende meganisme te manipuleer in transgenies plante het aangetoon dat die sisteem in plante, alhoewel effektief, nie optimaal is nie. Enige verbetering in 'n plant se inherente vermoë om streskondisies te weerstaan sal die plant se algemene gesondheid en dus produktiwiteit beïnvloed. As sulks sal hierdie in meeste gewasspesies toepassing vind. Hierdie studie beskryf die isolering en karakterisering van gene wat direk, of indirek, by karotenoïedbiosintese betrokke is. Verdere studies, en veral die manipulering van hierdie gene in model plante, sal die fisiologiese rol van spesifieke karotenoïeede in fotosintese, en die plant as 'n geheel, ontrafel.

# ACKNOWLEDGEMENTS

I wish to express my sincere gratitude and appreciation to the following persons and institutions:

**My family**, for supporting me (in every sense of the word) as only a family can;

**Claudia**; for sharing this experience with me;

**My friends**, for providing a life outside of the laboratory;

**My colleagues**; for providing a life inside the laboratory;

**Dr Marco Gagiano** and **Albert Joubert,** for their time, energy, enthusiasm and assistance;

**Prof. Isak S. Pretorius**, for introducing me to Biotechnology;

**Prof. Melané A. Vivier**; for keeping me interested in Biotechnology and, more importantly, supervising me as both a researcher and as a person.

The **National Research Foundation**, the **Harry Crossley Foundation** and the **Institute for Wine Biotechnology**; for financial support for the duration of this study.

This dissertation is dedicated to my family

# BIOGRAPHICAL SKETCH

Philip Richard Young was born in Cape Town, South Africa on 11 July 1973. He matriculated at the Hermanus High School in 1991. Philip enrolled at the Stellenbosch University in 1993 and obtained a B.Sc. degree (Microbiology and Genetics) in December, 1995. The Hons. B.Sc. (Microbiology) degree was awarded in December, 1996. Philip enrolled for an M.Sc. degree (Wine Biotechnology) in 1997, and the study was upgraded to a Ph.D. degree in 1999.

# PREFACE

This dissertation is presented as a compilation of six chapters. Each chapter is introduced separately and is written according to the style of the journal ***European Journal of Biochemistry***.

**Chapter 1** **GENERAL INTRODUCTION AND SPECIFIC PROJECT AIMS**

**Chapter 2** **LITERATURE REVIEW**
Plants, light and stress

**Chapter 3** **RESEARCH RESULTS**
Overexpression of the *Vitis vinifera* L. β-carotene hydroxylase encoding gene in tobacco leads to improved photoprotection

**Chapter 4** **RESEARCH RESULTS**
Isolation and characterization of candidate genes in the isoprenoid- and carotenoid biosynthetic pathways of *Vitis vinifera* L. I

**Chapter 5** **RESEARCH RESULTS**
Isolation and characterization of candidate genes in the isoprenoid- and carotenoid biosynthetic pathways of *Vitis vinifera* L. II

**Chapter 6** **GENERAL DISCUSSION AND CONCLUDING REMARKS**

I hereby declare that I was the primary contributor with respect to the experimental data presented on the multi-author manuscripts presented in Chapters 3, 4 and 5.
My supervisor, Prof M.A. Vivier, was involved in the conceptual design of the study, and together with my co-supervisor, Prof I.S. Pretorius, the critical evaluation of the manuscript.
Dr S. Chen assisted in the characterisation of the transgenic plants by optimising the photosynthetic measurements discussed in Chapter 3.
Ms K.L. Taylor was involved in the isolation of the genes discussed in Chapter 4 by assisting in the construction and subsequent screening of the sub-genomic libraries.

# CONTENTS

# CHAPTER 1

# GENERAL INTRODUCTION AND SPECIFIC PROJECT AIMS

# 1. INTRODUCTION AND SPECIFIC RESEARCH AIMS

## 1.1. INTRODUCTION

Light is possibly the most obvious prerequisite for photosynthesis, yet it can rapidly become damaging when the amount of light energy absorbed by plants exceeds the inherent photosynthetic capacity of the plant. Any excess light energy that is absorbed and not used in the photochemical reactions of photosynthesis can potentially form harmful singlet oxygen and/or triplet chlorophyll. If not quenched, these molecules will cause oxidative damage to the photosynthetic apparatus and eventually result in the entire photosynthetic process shutting down [1].

This has necessitated plants to evolve multiple mechanisms to cope with the absorption of excessive light and its consequences. Carotenoids, including the xanthophylls, represent one of these mechanisms. Carotenoids are formed in the plastids of plants and represent a class of pigments with antioxidant properties. Carotenoids present in the photosynthetic membranes of plants play an essential photoprotective role in plants by quenching triplet chlorophyll and singlet oxygen and preventing lipid peroxidation [2;3].

## 1.2 CAROTENOIDS AND PHOTOPROTECTION

The most notable characteristic of carotenoids are the bright colours they form in the leaves, flowers and fruits of plants. These pigments also fulfil a vital role in the photosynthetic process. Carotenoids, especially the oxygenated carotenoids (xanthophylls), participate in the photosynthetic process by acting as accessory light-harvesting pigments and also protect the photosynthetic apparatus from excessive light energy by quenching the potentially harmful singlet oxygen and triplet chlorophylls [4;5].

Recent genetic studies on *Arabidopsis* plant lines with mutations in their carotenoid biosynthetic genes have underlined the protective role of carotenoids during photo-oxidative stress conditions in the photosynthetic membranes of plants. These studies have shown that under saturating light conditions plants have an absolute requirement for the xanthophylls (zeaxanthin, antheraxanthin and violaxanthin). Although certain carotenoids (i.e. lutein) can compensate for the lack of xanthophylls under unsaturating light conditions, plants lacking the full suite of xanthophylls can not cope when light conditions becomes saturating for photosynthesis [3;6-10].

The manipulation of carotenoid biosynthetic pathway has received much attention in the last few years (reviewed in [11]). The most notable example is the much publicised (and debated) "Golden Rice" where β-carotene production was engineered in the endosperm of rice [12]. Since humans are incapable of synthesising carotenoids, they require plant-derived β-carotene (pro-Vitamin A) in their diet. This dietary β-carotene is converted to retinol that is subsequently used for a number of vital functions in the human body. Vitamin A deficiency can result in varying degrees of blindness and also intensifies the symptoms of diarrhea, respiratory diseases and certain childhood diseases such as measles [13]. Due to the widespread occurrence of Vitamin A deficiency (especially in poor and under developed countries), the manipulation of the carotenoid biosynthetic pathway has become a focus in a number of recent studies [14;15]. Although not discussed in any of the subsequent chapters, these studies are of interest since they show that the metabolic manipulation of the carotenoid biosynthetic pathway is possible in plants.

From a plant's perspective, an analogous breakthrough was achieved by increasing the relative amounts of xanthophylls in the model plant, *A. thaliana* [16]. Although not as visually striking as the "Golden Rice", these transgenic plants contained twice as much xanthophylls as the wild-type plant and were shown to be more tolerant to both high light conditions (1000 μmol photons.$m^{-2}$.$s^{-1}$) as well as elevated temperatures (40°C). On the other hand, similar studies have shown that biosynthetic pathways cannot be viewed in isolation, but rather as complex networks of overlapping pathways with common precursors and intermediates. This complexity was strikingly demonstrated in a study that attempted to increase the production of lycopene in *Lycopersicon esculentum*. Although the primary goal was achieved and the transgenic plants did contain higher levels of lycopene; the levels of the plant growth regulator, gibberellic acid, was so severely reduced that the plants were dwarfed [17].

## 1.3 WHY MANIPULATE CAROTENOID BIOSYNTHESIS IN GRAPEVINE?

The ability to successfully manipulate the carotenoid levels in a crop plant (like grapevine) will have several potentially positive outcomes. Firstly, increasing the β-carotene levels in the fruit will concomitantly improve the nutritional value of the product (grape berries). Secondly, carotenoids are thought to be precursors of

β-damascenone, vitispirane and other $C_{13}$-norisoprenoids compounds that are associated with grape- and wine quality [18]. Increasing the flux into the carotenoid pathway could lead to an increase in these compounds. Thirdly, the carotenoid biosynthetic pathway has been identified as a promising target for genetic manipulation to produce stress tolerant plants [16]. In all three of these cases elevating the carotenoid levels will provide benefits to both the consumer and the general fitness of field grown crops.

This study represents the initial stages in the manipulation of carotenoid biosynthesis in *V. vinifera* by describing the isolation and characterisation of genes involved in carotenoid- and carotenoid associated biosynthetic pathways.

## 1.4 SPECIFIC RESEARCH AIMS

The aim of this study was to isolate genes involved in the isoprenoid biosynthetic pathways, with particular focus on the carotenoid biosynthetic pathway and the subsequent reactions to abscisic acid from *V. vinifera*. The molecular analysis and characterisation of these genes will provide information on the regulation, structure and function of these genes and their encoded products. The isolated genes will serve as a genetic resource for future studies on carotenoid biosynthesis. The manipulation of the expression of these genes in model plants will provide further information on the physiological role(s) of these genes and their associated products *in planta*. To achieve these general aims the following specific research objectives were formulated:

i. The identification and isolation of genes that are either directly, or indirectly, involved in carotenoid biosynthesis in *V. vinifera*. This includes the genes that encode the enzymes catalysing the reactions in: (a) the 1-deoxy-D-xylulose 5-phosphate/2-C-methyl-D-erythritol 4-phosphate pathway to isopentenyl diphosphate (i.e. isoprenoid precursors of carotenoid biosynthesis); (b) the carotenoid biosynthetic pathway itself, and (c) the indirect biosynthetic pathway to abscisic acid (ABA) (i.e. where ABA is formed as a cleavage product of carotenoids);

ii. Characterisation of the carotenoid biosynthetic genes from *V vinifera* that were isolated in objective (i). This includes the analysis of the occurrence of the

isolated genes in the *Vitis* genome, as well as establishing expression profiles of the isolated genes in *V. vinifera*;

iii. Analysis of the nucleotide sequences of the isolated carotenoid biosynthetic genes from *V. vinifera*. This will entail the *in silico* analysis of the genomic- and cDNA sequences of the genes obtained from objective (i). These analyses include the comparison of the genomic and cDNA copies of the isolated genes in order to identify potential intron-exon splice sites, as well as analysis of the 5'- and 3'-flanking sequences for potential homologies to other known regulatory elements in plants. Analysis of the predicted amino acid sequences (derived from the cDNA sequences of the isolated genes) for homology to related proteins or protein families will follow, as well as the identification of any potential post-translational modifications;

iv. Due to the logistical impracticality of analysing the overexpression of all the isolated genes in model plants, this study will focus on the detailed analysis of the effect of overexpression of only one candidate gene in a model plant. The resultant transgenic plants will be analysed to determine the *in planta* effect of the overexpressed gene. The transgenic plants overexpressing the genes of interest will be analysed by phenotypical evaluation, measurement of the relative carotenoid- and chlorophyll levels, and quantification of the photosynthetic parameters of the plants under different stress conditions. The photosynthetic parameters of the plants will be determined by measuring $CO_2$ assimilation rates and stomatal conductance (as indicators of carbon fixation) as well as chlorophyll fluorescence. Chlorophyll fluorescence measurements will be used to determine both the photochemical- and non-photochemical capability of the transgenic plants. All the measurements will be interpreted relative to untransformed wild-type plants.

The data acquired from these analyses will provide insights into the physiological function of these genes and their encoded products *in planta* and so doing assist in elucidating the role that specific carotenoids play in photosynthesis and photoprotection. The assimilation of all these data will enable the formulation of a strategy for the prospective manipulation of the carotenoid biosynthetic pathway in *V. vinifera*.

## 1.5 LITERATURE CITED

[1] Arora,A., Sairam,R.K., & Srivastava,G.C. (2002) Oxidative stress and antioxidative system in plants. *Curr Sci*, **82,** 1227-1238.

[2] Aro,E.M., Virgin,I., & Andersson,B. (1993) Photoinhibition of photosystem II. Inactivation, protein damage and turnover. *Biochim Biophys Acta*, **1143,** 113-134.

[3] Niyogi,K.K., Grossman,A.R., & Björkman,O. (1998) *Arabidopsis* mutants define a central role for the xanthophyll cycle in the regulation of photosynthetic energy conversion. *Plant Cell*, **10,** 1121-1134.

[4] Bartley,G.E. & Scolnik,P.A. (1995) Plant carotenoids: pigments for photoprotection, visual attraction, and human health. *Plant Cell*, **7,** 1027-1038.

[5] Cunningham,F.X., Jr. & Gantt,E. (1998) Genes and enzymes of carotenoid biosynthesis in plants. *Annu Rev Plant Physiol Plant Mol Biol*, **49,** 557-583.

[6] Baroli,I. & Niyogi,K.K. (2000) Molecular genetics of xanthophyll-dependent photoprotection in green algae and plants. *Philos Trans R Soc Lond B: Biol Sci*, **355,** 1385-1393.

[7] Havaux,M. & Niyogi,K.K. (1999) The violaxanthin cycle protects plants from photooxidative damage by more than one mechanism. *Proc Natl Acad Sci USA*, **96,** 8762-8767.

[8] Havaux,M., Bonfils,J.P., Lutz,C., & Niyogi,K.K. (2000) Photodamage of the photosynthetic apparatus and its dependence on the leaf developmental stage in the *npq1 Arabidopsis* mutant deficient in the xanthophyll cycle enzyme violaxanthin de-epoxidase. *Plant Physiol*, **124,** 273-284.

[9] Muller,P., Li,X.P., & Niyogi,K.K. (2001) Non-photochemical quenching. A response to excess light energy. *Plant Physiol*, **125,** 1558-1566.

[10] Niyogi,K.K., Shih,C., Chow,W.S., Pogson,B.J., DellaPenna,D., & Björkman,O. (2001) Photoprotection in a zeaxanthin- and lutein-deficient double mutant of *Arabidopsis*. *Photosynth Res*, **67,** 139-145.

[11] Giuliano,G., Aquilani,R., & Dharmapuri,S. (2000) Metabolic engineering of plant carotenoids. *Trends Plant Sci*, **5,** 406-409.

[12] Ye,X., Al Babili,S., Kloti,A., Zhang,J., Lucca,P., Beyer,P., & Potrykus,I. (2000) Engineering the provitamin A (β-carotene) biosynthetic pathway into (carotenoid-free) rice endosperm. *Science*, **287,** 303-305.

[13] Castenmiller,J.J.M. & West,C.E. (1998) Bioavailability and bioconversion of carotenoids. *Annu Rev Nutr*, **18,** 19-38.

[14] Rosati,C., Aquilani,R., Dharmapuri,S., Pallara,P., Marusic,C., Tavazza,R., Bouvier,F., Camara,B., & Giuliano,G. (2000) Metabolic engineering of β-carotene and lycopene content in tomato fruit. *Plant J*, **24,** 413-419.

[15] Dharmapuri,S., Rosati,C., Pallara,P., Aquilani,R., Bouvier,F., Camara,B., & Giuliano,G. (2002) Metabolic engineering of xanthophyll content in tomato fruits. *FEBS Lett*, **519,** 30-34.

[16] Davison,P.A., Hunter,C.N., & Horton,P. (2002) Overexpression of β-carotene hydroxylase enhances stress tolerance in Arabidopsis. *Nature*, **418,** 203-206.

[17] Fray,R.G., Wallace,A., Fraser,P.D., Valero,D., Hedden,P., Bramley,P.M., & Grierson,D. (1995) Constitutive expression of a fruit phytoene synthase gene in transgenic tomatoes causes dwarfism by redirecting metabolites from the gibberellin pathway. *Plant J*, **8,** 693-701.

[18] Steel,C.C. & Keller,M. (2000) Influence of UV-B irradiation on the carotenoid content of *Vitis vinifera* tissues. *Biochem Soc Trans*, **28,** 883-885.

# CHAPTER 2

# LITERATURE REVIEW

## Plants, light and stress

# 2. PLANTS, LIGHT AND STRESS

Plants are continuously exposed to a wide range of both biotic and abiotic stresses that includes water stress (drought), high light intensities and nutrient limitation, as well as the more recent additional stresses caused by human activity (i.e. pollution). Since plants are sessile and therefore physically incapable of avoiding these daily (and seasonal) stresses, they must be capable of responding to such changes in both a rapid and flexible way in order to cope with their highly variable and often extreme environmental conditions. There is a complex overlapping of mechanisms within the plant's cells that helps to maintain normal cell function even under stress conditions [1].

Although diverse, a feature common to these different stress factors is their potential to increase the production of reactive oxygen species in affected plant tissues. These highly reactive molecules result in photo-oxidative cell damage to the photosynthetic apparatus of plants and this in turn results in a decrease in the plants photosynthetic abilty due to photoinhibition or photodamage [2;3]. Since light is the primary source of energy for the photosynthetic process, it is clear that plants are required to continuously counterbalance the light energy absorbed for photosynthesis against photoprotection of the photosynthetic apparatus in a dynamic way in order to survive [4].

## 2.1 PLANTS AND LIGHT

### 2.1.1 The light reactions of photosynthesis

#### 2.1.1.1 Chloroplasts as the site of photosynthesis

The photosynthetic processes in plants occur in sub-cellular organelles known as chloroplasts. Chloroplasts are located in specialised leaf cells, which typically contain fifty or more chloroplasts. Although the number of chloroplasts per cell fluctuates from one plant species to another, they generally increase with cell size. Distribution of the chloroplasts inside the cell varies according to the light conditions. Under low light intensities, light absorption is maximised by the accumulation of chloroplasts at the cell surface (parallel to the plane of the leaf) and their arrangement that occurs perpendicular to the incident light. Under high light, however, the chloroplasts move to the cell surfaces that are parallel to the incident light, thereby minimising the absorption of excess light (Fig 2.1). This mechanism can decrease the amount of light absorbed by the leaf by about 15% [5].

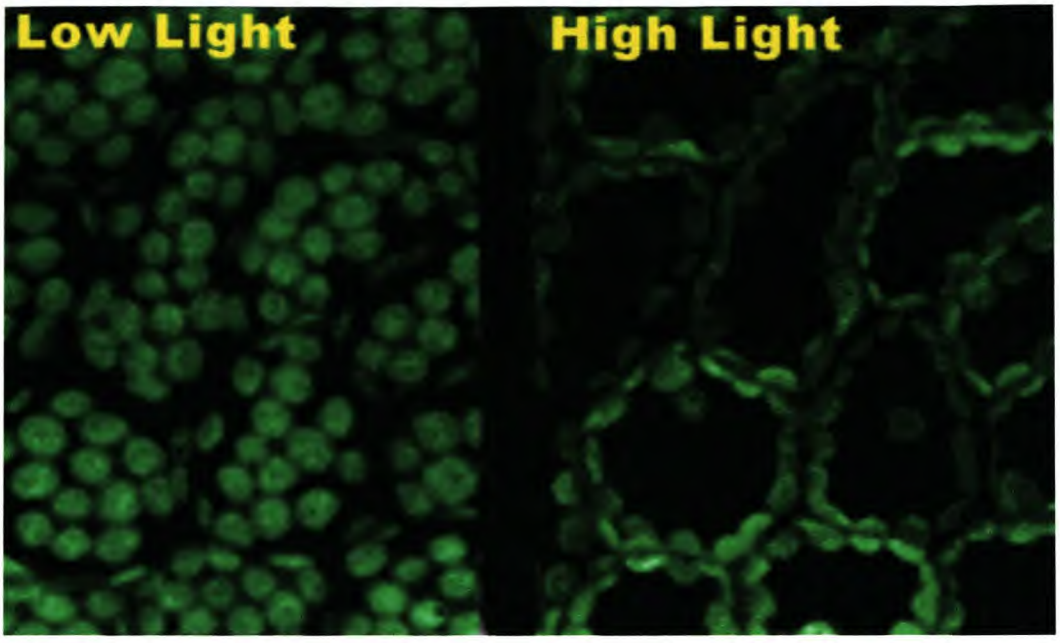


Figure 2.1 . Chloroplast movement in leaf cells under different light intensities. Under high light the chloroplasts change their orientation and distribution and move to the cell surfaces that are parallel to the incident light in order to minimise the absorption of excess light. The light is travelling perpendicular to the page [6].

Chloroplasts consist of three membranes (and the associated spaces they enclose): the outer-, inner-, and thylakoid membrane. The outer membrane is permeable to metabolites of small molecular weight, and contains proteins that form large aqueous channels. The inner envelope membrane on the other hand serves as the permeability barrier of the chloroplast and contains transporters that regulate and control the movement of metabolites (both organic and charged) in and out of the organelle [7]. Water, as well as small neutral molecules (such as $CO_2$ and $O_2$), can pass freely through the membranes. These two membranes collectively referred to as the envelope, do not contain any chlorophyll and as a result cannot directly contribute to the photosynthetic reactions. It is the third membrane, the thylakoid membrane that contains all the chlorophyll and is the site of the light reactions of photosynthesis. The carbon reduction reactions required for carbon fixation and carbohydrate synthesis, occurs in the outer soluble phase located between the thylakoid membrane and the inner membrane (i.e. the stroma).

In each chloroplast the thylakoid membrane can be regarded as a single, interconnected sheet that forms small flattened vesicles (the thylakoids) which are arranged in stacks, called grana. The thylakoid vesicles form enclosed spaces, the inner aqueous lumenal space and the outer aqueous stromal space. The lumenal spaces between the grana form a single continuous compartment. The thylakoid

membrane contains a wide variety of proteins essential for photosynthesis. Most of these proteins are integral membrane proteins to which several important side groups and light-absorbing pigments are bound. These bound proteins extend into the aqueous regions on both sides of the thylakoid membrane. The reaction centres (RC), the antennae pigment-protein complexes, as well as most of the electron transport enzymes are all integral membrane proteins [5].

Although one-dimensional, the photosynthetic process in plants can be regarded as occurring in four discrete stages, each occurring in a defined area of the chloroplast: (i) light absorption, (ii) electron transport, (iii) ATP synthesis, and (iv) carbon fixation. All four stages are functionally coupled and controlled to meet the specific carbohydrate requirements of the plant. The reactions in stages i, ii and iii are catalysed by proteins in the thylakoid membrane. The enzymes required for carbon fixation (stage iv), on the other hand, are soluble constituents of the stroma (Fig. 2.2).

#### 2.1.1.2 The photosystems

In the chloroplast, light energy is harvested by two different functional units called photosystems (PSs), specifically PSI and PSII. The PSs can be regarded as supramolecular complexes of the thylakoid membranes of higher plants that facilitate photosynthesis. Each PS consists of two multiprotein binding complexes, namely, the core complex or RC, and a complex of pigment-binding proteins that are organised into functional clusters, the light-harvesting complexes (LHCs). The light harvesting antenna is composed of two classes of proteins (together with their associated chlorophylls and carotenoids): the plastid-encoded proteins of the inner antenna, which bind chlorophyll *a* and β-carotene, and the chlorophyll *a*/*b* binding LHCs of the outer antenna [9;10]. All the pigment molecules in a PS can absorb photons (hence they are referred to as light-harvesting or antennae molecules), but only one molecule per cluster is capable of converting light energy into chemical energy and is, therefore, referred to as the RC (Fig. 2.3). The light energy used to drive the photosynthetic reactions is captured by a large number of chlorophyll *a* and *b* (approximately 250 per RC) and carotenoid (β-carotene, lutein, neoxanthin and violaxanthin) molecules associated with the light-harvesting antennae proteins.

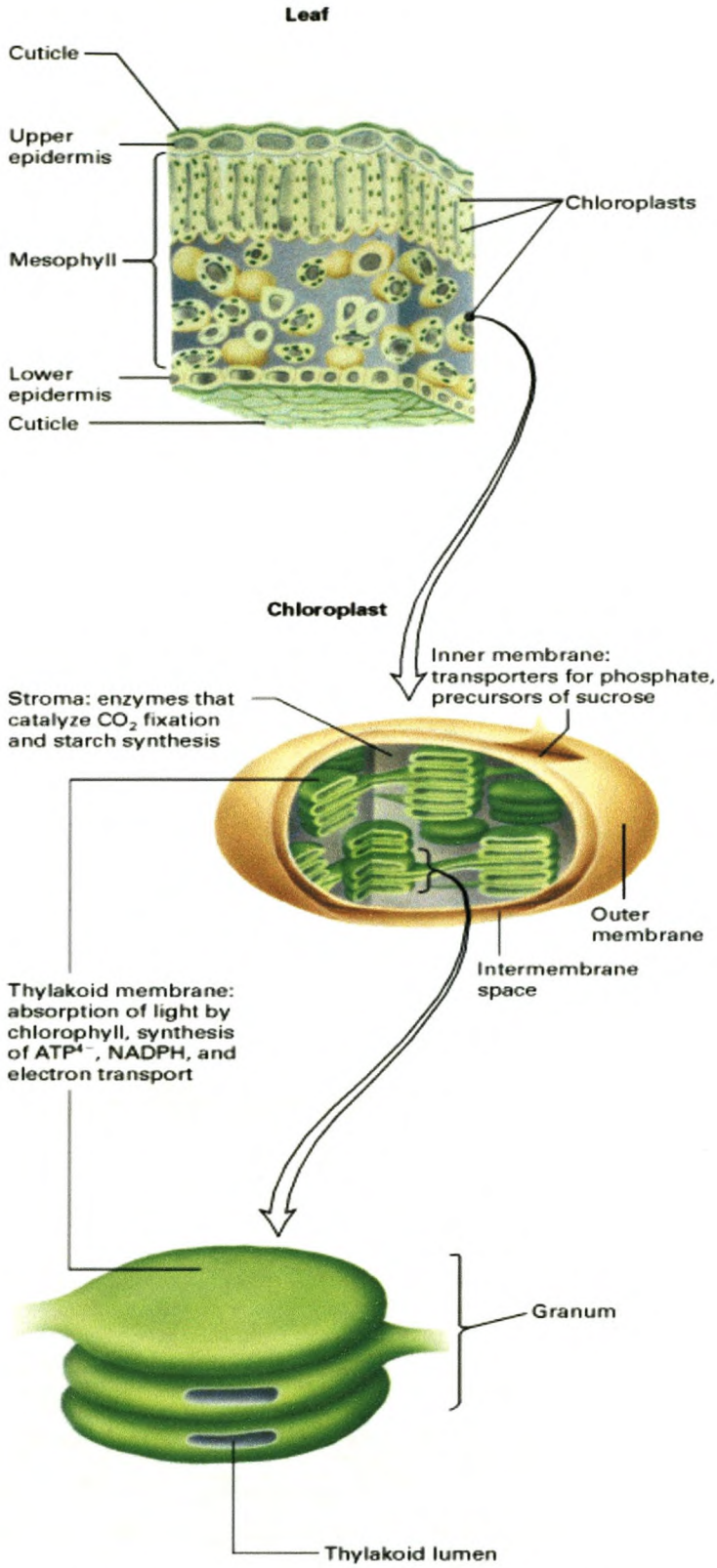


Figure 2.2. The structure of a leaf and chloroplast. Photosynthesis occurs on the thylakoid membrane, which forms a series of flattened vesicles (thylakoids) enclosing a single interconnected lumenal space. A granum is a stack of adjacent thylakoids. The stroma is the space within the inner membrane surrounding the thylakoids [8]

The PSI-PSII photosynthetic reactions serve as a shuttle system for transferring electrons from water to $NADP^+$ by using the absorption of two light-derived photons providing the energy. During this process NADPH is formed and protons are pumped across the thylakoid membrane providing the electrochemical gradient necessary for adenosine triphosphate (ATP) synthesis.

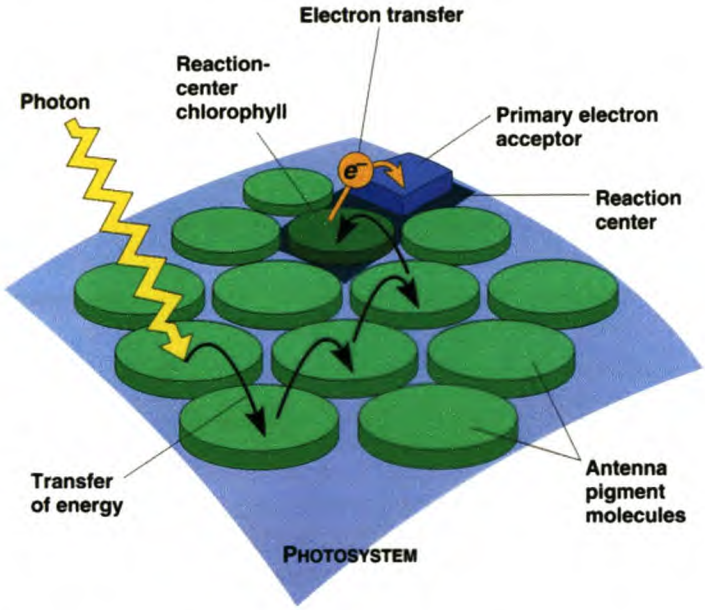


Figure 2.3. Antenna chlorophylls and carotenoid pigments of a photosystem harvest light and transfer the energy to the reaction center where chlorophyll P680 (in PSII) or P700 (in PSI) undergoes charge separation [11].

#### 2.1.1.2.1 Photosystem II (PSII)

The PSII complex consists of approximately 25 different proteins (PsbA-W), of which more than 20 are intregral membrane proteins. The RC, composed of the D1 and D2 proteins, is found at the center of this multi-subunit complex. The rest of the PSII subunits are situated around the D1 and D2 proteins. These subunits include the two chlorophyll *a* binding proteins (CP43 and CP46), which together act as an internal light-harvesting system that transfers excitation energy to the RC. The PSII core complex consists of the RC proteins, the oxygen evolving complex, the CP43/CP47 internal antenna, cytochrome b559, and the minor subunits. The core complex, therefore, contains all the proteins, pigments, and cofactors necessary for the light-driven movement of electrons from $H_2O$ to reduced plastoquinone. In addition to the internal light-harvesting antenna, plants have an outer light-harvesting system composed of proteins that bind both chlorophyll *a* and *b* (Lhcb proteins). The

Lhcb1-3 proteins that make up the majority of the light-harvesting system are organised as a trimer, and are known as the light-harvesting complex II (LHCII). The Lhcb4-6 proteins (also referred to as CP29, CP26 and CP24) bind less chlorophyll *b* than LHCII and are thought to be monomeric. These proteins possibly shuttle excitation energy from CP43/CP47 to the RC [9;12-15].

At least nine different redox components are capable of light-induced electron transfer (i.e. chlorophyll, pheophytin, plastoquinone [Q], tyrosine [Tyr], the water-oxidising cluster consisting of four manganese [Mn] atoms [4MnC], iron [Fe], cytochrome b559, carotenoid(s) and histidine). However, only five of these redox components are involved in the transfer of electrons from $H_2O$ to the plastoquinone pool: 4MnC, Tyr, the RC chlorophyll (P680), pheophytin, and the plastoquinone molecules, $Q_A$ and $Q_B$. Of these redox components, Tyr, P680, pheophytin, $Q_A$ and $Q_B$ have been shown to be bound to the D1 and D2 proteins that form the heterodimeric RC core of PSII [11].

A photon of light energy absorbed by an antenna chlorophyll or carotenoid molecule of the light harvesting complex is transferred to the RC of PSII. Photochemistry in the RC of PSII is initiated when the excitation energy from the photon raises the energy level of the primary oxidant P680, to $P680^+$. Under conditions ideal for photosynthetic activity, the excited $P680^*$ donates a single high-energy unpaired electron to the primary electron acceptor, pheophytin, creating $P680^+$/pheophytin$^-$. The electron from pheophytin is transferred to a plastoquinone molecule ($Q_A$) that is permanently bound to PSII. The electron from $Q_A^-$ is then transferred to a second mobile plastoquinone molecule ($Q_B$) that is loosely bound at the $Q_B$-site on the D1 protein. Plastoquinone at the $Q_B$-site differs from $Q_A$ in that it functions as a two-electron acceptor, by only becoming fully reduced and protonated after two photochemical turnovers of the RC. The full reduction of plastoquinone, therefore, requires the addition of two electrons (from $Q_A$) and two protons (from the stroma). The reduced plastoquinone ($PQH_2$) then dissociates from the RC and diffuses into the hydrophobic core of the membrane. The hydrophobicity of $PQH_2$ restricts its movement to the lipid bilayer of the photosynthetic membrane. $PQH_2$ diffuses through the membrane until it becomes bound to cytochrome $b_6/f$, a complex of cytochromes and iron-sulphur (FeS) proteins that is also membrane-bound. A "new" (i.e. re-oxidised) plastoquinone molecule can then find its way to the $Q_B$-binding site and the whole process can be repeated. Since the $Q_B$-site is near the

outer aqueous phase, the protons added to plastoquinone during the reduction are recruited from the outside of the thylakoid membrane (i,e, the stroma) (Fig. 2.4) [9;12-17].

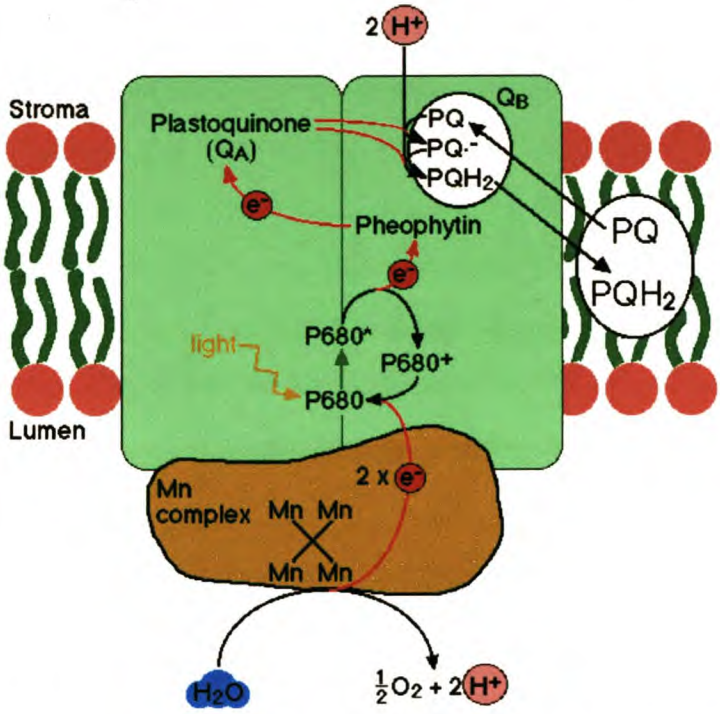


Figure 2.4. The electron transport reactions in PSII. Light energy causes charge separation of chlorophyll P680 and results in a series of electron transport reactions from (i) excited P680 ($P680^*$) to pheophytin; (ii) pheophytin to plastoquinone ($Q_A$); (iii) and from $Q_A$ to a mobile plastoquinone ($Q_B$) resulting in the formation of reduced plastoquinone ($PQH_2$) that diffuses into the lipid bilayer. The four Mn complex reduces $P680^+$ to P680 by the oxidation of water and the concomitant formation of $O_2$. [18].

### 2.1.1.2.2 The oxygen-evolving complex

In order for P680 to be recycled, the oxidised $P680^+$ has to be reduced. This is facilitated by the oxidation of $H_2O$ by the oxygen-evolving complex. This is considered to be the most oxidative reaction to occur in nature, and is responsible for the production of atmospheric $O_2$ as a byproduct of photosynthesis. A specific Tyr amino acid residue (Tyr161) on the D1 protein (D1-Tyr161) donates one electron to $P680^+$. The oxidised D1-Tyr161 is subsequently reduced by the 4MnC. The 4MnC is a metalloprotein that is bound to the lumenal surface of PSII and can exist in a series of oxidation states ($S_0$-$S_4$) enabling it to bind two $H_2O$ molecules and in so doing extract a total of four electrons. After four oxidations, molecular $O_2$ and protons ($H^+$)

are released into the thylakoid lumen. Illumination of PSII, therefore, allows the P680/P680*/P680+ cycle to be repeated and P680+ is recycled back to P680 (Fig. 2.5) [17].

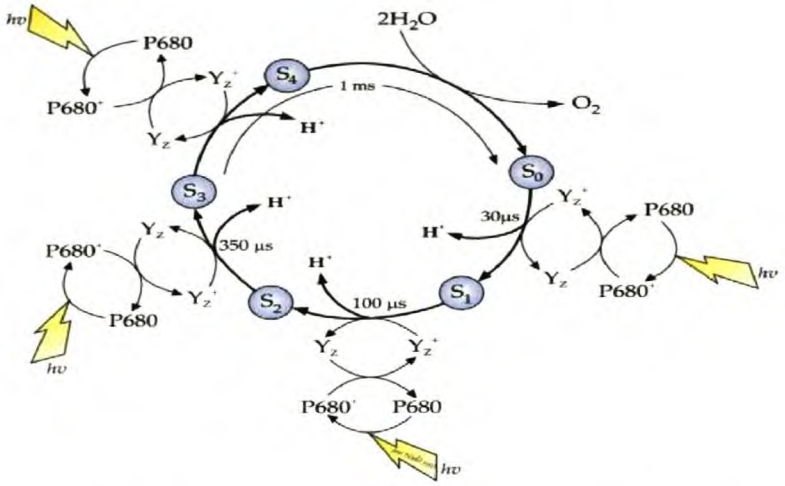


Figure 2.5. The oxygen-evolving reactions of PSII. P680 of PSII undergoes a cycle of oxidation and reduction. $P680^+$ is a very strong oxidising agent, and removes electrons from the oxygen evolving complex that causes the reduction of P680 and the oxidation of water. $O_2$ is formed as a byproduct [19].

### 2.1.1.2.3 The cytochrome $b_6/f$ complex

The cytochrome $b_6/f$ complex serves as a shuttle for electrons from PSII to PSI by accepting two electrons to $PQH_2$ and catalysing the transfer of one electron for both plastocyanin and cytochrome b563. Plastoquinone, bound on the stromal side of the complex, can then take up two more protons ($H^+$). Plastocyanin is mobile, water-soluble and operates in the thylakoid lumen where it reduces $P700^+$, the oxidised RC chlorophyll of PSI (Fig. 2.6).

### 2.1.1.2.4 Photosystem I (PSI)

PSI contains a RC that consists predominantly of β-carotene and chlorophyll *a*. The LHC of PSI (LHCI) includes 80-120 chlorophyll molecules, with a high ratio of chlorophyll *a* to chlorophyll *b*. PSI is monomeric and the LHCI remains associated to the PSI core under all physiological conditions [20]. In PSI, the RC and internal antenna are combined in a single chlorophyll-protein complex that accepts electrons from plastocyanin (or cytochrome) and delivers them to ferredoxin. This chlorophyll-carotenoid protein consists of the D1 and D2 proteins, that bind the chlorophyll *a* dimer, P700, and the initial electron acceptors $A_0$ (chlorophyll *a*), $A_1$ (phylloquinone),

and $A_2$ (an iron-sulphur complex, the 4Fe-4S center). The D1-D2 complex binds an additional 75-100 chlorophyll *a*, and 12-15 β-carotene molecules [11;17;21].

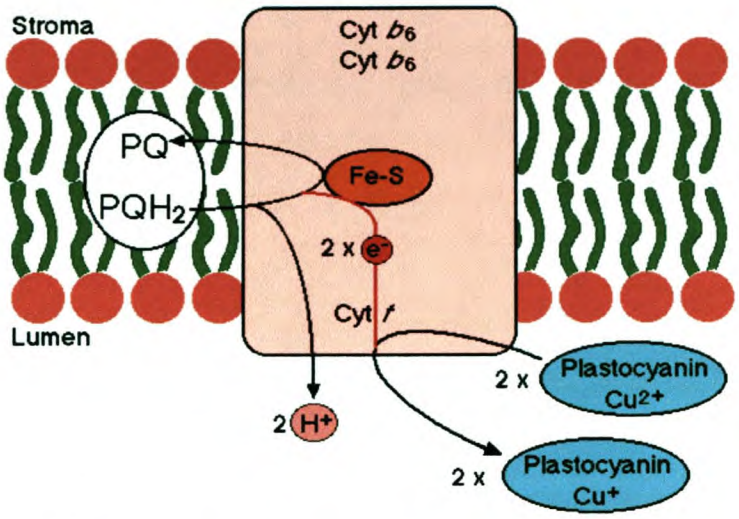


Figure 2.6. Electron transport reactions in the cytochrome $b_6/f$ complex. The cytochrome $b_6/f$ complex accepts electrons from reduced plastoquinone ($PQH_2$ from PSII) and reduces plastocyanin and cytochrome b563 and so doing shuttles electrons from PSII to PSI [18].

In much the same manner as in PSII, electron transfer in PSI is initiated when a photon of light energy is absorbed by a chlorophyll molecule of the LHC and is transferred to the RC chlorophyll, P700. P700 is raised from the ground state to an excited state (P700*) and an electron is passed sequentially on to $A_0$, $A_1$, $A_2$ and finally to ferredoxin that is present in the stroma. Ferredoxin-NADP oxidoreductase catalyses the reduction of $NADP^+$ to NADPH. In the photosynthetic process, much of the energy harvested from light is stored in NADPH as redox free energy (a form of chemical free energy) and is available for subsequent use in the reduction of carbon by the Calvin cycle (Fig. 2.7) [10;11;17].

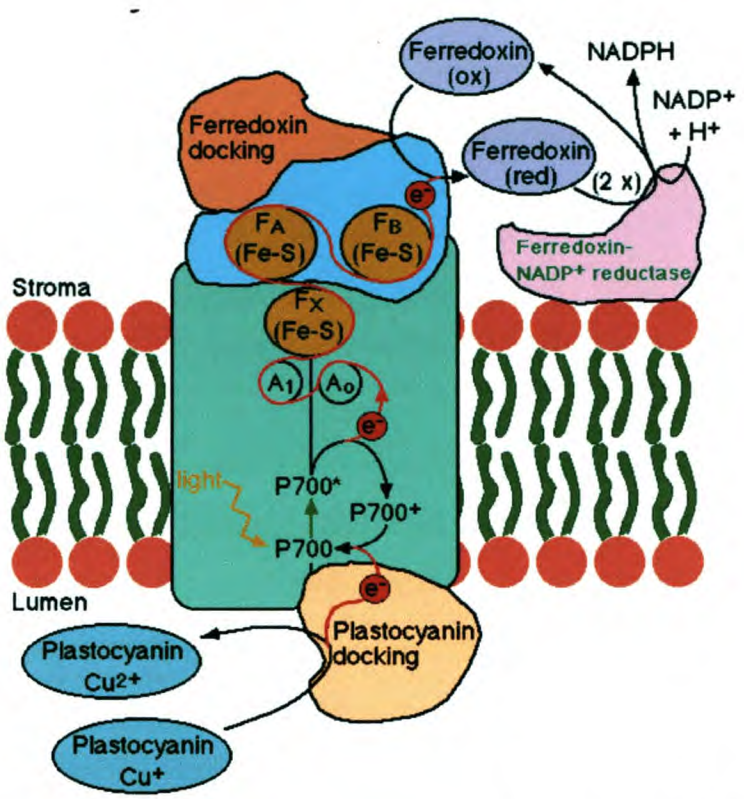


Figure 2.7. The electron transfer reactions from chlorophyll P700 to ferredoxin in PSI. P700, electron donor; $A_0$, primary electron acceptor; $A_1$, intermediate electron acceptor; $F_X/F_A/F_B$, iron-sulphur centers [18].

### 2.1.1.2.5 The ATP synthase ($CF_0$-$CF_1$) complex

The net result of these electron transport reactions is an accumulation of protons inside the membrane vesicles (i.e. the lumen) which creates an electrical field across the thylakoid membrane. In the process, the electron transfer reactions convert redox free energy into an electrochemical potential of protons. If this pH gradient ($\Delta$pH) across the thylakoid membrane is 2 (i.e. if the pH in the stroma is 8, and the pH in the lumen is 6, as typically occurs during photosynthesis), the electrochemical potential will be equivalent to 120 mV [11]. The energy stored in the proton electrochemical potential is used by the ATP synthase complex to covalently attach a phosphate group to adenosine diphosphate (ADP), forming ATP. The ATP synthase complex is responsible for the conversion of the generated proton electrochemical energy into chemical free energy (in the form of high energy phosphate bonds).

The ATP synthase complex is composed of two subunits, $CF_0$ and $CF_1$. The $CF_0$ subunit spans the thylakoid to form a proton channel through the membrane. The $CF_1$ subunit is bound to $CF_0$ on the outside of the membrane and is located in the aqueous space (stroma). The processes that couple proton transfer through the protein to the chemical addition of phosphate to ADP are poorly understood. It is

known, however, that phosphorylation can be driven by a pH gradient, a transmembrane electrical field, or a combination of both. Experimental evidence indicates that approximately three protons must pass through the ATP synthase complex for the synthesis of one molecule of ATP to occur [11]. The protons themselves are not involved in the chemistry of adding phosphate to ADP. One model suggests that there are three catalytic sites on each $CF_1$ that cycle between three different states. These states differ in their affinity for ADP, inorganic phosphate ($P_i$) and ATP. Initially, one ADP and one $P_i$ molecule binds loosely to one of the catalytic sites on $CF_1$. Due to conformational changes of the protein, the catalytic site becomes a tight binding site that stabilises the ATP. A second conformational change causes the site to release the new ATP molecule into the aqueous phase. It is thought that the energy from the proton electrochemical gradient is used to lower the affinity of the catalytic site for ATP, resulting in its release. The energy stored in this ATP can subsequently be transferred to other molecules by removal of the phosphate group(s) (Fig. 2.8) [11].

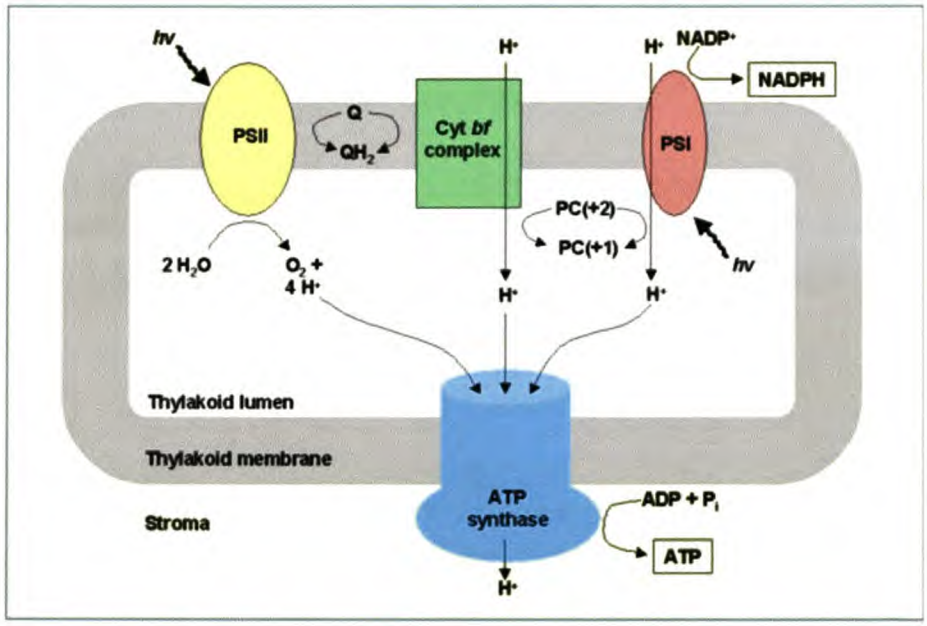


Figure 2.8. The ATP synthase complex utilises the accumulation of protons in the thylakoid lumen to drive the formation of ATP from ADP and organic phosphate [22].

### 2.1.1.3. Stoichiometry of the light reactions of photosynthesis

In summary, the light dependent reactions of photosynthesis convert light energy into chemical energy. Light energy is used to excite electrons of chlorophyll molecules in the RCs of PSI and -II. Some electrons are used to reduce NADP+ to NADPH. Other electrons are passed from P680 to the electron transport system in the thylakoid membranes, ultimately providing energy to synthesise ATP (via

chemiosmosis). The ATP and NADPH formed in the light-dependent reactions provide the energy (and protons) required to reduce $CO_2$ and synthesise glucose via the Calvin cycle. Atmospheric $CO_2$ provides the carbon source for photosynthesis and the electrons and protons needed to reduce the $CO_2$ to carbohydrate molecules are provided by $H_2O$ [10].

The overall photosynthetic reaction is represented by the equation:

$$6CO_2 + 6H_2O + \text{light energy (48 photons)} \rightarrow C_6H_{12}O_6 + 6O_2$$

The net result of the light reactions of photosynthesis can be represented by the equation (Fig. 2.9) [23]:

$$6H_2O + 12NADP^+ \; 18ADP + 18P_i + 6H^+ + 48 \text{ photons} \rightarrow 6O_2 + 12NADPH + 18ATP$$

i. One $H_2O$ is oxidised for every $NADP^+$ reduced (or alternatively, two NADPH are generated for every $O_2$ generated);

ii. For every $H_2O$ oxidised and $NADP^+$ reduced, five protons ($H^+$) are removed from the stroma and six are pumped into the lumen;

iii. The proton gradient generated is used by the ATP synthase complex to generate ATP. Approximately one ATP is generated for every $H_2O$ oxidised and $NADP^+$ reduced (to NADPH);

iv. The Calvin cycle uses two molecules of NADPH and three molecules of ATP to fix one molecule of $CO_2$. Thus an excess of ATP over NADPH is needed. This problem is solved by cyclic photophosphorylation: ferredoxin transfers its electrons back to plastoquinone, which can then donate them to the cytochrome $b_6/f$ complex.

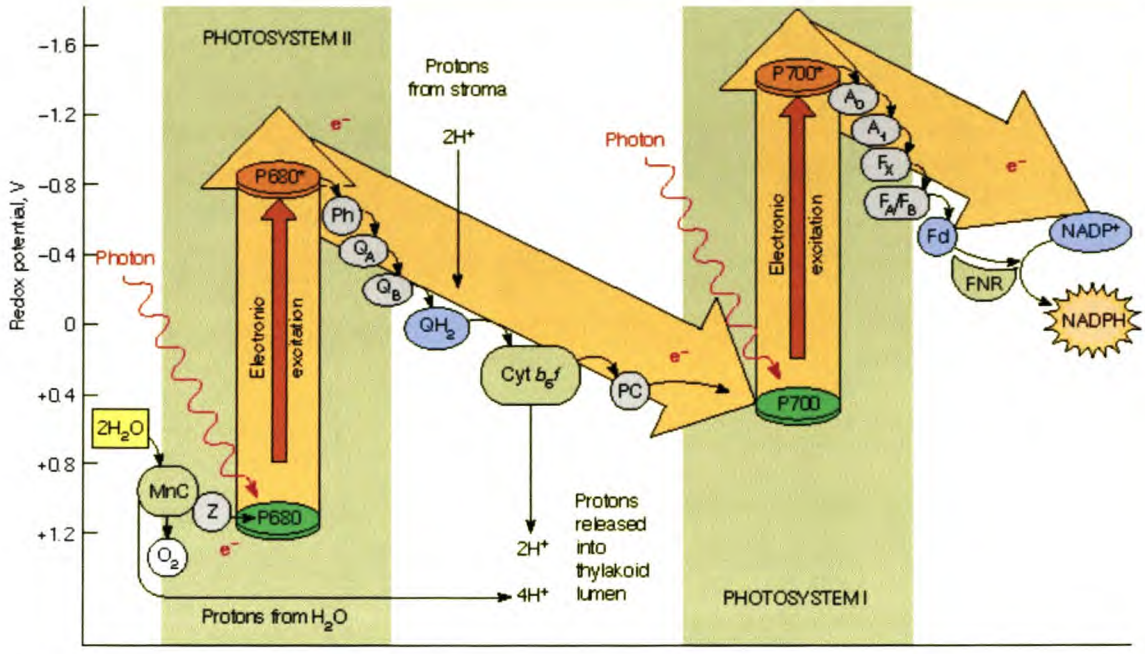


Figure 2.9. An overview of the electron transfer reactions that take place during the light-dependent reactions of photosynthesis in PSII, cytochrome $b_6/f$ and PSI [23].

## 2.1.2 PHOTOINHIBITION AND PHOTODAMAGE

### 2.1.2.1 How are the reactive molecules formed during photosynthesis?

The pigment-protein LHCs of PSII absorb light energy for photosynthesis. This light energy causes the primary charge separation of P680 in the RC of PSII to form the excited singlet state chlorophyll $P680^*$ molecule. Excess light intensities, however, cause alterations of the PSII RC that effectively blocks electron transfer from P680* to $Q_A$, or from reduced $Q_A$ ($Q_A^-$) to $Q_B$, which gives rise to an increase in charge recombination events of $P680^+/Pheo^-$ leading to the formation of triplet chlorophyll ($^3P680$). $^3P680$ is a long-lived excited state, and is incapable of initiating photosynthetic electron transfer. The oxidation of water by the oxygen-evolving complex of PSII gives rise to molecular $O_2$, that normally exists in the triplet ground state ($^3O_2$). Problems arise, however, when $^3O_2$ quenches $^3P680$ and is consequently converted to the excited singlet oxygen state ($^1O_2$) [12]. This reactive oxygen is a powerful oxidant and will attack proteins and pigments in the immediate vicinity of its formation.

There are strategies for defence against $^1O_2$ in the thylakoid membranes. Firstly, minimising the production of $^3P680$ by regulating the light-harvesting apparatus, and secondly, quenching of both $^3P680$ and $^1O_2$ reactive molecules by membrane-bound "quenchers". P680* can be quenched to the ground state by photochemistry (electron transport in the RCs) or the harmless dissipation of excess

excitation energy as heat. This thermal energy dissipation plays a crucial role in photoprotection since it limits the actual rate of reduction of $Q_A$ [1]. Thermal dissipation is increased by non-photochemical quenching (NPQ), and especially the activity of the xanthophyll cycle (i.e. the reversible conversion of violaxanthin to zeaxanthin).

The oxidative damage caused by the short-lived $^1O_2$ molecule seems to be confined to PSII, and specifically targets the D1 protein for degradation. Photo-oxidative damage, especially to PSII, appears to be an unavoidable consequence of the photosynthetic activity and is one of the major factors affecting photosynthetic efficiency [24-26].

In PSI, charge separation between P700 and the primary acceptor, $A_0$, is stabilised by electron transfer to $A_1$ (and $A_2$). In addition, $P700^+$ is less oxidative (and more stable) than $P680^+$ and is, therefore, an efficient quencher of the excitation energy from the PSI RC. The acceptor side of PSI, however, has a redox potential that is low enough to catalyse the reduction of $NADP^+$, and can also reduce $O_2$ to the superoxide anion radical ($O_2^-$). $O_2^-$ can subsequently be metabolised to peroxide ($H_2O_2$), as well as the extremely toxic hydroxyl radical, OH [26].

### 2.1.2.2 Targets of photo-oxidative damage in the photosynthetic membranes

The exact mechanism(s) of damage has not been determined, but the primary site of photo-oxidative damage is the components of the photosynthetic system located in the thylakoid membranes [27]. Within the thylakoid membrane PSII is the component most susceptible to photo-oxidative damage. This sensitivity is partially due to the action of the oxygen-evolving complex, as well as the intrinsic formation of reactive oxygen species [28]. Generation of $^1O_2$ (via $^3P680$) in the LHCs can potentially cause the oxidation of adjacent lipids, proteins, and pigments. The thylakoid membranes have a unique lipid composition, characterised by a high proportion of galactolipids (approximately 75%), containing mostly polyunsaturated fatty acids. This causes the membrane to adopt a relatively fluid system. This fluidity is thought to be essential for the photosynthetic process that requires numerous lateral, rotational, and transmembrane diffusion of its respective components. However, this fluidity is at the cost of susceptibility to high light intensities and elevated temperatures. The sensitivity of membrane lipids to oxidative damage by active forms of oxygen is generally proportional to their level of saturation. Heat-induced

membrane damage is attributed to lipid hyperfluidity, which alters lipid-protein interactions and subsequently causes protein denaturation (Fig. 2.10) [29;30].

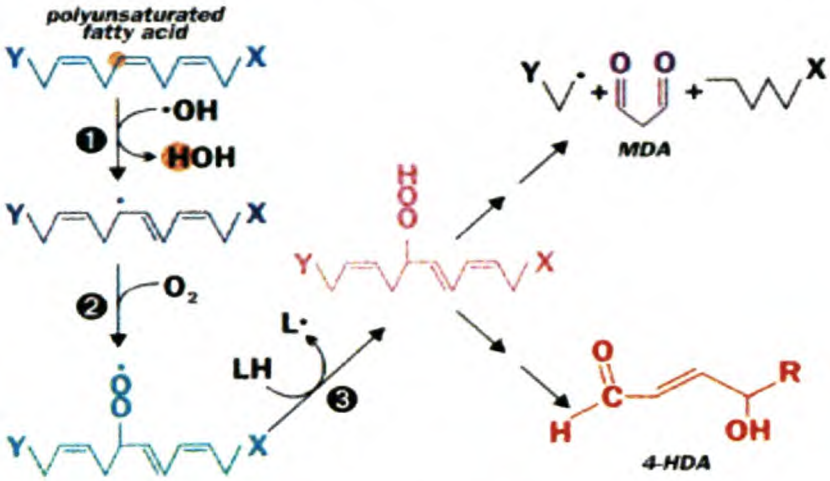


Figure 2.10. Peroxidation of unsaturated lipids. The variety of lipids and the random nature of free radical reactions leads to many products. These include 4-hydroxyalkenals (4-HDA) and, when there are three or more unsaturated bonds, malondialdehyde (MDA). These are useful for quantifying lipid peroxidation. Since a radical is also produced in the process, it is referred to as a chain reaction [31].

Lipid peroxidation is initiated by a reaction between ROS and fatty acid side chains of cell membranes. The ROS extracts a hydrogen atom, forming a fatty acid side chain peroxyl radical, which in turn can attack other fatty acid side chains and propagate lipid peroxidation. The ROS can therefore lead to the formation of peroxides and ketones with adjacent lipids and proteins (or any other oxidisable molecules). These ROS specifically damage the acyl side chains of polyunsaturated fatty acids causing the initiation of peroxidation chain reactions. Once initiated these chain reactions are autocatalytic and continue causing lipid peroxides to accumulate in the membrane. This peroxidation affects cellular function by altering membrane function - increasing fluidity, disrupting permeability, and inactivating membrane-bound receptors and enzymes.

Although $\alpha$-tocopherol is regarded as the major antioxidant responsible for controlling lipid peroxidation chain reactions, carotenoids are also involved in this protection. It is thought that a relatively small pool of free xanthophylls found in the lipid bilayer of the thylakoid membrane is responsible for this photo-oxidative protection [29]. In artificial lipid membranes, both lutein and zeaxanthin are capable

of preventing lipid peroxidation reactions. The interaction of these xanthophylls with free radicals has, to date, not been documented *in vivo* [32;33].

### 2.1.2.3 Mechanism of photoinhibition

Photoinhibition (or photoinactivation) is the light-induced loss of charge separation that is accompanied by the irreversible oxidative damage to the PSII protein complex, requiring the degradation and replacement of the D1 protein (as well as other PSII proteins) to re-establish photosynthetic function. Photodamage to the RCs appears to involve two separate mechanisms that both lead to loss of charge separation. The first is observed when the RC is unable to supply enough electrons for the reduction of $P680^+$ (donor-side photoinhibition); and the second results when the electron acceptor, $Q_A$ (and indirectly $Q_B$), cannot transfer electrons from the RC fast enough (acceptor-side photoinhibition). Both donor- and acceptor-side photoinhibition will lead to chlorophyll oxidation and damage to the D1 protein. In PSII, two membrane-bound proteases (DegP2 and FtsH) are activated by light, and catalyse the cleavage of the D1 protein into discrete fragments [28;34;35]. It is possible that the cleavage of the D1 protein causes structural alterations resulting in the targeting of the RC for either disassembly and replacement, or conversion to an energy-dissipating form. Furthermore, phosphorylation of the D1 protein is thought to play an important role in determining the ultimate fate of the affected RC [36-38].

The D1 protein has the fastest turnover among the chloroplast proteins. Under unsaturating light conditions, the rate of *de novo* synthesis of the D1 protein is balanced by its degradation, resulting in no visible signs of photoinhibition in the leaf. Saturating light conditions, however, will result in an increase in the flux of electrons from $P680^+$/pheophytin$^-$ to the D1 bound $Q_A$, causing $Q_A$ to be reduced beyond its normal level. This effectively blocks the electron transfer from the RC to $Q_A$, leading to the formation of $^3P680$. Under aerobic conditions $^3P680$ can react with molecular $O_2$ and form $^1O_2$. $^1O_2$ has been implicated in the initiation of the D1 protein degradation [34]. The repair process entails the disassembly of the PSII complex and the selective removal and replacement of the photodamaged D1 protein. When the photo-oxidative damage to PSII occurs faster than its enzymatic repair, the photosynthetic capacity will decrease and eventually stop.

## 2.2 PLANTS AND PHOTOPROTECTION

Light is probably the most obvious prerequisite for photosynthesis, yet plants frequently require protection from light. Reactive intermediates are unavoidable by-products of the photosynthetic process and can, if not controlled, cause damage to the photosynthetic apparatus (photo-oxidative damage or photodamage). If the damage is not repaired, it will affect both the rate and efficiency of photosynthesis [39]. If this light-induced damage exceeds the repair capacity of the plant, then the overall photosynthetic activity will decrease and eventually stop (photoinhibition). In exposed habitats, this phenomenon can occur daily during periods of peak irradiance, and although plants are efficient at converting light energy into chemical energy, the capacity of these reactions becomes limited when the light conditions become saturating [40]. This has necessitated plants to evolve numerous biochemical and developmental responses to light that help to optimise both photosynthesis and growth (collectively referred to as photoprotection).

Light stress is typically caused when the amount of absorbed light exceeds the capability of the photosynthetic apparatus. This will occur if the ratio of photon flux density (PFD) to photosynthesis is high. However, this ratio does not only increase when the PFD increases (i.e. high light conditions), but also if the rate of photosynthesis is decreased under moderate PFD, normally due to environmental stresses from temperature, nutrition, drought, etc. Plants exhibit an entire spectrum of responses to increasing PFD. Over a range of PFDs, an increase in the absorption of light by chlorophyll will result in an increase in photosynthetic $CO_2$ fixation. Above a certain PFD, however, photosynthesis will be incapable of utilising all the energy absorbed by chlorophyll. It is in this range of PFDs that various mechanisms must function to protect the photosynthetic apparatus against damage from the accumulation of excess energy.

Certain plants can avoid absorption of excess light by movement of their leaves, cells, or chloroplasts. Within the chloroplasts, both the absorption and utilisation of light energy is further balanced by regulation of photosynthetic light harvesting and electron transport. An adjustment in light-harvesting antenna size and photosynthetic capacity can decrease light absorption and increase light utilisation, respectively. Furthermore, alternative electron transport pathways and heat dissipation remove excess absorbed light energy from the photosynthetic apparatus. Antioxidant molecules (e.g. carotenoids, ascorbate, glutathione and $\alpha$-tocopherol) and the so

called "scavenging enzymes" (e.g. superoxide dismutase and catalase) control the inevitable generation of reactive molecules. However, despite these photoprotective defenses; photodamage to the photosynthetic apparatus still occurs, necessitating the turnover and replacement of damaged proteins (Fig. 2.11).

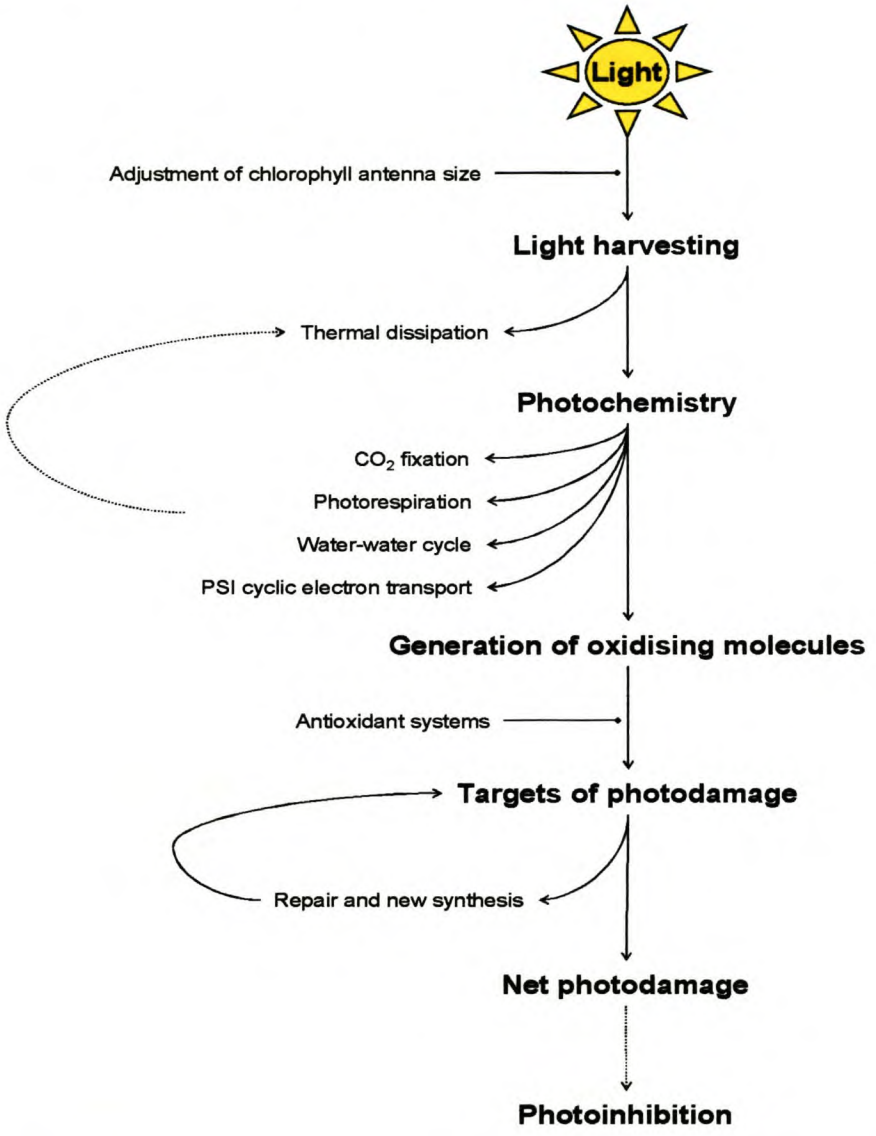


Figure 2.11. Schematic diagram of the photoprotective processes that occur in the chloroplast [4].

### 2.2.1 Photoprotection and photoadaptation

It is clear that plants need to be able to cope with any imbalances between the light energy absorbed and the energy that is actually used for photosynthesis. Plants have developed a whole range of acclimation and protection strategies against photoinhibition of PSII under saturating light conditions. These mechanisms can typically be grouped into two categories: strategies that are related to the harvesting

and transfer of light energy to PSII RC; and those directly involved in the functioning of the RC [41].

The first category includes the re-arrangement of light-harvesting pigments associated with PSII due to acclimation or genetic variability between plant species. These include changes in both the amount and composition of the antennae pigments, increases in the levels of the photosynthetic electron transport carriers, as well as an increase in ribulose-1,5-bisphosphate carboxylase (Rubisco, the key enzyme involved in carbon fixation). Other mechanisms are the spill-over of excess energy from PSII to PSI as well as phosphorylation of LHCII (that results in the rapid detachment of the chlorophyll-binding proteins from PSII complex). The waxy layers found in the epidermis of certain plants should also be included in this category since these layers reflect a significant amount of light energy and, therefore, also play a role in photoprotection [41;42]. This review will, however, focus only on the second category. This includes the dynamic processes that facilitate the harmless dissipation of excess (absorbed) light energy as heat. In this category, the xanthophyll cycle facilitates the major photoprotective process, and is activated by the build-up of a transmembrane pH gradient that is formed under saturating light conditions. Zeaxanthin, antheraxanthin and lutein are necessary especially under these conditions for the efficient transition of the LHCs of PSII from a conformation that favours light harvesting, to one that allows for the harmless dissipation of the excess light energy as heat. Plants also make use of a series of antioxidant molecules and enzymes to detoxify reactive oxygen species and free radicals once they have formed (Fig. 2.12).

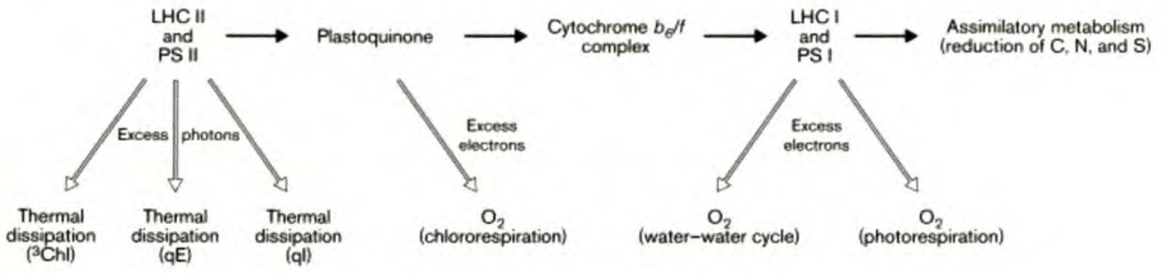


Figure 2.12. "Safety valves" for excess photons and electrons. Thermal dissipation of excess photons is accomplished by triplet chlorophyll, inducible energy-dependent quenching (*q*E), and sustained photoinhibition (*q*I). Additional mechanisms include oxygen-dependent alternative electron sinks and photorespiratory metabolism, photoreduction of $O_2$ in the water–water cycle, and a chlororespiratory alternative oxidase [43].

This section has only touched on some of the mechanisms plants possess to deal with excessive light, the rest of this review will focus on the protective role that carotenoids play in preventing photo-oxidative damage to the photosynthetic membranes of plants. The different photoprotective mechanisms that plants possess should not be considered in isolation, but rather be seen as a complex overlapping network of responses to a perceived stress condition (reviewed in [4;20;44]).

## 2.3 CAROTENOIDS: PIGMENTS WITH ROLES IN LIGHT-HARVESTING AND PHOTOPROTECTION

Carotenoids are one of the most abundant and widely distributed classes of natural pigments and perform a variety of essential biological functions in plants. Carotenoids are both integral and indispensable components of the photosynthetic membranes of plants. RCs bind carotenoids for light-harvesting, quenching of $^3$P680 and electron transport between cytochrome b559 and P680$^+$. Xanthophylls (lutein, neoxanthin and violaxanthin) that are bound to the LHC proteins, serve as accessory pigments for light harvesting and the consequent transfer of excitation energy to chlorophyll [45]. Xanthophylls are indispensable for photoprotection by contributing to NPQ (via the xanthophyll cycle), the direct and indirect quenching of excited chlorophyll, and as scavengers of photosynthetically generated $^1O_2$. In addition to these photoprotective functions, xanthophylls are also essential structural components of the LHCs [46;47]. Carotenoids are also precursors for the plant growth regulator, abscisic acid (ABA) [48;49].

### 2.3.1 Properties of carotenoids in relation to function

The majority of carotenoids are $C_{40}$-tetraterpenes made up of eight isoprene ($C_5$) units bound in a "head-to-tail" manner. This terpenoid backbone can be modified by desaturation, cyclisation or hydroxylation. Very few of the carotenoids found in the photosynthetic apparatus of higher plants are hydrocarbons, and typically contain two cyclised end-groups, and for the majority, at least one oxygen function (usually a hydroxyl- or epoxy-group). The different carotenoids found in the photosynthetic apparatus possess a whole range of physical, chemical and spectroscopic properties and, since the carotenoid composition of the various pigment-protein complexes is largely heterogeneous, this potentially leads to different functions for each of these carotenoids in the different protein-lipid environments (Fig. 2.14) [50].

For carotenoids to be effective light harvesting pigments, they must be capable of transferring the singlet-singlet energy (from the excitation by light) to chlorophyll.

The photoprotective role of carotenoids, on the other hand, relies on the triplet-triplet energy transfer from the excited $^3$P680 to a carotenoid molecule, thereby preventing the formation (via triplet-sensitisation) of harmful $^1O_2$. The rate of carotenoid de-excitation of $^3$P680 is much faster than the rate of $^1O_2$ sensitisation, and is, therefore, the preferred reaction. Carotenoids have been shown *in vitro* to be capable of directly quenching $^1O_2$. *In vivo*, carotenoids are found bound in pigment-protein complexes, and it is not known how this conformational change affects the quenching mechanism.

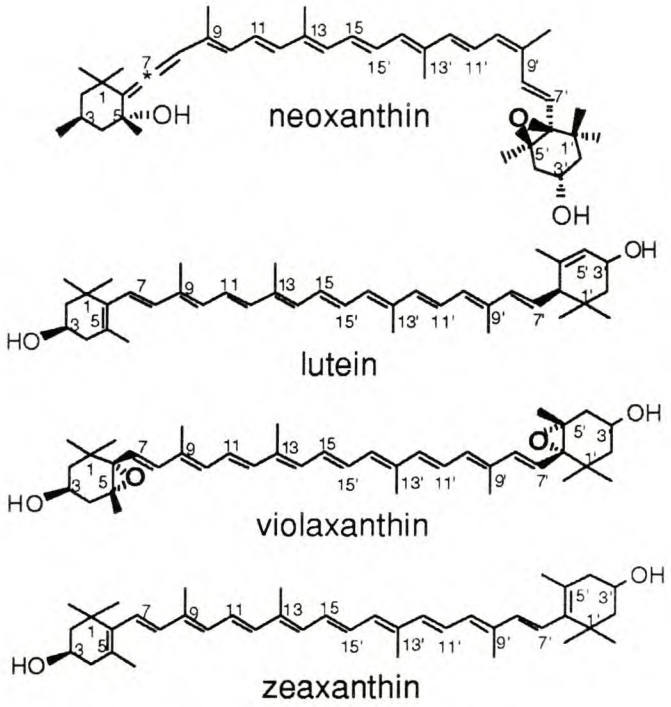


Figure 2.14 . Structural formulae of the four major photosystem II antenna xanthophylls: neoxanthin, lutein, violaxanthin and zeaxanthin [51].

The interconversion of violaxanthin and zeaxanthin by the action of the xanthophyll cycle, results in major alterations to the properties of these molecules. De-epoxidation of violaxanthin to zeaxanthin, results in a change from nine to eleven conjugated carbon-carbon double bonds (and the inverse for the epoxidation reaction). This conversion will affect both the energies and lifetimes of the excited states of these molecules, as well as preventing rotation of the β end-groups around the main polyene chain and resulting in near-planar conformations. This does not occur in carotenoids which have an epoxide-group in the C-5,6 position (e.g. violaxanthin) or possess an ε end-group (e.g. lutein). As a result the conformations of zeaxanthin and violaxanthin are quite different, and the end-groups may adopt

either perpendicular or near-planar positions relative to the main conjugated chain. These conformations are associated with the tendency of these carotenoids to form aggregates, and possibly plays a role in the control of the organisation of the LHCs [50]. Xanthophylls with these characteristics will alter the fluidity of photosynthetic membranes, as well as the aggregation state of the LHCs within the membranes. The lack of an epoxide on at least one cyclohexenyl ring could facilitate a direct photochemical reaction with $^1O_2$, whereas having additional double bonds might make these xanthophylls more effective in preventing lipid peroxidation [52].

### 2.3.2 Carotenoid biosynthesis

All isoprenoids are synthesised from just two $C_5$ precursors: isopentenyl diphosphate (IPP) and its isomer dimethylallyl diphosphate (DMAPP). Two distinct pathways are utilised by plants for the biosynthesis of IPP: the classical acetate/mevalonate pathway and the novel mevalonate-independent route, the 1-deoxy-D-xylulose 5-phosphate (DOXP)/2-C-methyl-D-erythritol 4-phosphate (MEP) pathway (Fig. 2.15) [53]. The acetate/mevalonate pathway operates in the cytosol and is responsible for the formation of sterols, certain sesquiterpenes, etc, whereas plastidic isoprenoids (such as isoprene, phytol and carotenoids) originate via the DOXP/MEP pathway [54]. Although there is evidence that suggests that some exchange occurs between the different cytoplasmic and plastidic derived IPP, each pathway seems to produce unique isoprenoids [55].

The formation of the $C_6$-compound 3-hydroxy-3-methylglutaryl-CoA (HMG-CoA) by the fusion of three molecules of acetyl-CoA signals the start of the acetate/mevalonate pathway. This reaction is catalysed by HMG-CoA synthase (HMGS). HMG-CoA reductase (HMGR) subsequently catalyses the two-step reduction of HMG-CoA to form mevalonate. Mevalonate is in turn sequentially phosphorylated by first mevalonate kinase (MK), and secondly phosphomevalonate kinase (PMK) to form mevalonate 5-diphosphate (via the intermediate mevalonate 5-phosphate). Finally mevalonate decarboxylase (MDC) catalyses the decarboxylation of mevalonate 5-diphosphate to yield IPP.

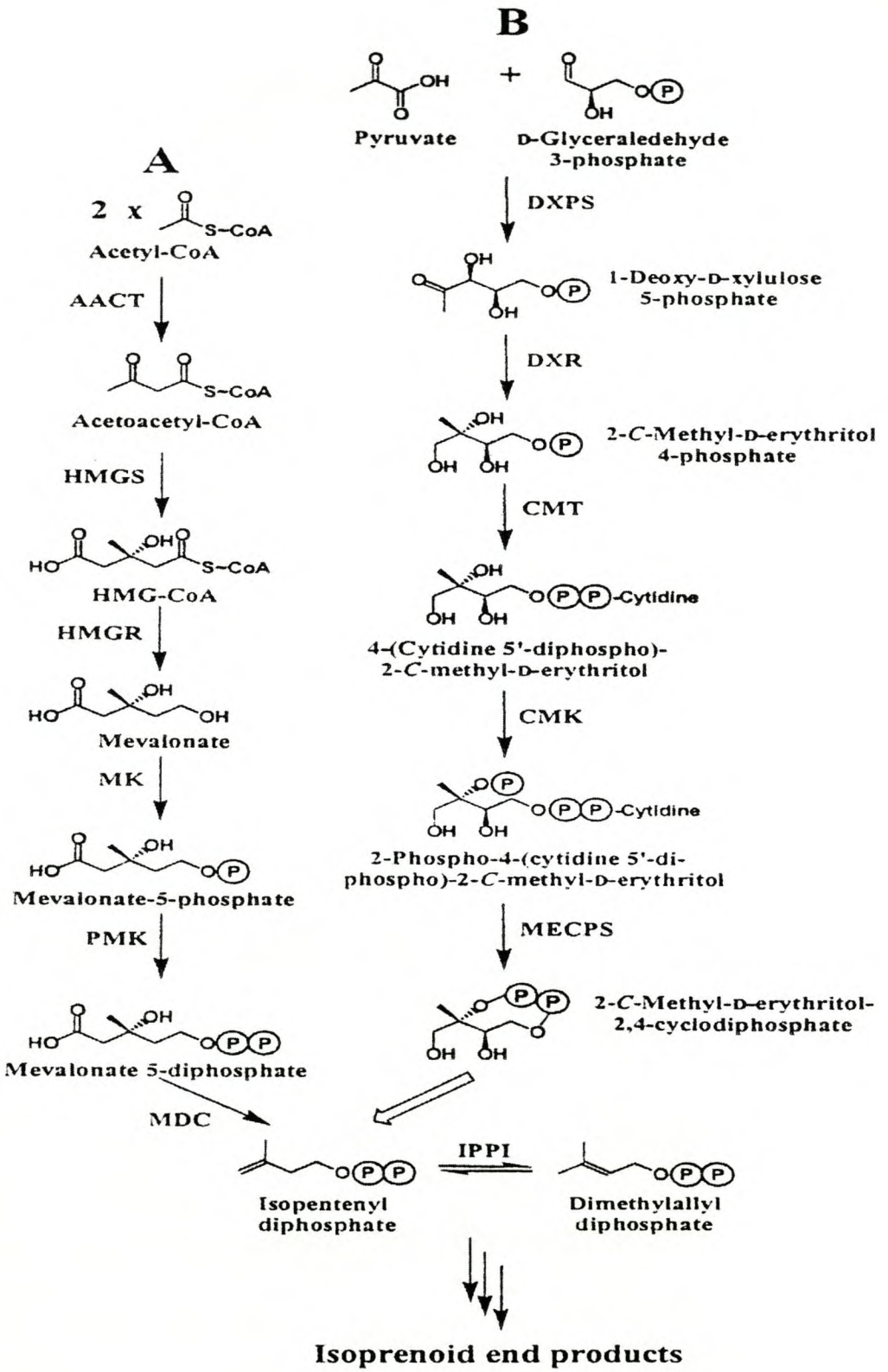


Figure 2.15. The acetate/mevalonate pathway (A) and the 1-deoxy-D-xylulose 5-phosphate/2-C-methyl-D-erythritol 4-phosphate pathway (B) to isopentenyl diphosphate. Abbreviations for the enzymes catalysing the reactions are as used in the text [56].

The DOXP/MEP pathway for IPP biosynthesis requires the condensation of pyruvate and D-glyceraldehyde-3-phosphate to yield DOXP by the action of DOXP synthase (DXS) [55;57]. Estevez and co-workers [55] showed that overexpressing DXS in *Arabidopsis* plants increased the levels of a range of isoprenoids (chlorophylls, tocopherols, carotenoids, ABA, and gibberillic acid [GA]) and that suppressing the levels of DXS decreased the amounts of all of these products. The fact that manipulation of the DXS levels leads to changes of various isoprenoids indicates that DXS is one of the limiting steps in the production of plastidic IPP and, therefore, of isoprenoids in general [55;58].

DOXP reductoisomerase (DXR, IspC) catalyses the first step of this pathway by the conversion of DOXP to MEP [59]. MEP is further converted to 4-diphosphocytidyl-2C-methyl-D-erythritol (DPME) by the action of DPME synthase (ispD), and DPME kinase (IspE) in turn phosphorylates DPME [60;61]. 2C-Methyl-D-erythritol (ME) 2, 4-cyclodiphosphate synthase (IspF) converts the phosphorylated DPME to ME 2, 4-cyclodiphosphate [62;63]. In turn, hydroxymethylbutenyl diphosphate synthase (GcpE, IspG) has been shown (in *Escherichia coli*) to catalyse the reduction of ME 2, 4-cyclodiphosphate to 1-hydroxy-2-methyl-2-(E)-butenyl 4-diphosphate [64;65]. The gene product of 4-hydroxy-3-methylbut-2-enyl diphosphate reductase (*lytB*, i*spH*) is thought to affect the ratio of IPP to DMAPP, but the specific reaction that is catalysed is not entirely clear [66]. An *E. coli* strain expressing the *lytB* gene, however, was capable of converting 1-hydroxy-2-methyl-2-(E)-butenyl 4-diphosphate to IPP and DMAPP in a 6:1 ratio [64;67;68].

IPP is itself not reactive enough to undergo the ionisation that initiates the subsequent condensation reactions that gives rise to the more complex isoprenoids. DMAPP, the more reactive isomer of IPP, is formed by the reversible isomerisation of IPP, catalysed by IPP isomerase (IPI). Additional IPP molecules can be added to DMAPP by sequential head-to-tail condensation reactions [68-70]. Geranylgeranyl diphosphate (GGPP) synthase (GGPS) catalyses the condensation of three IPP molecules with one DMAPP molecule to form the $C_{20}$-hydrocarbon GGPP. GGPP serves as an important branchpoint in isoprenoid biosynthesis, and is the precursor for tocopherols, gibberellins, plastoquinones, chlorophylls and carotenoids (Fig. 2.16)

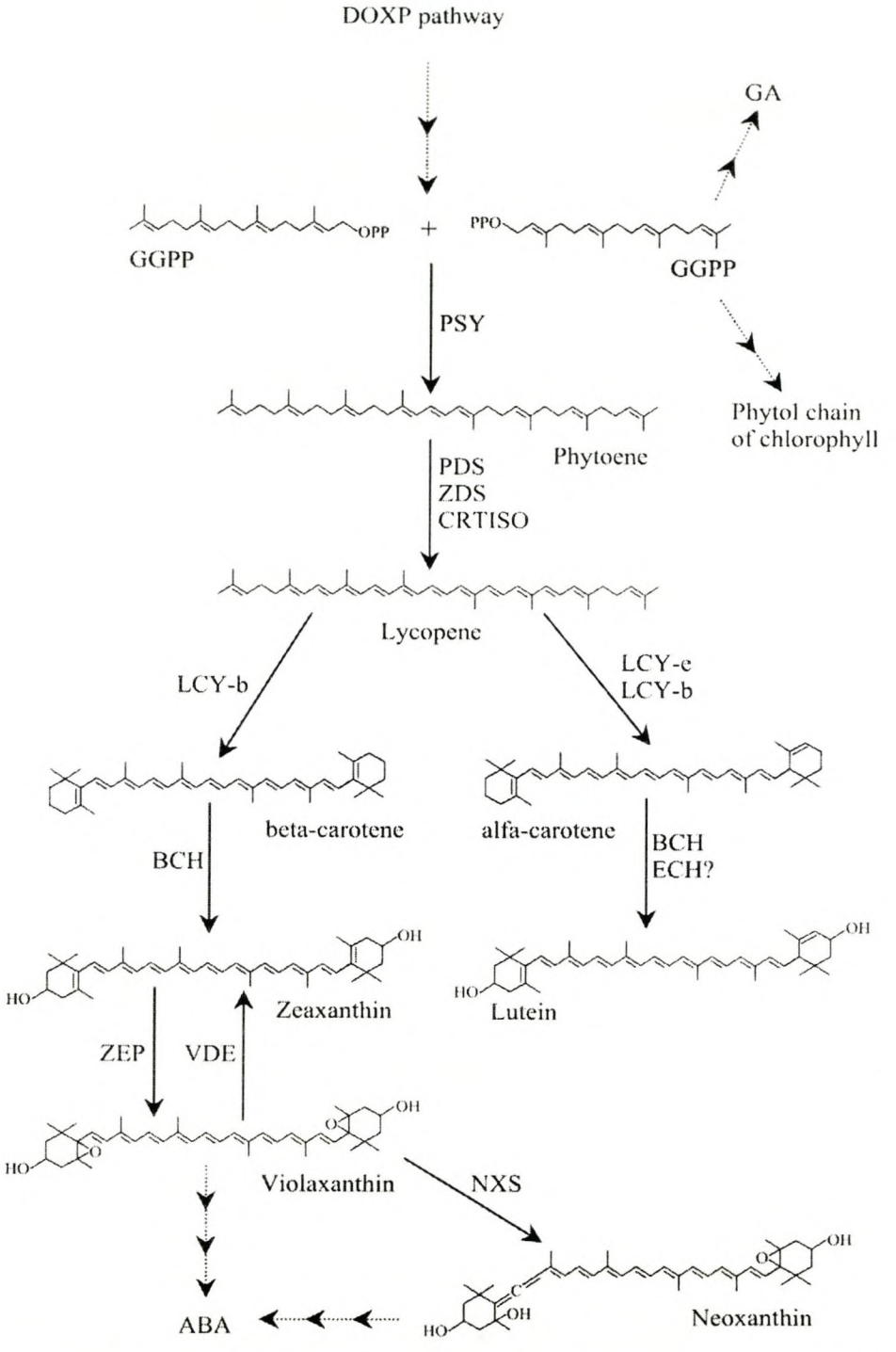


Figure 2.16. A brief overview of the biosynthesis of carotenoids in plastids. PSY, phytoene synthase; PDS, phytoene desaturase; ZDS, ζ-carotene desaturase; CRTISO, carotene isomerase; LCY-b, lycopene β-cyclase; LCY-e, lycopene ε-cyclase; BCH, β-carotene hydroxylase; ECH, ε-carotene hydroxylase; ZEP, zeaxanthin epoxidase; VDE, violaxanthin de-epoxidase; NXS, neoxanthin synthase. Some of the steps have been omitted for simplification [71].

The 20-carbon molecule geranylgeranyl diphosphate (GGPP) is formed by the linear addition of three IPP molecules to DMAPP by GGPP synthase (GGPS). As many as eleven genes in the *Arabidopsis* genome encode for GGPS. A large gene family is most probably required due to the need for the different isoforms that are targeted to the different organelles [72;73]. It has been reported that GGPS can combine with phytoene synthase (PSY) and IPI to form a complex that is associated with the internal membranes of the plastids [74]. In addition to carotenoids, a number of other compounds made in the plastids require GGPP as a precursor, among them GA. In tomato plants overexpressing PSY, the total amount of carotenoids was increased in the fruits, but the levels of GA were drastically reduced [75]. Similarly, in tomato plants expressing an antisense PSY, the carotenoid levels were reduced, but GA levels were much higher than the wild-type [76]. These results would suggest that both the carotenoid- and GA pathways are in direct competition for substrate (GGPP), or alternatively, for GGPS.

PSY catalyses the first step specific to carotenoid biosynthesis by condensation of two soluble GGPP molecules to produce the lipophilic phytoene. PSY has been identified as a rate-limiting step in carotenoid biosynthesis [77]. Furthermore, there is evidence for post-translational regulation of PSY activity in plants. For example, in daffodil flowers an inactive, soluble pool of PSY becomes functional only after association with chromoplast membranes [78]. Similarly, in etioplasts of *Sinapsis alba*, a PSY pool is found that is only activated when chloroplast differentiation is initiated by illumination. The activated PSY then binds to the membrane [77].

Phytoene desaturase (PDS) and ζ-carotene desaturase (ZDS) catalyse four stepwise desaturations of phytoene to ζ-carotene (via phytofluene), and poly-*cis* lycopene (via neurosporene), respectively. These desaturation reactions serve to lengthen the conjugated series of carbon-carbon double bonds that form the typical chromophore of carotenoid pigments. An electron acceptor is required for PDS and ZDS function. It has been reported that the enzymatic activity of PDS in daffodil flowers depends on the redox state of quinones in the chromoplast membranes. This has been identified as a possible regulatory mechanism for the control of flux through the pathway [79].

Since only all-*trans* lycopene serves as a substrate for the subsequent cyclase reactions, it is clear that an isomerisation is necessary to convert the poly-*cis* lycopene to all-*trans* lycopene. This can be catalysed by either a carotenoid

isomerase (CrtISO), or by light (photoisomerisation). Since photoisomerisation only occurs in chlorophyll-synthesising tissues, the enzymatic action of CrtISO is usually also required [80-82].

In any oxygen-evolving photosynthetic organism an inability to form cyclic carotenoids is eventually lethal. Carotenoids in the photosynthetic membranes of plants typically contain two β-rings (e.g. β-carotene and zeaxanthin) or one ε- and one β-ring (e.g., lutein). Carotenoids with two ε-rings are uncommon and to date have only been found in lettuce [83]. All-*trans* lycopene serves as the substrate for both lycopene β-cylase (LCYB) and lycopene ε-cyclase (LCYE) and as such represents a branchpoint in the carotenoid pathway. LCYB catalyses a two-step reaction that adds an identical β-ionone ring on each end of the symmetrical lycopene molecule and forms the bicyclic β-carotene (via the intermediate γ–carotene). LCYE, on the other hand, creates an ε-ring on only one end of the lycopene molecule to form the monocyclic δ-carotene (with the β- and ε-rings differing only in respect of the position of the double bond within the cyclohexene endgroup). The action of both LCYB and LCYE is required to form the lutein precursor, α-carotene (β, ε-carotene). Adjustment of the relative activities of the two cyclases might be a mechanism by which plants can control the flux of substrates to either the β,β-carotenoids that are essential for photoprotection, or the β,ε–carotenoids that serve primarily to capture light energy for photosynthesis. This serves to regulate the formation of carotenoids with two ε-rings [83]. This hypothesis is supported by mutations that affect xanthophyll biosynthesis in *Arabidopsis* where the loss of a specific carotenoid causes a concomitant increase in other carotenoids. Although the carotenoid composition in these mutant lines is different, the total carotenoid content still remains the same [45]. This phenomenon could be controlled by the adjustment of the two cyclase activities.

The action of two hydroxylases is required to convert β-carotene to zeaxanthin (via β-cryptoxanthin), and α-carotene to lutein (via zeinoxanthin/α-cryptoxanthin). As the name suggests, β-carotene hydroxylase activity is specific for β-rings, and likewise ε-carotene hydroxylase is specific for ε-rings. β-Carotene, therefore, requires two β-ring hydroxylations, whereas α-carotene requires the action of both a β- and ε-ring hydroxylation to form their respective xanthophylls (oxygenated carotenoids). To date, however, no ε-carotene hydroxylase encoding gene has been

cloned from any organism, but it has been identified genetically in the *Arabidopsis* mutant, *lut1* [84]. Most of the carotenoid pigments in the thylakoid membranes of plants are xanthophylls, with lutein and zeaxanthin representing the first carotenoids formed in the pathway. Zeaxanthin has been shown to play a central role in the non-radiative dissipation of light energy under conditions of excess photon capture by the photosynthetic light-harvesting apparatus [reviewed in [4;85].

In some plants, non-photosynthetic cells are able to accumulate large amounts of carotenoids in specialised plastids called chromoplasts. Many species-specific chromoplast-carotenoids have been described. The characteristic red colour in ripening *Capsicum annuum* fruits, for example, is due to the accumulation of two such ketoxanthophylls: capsanthin and capsorubin. The conversion of antheraxanthin and violaxanthin into capsanthin and capsorubin, respectively, is catalysed by only one bifunctional enzyme, capsanthin-capsorubin synthase (CCS) (or keto carotenoid synthase) [86;87].

The conversion of zeaxanthin to violaxanthin (via the intermediate antheraxanthin) is catalysed by zeaxanthin epoxidase (ZEP). This reaction typically occurs under low (or limiting) light in photosynthetic tissues. Under excessive light this epoxidation reaction is reversed and VDE converts violaxanthin back to zeaxanthin (via antheraxanthin) causing a rapid change in the carotenoid composition of the LHCs in the thylakoid membranes [88]. The high light-induced formation of zeaxanthin facilitates a state of high energy dissipation in PSII.

In photosynthetic plants, the final step of carotenoid biosynthesis involves the formation of the epoxy-carotenoid, neoxanthin which serves as a precursor for the plant growth regulator, ABA. Neoxanthin synthase (NSY) catalyses the conversion of violaxanthin to neoxanthin. Interestingly, the amino acid sequence of the *NSY*-encoding gene from tomato was found to be practically identical to the chromoplast-specific LCYB (CYC-B) from tomato, and to a lesser degree, CCS from pepper [86].

### 2.3.3 Abscisic acid biosynthesis

The plant hormone ABA is an important regulator that plays a role in co-ordinating plant growth and development in response to external environmental conditions. ABA is involved in many cellular processes including seed development, dormancy, germination, vegetative growth, and environmental stress [89].

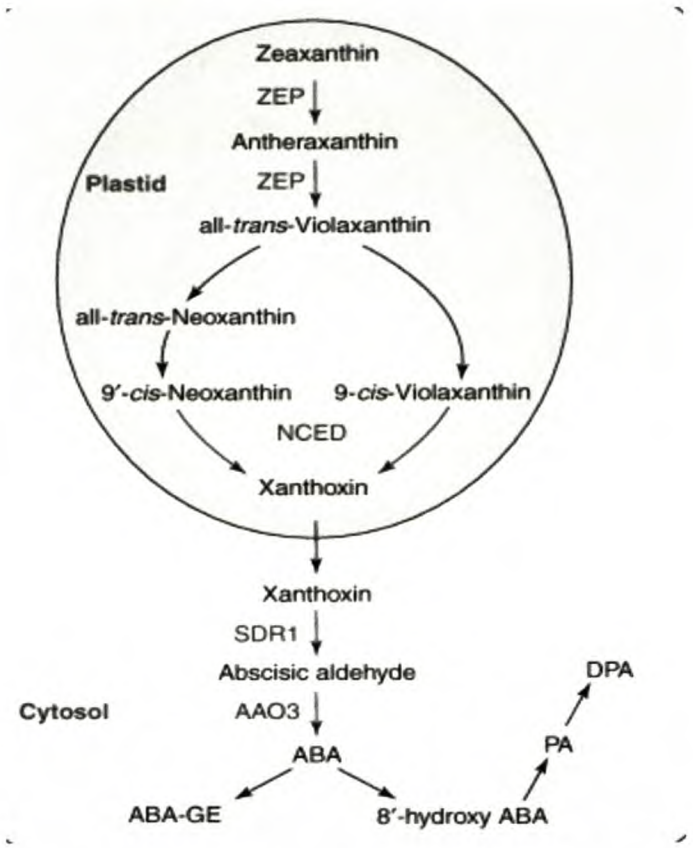


Figure 2.17. Abscisic acid (ABA) biosynthesis pathway in plants. Zeaxanthin is converted to violaxanthin by zeaxanthin epoxidase (ZEP). Cleavage of cis-xanthophylls (i.e. violaxanthin and neoxanthin) is catalysed by a family of 9-cis-epoxycarotenoid dioxygenases (NCED) to form xanthoxin. Xanthoxin moves to the cytosol and is converted into abscisic aldehyde by a short-chain dehydrogenase reductase (SDR1), which is then oxidised into ABA by an abscisic aldehyde oxidase (AAO3). The most abundant ABA-catabolite is phaseic acid (PA), which is formed via the hydroxylation of ABA into 8'-hydroxy ABA. Phaseic acid is subsequently converted into dihydrophaseic acid (DPA) [90].

Two pathways for ABA biosynthesis have been proposed. A direct pathway from IPP via farnesyl diphosphate (FPP) to ABA; and an indirect pathway in which ABA is a cleavage product of carotenoids [91;92]. The direct pathway has been shown to function in fungi, whereas the indirect pathway functions in plants. Only the indirect pathway will be discussed (Fig. 2.17). The contribution of carotenoid synthesis to the regulation of ABA biosynthesis remains unclear. Data obtained from overexpression of PSY in tomato indicated that the rate of carotenoid biosynthesis had no significant effect on the overall rate of ABA synthesis [75].

The first step in ABA biosynthesis is the oxidative cleavage of 9-*cis*-epoxy carotenoids (e.g. violaxanthin or neoxanthin) to *cis*-xanthoxin. This reaction occurs in

the thylakoids and is catalysed by the enzyme 9-*cis* epoxy carotenoid dioxygenase (NCED) [93]. NCED is the first committed step in ABA biosynthesis, and most probably the overall rate-limiting step of ABA production [90;91]. In most plant species studied, NCED comprises a gene family consisting of several members. Nine hypothetical genes in the *Arabidopsis* genome encode for NCED, of which four (*AtNCED2, -3, -6,* and *-9*) have been shown to catalyse the cleavage reaction in ABA synthesis. It is thought that the different NCED-encoding genes in *Arabidopsis* are expressed in different tissues and at different developmental stages [94]. Overexpression of the *NCED* from *Phaseolus vulgaris* (*PvNCED*) in tobacco plants leads to increased ABA and its catabolite, phaseic acid. These plants displayed slower germination rates (four days later than the wild-type), but also displayed reduced transpiration water loss than the wild-type plants and were therefore more tolerant to drought stress conditions [95].

In the cytosol, xanthoxin is converted to abscisic-aldehyde by an enzyme that is similar to the short-chain dehydrogenases/reductases (SDRs). However, unlike NCED, the expression of the *Arabidopsis* SDR (encoded by *AtABA2*) remained unaffected by stress, but was upregulated by glucose [96;97]. Abscisic-aldehyde is oxidised by abscisic aldehyde oxidase (AAO) to yield ABA. Four *AAO* genes (*AAO1-4*) have been identified in *Arabidopsis*, but only one, *AAO3*, is responsible for ABA synthesis in vegetative tissue [98]. In some mutants defective in aldehyde oxidation a "shunt pathway" has been identified. This pathway oxidises abscisic aldehyde to ABA (via abscisic alcohol), but the final levels of ABA in these mutants is still very low. This shunt pathway possibly functions in normal (wild-type) plants as well, and serves as a minor source of ABA [92].

### 2.3.4 The location and site(s) of action of carotenoids in photosynthetic membranes

Carotenoids are biosynthesised and accumulated in photosynthetic tissues of all higher plants. Unlike algae and bacteria, the carotenoid composition of higher plants is remarkably uniform. The main carotenoids in photosynthetic tissues of plants are lutein (45%), β-carotene (25-30%), violaxanthin (10-15%) and neoxanthin (10-15%). Under normal conditions zeaxanthin and antheraxanthin are found only in trace amounts. High light conditions cause a conversion of violaxanthin to zeaxanthin. The majority of the carotenoids (and chlorophylls) are located in functional pigment-binding proteins that are embedded in the thylakoid membrane [21].

The RC complex binds β-carotene and chlorophyll *a*, while the light-harvesting proteins bind chlorophyll *a* and *b*, as well as the three xanthophylls lutein, violaxanthin and neoxanthin. Under excess illumination, however, two additional xanthophylls (antheraxanthin and zeaxanthin) are found associated with the light harvesting proteins. This is due to the xanthophyll cycle mediated conversion of violaxanthin to zeaxanthin (via antheraxanthin) [99].

β-carotene, lutein, neoxanthin and the carotenoids of the xanthophyll cycle (zeaxanthin, antheraxanthin and violaxanthin) are ubiquitously present in the thylakoid membranes of higher plants, emphasising their importance in growth and development of photosynthetic organisms. In both PSI and PSII, the carotenoids are usually bound to specific chlorophyll/carotenoid-binding protein complexes. The distribution of the different carotenoids in PSI and PSII is highly uneven. PSI contains predominantly β-carotene, and PSII lutein. Both bound and unbound pools of the xanthophyll cycle pigments are found in the thylakoid membrane. Zeaxanthin would have to be bound to the antenna proteins of PSII to perform its function in heat dissipation, whereas xanthophylls that are not associated with proteins would function as membrane stabilisers and antioxidants [29].

Violaxanthin is thought to be the only photosynthetic pigment in the thylakoid that is not directly associated with proteins. Only a fraction (50-80%) of the total violaxanthin is available for conversion into zeaxanthin. This suggests a heterogeneous organisation of violaxanthin and some plants, especially those adapted to high PFD, are able to convert nearly 100% of their violaxanthin into zeaxanthin. It was shown that high levels of de-epoxidation could also be obtained if the thylakoids were unstacked in the presence of $Mg^{2+}$, suggesting that the availability of violaxanthin depends on the organisation of the complexes [100].

Although the carotenoid composition of plants is well conserved, the carotenoid composition of each of the LHC proteins is surprisingly unique. This means that the same xanthophyll is bound to different sites in LHC proteins, and the xanthophyll localisation between LHC proteins is not conserved [100].

### 2.3.5 The role of carotenoids in photoprotection

As discussed in the preceding section, photoprotection via thermal dissipation of excess energy within the chlorophyll-pigment complex is facilitated by specific carotenoids of the xanthophyll cycle. These xanthophylls are located in the thylakoid membranes of all higher plants and rapidly respond to changes in PFD [101]. Since the carotenoids are distributed in the thylakoid pigment-protein complexes in very close proximity to the chlorophylls (and therefore the potential site of $^1O_2$ formation), they are considered the most important quenchers of excited states in the thylakoid membrane. $^3$P680 or $^1O_2$ transfers its excitation energy to an adjacent carotenoid molecule to form a carotenoid triplet that decays harmlessly to the stable ground state by heat dissipation. β-carotene molecules are found bound to the D1 and D2 proteins of the PSII RC, but they are not directly involved in the quenching of $^3$P680, and are instead rapidly hydroxylated to zeaxanthin during the degradation of the D1 protein under high light conditions. If β-carotene could accept electrons from $^3$P680 (i.e. direct quenching), this would imply that β-carotene would also compete with the primary electron acceptor ($Q_A$) for electron transfer during normal photochemical quenching [12].

In addition to the total amount of zeaxanthin formed, it is also important to consider the ratio of zeaxanthin to chlorophyll *a* for each complex, especially if a direct, singlet-singlet interaction between these molecules leads to fluorescence quenching, as opposed to an indirect action through carotenoid-mediated alterations to LHC organisation.

In addition to their quenching function in the antenna, the xanthophyll cycle pigments play a crucial role in membrane fluidity and the protection of the thylakoid membrane against lipid peroxidation [25;102;103]. The *Arabidopsis npq1* mutant is defective in VDE activity, and is unable to form zeaxanthin in response to high light. Generation of $^1O_2$ in these leaves by infiltration with the photosensitising chemical eosin causes severe lipid peroxidation (relative to the wild-type leaves). This would suggest that photoprotection by zeaxanthin is not restricted to the LHCs.

In addition, zeaxanthin may be an important antioxidant in the lipid bilayer of the thylakoid membrane, where it could inactivate reactive oxygen species and/or terminate lipid peroxidation chain reactions. This was demonstrated *in vitro* by treating artificial membranes (made from egg yolk lecithin) with a peroxyl radical

generator. Both zeaxanthin and lutein were able to slow down the lipid peroxidation reaction [30;32].

### 2.3.5.1 The xanthophyll cycle enzymes

The xanthophyll cycle is the reversible light-dependent de-epoxidation of violaxanthin to zeaxanthin (via antheraxanthin), that is functional under saturating light conditions [20]. When a high pH gradient is formed across the thylakoid membrane, VDE is activated and removes the epoxide groups from the available violaxanthin, forming zeaxanthin. Violaxanthin can be regenerated by a light-independent epoxidation, catalysed by ZEP. The xanthophyll cycle has been shown to function in the LHCs of both PSI and PSII. When light conditions are not saturating, violaxanthin functions as an antenna pigment by absorbing and transferring light energy to chlorophyll (Fig. 2.18).

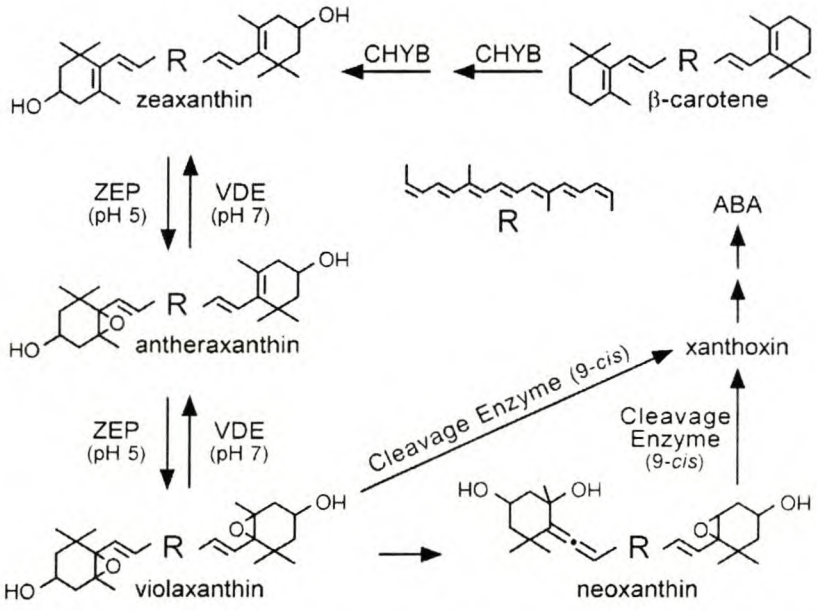


Figure 2.18. The reversible pH-dependent xanthophyll cycle and the enzymes involved. The subsequent enzymatic reactions to abscisic acid (ABA) are also shown. CHYB, β-carotene hydroxylase; ZEP, zeaxanthin epoxidase; VDE, violaxanthin de-epoxidase [104].

VDE is a water-soluble enzyme that is present at very low concentrations (estimated at approximately one enzyme per 20-100 RCs) in the thylakoid lumen under neutral pH. Light-induced acidification of the lumen, however, causes VDE to bind to the lumenal surface of the thylakoid, and rapidly convert violaxanthin to zeaxanthin. Apart from the high transmembrane ΔpH, the de-epoxidation reaction also requires ascorbate. In addition to activating VDE, ascorbate also serves as a direct antioxidant of reactive oxygen species ($^1O_2$ and $H_2O_2$). Due to its role in both

the activation of the xanthophyll cycle and antioxidation, it has been suggested that ascorbate availability may serve as a regulator for both processes [42]. ZEP, on the other hand, is a multi-component enzymatic complex that is constitutively active on the stromal side of the thylakoid membrane at a pH of 7.0-7.5 (i.e. neutral). The transmembrane organisation of the VDE and ZEP enzymes suggests that the xanthophyll cycle pigments are free to move within the lipid phase of the thylakoid membrane [29].

The xanthophyll cycle pigments are localised in the LHCs of both PSs. Their location within the antennae allows for the effective dissipation of excess light energy, thereby preventing the over-reduction of the electron transport chain, and minimising the formation of $^1O_2$. Changes in the epoxidation/de-epoxidation state of the xanthophyll cycle, availability of ascorbate, as well as the magnitude of the transmembrane $\Delta$pH formed, allows plants to control thermal energy dissipation such that only excess absorbed light energy is dissipated [105]. Relative to the major LHC of PSII, the xanthophyll pigments have been found to be enriched in the minor LHC components (CP29, CP26 and CP24). Based on these observations it has been suggested that the minor CPs play an important role in photoprotection [105]. The conversion of violaxanthin to antheraxanthin and zeaxanthin has been reported in all complexes, with only the degree of epoxidation/de-epoxidation varying [106].

Zeaxanthin facilitates energy dissipation by either directly, or indirectly, quenching excited chlorophyll. Direct quenching is possible due to the physical properties of zeaxanthin that makes it thermodynamically viable to accept excitation energy directly from chlorophyll. Carotenoids possess a low-lying excited state, of which the energy level is inversely proportional to the number of conjugated double bonds within the molecules (nine for violaxanthin, ten for antheraxanthin, and eleven for zeaxanthin). After the transfer of absorbed excitation energy from chlorophyll, the carotenoid molecule undergoes a rapid radiationless de-excitation and so doing harmlessly releases the absorbed energy as heat (thermal dissipation). In this model the xanthophyll cycle facilitates the formation of the quencher, zeaxanthin. The function of the transmembrane $\Delta$pH is then to cause the conformational change in LHCII needed to bring chlorophyll and zeaxanthin close enough together for energy transfer [99;102].

Alternatively, zeaxanthin can indirectly facilitate quenching by causing a $\Delta$pH-dependent conformational change in some of the LHC proteins that allows the direct

conversion of excited state chlorophyll to the ground state, with the concomitant harmless release of heat. The removal of the epoxide group from violaxanthin not only affects the excited state, but also the polarity of the molecule; making zeaxanthin much more hydrophobic than violaxanthin. In general, the xanthophylls resemble detergents and this amphipathic property is strongest for violaxanthin (and weakened by conversion to zeaxanthin). In this model a ΔpH regulates the xanthophyll cycle, which in turn alters the amphipathic properties of the xanthophylls bound to LHCII. Both the altered thylakoid membrane structure and protonation leads to the formation of a quenching complex [30;107].

A leaf responding to high-light stress shows strong correlation between zeaxanthin (and antheraxanthin) formation by the xanthophyll cycle, and the level of excess excitation energy dissipated (as measured by NPQ). In addition, the extent of NPQ has also been correlated to the antenna size of PSII [108].

## 2.4. MECHANISMS TO ANALYSE THE PHOTOPROTECTIVE ABILITY OF CAROTENOIDS

### 2.4.1 Non-photochemical quenching (NPQ) as it occurs in plants

Quenching of fluorescence can occur by photochemical- and non-photochemical mechanisms. Under non-saturating light conditions the photosynthetic apparatus is more than capable of quenching the absorbed energy via electron transport mechanisms (photochemistry). Under saturating light conditions, however, the dissipation of excess absorbed light energy is known to play a key role in the regulation of both light harvesting and electron transport, and appears to be critical for the prevention of photo-oxidative damage to the photosynthetic apparatus. An increase in the proton gradient (ΔpH) across the thylakoid membrane in saturating light triggers the dissipation of excess energy as heat in the LHCs of PSII. This process can be measured and is referred to as non-photochemical quenching (NPQ) of chlorophyll fluorescence.

Three quenching processes have been identified that contribute to NPQ: (i) high energy state quenching (i.e. *q*E); (ii) state transition (*q*T); and (iii) photoinhibition (*q*I). Although the pH-dependent energy dissipation (*q*E) is the major component of NPQ under most conditions, decreases in PSII fluorescence due to both *q*T and *q*I may also contribute to what is measured as NPQ. These different quenching processes have different relaxation times, ranging from a few minutes to several

hours, and the kinetics of the relaxation of these processes can be used to distinguish them from each other [26].

Energy-dependent quenching (*q*E) is considered the major quenching process, and is essential in protecting the leaf (or any photosynthetically active tissue) from light-induced damage. It involves the formation of zeaxanthin (via the xanthophyll cycle), is rapidly (within minutes) reversible and requires acidification of the thylakoid lumen. The *q*E mechanism can be regarded as a feed-back regulated "safety valve" for photosynthesis since it is controlled primarily by the thylakoid ΔpH that is generated via photosynthetic electron transport (Fig. 2.12) [43].

State transitions (*q*T) occur after a shift to high light and are caused by $PQH_2$ occupying the quinone-binding site of cytochrome $b_6/f$ [109]. It involves the reversible phosphorylation of light-harvesting proteins and is thought to play a role in the balancing of the distribution of the absorbed light energy between PSI and PSII. Although the relaxation kinetics of *q*E and *q*T are similar, the contribution of *q*T to NPQ is considered negligible; it only seems to make a significant contribution in low light conditions [110].

Under more prolonged and severe light stress, *q*E is replaced by a sustained, slowly reversible component of NPQ, called *q*I. The latter is the collective term for the photoprotective processes with long relaxation times (hours) and has been attributed to a range of processes including PSII damage and inactivation, as well as zeaxanthin quenching in the antenna complexes. Although both *q*E and *q*I are induced under conditions of light stress, *q*E is dependent on the thylakoid ΔpH formed, whereas *q*I remains after dissipation of ΔpH, and it relaxes only slowly [20;110]. An example of *q*I is seen in overwintering plants that acclimatise to the cold by increasing their xanthophyll pool size, increasing the retention of both zeaxanthin and antheraxanthin (possibly by limiting the epoxidation of zeaxanthin), and the formation of a chlorophyll-quenching complex that can effectively dissipate excess excitation energy [111].

Xanthophyll pigments in the LHCs play an indispensable role in NPQ. The extent of NPQ (specifically *q*E) in plants has been correlated with the levels of zeaxanthin (and antheraxanthin) that are formed from violaxanthin, via the xanthophyll cycle. It has been suggested that the light-induced accumulation of protons in the lumen (ΔpH) not only stimulates violaxanthin de-epoxidase (VDE) activity, but also the protonation of one or more of the proteins in the LHC that are

associated with PSII. Protonation of the antenna complexes of PSII could have two possible effects. Firstly, it could cause a transient interaction between zeaxanthin and $P680^*$. This interaction would facilitate the transfer of the excitation energy from P680* to zeaxanthin, and the excess energy would subsequently be dissipated from zeaxanthin as heat (i.e. direct quenching). Secondly, it could result in a conformational change in the antenna complexes leading to increased heat loss from $P680^*$ (i.e. indirect quenching). It is not known which of these two routes function in PSII, yet the possibility exists that both of these mechanisms are functional, and only vary relative to the environmental conditions and/or the plant species.

Muller and co-workers [30] proposed a working model that integrates most of the phenomena observed during the induction and functioning of the *q*E component of NPQ (Fig. 2.19). The model proposes that under non-saturating light conditions, *q*E is not induced and the photosynthetic apparatus can effectively quench the absorbed energy (via electron transport). Under saturating light conditions, however, antenna proteins (including PsbS/CP22) are protonated. The ΔpH causes VDE to be activated, but the conversion of violaxanthin to zeaxanthin is much slower than the protonation reaction. Zeaxanthin binding to the protonated proteins forms a "quenching complex". The quenching complex causes a conformational shift in the PSII antenna, possibly due to the interaction between the different components (i.e. PsbS, zeaxanthin and protons). The formation of the quenching complex could further involve structural changes in PSII, or changes in the interactions of several of the complexes with each other. Once the light intensity decreases, the thylakoid ΔpH will concomitantly decrease, and the antenna proteins will be rapidly deprotonated, causing the quenching complex to uncouple. The epoxidation of zeaxanthin to violaxanthin will also occur, but at a much slower rate (Fig. 2.19).

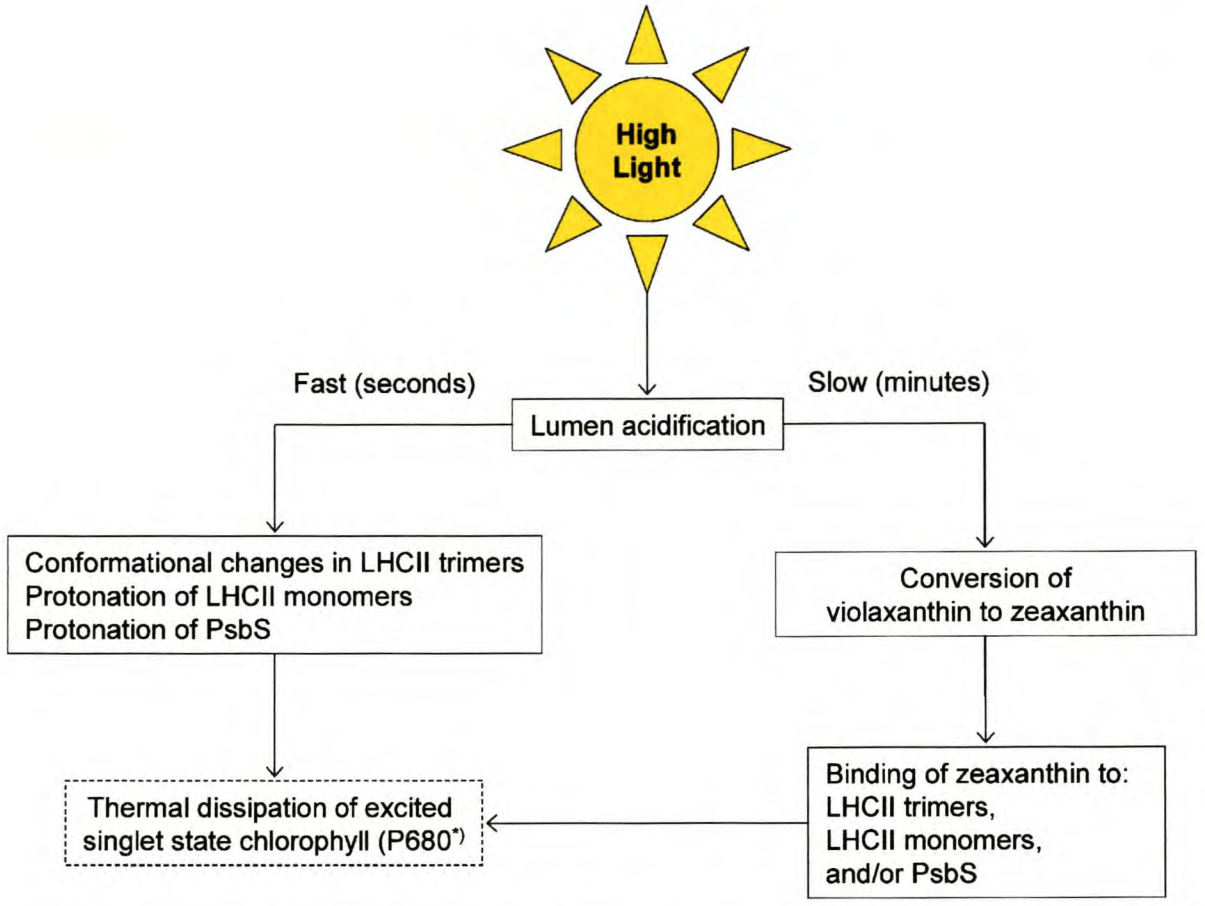


Figure 2.19. A model of thermal dissipation in plants. High light generates proton accumulation in the lumen, causing acidification. This in turn induces alterations in the antenna of PSII that promote thermal dissipation. These changes include conformational changes in LHCII trimers, protonation of the LHCII monomers and/or minor antenna, and/or protonation of PsbS. Protonation will result in conformational changes. The ΔpH also stimulates the de-epoxidation of violaxanthin to zeaxanthin. Zeaxanthin either acts "directly" (by accepting excitation energy from $P680^*$ and dissipating it as heat) or "indirectly" (by altering antenna conformation) to increase the rate of thermal dissipation [30;112].

## 2.4.2 Using chlorophyll fluorescence as a measure of photosynthesis

### 2.4.2.1 Background

As is the case with any energy transduction system, the conversion of light energy to chemical energy during photosynthesis is not a perfect process. In the photosynthetic apparatus, light is absorbed by the antenna pigments (chlorophyll and/or carotenoids), and this absorbed excitation energy is transferred to P700 or P680 in the RCs of PSI and PSII, respectively. Chlorophyll fluorescence analysis is based on the observation that this absorbed light energy can undergo one of three fates: it can be used to drive the reactions that initiate the photosynthetic energy conversions for photochemistry, it can be dissipated as heat (radiationless deactivation), or it can be re-emitted as light [110]. In low light and under optimal

conditions, approximately 90% of absorbed light energy will be utilised by photosynthesis and primary photochemistry is considered to be highly efficient [113]. However, not all electrons that are raised to a higher energy level are successfully passed on to the electron acceptors. These electrons can return to their "parent" chlorophyll molecules (without the production of ATP and/or $NADPH_2$) and this energy is consequently lost as either heat or light during the return to the ground state. If light is produced, it is emitted at a longer wavelength than the light that was initially absorbed by the chlorophyll molecule, causing the chlorophyll molecule to fluoresce (hence chlorophyll fluorescence). This fluorescence can be quantified by exposing a leaf to light of a defined wavelength, and measuring the amount of light re-emitted at a longer wavelength. It has been shown that most of the emitted fluorescence measured at room temperature, originates from PSII [114]. The three mentioned processes occur in competition, such that an increase in the efficiency of one component will result in a concomitant decrease in the yield of the other two components. Chlorophyll fluorescence will occur maximally when both photochemistry and heat dissipation are minimal. If all the RCs of PSII are "closed" (i.e. the electron acceptor, QA, is fully reduced), the maximum fluorescence yield of PSII can be measured. Under these conditions chlorophyll fluorescence accounts for only a small fraction (approximately 1-3%) of the total light absorbed by the light harvesting complex. When all the RCs are "open" (or active) the theoretical minimum fluorescence yield is usually much lower (approximately 0.6%) due to competition with photochemistry for electrons. Since the fluorescence yield is inversely proportional to the number of open RCs, it represents a useful tool for the *in vivo* assaying of the various physiological parameters that affect the photosynthetic processes of PSII [115].

If a dark-adapted leaf is transferred into light, an increase in the yield of chlorophyll fluorescence is observed. This increase, also called the Kautsky effect, is caused by the reduction of electron acceptors in PSII [113]. This can be explained if one considers that during the dark-adaptation, several of the enzymes involved in the Calvin cycle become deactivated and must be re-activated by light before they can operate again. $CO_2$ fixation can only occur at optimal rates once the metabolites involved in the reactions have reached certain basal levels. This period of slow $CO_2$ fixation is termed the photosynthetic induction period or the slow induction phase. During the photosynthetic induction period the PSII electron acceptors (mostly $Q_A$) continue to accept electrons from excited $P680^*$, but have no way of dissipating the

energy from these electrons. This is because the enzymes involved in the dark (light-independent) reactions of photosynthesis are not yet activated. As a result, the number of acceptors that can accept electrons are rapidly diminished. These RCs are consequently regarded as "closed", and will lead to an overall decrease in the efficiency of photochemistry, and a concomitant increase in the yield of fluorescence [110]. If the actinic light is strong enough, all the RCs become closed, and the maximum level of fluorescence is attained with no photochemistry taking place [113-116].

At room temperature, fluorescence is emitted only from the chlorophyll surrounding PSII. Chlorophyll of PSI either does not emit fluorescence at all, or emits a weak constant fluorescence which does not change in response to the PSI acceptor side reduction. These differences between the two PSs are probably caused by differences in the acceptor side carriers. Due to the presence of a sequence of carriers at the PSI acceptor side, the primary acceptor can probably never become reduced, except at very low temperatures [117].

Chlorophyll fluorescence enables the non-invasive study of photosynthesis and the different mechanisms dissipating excitation energy in the LHCs and RCs. Information is obtained on both the extent to which PSII is using the energy absorbed by chlorophyll, as well as the extent to which it (PSII) is being damaged by the excess light. Under many conditions, the electron flow through PSII is indicative of the net rate of photosynthesis and, therefore, gives a good estimation of the overall photosynthetic performance. PSII is considered to be the most susceptible component of the photosynthetic apparatus to photo-oxidation, and this damage to PSII is regarded as the first sign of stress in a plant. Data can be obtained both easily and rapidly using chlorophyll fluorescence, but it is considered even more useful when used in conjunction with other plant analyses (i.e. gas exchange or $CO_2$ assimilation) [110].

#### 2.4.2.2 Parameters and measurements

A fluorometer typically consists of four radiation sources. These different light sources produce quantitatively and qualitatively different radiation incidence on a photosynthetic object (typically a leaf) causing chlorophyll fluorescence namely: (i) modulated measuring radiation, (ii) actinic radiation, (iii) saturating pulses, and (iv) far-red radiation [118]. Different coefficients have been proposed to quantify the photochemical and non-photochemical quenching events. These different

parameters are probably best explained using an experimental fluorescence trace (Fig. 2.20).

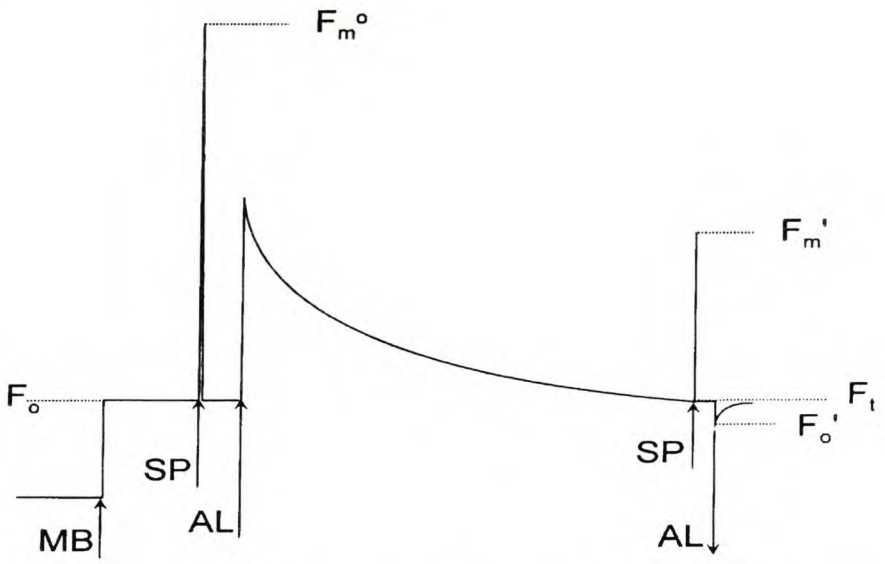


Figure 2.20. A typical chlorophyll fluorescence trace. A modulated measuring light (MB) is used in order to measure the minimal fluorescence ($F_o$) of a dark-adapted leaf. A pulse of saturating light (SP) enables the measurement of the maximum fluorescence level ($F_m^0$). An actinic light (AL) is applied, and after a period of time, another saturating light flash (SP) allows the maximum fluorescence in the light ($F_m'$) to be measured. The level of fluorescence immediately before the saturating flash is termed ($F_t$). Turning off the AL, in the presence of a far-red light, allows the minimal fluorescence 'in the light' to be estimated ($F_0'$) [110].

It is important that the experimental leaf be dark-adapted prior to the initial measurements. This will ensure the complete relaxation of any thylakoid pH gradient that may have formed and also ensure the epoxidation of zeaxanthin and antheraxanthin (to violaxanthin). The fluorescence measurement is initiated by switching on the modulated light, giving a measure of the minimal level of fluorescence ($F_0$). Pulse-modulated chlorophyll fluorometers use a very weak light emitting diode (LED) source (approximately 6 $nmol.m^{-2}.s^{-1}$ at 660 nm peak wavelength) that is pulsed between 1 and 100 times per second (i.e. modulated at a frequency of between 1 and 100 Hz). The duration of each flash is so short that in a dark-adapted leaf this light induces such a low rate of electron transfer to PSII RCs that the re-oxidation processes are fast enough to keep all the RCs open, and no variable fluorescence is generated or measured. This weak initial rise in fluorescence is assumed to be $F_0$, and, therefore, represents the amount of

background fluorescence. At this point photochemical quenching (*q*P) is considered to be maximal and NPQ minimal (i.e. *q*P = 1, and NPQ = 0).

Secondly, a saturating pulse of light is applied, allowing the measurement of $F_m$ in the dark-adapted state ($F_m$, or $F^0_m$). The saturating light (>5000 $\mu mol.m^{-2}.s^{-1}$, $400 < \lambda > 700$ nm, applied for 0.5- 2.0 seconds) causes the fluorescence to be raised from $F_0$ to $F_m$ due to the complete reduction of all available $Q_A$ (i.e. all RC are closed), and so doing *q*P is completely eliminated (i.e. *q*P=0). It is assumed that the saturating pulse does not affect NPQ (i.e. NPQ = 0), and therefore fluorescence is at its maximum [119].

An actinic light is then applied and, at appropriate intervals, further saturating flashes can be applied. From each of these a value for the fluorescence maximum in the light ($F'_m$), can be measured. The steady-state value of fluorescence immediately prior to the flash is termed F' (alternatively $F_s$ or $F_t$). After a saturating flash, removal of the actinic light, while simultaneously giving a far-red light (approximately 6 $\mu mol.m^{-2}.s^{-1}$, with a wavelength of > 700 nm), allows the measurement of $F'_0$ (i.e. an estimation of $F_0$ at the time of the measurement). This far-red light ensures that all the PSII RC open rapidly after illumination (Fig. 2.20) [110;119].

Important information about the photochemical and non-photochemical, protective, regulative, destructive, and other processes acting in PSII (and the photosynthetic apparatus as a whole) can be gained. The maximum (or intrinsic) efficiency of PSII can be calculated using the $F_0$ and $F_m$ values, and the following formula:

$$F_v/F_m = (F_m - F_0)/F_m$$

$F_v$ is not a measured parameter, but merely a representation of the maximum variable fluorescence. $F_v/F_m$ represents the efficiency of energy capture (or photon yield) by open RCs of PSII. Bjorkman and Demmig [120] showed that irrespective of the plant species or ecotypes being studied, the $F_v/F_m$ ratio stays remarkably constant in healthy, unstressed leaves (0.832 ± 0.004). A lower $F_v/F_m$ value reflects a change in the efficiency of non-photochemical quenching (NPQ), due to damage to PSII, a phenomenon that is often observed in stressed plants. $F'_v/F'_m$ (where $F'_v = F'_m - F'_0$) is another useful calculation and reflects the quantum yield of open PSII, as opposed to the maximum yield obtained from $F_v/F_m$ in dark adapted plants.

Photochemical quenching parameters typically relate to the relative value of $F'_m$ and $F_t$. The efficiency of PSII photochemistry ($\phi$PSII), gives a measure of the proportion of absorbed light that is actually used in photochemistry, and is calculated as:

$$\phi PSII = (F'_m - F_t)/F'_m$$

$\phi$PSII gives a measure of the linear photosynthetic electron transport, and, therefore, an indication of overall photosynthesis. In unstressed leaves, a linear relationship exists between $\phi$PSII and the efficiency of carbon fixation (measured independently using gas exchange).

Another widely used fluorescence parameter is photochemical quenching (*q*P), which is calculated as:

$$qP = (F'_m - F_s)/(F'_m - F'_0)$$

Where $\phi$PSII reflects the proportion of absorbed energy being used in photochemistry, *q*P gives an indication of the proportion of PSII RC that are open and, therefore gives an indication of the redox state of $Q_A/Q_A^-$. A change in *q*P is due to closure of the RCs, resulting from a saturation of photosynthesis by light. Any reduction in *q*P will be due to alternative quenching mechanisms. An alternative expression of this is 1 - *q*P, which reflects the proportion of closed RCs, i.e. the fraction of $Q_A$ in the reduced state.

Another useful parameter is the effective photosynthetic electron transport rate (ETR) that takes into account the actual PFD, $\phi$PSII, and two semi-empirical factors: $F_1$ (=0.5) and $F_2$ (typically 0.83-0.86).

$$ETR = PFD \times \phi PSII \times F_1 \times F_2$$

$$= PFD \times \phi PSII \times 0.5 \times 0.84$$

PFD is the absorbed light (measured and expressed in $\mu mol.m^{-2}.s^{-1}$). The $F_1$ factor reflects that two photons must be absorbed by PSII and PSI for every electron transported, and the $F_2$ factor represents an absorption coefficient [118]. The calculated ETR therefore gives an indication of the linear electron transport rate and, therefore, the overall photosynthetic capacity *in vivo*.

Quenching of fluorescence can occur by photochemical (*q*P) and non-photochemical mechanisms. The non-photochemical quenching (NPQ) is of importance since it gives an indication of photoprotection (or photodamage). NPQ is

a co-operative phenomenon consisting of a number of processes occurring in the thylakoid membrane, but the major proportion arises from an increase in heat dissipation [4]. NPQ can be quantified by measuring the ratio of change in $F_m$, relative to the dark-adapted state ($F^0_m$), and is calculated as:

$$NPQ = (F^0_m - F'_m)/F'_m$$

$$= (F^0_m /F'_m) - 1$$

NPQ has been shown to be linearly related to heat dissipation [114]. At saturating light intensities, values of 0.5 - 3.5 (on a scale from 0 to infinity) are typically obtained, but this will depend on the physiological condition of the plant, as well as the species being studied. Any change in the obtained NPQ value reflects the change in the efficiency of heat dissipation, relative to the dark-adapted state. An increase in NPQ will therefore reflect the plants intrinsic quenching processes that are actively protecting the leaf from light-induced damage. An alternative equation to calculate NPQ is:

$$NPQ = (F^0_m - F_0)/(F'_m - F_0)$$

As discussed in section 2.2.5., the different quenching processes (i.e. *q*E, *q*I and *q*T) have different relaxation times, that range from a few minutes to several hours, and the kinetics of the relaxation of these processes are used to distinguish them from each other (Fig. 2.21) [26]. Relaxation experiments can be performed in order to distinguish the fast- from the slow relaxing quenching processes. During these experiments quenching is allowed to relax and a saturating light pulse is applied at regular intervals in order to calculate the $F_m$ value. The interval between the $F_m$ values is chosen based on the time it takes the effect of the initial saturating flash to relax before the next flash is applied. Under normal conditions five minutes is sufficient time for this recovery, and the relaxation is usually recorded for approximately one hour. A graph of the log($F_m$) values against time is used to calculate the $F_m$ value that would have been attained if only slow quenching was active in the light (i.e. $F_m$ of the relaxing/relaxation graph, $F^r_m$,). Using this value, the slow ($NPQ_S$) and rapid ($NPQ_F$) relaxing quenching can be calculated as:

$$NPQ_S = (F^0_m - F^r_m)/F^r_m$$

$$NPQ_F = (F^0_m - F'_m)/ (F^0_m - F^r_m)$$

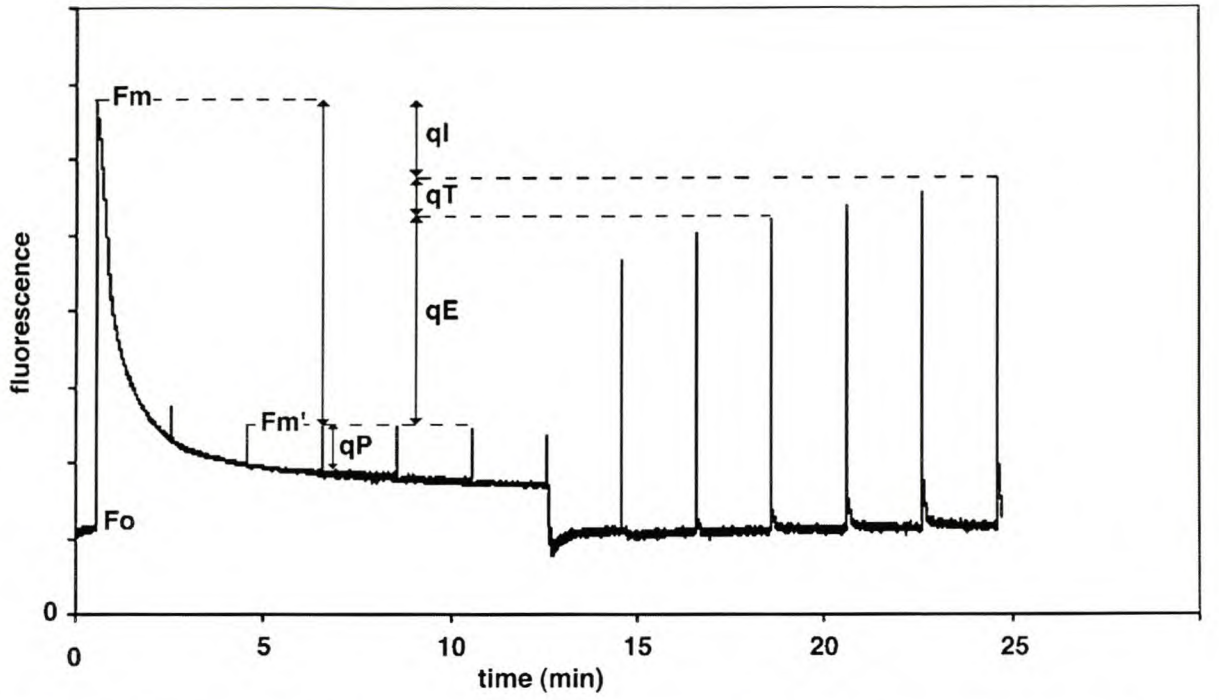


Figure 2.21. Chlorophyll fluorescence measurements from a dark-adapted *Arabidopsis* leaf. A weak modulating light is used to determine the minimal fluorescence ($F_o$). A pulse of saturating light will saturate all the PSII reaction centers, and the maximum fluorescence can be measured ($F_m$). Continuous illumination with an actinic light will result in both *q*P and NPQ lowering the fluorescence yield. NPQ (i.e. *q*E + *q*T + *q*I) can be seen as the difference between $F_m$ and the measured maximal fluorescence after a saturating light pulse during illumination ($F_m$'). After switching off the actinic light, the rate of recovery of $F_m$' reflects the relaxation of the *q*E component of NPQ [30].

### 2.4.3. Chlorophyll fluorescence characteristics of *Arabidopsis* NPQ mutants

Genetic analyses of *Arabidopsis* mutants defective in NPQ have helped in elucidating the *in vivo* roles of specific xanthophylls in NPQ. Research on these *Arabidopsis* mutants has established a central role for the xanthophyll cycle in NPQ and therefore in photoprotection. The isolated mutations can be grouped into two general categories: those that affect NPQ without altering the pigment composition of unstressed leaves (e.g. *npq1*, *npq4*, *vtc2*), and those that affect both NPQ and the pigment composition in unstressed leaves (e.g. *lut1*, *lut2* and *aba1/npq2*) (Fig. 2.22) [26].

The *npq1* mutant is defective in VDE activity, and is unable to form zeaxanthin in response to high light (due to a dysfunctional xanthophyll cycle). The *npq1* mutants retain the rapid, initial pH-dependent component of NPQ, but lack the characteristic slower phase. The amplitude of NPQ is also lower than that of the wild-type plants (Fig. 2.23) [26;102;121]. After short illumination with intense white light, leaves of *npq1* mutants exhibit enhanced photoinhibition and lipid peroxidation.

Interestingly, the growth of *npq1* plants that are acclimatised to high light conditions, are not significantly different from that of the wild type plants. The xanthophyll cycle, although essential for most of the observed NPQ, is therefore not an absolute requirement for long-term photoprotection (*q*I) in plants. It is clear that other overlapping compensatory mechanisms are involved in this long-term adaptation [26]. The *npq1* phenotype can be induced in wild-type plants by using dithiothreitol (DTT), an inhibitor of VDE. Blocking zeaxanthin synthesis in leaves with DTT, resulted in the suppression of *q*E [30].

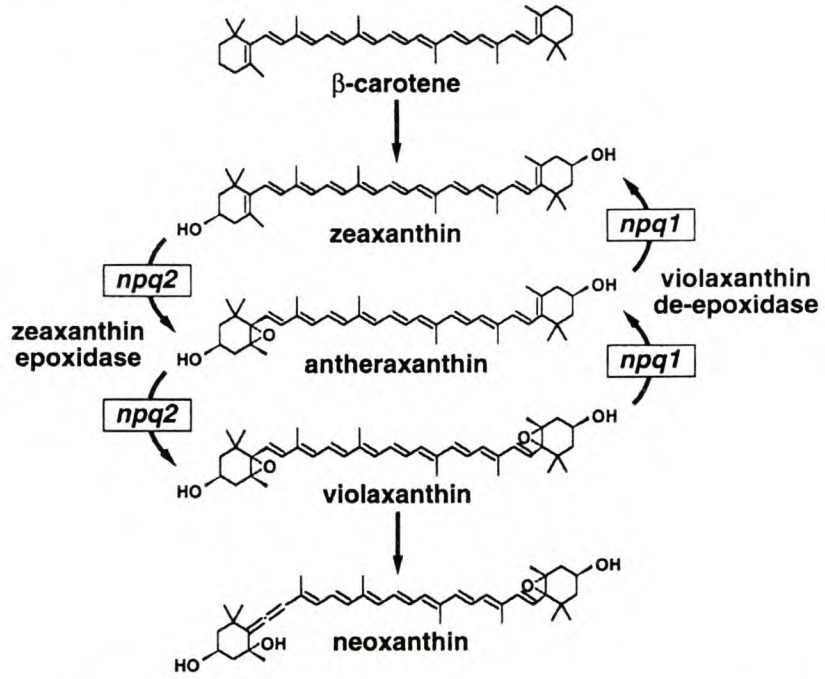


Figure 2.22. The reversible xanthophyll cycle in the β-carotene branch of the carotenoid biosynthetic pathway in plants. The *npq1* mutation in the zeaxanthin epoxidase gene, and the *npq2* mutations in the violaxanthin de-epoxidase gene are indicated [26].

The *npq4* mutation is unable to form the PSII protein, PsbS, and lacks the *q*E component of NPQ. Despite the absence of the PsbS protein, the *npq4* mutant is not impaired in light-harvesting or xanthophyll cycle activity, and the levels of the other LHC proteins are also normal [122;123]. After intense white light illumination, the *npq4* mutants were more resistant to lipid peroxidation than the *npq1* mutant. This has been attributed to the presence of zeaxanthin in the *npq4* mutant, and not due to the lack of NPQ [123].

The *lut1* mutation has a disruption in ε-ring hydroxylation, and as a result the intermediate, α-cryptoxanthin (zeinoxanthin) accumulates instead of lutein. This results in an 80-100% reduction in lutein when compared to the wild-type plants

[84;124;125]. The *lut2* mutant lacks ε-ring cyclisation activity (lycopene ε–cyclase, LCYE) and consequently contains no lutein (or any other α-carotene-derived xanthophylls). Both *lut1* and *lut2* have reduced lutein levels, elevated levels of the β-carotene derived xanthophylls, slower NPQ inductions, and decreased NPQ amplitudes (Fig. 2.25). This suggests that, in addition to antheraxanthin and zeaxanthin, lutein is also required for NPQ, but the specific role it plays, is as yet, unknown. The absence of lutein possibly alters the LHC antenna structure to such an extent that quenching is indirectly affected. It is also possible that lutein contributes to direct fluorescence quenching [84;124;125].

The *aba1* (*npq2*) mutant is defective in ZEP activity, and consequently has constitutively high levels of zeaxanthin. The *aba1* mutant induces NPQ much faster, but the amplitude of NPQ is lower than the wild-type (Fig. 2.25). A possible explanation is that energy dissipation will occur even in moderate (unsaturating) light conditions in the plant lines having constitutively high levels of zeaxanthin (i.e. *aba1*). After a decrease in light intensity, the slower NPQ reversibility would imply that NPQ remains active for a longer. This extended NPQ causes an overall decrease in the efficiency of photosynthesis in limiting light (Fig. 2.25) [26;124;125].

The *lut1, lut2* and *aba1 Arabidopsis* xanthophyll biosynthetic mutants that are all defective in NPQ, illustrates that an altered xanthophyll composition impairs the ability of plants to cope with light in excess of what is needed for photosynthesis. The mutations in the *lut1, lut2* and *aba1* genes have provided insights into the regulation of carotenoid biosynthesis, and has also shown the flexibility of plant LHCs with respect to their carotenoid binding specificities.

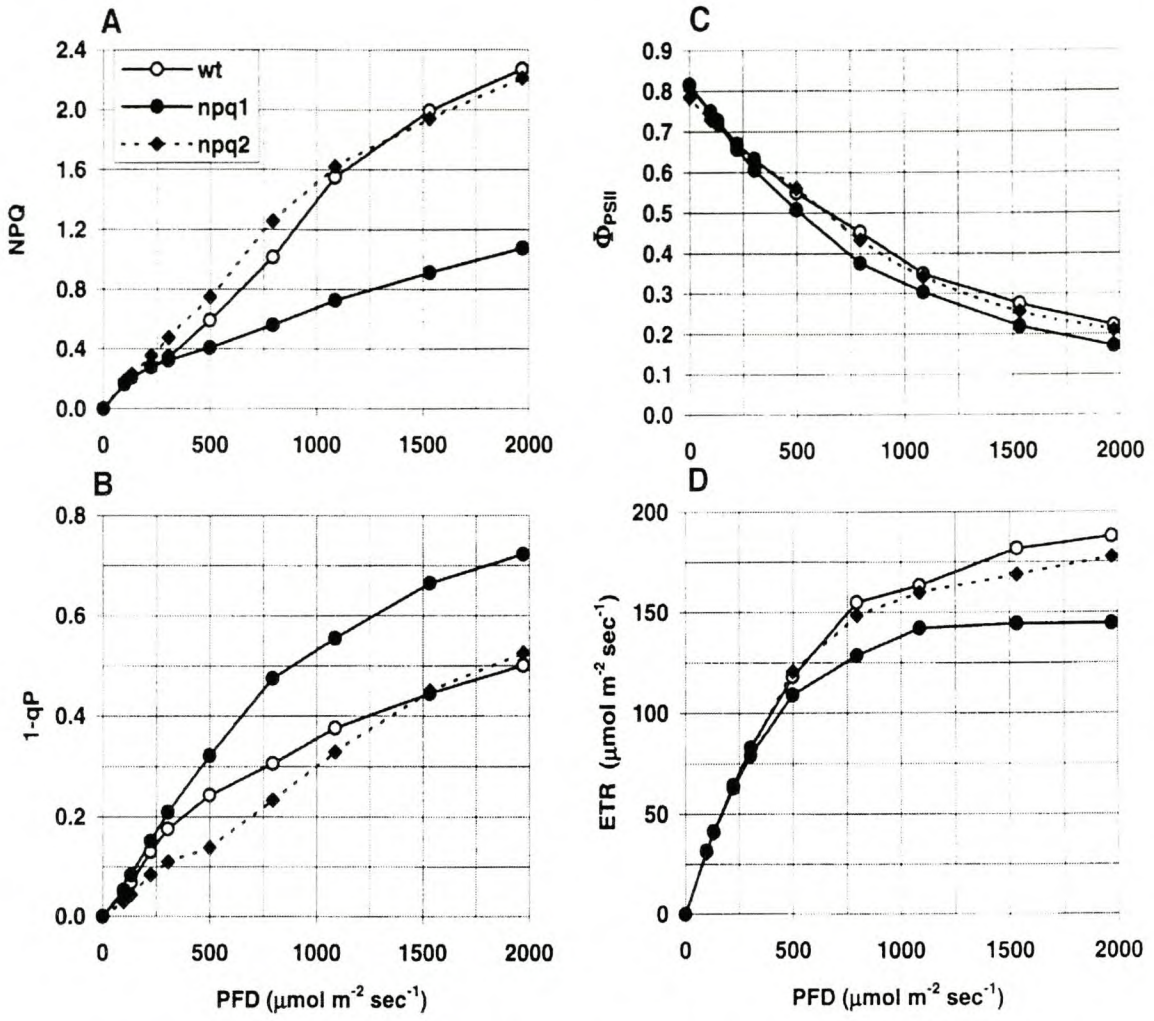


Figure 2.23. The effect of increasing PFD on the chlorophyll fluorescence parameters in leaves of wild-type (wt), *npq1*, and *npq2 Arabidopsis* mutant plant lines. (A) Total non-photochemical quenching (NPQ), where NPQ = $(F^0_m - F'_m)/F'_m$. (B) The fraction of $Q_A$ in the reduced state was estimated as 1-*q*P, where *q*P = $(F'_m - F_t)/(F'_m - F'_0)$. (C) The efficiency of PSII photochemistry ($\phi$PSII) was calculated as $(F_m - F_o)/F_m$ in the absence of actinic light, and as $(F_m' - F_t)/F_m'$ in the presence of actinic light. (D) Relative PSII electron transport rate (ETR). The rate of electron transport through PSII was calculated as $\phi$PSII × PFD × 0.5 × $F_2$ (where $F_2$ is the fraction of incident light absorbed by the leaf. In all leaves, $F_2$ was between 0.84 and 0.86) [26].

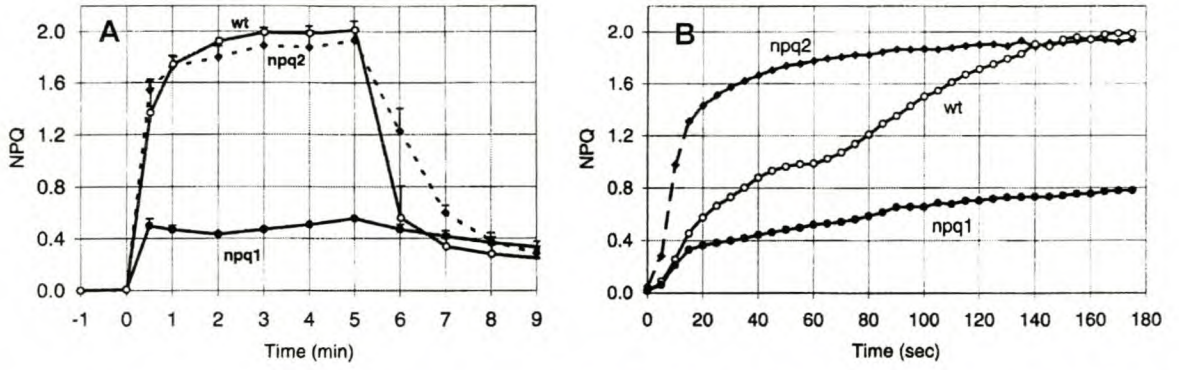


Figure 2.24. (A). Time course analysis of the induction and relaxation of NPQ in leaves of the wild-type (wt), *npq1*, and *npq2 Arabidopsis* plant lines. Actinic light (1900 µmol photons $m^{-2}$ $sec^{-1}$) was switched on at time zero, and then leaves were left in the dark after 5 min. (B). Rapid time course of NPQ induction in leaves of the wt, *npq1*, and *npq2* lines. Leaves were exposed to a PFD of 1083 µmol photons $m^{-2}$ $sec^{-1}$ at time zero, and gross NPQ was measured at 5-sec intervals [26].

The total amount of carotenoids in these mutant lines did not change significantly, but instead showed a degree of compensation by increasing the levels of other carotenoids. No net alteration in carbon flow to the pathway occurs in mutations that are disrupted in either of the two branches of xanthophyll biosynthesis [26]. Although specific xanthophylls (i.e. violaxanthin, antheraxanthin and zeaxanthin) are able to assume the structural role of lutein, the altered xanthophyll composition in these mutants has a drastic effect on their photosynthetic apparatus. It seems that these "substitute" xanthophylls can not provide the same degree of antennae stability, flexibility and function that lutein does in regulating and protecting the photosynthetic apparatus under fluctuating environmental conditions. These findings suggest that the observed differences in NPQ in these mutants are due to changes in the stability of the LHCII-complex, PSII antenna size and/or superstructure [124;125].

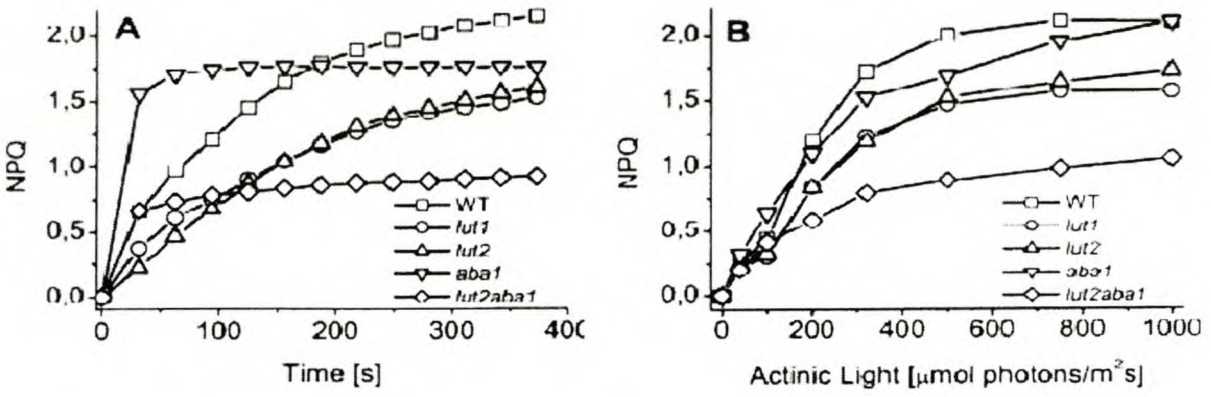


Figure 2.25. (A) Nonphotochemical fluorescence quenching (NPQ) in leaves of *Arabidopsis* wild-type (WT) and xanthophyll biosynthesis mutants (*lut1, lut2, aba1* and *lut2/aba1*), as a function of time of exposure to 500 µmol photons.$m^{-2}$.$s^{-1}$. (B) NPQ as a function of actinic light intensity [124].

An *Arabidopsis v*itamin C-deficient mutant, *vtc2*, has shown that ascorbate availability affects the rate of the VDE enzyme, xanthophyll cycle activity, and NPQ levels. The *vtc2* mutants contain only 25% of the wild-type ascorbate levels in their chloroplasts and as a result VDE activity is decreased, and the level of NPQ is lower than that of wild-type plants. The *vtc2* plants showed both a slower induction of NPQ, and a lower amplitude of NPQ than the wild-type plants under light intensities above that of the original growth conditions. Ascorbate feeding of detached *vtc2* leaves partially restored VDE activity and NPQ to wild-type levels. Even though the NPQ levels of *vtc2* plants are altered, the ETRs were unaffected (Fig. 2.26). It is thought that ascorbate influences the xanthophyll cycle directly by acting as a reductant for VDE [126;127]. Ascorbate is involved in the Mehler-peroxidase pathway (water-water cycle) and therefore also influences the ΔpH which will alter the activity of VDE (optimum at pH 5). The protein protonation that is required for *q*E could possibly also be affected by ascorbate availability [128].

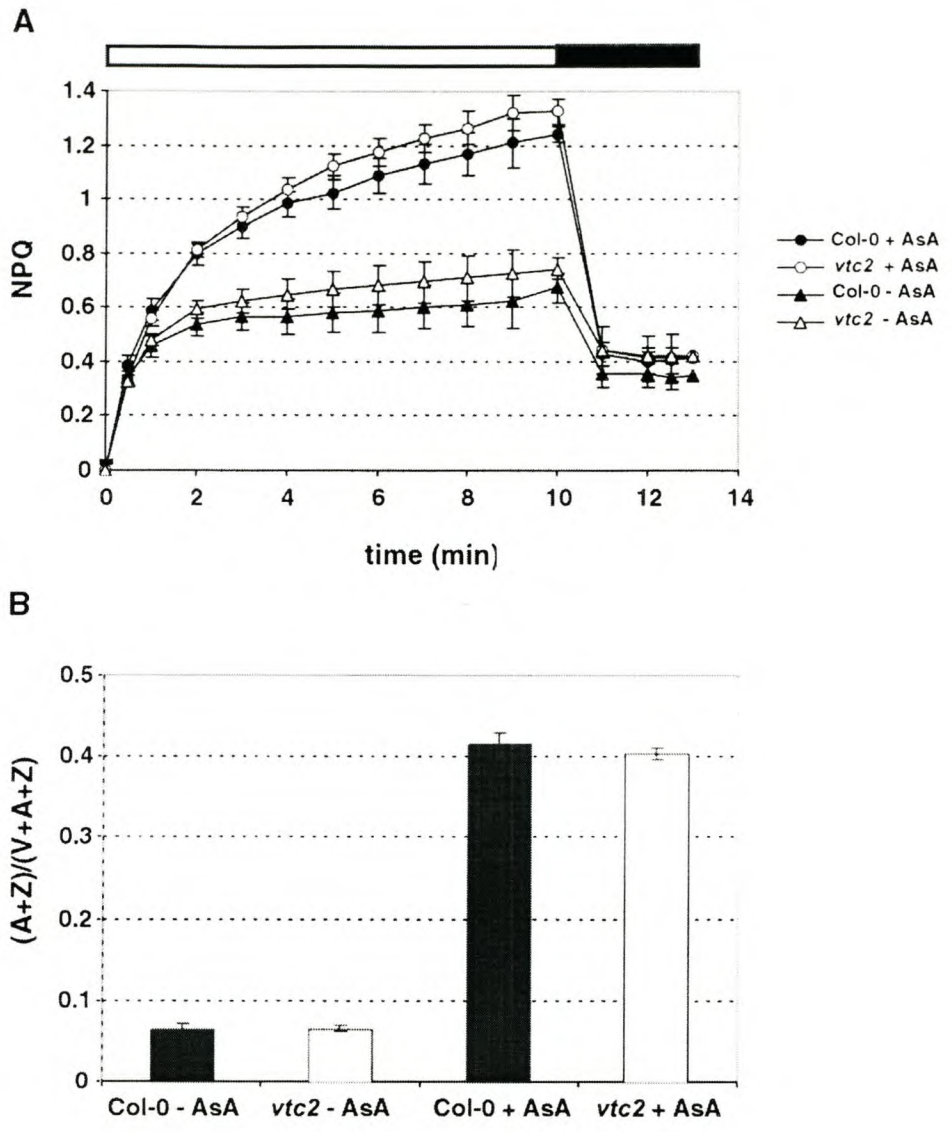


Figure 2. 26. Addition of ascorbate to isolated thylakoids from *Arabidopsis*. (A), NPQ measurements in isolated thylakoids of wild-type *Arabidopsis* (Co-0) and *vtc2* mutant plant lines with added buffer (-AsA) or with added ascorbate (+AsA) during 10 min of illumination and 3 min of darkness. (B), De-epoxidation state of the thylakoids after illumination [126].

## 2.5 CONCLUDING REMARKS

Genetic analyses of plants with mutations in their carotenoid biosynthetic genes, as well as transgenic studies utilising overexpressed carotenoid biosynthetic genes, have underlined the importance of carotenoids, and especially the xanthophylls, in photosynthesis and photoprotection. The specific role of individual carotenoids, as well as the interaction of different carotenoids in the photosynthetic apparatus, is a focus of numerous research groups.

The mutant studies in *Arabidopsis* have shown that under moderate light conditions a degree of flexibility exists by which various carotenoid combinations are capable of assembly of functional pigment:protein complexes in the photosynthetic apparatus. Under high light conditions, however, this flexibility is less obvious. This implies that when the excitation pressure is high (i.e. saturating light conditions), certain carotenoids are more effective at fulfilling their protective function. This difference could be due to the physico-chemical properties of the individual carotenoids, or more likely due to a more optimal association of the pigments in the photosynthetic complexes that results in a closer association with the photosynthetic membranes.

The contribution of specific carotenoids to the *in vivo* structure and function of the photosynthetic apparatus is necessary in order to fully understand the mechanism of photoprotection in plants. An understanding of photoprotection will pave the way for targeted manipulation of the carotenoid biosynthetic pathway in plants in order to upregulate the plants natural defence response and produce plants with enhanced stress tolerance.

## 2.6 LITERATURE CITED

[1] Arora,A., Sairam,R.K., & Srivastava,G.C. (2002) Oxidative stress and antioxidative system in plants. *Curr Sci*, **82,** 1227-1238.

[2] Aro,E.M., Virgin,I., & Andersson,B. (1993) Photoinhibition of Photosystem II. Inactivation, protein damage and turnover. *Biochim Biophys Acta*, **1143,** 113-134.

[3] Yordanov,I. & Velikova,V. (2000) Photoinhibition of Photosystem II. *Bulg J Plant Physiol*, **26,** 70-92.

[4] Niyogi,K.K. (1999) Photoprotection revisited: Genetic and molecular approaches. *Annu Rev Plant Physiol Plant Mol Biol*, **50,** 333-359.

[5] Vogelmann,T.C. (1998) Photosynthesis: physiological and ecological considerations. In *Plant physiology* (Taiz,L. & Zeiger,E., eds), pp. 227-249. Sinauer Associates, Inc., Sunderland (USA).

[6] Reisch P. (2003) Forest Ecology: Light responses. http://www.cnr.umn.edu/forestecology.

[7] Hall,D.O. & Rao,K.K. (2003) *Photosynthesis*, 6th edn. Cambridge University Press, Cambridge (UK).

[8] Lodish,H., Berk,A., Zipursky,L., Matsudaira,P., Baltimore,D., & Darnell,J. (2003) Cellular Energetics: Glycolysis, Aerobic Oxidation, and Photosynthesis. In *Molecular Cell Biology* (Tenney,S., ed), W. H. Freeman, New York.

[9] Barber,J. & Kuhlbrandt,W. (1999) Photosystem II. *Curr Opin Struct Biol*, **9,** 469-475.

[10] Blankenship,R.E. (1998) Photosynthesis: the light reactions. In *Plant physiology* (Taiz,L. & Zeiger,E., eds), pp. 155-193. Sinauer Associates, Inc., Sunderland (USA).

[11] Whitmarsh,J. & Govindjee (1999) The photosynthetic process. In *Concepts in photobiology: photosynthesis and photomorphogenesis* (Singhal,G.S., Renger,G., Sopory,S.K., Irrgang,K.D., & Govindjee, eds), pp. 11-52. Kluwer Academic Publishers, Dordrecht (The Netherlands).

[12] Barber,J. & Archer,M.D. (2001) P680, the primary electron donor of photosystem II. *J Photochem Photobiol A: Chem*, **142,** 97-106.

[13] Barber,J. (2002) P680: what is it and where is it? *Bioelectrochemistry*, **55,** 135-138.

[14] Barber,J., Nield,J., Morris,E.P., & Hankamer,B. (1999) Subunit positioning in photosystem II revisited. *Trends Biochem Sci*, **24,** 43-45.

[15] Barber,J. (2002) Photosystem II: a multisubunit membrane protein that oxidises water. *Curr Opin Struct Biol*, **12,** 523-530.

[16] Hankamer,B., Nield,J., Zheleva,D., Boekema,E.J., Jansson,S., & Barber,J. (1997) Isolation and biochemical characterisation of monomeric and dimeric photosystem II complexes from spinach and their relevance to the organisation of photosystem II *in vivo*. *Eur J Biochem*, **243,** 422-429.

[17] Hankamer,B. & Baber,J. (1997) Structure and memberane organization of photosystem II in green plants. *Annu Rev Plant Physiol Plant Mol Biol*, **48,** 641-671.

[18] Orr,L. & Govindjee (2002) Photosynthesis and the web: 2002. http://photoscience.la.asu.edu/photosyn/photoweb/default.html.

[19] Rutherford,A.W. (1989) Photosystem II, the water-splitting enzyme. *Trends Biochem Sci*, **14,** 227-232.

[20] Horton,P., Ruban,A.V., & Walters,R.G. (1996) Regulation of light harvesting in green plants. *Annu Rev Plant Physiol Plant Mol Biol*, **47,** 655-684.

[21] Green,B.R. & Durnford,D.G. (1996) The chlorophyll-carotenoid proteins of oxygenic photosynthesis. *Annu Rev Plant Physiol Plant Mol Biol*, **47,** 685-714.

[22] Gibson,L. (2001) Principles of weed science: Photosynthesis inhibitors. http://www.agron.iastate.edu/courses/agron317/Photosynthesis_Inhibitors.htm.

[23] Matthews,C.K. & van Holde,K.E. (1990) Photosynthesis. In *Biochemistry* (Bowen,D., ed), pp. 643-669. The Benjamin/Cummings Publishing Company, Inc., Redwood city.

[24] Havaux,M. & Tardy,F. (1996) Temperature-dependent adjustment of the thermal stability of photosystem II *in vivo*: possible involvement of xanthophyll-cycle pigments. *Planta*, **198,** 324-333.

[25] Havaux,M., Tardy,F., & Lemoine,Y. (1998) Photosynthetic light-harvesting function of carotenoids in higher-plant leaves exposed to high light irradiances. *Planta*, **205,** 242-250.

[26] Niyogi,K.K., Grossman,A.R., & Björkman,O. (1998) *Arabidopsis* mutants define a central role for the xanthophyll cycle in the regulation of photosynthetic energy conversion. *Plant Cell*, **10,** 1121-1134.

[27] Georgieva,K. (1999) Some mechanisms of damage and acclimation of the photosynthetic apparatus due to high temperature. *Bulg J Plant Physiol*, **25,** 89-99.

[28] Lindahl,M., Spetea,C., Hundal,T., Oppenheim,A.B., Adam,Z., & Andersson,B. (2000) The thylakoid FtsH protease plays a role in the light-induced turnover of the photosystem II D1 protein. *Plant Cell*, **12,** 419-432.

[29] Havaux,M. (1998) Carotenoids as membrane stabilizers in chloroplasts. *Trends Plant Sci*, **3,** 147-151.

[30] Muller,P., Li,X.P., & Niyogi,K.K. (2001) Non-photochemical quenching. A response to excess light energy. *Plant Physiol*, **125,** 1558-1566.

[31] Esterbauer,H. & Cheeseman,K.H. (1990) Determination of aldehydic lipid peroxidation products: malonaldehyde and 4-hydroxynonenal. *Methods Enzymol.*, **186,** 407-421.

[32] Sujak,A., Okulski,W., & Gruszecki,W.I. (2000) Organisation of xanthophyll pigments lutein and zeaxanthin in lipid membranes formed with dipalmitoylphosphatidylcholine. *Biochim Biophys Acta*, **1509,** 255-263.

[33] Baroli,I. & Niyogi,K.K. (2000) Molecular genetics of xanthophyll-dependent photoprotection in green algae and plants. *Philos Trans R Soc Lond B: Biol Sci*, **355,** 1385-1393.

[34] Hauβühl,K., Andersson,B., & Adamska,I. (2001) A chloroplast DegP2 protease performs the primary cleavage of the photodamaged D1 protein in plant photosystem II. *EMBO J*, **20,** 713-722.

[35] Adam,Z. & Clarke,A.K. (2002) Cutting edge of chloroplast proteolysis. *Trends Plant Sci*, **7,** 451-456.

[36] Young,A.J., Phillip,D., & Savill,J. (1997) Carotenoids in higher plant photosynthesis. In *Handbook of photosynthesis* (Pessarakli,M., ed), pp. 575-596. Marcel Dekker, Inc., New York (USA).

[37] Rintamaki,E., Salo,R., Lehtonen,E., & Aro,E.M. (1995) Regulation of D1-protein degradation during photoinhibition of photosystem II in vivo: phosphorylation of the D1 protein in various plant groups. *Planta*, **195,** 379-386.

[38] Rintamaki,E., Kettunen,R., & Aro,E.M. (1996) Differential D1 dephosphorylation in functional and photodamaged photosystem II centers. Dephosphorylation is a prerequisite for degradation of damaged D1. *J Biol Chem*, **271,** 14870-14875.

[39] Ma,Y.Z., Holt,N.E., Li,X.P., Niyogi,K.K., & Fleming,G.R. (2003) Evidence for direct carotenoid involvement in the regulation of photosynthetic light harvesting. *Proc Natl Acad Sci USA*, **100,** 4377-4382.

[40] Munne-Bosch,S. & Alegre,L. (2000) Changes in carotenoids, tocopherols and diterpenes during drought and recovery, and the biological significance of chlorophyll loss in *Rosmarinus officinalis* plants. *Planta*, **210,** 925-931.

[41] Gilmore,A.M. & Govindjee (1999) How higher plants respond to excess light: energy dissipation in photosystem II. In *Concepts in photobiology: photosynthesis and photomorphogenesis* (Singhal,G.S., Renger,G., Sopory,S.K., Irrgang,K.D., & Govindjee, eds), pp. 513-548. Kluwer Academic Publishers, Dordrecht (The Netherlands).

[42] Logan,B.A., Demmig-Adams,B., & Adams,W.W., III (1999) Acclimation of photosynthesis to the environment. In *Concepts in photobiology: photosynthesis and photomorphogenesis* (Singhal,G.S., Renger,G., Sopory,S.K., Irrgang,K.D., & Govindjee, eds), pp. 477-512. Kluwer Academic Publishers, Dordrecht (The Netherlands).

[43] Niyogi,K.K. (2000) Safety valves for photosynthesis. *Curr Opin Plant Biol*, **3,** 455-460.

[44] Demmig-Adams,B. & Adams,W.W., III (1992) Photoprotection and other responses of plants to high light stress. *Annu Rev Plant Physiol Plant Mol Biol*, **43,** 599-626.

[45] DellaPenna,D. (1999) Carotenoid synthesis and function in plants: Insights from mutant studies in *Arabidopsis*. *Pure Appl Chem*, **71,** 2205-2212.

[46] Gastaldelli,M., Canino,G., Croce,R., & Bassi,R. (2003) Xanthophyll binding sites of the CP29 (Lhcb4) subunit of higher plant photosystem ii investigated by domain swapping and mutation analysis. *J Biol Chem*, **278,** 19190-19198.

[47] Armstrong,G.A. & Hearst,J.E. (1996) Carotenoids 2: Genetics and molecular biology of carotenoid pigment biosynthesis. *FASEB J*, **10,** 228-237.

[48] Jiang,M.Y. & Zhang,J.H. (2001) Effect of abscisic acid on active oxygen species, antioxidative defence system and oxidative damage in leaves of maize seedlings. *Plant Cell Physiol*, **42,** 1265-1273.

[49] Taylor,I.B., Burbidge,A., & Thompson,A.J. (2000) Control of abscisic acid synthesis. *J Exp Bot*, **51,** 1563-1574.

[50] Young,A.J. & Frank,H.A. (1996) Energy transfer reactions involving carotenoids: quenching of chlorophyll fluorescence. *J Photochem Photobiol B: Biol*, **36,** 3-15.

[51] Ruban,A.V., Pascal,A., Lee,P.J., Robert,B., & Horton,P. (2002) Molecular configuration of xanthophyll cycle carotenoids in photosystem II antenna complexes. *J Biol Chem*, **277,** 42937-42942.

[52] Ruban,A.V., Young,A.J., & Horton,P. (1996) Dynamic properties of the minor chlorophyll *a/b* binding proteins of photosystem II, an in vitro model for photoprotective energy dissipation in the photosynthetic membrane of green plants. *Biochemistry*, **35,** 674-678.

[53] Laule,O., Furholz,A., Chang,H.S., Zhu,T., Wang,X., Heifetz,P.B., Gruissem,W., & Lange,M. (2003) Crosstalk between cytosolic and plastidial pathways of isoprenoid biosynthesis in *Arabidopsis thaliana*. *Proc Natl Acad Sci USA*, **100,** 6866-6871.

[54] Lichtenthaler,H.K. (2000) Non-mevalonate isoprenoid biosynthesis: Enzymes, genes and inhibitors. *Biochem Soc Trans*, **28,** 785-789.

[55] Estevez,J.M., Cantero,A., Reindl,A., Reichler,S., & Leon,P. (2001) 1-Deoxy-D-xylulose-5-phosphate synthase, a limiting enzyme for plastidic isoprenoid biosynthesis in plants. *J Biol Chem*, **276,** 22901-22909.

[56] Lange,B.M., Rujan,T., Martin,W., & Croteau,R. (2000) Isoprenoid biosynthesis: The evolution of two ancient and distinct pathways across genomes. *Proc Natl Acad Sci USA*, **97,** 13172-13177.

[57] Walter,M.H., Hans,J., & Strack,D. (2002) Two distantly related genes encoding 1-deoxy-d-xylulose 5-phosphate synthases: differential regulation in shoots and apocarotenoid-accumulating mycorrhizal roots. *Plant J*, **31,** 243-254.

[58] Lois,L.M., Rodriguez-Concepcion,M., Gallego,F., Campos,N., & Boronat,A. (2000) Carotenoid biosynthesis during tomato fruit development: Regulatory role of 1-deoxy-D-xylulose 5-phosphate synthase. *Plant J*, **22,** 503-513.

[59] Schwender,J., Muller,C., Zeidler,J., & Lichtenthaler,H.K. (1999) Cloning and heterologous expression of a cDNA encoding 1-deoxy-D-xylulose-5-phosphate reductoisomerase of *Arabidopsis thaliana*. *FEBS Lett*, **455,** 140-144.

[60] Rohdich,F., Wungsintaweekul,J., Luttgen,H., Fischer,M., Eisenreich,W., Schuhr,C.A., Fellermeier,M., Schramek,N., Zenk,M.H., & Bacher,A. (2000) Biosynthesis of terpenoids: 4-diphosphocytidyl-2-C-methyl-D-erythritol kinase from tomato. *Proc Natl Acad Sci USA*, **97,** 8251-8256.

[61] Rohdich,F., Wungsintaweekul,J., Eisenreich,W., Richter,G., Schuhr,C.A., Hecht,S., Zenk,M.H., & Bacher,A. (2000) Biosynthesis of terpenoids: 4-diphosphocytidyl-2C-methyl-D-erythritol synthase of *Arabidopsis thaliana*. *Proc Natl Acad Sci USA*, **97,** 6451-6456.

[62] Rohdich,F., Zepeck,F., Adam,P., Hecht,S., Kaiser,J., Laupitz,R., Grawert,T., Amslinger,S., Eisenreich,W., Bacher,A., & Arigoni,D. (2003) The deoxyxylulose phosphate pathway of isoprenoid biosynthesis: studies on the mechanisms of the reactions catalyzed by IspG and IspH protein. *Proc Natl Acad Sci USA*, **100,** 1586-1591.

[63] Veau,B., Courtois,M., Oudin,A., Chenieux,J.C., Rideau,M., & Clastre,M. (2000) Cloning and expression of cDNAs encoding two enzymes of the MEP pathway in *Catharanthus roseus*. *Biochim Biophys Acta*, **1517,** 159-163.

[64] Altincicek,B., Kollas,A.K., Sanderbrand,S., Wiesner,J., Hintz,M., Beck,E., & Jomaa,H. (2001) GcpE is involved in the 2-C-methyl-D-erythritol 4-phosphate pathway of isoprenoid biosynthesis in *Escherichia coli*. *J Bacteriol*, **183,** 2411-2416.

[65] Kollas,A.K., Duin,E.C., Eberl,M., Altincicek,B., Hintz,M., Reichenberg,A., Henschker,D., Henne,A., Steinbrecher,I., & Ostrovsky,D.N. (2002) Functional characterization of GcpE, an essential enzyme of the non-mevalonate pathway of isoprenoid biosynthesis. *FEBS Lett*, **532,** 432-436.

[66] Cunningham,F.X., Jr., Lafond,T.P., & Gantt,E. (2000) Evidence of a role for LytB in the nonmevalonate pathway of isoprenoid biosynthesis. *J Bacteriol*, **182,** 5841-5848.

[67] Rohdich,F., Hecht,S., Gartner,K., Adam,P., Krieger,C., Amslinger,S., Arigoni,D., Bacher,A., & Eisenreich,W. (2002) Studies on the nonmevalonate terpene biosynthetic pathway: metabolic role of IspH (LytB) protein. *Proc Natl Acad Sci USA*, **99,** 1158-1163.

[68] Cunningham,F.X., Jr. & Gantt,E. (2000) Identification of multi-gene families encoding isopentenyl diphosphate isomerase in plants by heterologous complementation in *Escherichia coli*. *Plant Cell Physiol*, **41,** 119-123.

[69] Nakamura,A., Shimada,H., Masuda,T., Ohta,H., & Takamiya,K. (2001) Two distinct isopentenyl diphosphate isomerases in cytosol and plastid are differentially induced by environmental stresses in tobacco. *FEBS Lett*, **506,** 61-64.

[70] Sun,Z., Cunningham,F.X., Jr., & Gantt,E. (1998) Differential expression of two isopentenyl pyrophosphate isomerases and enhanced carotenoid accumulation in a unicellular chlorophyte. *Proc Natl Acad Sci USA*, **95,** 11482-11488.

[71] Lindgren,L.O., Stalberg,K.G., & Hoglund,A.S. (2003) Seed-specific overexpression of an endogenous *Arabidopsis* phytoene synthase gene results in delayed germination and increased levels of carotenoids, chlorophyll, and abscisic acid. *Plant Physiol*, **132,** 779-785.

[72] Oh,S.K., Kim,I.J., Shin,D.H., Yang,J., Kang,H., & Han,K.H. (2000) Cloning, characterization, and heterologous expression of a functional geranylgeranyl pyrophosphate synthase from sunflower (*Helianthus annuus* L.). *J Plant Physiol*, **157,** 535-542.

[73] Okada,K., Saito,T., Nakagawa,T., Kawamukai,M., & Kamiya,Y. (2000) Five geranylgeranyl diphosphate synthases expressed in different organs are localized into three subcellular compartments in *Arabidopsis*. *Plant Physiol*, **122,** 1045-1056.

[74] Fraser,P.D., Schuch,W., & Bramley,P.M. (2000) Phytoene synthase from tomato (*Lycopersicon esculentum*) chloroplasts--partial purification and biochemical properties. *Planta*, **211,** 361-369.

[75] Fray,R.G., Wallace,A., Fraser,P.D., Valero,D., Hedden,P., Bramley,P.M., & Grierson,D. (1995) Constitutive expression of a fruit phytoene synthase gene in transgenic tomatoes causes dwarfism by redirecting metabolites from the gibberellin pathway. *Plant J*, **8,** 693-701.

[76] Fraser,P.D., Hedden,P., Cooke,D.T., Bird,C.R., Schuch,W., & Bramley,P.M. (1995) The effect of reduced activity of phytoene synthase on isoprenoid levels in tomato pericarp during fruit-development and ripening. *Planta*, **196,** 321-326.

[77] Welsch,R., Beyer,P., Hugueney,P., Kleinig,H., & Von Lintig,J. (2000) Regulation and activation of phytoene synthase, a key enzyme in carotenoid biosynthesis, during photomorphogenesis. *Planta*, **211,** 846-854.

[78] Bonk,M., Hoffmann,B., VonLintig,J., Schledz,M., Al Babili,S., Hobeika,E., Kleinig,H., & Beyer,P. (1997) Chloroplast import of four carotenoid biosynthetic enzymes *in vitro* reveals

differential fates prior to membrane binding and oligomeric assembly. *Eur J Biochem*, **247,** 942-950.

[79] Nievelstein,V., Vandekerckhove,J., Tadros,M.H., Lintig,J.V., Nitschke,W., & Beyer,P. (1995) Carotene desaturation is linked to a respiratory redox pathway in *Narcissus pseudonarcissus* chromoplast membranes - involvement of a 23-kDa oxygen-evolving-complex-like protein. *Eur J Biochem*, **233,** 864-872.

[80] Giuliano,G., Giliberto,L., & Rosati,C. (2002) Carotenoid isomerase: a tale of light and isomers. *Trends Plant Sci*, **7,** 427-429.

[81] Isaacson,T., Ronen,G., Zamir,D., & Hirschberg,J. (2002) Cloning of *tangerine* from tomato reveals a carotenoid isomerase essential for the production of β-carotene and xanthophylls in plants. *Plant Cell*, **14,** 333-342.

[82] Park,H., Kreunen,S.S., Cuttriss,A.J., DellaPenna,D., & Pogson,B.J. (2002) Identification of the carotenoid isomerase provides insight into carotenoid biosynthesis, prolamellar body formation, and photomorphogenesis. *Plant Cell*, **14,** 321-332.

[83] Cunningham,F.X., Jr. & Gantt,E. (2001) One ring or two? Determination of ring number in carotenoids by lycopene ε-cyclases. *Proc Natl Acad Sci USA*, **98,** 2905-2910.

[84] Pogson,B., McDonald,K.A., Truong,M., Britton,G., & DellaPenna,D. (1996) *Arabidopsis* carotenoid mutants demonstrate that lutein is not essential for photosynthesis in higher plants. *Plant Cell*, **8,** 1627-1639.

[85] Eskling,M., Arvidsson,P.O., & Akerlund,H.E. (1997) The xanthophyll cycle, its regulation and components. *Physiol Plant*, **100,** 806-816.

[86] Bouvier,F., Hugueney,P., d'Harlingue,A., Kuntz,M., & Camara,B. (1994) Xanthophyll biosynthesis in chromoplasts: isolation and molecular cloning of an enzyme catalyzing the conversion of 5,6-epoxycarotenoid into ketocarotenoid. *Plant J*, **6,** 45-54.

[87] Hugueney,P., Badillo,A., Chen,H.C., Klein,A., Hirschberg,J., Camara,B., & Kuntz,M. (1995) Metabolism of cyclic carotenoids: a model for the alteration of this biosynthetic pathway in *Capsicum annuum* chromoplasts. *Plant J*, **8,** 417-424.

[88] Demmig-Adams,B., Moeller,D.L., Logan,B.A., & Adams,W.W., III (1998) Positive correlation between levels of retained zeaxanthin plus antheraxanthin and degree of photoinhibition in shade leaves of *Schefflera arboricola* (Hayata) Merrill. *Planta*, **205,** 367-374.

[89] Xiong,L. & Zhu,J.K. (2003) Regulation of abscisic acid biosynthesis. *Plant Physiol*, **133,** 29-36.

[90] Nambara,E. & Marion-Poll,A. (2003) ABA action and interactions in seeds. *Trends Plant Sci*, **8,** 213-217.

[91] Kende,H. & Zeevaart,J.A.D. (1997) The five "classical" plant hormones. *Plant Cell*, **9,** 1197-1210.

[92] Rock,C.D. & Zeevaart,J.A. (1991) The *aba* mutant of *Arabidopsis thaliana* is impaired in epoxy-carotenoid biosynthesis. *Proc Natl Acad Sci USA*, **88,** 7496-7499.

[93] Qin,X. & Zeevaart,J.A. (1999) The 9-*cis*-epoxycarotenoid cleavage reaction is the key regulatory step of abscisic acid biosynthesis in water-stressed bean. *Proc Natl Acad Sci USA*, **96,** 15354-15361.

[94] Iuchi,S., Kobayashi,M., Yamaguchi-Shinozaki,K., & Shinozaki,K. (2000) A stress-inducible gene for 9-*cis*-epoxycarotenoid dioxygenase involved in abscisic acid biosynthesis under water stress in drought-tolerant cowpea. *Plant Physiol*, **123,** 553-562.

[95] Qin,X.Q. & Zeevaart,J.A.D. (2002) Overexpression of a 9-*cis*-epoxycarotenoid dioxygenase gene in *Nicotiana plumbaginifolia* increases abscisic acid and phaseic acid levels and enhances drought tolerance. *Plant Physiol*, **128,** 544-551.

[96] Cheng,W.H., Endo,A., Zhou,L., Penney,J., Chen,H.C., Arroyo,A., Leon,P., Nambara,E., Asami,T., Seo,M., Koshiba,T., & Sheen,J. (2002) A unique short-chain dehydrogenase/reductase in *Arabidopsis* glucose signaling and abscisic acid biosynthesis and functions. *Plant Cell*, **14,** 2723-2743.

[97] Gonzalez-Guzman,M., Apostolova,N., Belles,J.M., Barrero,J.M., Piqueras,P., Ponce,M.R., Micol,J.L., Serrano,R., & Rodriguez,P.L. (2002) The short-chain alcohol dehydrogenase ABA2 catalyzes the conversion of xanthoxin to abscisic aldehyde. *Plant Cell*, **14,** 1833-1846.

[98] Schwartz,S.H., Qin,X., & Zeevaart,J.A. (2003) Elucidation of the indirect pathway of abscisic acid biosynthesis by mutants, genes, and enzymes. *Plant Physiol*, **131,** 1591-1601.

[99] Bassi,R. & Caffarri,S. (2000) Lhc proteins and the regulation of photosynthetic light harvesting function by xanthophylls. *Photosynth Res*, **64,** 243-256.

[100] Heyde,S. & Jahns,P. (1998) The kinetics of zeaxanthin formation is retarded by dicyclohexylcarbodiimide. *Plant Physiol*, **117,** 659-665.

[101] Adams,W.W., III, Demmig-Adams,B., Verhoeven,A.S., & Barker,D.H. (1994) 'Photoinhibition' during winter stress: Involvement of sustained xanthophyll cycle-dependent energy dissipation. *Aust J Plant Physiol*, **22,** 261-276.

[102] Havaux,M. & Niyogi,K.K. (1999) The violaxanthin cycle protects plants from photooxidative damage by more than one mechanism. *Proc Natl Acad Sci USA*, **96,** 8762-8767.

[103] Havaux,M., Bonfils,J.P., Lutz,C., & Niyogi,K.K. (2000) Photodamage of the photosynthetic apparatus and its dependence on the leaf developmental stage in the *npq1 Arabidopsis* mutant deficient in the xanthophyll cycle enzyme violaxanthin de-epoxidase. *Plant Physiol*, **124,** 273-284.

[104] Cunningham,F.X., Jr. & Gantt,E. (1998) Genes and enzymes of carotenoid biosynthesis in plants. *Annu Rev Plant Physiol Plant Mol Biol*, **49,** 557-583.

[105] Verhoeven,A.S., Adams,W.W., III, Demmig-Adams,B., Croce,R., & Bassi,R. (1999) Xanthophyll cycle pigment localization and dynamics during exposure to low temperatures and light stress in *Vinca major*. *Plant Physiol*, **120,** 727-738.

[106] Ruban,A.V., Young,A.J., Pascal,A.A., & Horton,P. (1994) The effects of illumination on the xanthophyll composition of the photosystem II light-harvesting complexes of spinach thylakoid membranes. *Plant Physiol*, **104,** 227-234.

[107] Kramer,D.M., Cruz,J.A., & Kanazawa,A. (2003) Balancing the central roles of the thylakoid proton gradient. *Trends Plant Sci*, **8,** 27-32.

[108] Hartel,H., Lokstein,H., Grimm,B., & Rank,B. (1996) Kinetic studies on the xanthophyll cycle in barley leaves - Influence of antenna size and relations to nonphotochemical chlorophyll fluorescence quenching. *Plant Physiol*, **110,** 471-482.

[109] Elrad,D., Niyogi,K.K., & Grossman,A.R. (2002) A major light-harvesting polypeptide of photosystem II functions in thermal dissipation. *Plant Cell*, **14,** 1801-1816.

[110] Maxwell,K. & Johnson,G.N. (2000) Chlorophyll fluorescence - a practical guide. *J Exp Bot*, **51,** 659-668.

[111] Gilmore,A.M. & Ball,M.C. (2000) Protection and storage of chlorophyll in overwintering evergreens. *Proc Natl Acad Sci USA*, **97,** 11098-11101.

[112] Govindjee (2002) A role for a light-harvesting antenna complex of photosystem II in photoprotection. *Plant Cell*, **14,** 1663-1668.

[113] Krause,G.H. & Weis,E. (1991) Chlorophyll fluorescence and photosynthesis: The basics. *Annu Rev Plant Physiol Plant Mol Biol*, **42,** 313-349.

[114] Rohacek,K. (2002) Chlorophyll fluorescence parameters: the definitions, photosynthetic meaning, and mutual relationships. *Photosynthetica*, **40,** 13-29.

[115] Bolhar-Nordenkampf,H.R. (1993) Chlorophyll fluorescence as a tool in photosynthetic research. In *Photosynthesis and production in a changing environment: a field and laboratory manual* (Hall,D.O., Scurlock,J.M.O., Bolhar-Nordenkampf,H.R., Leegood,R.C., & Long,S.P., eds), Chapman and Hall, London (UK).

[116] Ruban,A.V., Pascal,A.A., Robert,B., & Horton,P. (2002) Activation of zeaxanthin is an obligatory event in the regulation of photosynthetic light harvesting. *J Biol Chem*, **277,** 7785-7789.

[117] Laisk,A. & Oja,V. (1998) Dynamics of leaf photosynthesis: rapid-response measurements and their interpretations. In *Techniques in plant sciences* (Osmond,B. ed) CSIRO Publishing, Melbourne (Australia).

[118] Rohacek,K. & Bartak,M. (1999) Technique of the modulated chlorophyll fluorescence: basic concepts, useful parameters, and some applications. *Photosynthetica*, **37,** 339-363.

[119] Van Kooten,O. & Snel,J.F.H. (1990) The use of chlorophyll fluorescence nomenclature in plant stress physiology. *Photosynth Res*, **25,** 147-150.

[120] Björkman,O. & Demmig,B. (1987) Photon yield of $O_2$ evolution and chlorophyll fluorescence characteristics at 77 K among vascular plants of diverse origins. *Planta*, **170,** 489-504.

[121] Havaux,M. & Kloppstech,K. (2001) The protective functions of carotenoid and flavonoid pigments against excess visible radiation at chilling temperature investigated in *Arabidopsis npq* and *tt* mutants. *Planta*, **213,** 953-966.

[122] Peterson,R.B. & Havir,E.A. (2000) A nonphotochemical-quenching-deficient mutant of *Arabidopsis thaliana* possessing normal pigment composition and xanthophyll-cycle activity. *Planta*, **210,** 205-214.

[123] Li,X.P., Muller-Moule,P., Gilmore,A.M., & Niyogi,K.K. (2002) PsbS-dependent enhancement of feedback de-excitation protects photosystem II from photoinhibition. *Proc Natl Acad Sci USA*, **99,** 15222-15227.

[124] Lokstein,H., Tian,L., Polle,J.E.W., & DellaPenna,D. (2002) Xanthophyll biosynthetic mutants of Arabidopsis thaliana: altered nonphotochemical quenching of chlorophyll fluorescence is due to changes in photosystem II antenna size and stability. *Biochim Biophys Acta*, **1553,** 309-319.

[125] Pogson,B.J., Niyogi,K.K., Björkman,O., & DellaPenna,D. (1998) Altered xanthophyll compositions adversely affect chlorophyll accumulation and nonphotochemical quenching in *Arabidopsis* mutants. *Proc Natl Acad Sci USA*, **95,** 13324-13329.

[126] Muller-Moule,P., Conklin,P.L., & Niyogi,K.K. (2002) Ascorbate deficiency can limit violaxanthin de-epoxidase activity *in vivo*. *Plant Physiol*, **128,** 970-977.

[127] Muller-Moule,P., Havaux,M., & Niyogi,K.K. (2003) Zeaxanthin deficiency enhances the high light sensitivity of an ascorbate-deficient mutant of *Arabidopsis*. *Plant Physiol*, **133,** 1-13103.

[128] Smirnoff,N. (1996) The function and metabolism of ascorbic acid in plants. *Ann Bot*, **78,** 661-669.

# CHAPTER 3

# RESEARCH RESULTS

## Overexpression of the *Vitis vinifera* L. β-carotene hydroxylase encoding gene in tobacco leads to improved photoprotection

This manuscript will be submitted for publication in ***Plant Physiology***

# Overexpression of the *Vitis vinifera* L. β-Carotene Hydroxylase Gene Improves the Photoprotective Ability of Tobacco

Philip R. Young[1], Shang W. Chen[2], Isak S. Pretorius[3] and Melané A. Vivier[1]*

[1]Institute for Wine Biotechnology, Department of Viticulture and Oenology, Stellenbosch University, Stellenbosch, South Africa, 7600; [2]Food Science and Nutritional Engineering College, China Agricultural University, Beijing, PR China [3]Australian Wine Research Institute, Adelaide, Australia

## ABSTRACT

Every year severe crop reductions are caused by extreme environmental conditions that typically cause oxidative damage to the photosynthetic membranes of plants. Carotenoids associated with these membranes serve a vital protective function under these conditions, and therefore serve as a promising target for genetic manipulation in order to enhance the plants inherent stress tolerance. To this end, the cDNA- and genomic copies of the β-carotene hydroxylase (BCH) encoding gene from *Vitis vinifera* L. cv. Pinotage has been isolated and characterized (Genbank accession number, AF499108). The BCH gene contains six introns and is present as a single-copy gene in the grapevine genome. The BCH gene is expressed at relatively low-levels in leaves, berries, and flowers. A 2.0 kb fragment of the putative BCH promoter showed no transcriptional activity in transient reporter gene assays. *Nicotiana tabacum* (cv Petite Havana SR1) was transformed with the BCH encoding gene from grapevine which was expressed in both the sense and antisense orientation under the control of the constitutive cauliflower mosaic virus (CaMV) 35S promoter. Under relatively mild photon flux density (PFD) of between 200- and 400 $\mu mol.m^{-2}.s^{-1}$ the $T_1$-generation transgenic tobacco lines expressing the BCH gene were phenotypically indiscernible from the wild-type control plants, and showed no differences in growth rate or total carotenoid content. Under high light intensities (1500-2500 $\mu mol.m^{-2}.s^{-1}$), however, the photosynthetic parameters of the transgenic tobacco lines showed significant differences relative to that of both the wild-type control plants, as well as the antisense lines. Chlorophyll *a* fluorescence assays revealed that the expressed BCH assisted the transgenic plants in coping with high light stress by reducing photodamage to the PSII reaction centre while maintaining a lower D1 protein turnover rate, as well as a higher net assimilation rate. The rate of recovery and relaxation of the active reaction centres during the dark phase of the transformants was higher than that of the wild-type tobacco. During the illumination phase the transgenic plants displayed slightly elevated xanthophyll pigment pools in leaves and managed to maintain a higher stomatal conductance in PFD growth. Cumulatively, these results indicate that the expression of the heterologous grapevine BCH functions in transgenic tobacco by enhancing the plants existing photoprotective system under high light stress. This can be accounted for by an increase in BCH (and the subsequent higher zeaxanthin levels) in the xanthophyll biosynthetic pathway.

*Corresponding author: Institute for Wine Biotechnology, Department of Viticulture and Oenology, Stellenbosch University, Private Bag X1, Matieland, ZA7602, South Africa. Tel: +27 21 8083773; Fax: +27 21 8083771; Email: mav@sun.ac.za

## 3.1 INTRODUCTION

Light is probably the most obvious prerequisite for photosynthesis, yet when light conditions become saturating, plants require protection. The reactive intermediates formed are unavoidable by-products of the photosynthetic process. If these reactive molecules are not controlled, they can cause damage to the photosynthetic apparatus (photo-oxidative damage or photodamage); and if this damage is not repaired, it will affect both the rate and efficiency of photosynthesis [1]. As soon as this damage exceeds the plants inherent ability for repair, the overall photosynthetic activity will decrease and eventually stop (i.e. photoinhibition).

PSII in the thylakoid membrane is the most susceptible to this photo-oxidative damage, and this sensitivity has been attributed to the activity of the oxygen-evolving complex of PSII, as well as the formation of reactive oxygen species. The main target of this photodamage in PSII is the D1 protein. Damage to the D1 protein will lead to photo-oxidative inactivation of the entire reaction centre. To recover the photosynthetic capacity, *de novo* synthesis and replacement of the degraded D1 protein is required [2-4].

An efficient system to protect plants from these damages must be capable of dissipating the excess energy that is absorbed by the light harvesting complexes. Carotenoids, especially epoxy-derivatives of the β-carotenoid branch pathway pigments (i.e. violaxanthin, antheraxanthin, and zeaxanthin), play a pivotal role in the photoprotection of green plants and other photosynthetic organisms [5-8]. The xanthophyll cycle facilitates the interconversion of violaxanthin and zeaxanthin (via antheraxanthin), and is catalyzed by two enzymes: violaxanthin de-epoxidase (VDE) and zeaxanthin epoxidase (ZEP). These enzymes are localized on opposite sides of the thylakoid membrane, and are regulated by the trans-thylakoid pH gradient (ΔpH), as well as the availability of ascorbate [9-12]. β-Carotene is the precursor of zeaxanthin, the first xanthophyll pigment in the carotenoid biosynthetic pathway. β-Carotene hydroxylase (BCH) catalyzes the metabolic reaction of adding hydroxyl groups to the β-ionone rings of β-carotene to form zeaxanthin [13]. BCH occupies a critical step in the control of the flow rate of pigments through the β-carotenoid branch in plants (Fig. 3.1) [14].

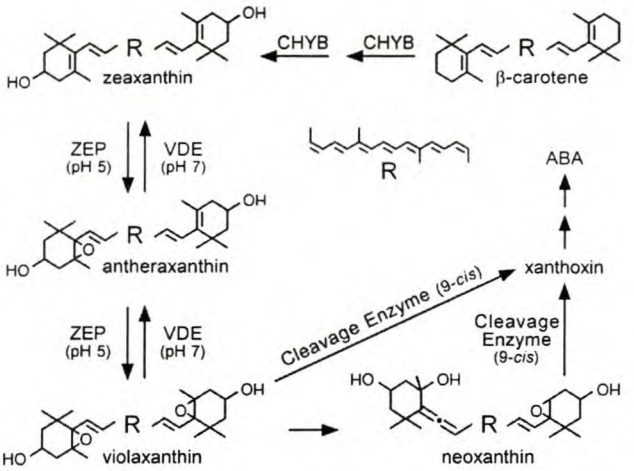


Figure 3.1. The reversible pH-dependent xanthophyll cycle and the relevant enzymes involved in relation to the carotenoid biosynthetic pathway: CHYB, β-carotene hydroxylase; ZEP, zeaxanthin epoxidase; VDE, violaxanthin de-epoxidase. R, represents the carotene hydrocarbon backbone. Cleavage enzyme (9-*cis*) refers to the 9-*cis* epoxy carotenoid dioxygenase (NCED) [15].

Several overlapping mechanisms are active in the thermal dissipation process in plants and can be measured as nonphotochemical quenching (NPQ) of chlorophyll *a* fluorescence [16]. Three quenching processes are known to contribute to NPQ: (i) high energy state quenching (qE), (ii) state transition (qT), and (iii) photoinhibition (qI). The xanthophyll cycle is considered the main contributor to the qE component of (NPQ) in PSII due to its role in dissipating excess excitation energy as heat, quenching singlet or triplet chlorophyll, and maintaining both the assembly and stability of the light harvesting antenna [7;17-19]. Zeaxanthin is required for both the xanthophyll cycle and the induction of NPQ in plants [20]. Overexpression of the native BCH in *Arabidopsis thaliana* lead to transgenic plants that were phenotypically more tolerant to conditions of high light (1000 μM photons.$m^{-2}$.$s^{-1}$) and elevated temperature (40°C). This stress protection was attributed to the function of zeaxanthin in preventing oxidative damage to photosynthetic membranes [21]. Similarly, the crucial role of the xanthophyll cycle and NPQ in protecting the photosynthetic apparatus from damage was shown in transgenic tobacco plants with suppressed zeaxanthin levels. The transgenic tobacco plants that expressed an antisense violaxanthin de-epoxidase encoding gene were more

susceptible to both high light (2000 μM photons.$m^{-2}$.$s^{-1}$) and water stress conditions than the wild-type plants [22].

Carotenoid biosynthesis and especially the xanthophyll cycle have been both extensively and intensively studied in the last few years, but how plants regulate this pathway to adapt to their variable environment still needs to be unraveled. Additional genetic analyses of plants with mutations in carotenoid biosynthetic genes, or overexpression of specific carotenoid biosynthetic genes, are needed to elucidate the effect of individual carotenoids in photoprotection *in vivo*.

The BCH gene from grapevine (*Vitis vinifera*) has been isolated and characterized and subsequently transformed into tobacco (*Nicotiana tabacum*) in both the sense and antisense orientation under the control of the constitutive cauliflower mosaic virus (CaMV) 35S promoter. The $T_1$-progenies were evaluated by monitoring the chlorophyll *a* fluorescence, pigment profiles, and D1 protein turnover rate to determine the effect of the expressed BCH gene on the photoprotective ability of plants under different light conditions. In addition to these measurements, the activity of the putative BCH promoter was evaluated in a transient reporter gene assay. Both the cDNA- and genomic copy of the BCH gene have been isolated and characterized. The native expression of the BCH gene in *V. vinifera* was investigated in different plant organs, at different developmental stages, and during different induced stress conditions. Collectively these data provided genetic, structural and functional information on the BCH gene (and its encoded product) in *V. vinifera.*

## 3.2 MATERIALS AND METHODS

### 3.2.1 Plant material

*Vitis vinifera* leaves cv Pinotage were collected in the field and flash frozen in liquid nitrogen. Berries were collected throughout the growth season (October, 2001 through to February, 2002) in one-week intervals. The frozen tissue was ground in liquid nitrogen and, if not used immediately, stored at -80°C. Plant material for biolistic bombardments was either from *in vitro* tissue culture plants (*Nicotiana tabacum* and *V. vinifera* leaves), commercially bought *Capsicum annuum* and *Lycopersicon esculentum* fruit, and *V. vinifera* berries, or collected in the field (*V. vinifera* berries), depending on the seasonal availability of each.

Field-grown leaf tissue was used for the induction experiments and subsequent RT-PCR analyses. The petioles of detached leaves were placed in (i) sterile water, (ii) 100 μM abscisic acid, (iii) without water (i.e. dehydration), (iv) 300 mM NaCl, and (v) wounding (by damaging the leaf blade with a pincer). Tissue was collected 1 h, 6 h, 16 h, and 24 h after the induction (corresponding to 16h00, 21h00, 08h00 and 15h00, respectively).

Seeds of the different transgenic $T_1$-lines: sense lines (SL), antisense lines (ASL), and the wild-type (WT), were germinated at 25°C. Four week old seedlings were potted and grown at 25°C (14 h light) and 22°C (10 h dark) in a green house at moderate light intensity (200 $\mu mol.m^{-2}.s^{-1}$, supplied by artificial light) for four to ten weeks. The first five fully expanded leaves (from top to bottom) of two different stages (vegetative and flowering) of each tobacco line were selected for subsequent assays. Sampling, treatment and the *in situ* assay were done according to the aim of each of the individual experiments.

### 3.2.2 Plasmids, bacterial strains and growth conditions

The pGEM-T Easy vector system was used to clone all PCR-generated fragments, according to the specifications of the supplier (Promega, Madison, WI). Transformed *E. coli* DH5α cultures were grown in LB media, supplemented with appropriate antibiotic(s) at 37°C. *Agrobacterium tumefaciens* EHA105 was cultured at 28°C in LB media containing 0.2% Glc (w/v), 15 $\mu g.ml^{-1}$ rifampcin and 50 $\mu g.ml^{-1}$ streptomycin. The plasmids, pAC-BETA and pAC-ZEAX were received from F. X. Cunningham and are described, together with the functional complementation assay, in Cunningham *et al.* 1993 and Cunningham *et al.* 1994 ([23;24]. The recombinant binary constructs in pART27 were transferred from *E. coli* DH5α into *A. tumefaciens* EHA105 via triparental mating with an HB101 *E. coli* strain containing the mobilizing plasmid, pRK2013 [25].

### 3.2.3 Isolation and manipulation of nucleic acids

High molecular weight genomic DNA was isolated from fully expanded *V. vinifera* leaves as described by Steenkamp *et al.* (1994) [26]. Total RNA from different grapevine tissue was extracted according to the methods described by Davies and Robinson [27]. Total RNA from *N. tabacum* was extracted according to Chomczynski and Sacchi [28]. Total RNA was extracted from the $T_1$-seedlings two weeks after potting, by taking three leaf

discs (11 mm in diameter) from the first fully expanded leaves. Unless otherwise stated, all standard methods for plasmid DNA isolation, manipulations and cloning of DNA fragments, agarose gel electrophoresis and purification of DNA fragments were used as described by Sambrook *et al.* [29].

### 3.2.4 Isolation of the *V. vinifera* BCH gene and construction of subsequent cloning and transformation vectors

BCHs display a high degree of homology in certain streches of their amino acid sequences. These stretches correspond to transmembrane helices in the protein sequence (Fig. 3.4). The BCH1 and BCH3 primer pair was designed from the corresponding nucleotide sequence in two of these homologous areas and subsequently used to amplify an internal 1000 bp BCH fragment using 100 ng of Pinotage genomic DNA as template (Table 3.1). PCR amplification was performed in a BioRad PCR thermal cycler (BioRad, Hercules, CA) using the following program: initial denaturation at 94°C for 2 min; subsequent denaturations at 94°C for 35 s; annealing at 55°C for 35 s; extension at 72°C for 1 min; and a final elongation at 72°C for 10 min. Amplifications were performed for 32 cycles and the fragment was isolated from a 1.0% (w/v) TAE agarose gel using the QIAquick Gel Extraction Kit (Qiagen GmbH, Hilden, Germany), and cloned into the pGEM-T Easy Vector. The plasmid containing the 950 bp product was subsequently called pBCH1. All DNA sequencing was performed at the Central Analytical Facility, Stellenbosch University, using an ABI Prism 3100 Genetic Analyzer.

Sub-genomic libraries had to be constructed and screened in order to isolate the full-length BCH gene with both the up- and downstream flanking sequences. This was achieved by digesting ten micrograms of *V. vinifera* L. cv Pinotage genomic DNA with a range of restriction enzymes. The fragments were separated in a 0.8% (w/v) TBE agarose gel and transferred to Hybond-N nylon membranes, and probed with the DIG PCR-labeled partial BCH. Subsequent hybridizations of the digested genomic DNA with the restriction enzyme, *Eco*RV showed a single band of approximately 5.6 kb in the subsequent Southern blot analysis. The *Eco*RV genomic DNA fragments (corresponding to the size of the hybridization signal from the Southern blot) were isolated, gel-purified and cloned into the dephosphorylated *Eco*RV sites of pBluescript II SK(+). The ligation mixtures were transformed into DH5α *E. coli* cells and the resultant sub-genomic libraries were screened to identify the genomic fragments containing the

entire BCH gene, as well as the up- and downstream flanking sequences. Similarly, a 5.0 kb *Pst*I sub-genomic library was constructed in pBluescript II SK(+) (digested with *Pst*I) and screened. A positive clone from each of the sub-genomic libraries was isolated and designated pBCH5.6 (for the 5.6 kb *Eco*RV fragment) and pBCH5.0 (for the 5.0 kb *Pst*I fragment).

Table 3.1. Primers used in this study.

| PRIMER | SEQUENCE |
|---|---|
| BCH1 | 5'-ATCGGATATCATGATGTCTAGCCTCGGC-3' |
| BCH3 | 5'-TAGCGGATCCTGATTTACTTGGTGGGCC-3' |
| 5'RTAseI | 5'-ATTAATATGGCGACAGGAATTTC-3' |
| BCHComp2 | 5'-ATCGCTCGAGTGCATACTGATTGATGTCATATTC-3' |
| BCH-TM-5' | 5'-ATGCCAGTTCTGGAAATGTTGGGTAC-3' |
| BCH-TM-3' | 5'-CTCGAGTCATGAAGAGTCAGATGATTTAATTC-3' |
| ATG-prom | 5'-ACCCAGTGGCCTCAATTCTTTCTGCCGTTT-3' |
| BCH5'-2.00 | 5'-GGTCCCAACTCATGAATCCT-3' |
| BCH5'-0.85 | 5'-ATCGAAGCTTTCCCAAAATGGAATTGAT-3' |
| BCH5'-0.50 | 5'-CCCACCCAATACATGTTTACC-3' |
| BCH5'-0.25 | 5'-TTGAAACGTCTGCTACAGGG-3' |
| BCH5'-1.00 | 5'-TCAAGTCTTCTCAAAGCTCGT-3' |
| BCH5'-0.05 | 5'-GATGTTTCTCATTTCCCAAGC-3' |
| ACTIN5' | 5'-GATACTGAAGATATCCAGCCCCTCG-3' |
| ACTIN3' | 5'-GCATGGGGAAGTGCATAACCTT-3' |
| EF1α5' | 5'-CACATCAACATTGTCGTCATTGGC-3' |
| EF1α3' | 5'-GGGACAAATGGAATCTTATCAGGG-3' |

The 957 bp full-length BCH RT-PCR product was cloned into pGEM-T Easy vector, and subsequently called pRT-BCH1. This product was isolated from pRT-BCH1 by digestion with *Asn*I/*Xho*I, and cloned (in-frame) into the *Nde*I/*Xho*I site of the IPTG-inducible expression vector, pET14b (Novagen, Madison, WI) to generate the expression construct, pET-BCH.

The 957 bp full-length BCH was isolated from pRT-BCH1 also as an *Eco*RI-fragment, and cloned into the *Eco*RI-site of pART7 [30] between the constitutive CaMV-35S promoter and the NOS 3' terminator (in both the sense and antisense orientation). Sense and antisense CaMV-35S$_P$-[RT-BCH]-NOS$_T$ cassettes were identified, isolated from pART7 as *Not*I-fragments, and cloned into the *Not*I-site of pART27 [30], and subsequently designated pART27-BCH$^S$ (for the sense construct), and pART27-BCH$^{AS}$ (for the antisense construct).

The CaMV-35S promoter and β-glucuronidase (GUS) reporter gene cassette was isolated from pBI221 (CLONTECH Laboratories, Palo Alto, CA) by digestion with *Pst*I/*Eco*RI and cloned into the *Pst*I/*Eco*RI-site of pBluescript II SK (+) (Stratagene, La Jolla, CA). This plasmid was subsequently designated pBS-[CaMV-GUS]. The BCH promoter fragments corresponding to -2000, -850, -500, -250, -100, -50 bp (relative to the putative predicted BCH ATG) were PCR amplified from Pinotage genomic DNA (Table 3.1) and cloned into pGEM-T Easy Vector. The recombinant vectors were digested with *Not*I/*Bam*HI and cloned into the *Not*I/*Bam*HI-site of pBS-[CaMV-GUS] (this effectively replaced the entire CaMV-35S promoter of pBS-[CaMV-GUS] with the promoter of interest, in front of the GUS reporter gene).

### 3.2.5 Southern and northern hybridizations

For Southern blot analyses 10 μg of digested genomic DNA was separated in a 0.8% TBE (w/v) agarose gel and transferred to a positively charged Hybond-N nylon membrane as described by the supplier (Amersham-Pharmacia Biotech, Buckinghamshire, UK). For northern blot analyses 10 μg of total RNA was separated in a 1.2% (w/v) formaldehyde-agarose gel, and transferred to a positively charged Hybond-N nylon membrane as described by the supplier. Labeling, hybridization of probes, and DIG detection were performed using the DIG non-radioactive nucleic acid labeling and detection system according to the specifications of the supplier (Roche Diagnostics, Mannheim, Germany).

### 3.2.6 RT-PCR

RT-PCR assays were performed to examine the relative expression levels of the isolated genes in an organ and developmental stage-specific manner. The RT-PCR assays were performed using the reverse transcriptase, *C. therm.* polymerase- (from *Carboxydothermus hydrogenoformans*), and supplied buffer. The "two-step" protocol of the supplier (Roche Diagnostics) was used. The forward primer, 5'RTAseI and the reverse primer, BCHComp2 were used to amplify the 957 bp full-length BCH cDNA fragment (Table 3.1). The first strand synthesis reaction was performed at 50°C, using 0.5-1.0 μg total RNA as template, and the subsequent PCR program was the same as described for the amplification of the internal partial BCH, but using 10% of the first strand reaction as template. Each RNA extraction was done in triplicate, pooled, and

the first-strand reactions were performed in triplicate. The subsequent RT-PCR was also done in triplicate in order to determine the degree of experimental variation.

The primers, BCH-TM-5' and BCH-TM-3', were used for the RT-PCR analysis of the BCH expression in different grapevine tissues (Table 3.1). A product of 800 bp was amplified from cDNA using the same program as described for the BCH1-BCH3 primer pair. Due to the occurrence of introns, these primers will amplify a 1200 bp product from genomic DNA.

The intensity of the bands on the autoradiograms and ethidium bromide stained gels were quantified using a digital camera (Alphalmager 1220; Alpha Innotech Corporation, San Leandro, CA) and densitometry software, AlphaEase v5.5 (Alpha Innotech Corporation).

### 3.2.7 Analysis of transient expression of the β-glucuronidase reporter gene by biolistic bombardment

Surface sterilized (or *in vitro*) plant tissue was bombarded using the Biolistic PDS-1000/He particle delivery system (BioRad) with 1100 p.s.i. rupture discs and the application of 80 kPa vacuum in the chamber. The microcarrier (1.0 μm gold particles) preparation and subsequent DNA-coating was performed as described by the supplier (BioRad). The macrocarrier was spaced 6 mm from the stopping screen and the samples were placed 9 cm from the macrocarrier. The pBS-[CaMV-GUS] plasmid was used as a positive control and the promoterless pBS-GUS was used as a negative control.

All tissue (except *in vitro* material) was surface sterilized by washing in 70% (v/v) ethanol (30 s), followed by gentle agitation in 7% (w/v) Ca-hypochloride (20 min), and thorough rinsing in sterile water. The different plant tissues were bombarded in triplicate and placed on MS-plates and incubated at 23°C (16 h light-8 h dark cycle). Histochemical GUS-staining was performed 24 h and 72 h after bombardment according to Jefferson [31]. The GUS-staining solution contained 0.1 M sodium phosphate buffer (pH 7.0), 1 mM 5-bromo-4-chloro-3-indolyl-ß-D-glucuronic acid, 10 mM EDTA, 0.5 mM $K_3Fe(CN)_6$, 0.5 mM $K_4Fe(CN)_6$ and 0.1% (v/v) Triton X-100. Samples were submerged in this solution at 37°C (in the dark) for at least 24 h.

### 3.2.8 Computer analyses

Intron- and exon splice sites in genomic sequences were predicted using the NetPlantGene server of the Center for Biological Sequence (CBS) Analysis (http://www.cbs.dtu.dk/services/NetPGene/). Transmembrane helices were predicted using the CBS TMHMM server (http://www.cbs.dtu.dk/services/TMHMM/). Subcellular localization of the predicted BCH protein was determined using the CBS TargetP (v1.01) server (http://www.cbs.dtu.dk/services/TargetP/) [32]. Protein and DNA sequences were aligned using ClustalX [33].

### 3.2.9 Plant transformations

The binary vectors, pART27-BCH(S) and pART27-BCH(AS) were mobilized into *A. tumefaciens* strain, EHA105 by triparental mating using the helper plasmid, pRK2013. The BCH gene was transformed into tobacco leaf discs (*N. tabacum* cv Petite Havana SR1) in both the sense- and antisense orientation. The transformation and subsequent regeneration of transgenic tobacco was performed according to the protocol described by Gallois and Marinho [34]. Integration of the expression cassette was verified by Southern blot hybridization.

### 3.2.10 Photosynthetic assays

Parameters of photosynthesis (net carbon assimilation rate, stomatal conductance and transpiration rate) at different constant photosynthetic photon flux density (PPFD) were measured at constant leaf temperature (22°C), 380 $\mu$mol.mol(air)$^{-1}$ $CO_2$, and 60% relative humidity with a portable $CO_2/H_2O$ open gas-exchange system LI-6400 (IRGAs; Li-Cor Inc., Lincoln, NE, USA). Where possible, the gas exchange measurements were conducted on the first five fully expanded leaves with a 6 cm$^2$ leaf chamber and the PPF was generated with a 6400-02B LED light source.

Net assimilation rate-PPFD respondence curves of the different lines were assayed at stepwise change of PPFD from 2000-, 1750-, 1500-, 750-, 500-, 250-, 100-, 50- to 0 $\mu$mol.m$^{-2}$.s$^{-1}$. The net assimilation rate – leaf position curves were assayed at PPFD 2000- and 100 $\mu$mol.m$^{-2}$.s$^{-1}$. All the gas exchange parameter assays were logged three times with at least six replicates.

### 3.2.11 Leaf chlorophyll *a* fluorescence and dark recovery assays

Chlorophyll *a* fluorescence was measured with a Hansatech Fluorescence Monitoring System FMS2 (Hansatech, Pentney, Norfolk, England). Tobacco leaves were dark-adapted for 2 h before the measurements. The initial level of chlorophyll fluorescence ($F_o$) was measured with modulated dim red light. The maximum fluorescence level ($F_m$) was obtained with an 800 ms pulse of 6000 $\mu mol.m^{-2}.s^{-1}$ saturated light. After 45 s an actinic light at a specific PFD was turned on, steady-state fluorescence ($F_s$) and maximum fluorescence in the light ($F_m'$) were noted at regular intervals both before and after the saturated light pulse was introduced. After 9.5 min illumination the actinic light was turned off and a two second pulse of far-red light was applied for the minimum fluorescence in the light ($F_o'$) detection. During darkness for NPQ relaxation and the photosynthetic center recovery assay, the saturated light pulse was applied at a regular interval and maximum fluorescence in the dark ($F^r_m$) was detected. All the chlorophyll fluorescence parameters were measured at room temperature (22°C) on the fifth and sixth fully expanded leaves, with three replicates per reading.

$F_v = F_m - F_o$ is the variable chlorophyll fluorescence, and $F_v/F_m = (F_m - F_o)/F_m$ is the maximum photochemical efficiency of PSII of the dark-adapted leaves. During the light illumination phase, $F_v'/F_m' = (F_m' - F_o)/F_m'$ was calculated to determine the extent of photoinhibition (alternatively, the efficiency of light-capture by PSII). $qP = (F_m' - F_s)/(F_m' - F_o')$ is the photochemical quenching coefficient (reflects the fraction of open PSII traps), and $NPQ = (F_m - F_m')/F_m'$ is the measure of nonphotochemical quenching. During the dark recovery phase, $F^r/F_m = (F_m^r - F_o')/Fm$ was calculated to determine the recovery of the photosynthetic reaction center, and $NPQs = (F_m - F^r_m)/F^r_m$, of the slowly relaxing NPQ was calculated. All the nomenclature was according to van Kooten and Snel [35], Maxwell and Johnson [36] and Peterson and Havir [37].

The PFD-chlorophyll fluorescence parameter response curves were assayed at different actinic PFDs: from 2500-, 2000-, 1500-, 750-, 500-, 250-, 100-, 50- and 25 $\mu mol.\ m^{-2}.s^{-1}$. The stress light illumination and dark recovery was assayed at 2500 $\mu mol.m^{-2}.s^{-1}$. All the different parameters were assayed with three or more replicates and the standard deviation was calculated.

### 3.2.12 Pigment extractions

Leaf pigments were extracted according to the methods described by Britton [38] (with some modifications) and Rock and Zeevaart [39]. Batch samples of four leaf discs of 11 mm in diameter were frozen and ground in liquid nitrogen in 2 ml polypropylene tubes. Pigments were extracted with 500 µl 85% (v/v) methanol (containing 1% (w/v) $Na_2CO_3$) on ice for 30 min, after which an equal volume of diethyl ether and 250 µl of 3 M NaCl were added sequentially. After centrifuging, the ether phase was collected and the water phase was washed twice with 250 µl diethyl ether. The ether phases were pooled, washed twice with water and vacuum-dried below 40°C in the dark. The dried pigment samples were resuspended in 250 µl of hexane for thin layer chromatography (TLC) separation [40], or dissolved in 1 ml methanol for spectrophotometrical assaying of chlorophylls and total carotenoids [41], or diluted with acetonitrile/methanol for HPLC analysis.

A Shimadzu HPLC system (Shimadzu, Columbia, MD) was used to separate and quantify pigments [42]. The HPLC system consisted of a SCL-10A vp system controller, a DGU-12A degasser, a SIL-10AD vp Auto-injector, a SPD-10A vp UV/VIS Detector, a CTO-10AS vp column oven and two LC-10AD vp pumps. Pigments were separated on a Phenomenex 5µ $C_{18}$ (ODS) 250 x 3.0 mm column, protected by a 4 x 3 mm ODS guard column at a flow rate of 1 $ml.min^{-1}$ and with 10 µl injection volume at a column temperature of 40°C. A 22.5 min linear gradient elution profile was used, that consisted of: 4.5 min in solvent A [acetonitrile:methanol, 92.5:7.5 (v/v)], followed by a 0.5 min linear gradient from 0 to 100% of solvent B [methanol:ethyl acetate, 68:32 (v/v)] and kept for 7.5 min running of solvent B at 100%. This was followed by 10 min of solvent A. Pigments were detected at 450 nm. The concentration of each pigment was identified and calculated using standards, published extinction coefficients, and elution profiles [38;42-44]. Authentic β-carotene and zeaxanthin standards were purchased from Sigma-Aldrich (Steinheim, Germany) and Roth (Karlsruhe, Germany), respectively.

Diurnal changes in leaf pigments were assayed by sampling leaf discs of plant lines grown in a greenhouse under low light intensity (peak PFD of 200-400 $\mu mol.m^{-2}.s^{-1}$) for six weeks, and then transferred to natural light conditions (peak PFD of 1500-1700 $\mu mol.m^{-2}.s^{-1}$) for one day. Six leaf discs (11 mm in diameter), with three

replicates of the 4th, 5th and 6th fully-expanded leaves were cut at predawn (06h00), noon (12h00), and afternoon (16h00). The leaf discs were frozen in liquid nitrogen, pigments were extracted under dim light and detected at 450 nm. Each value represents the mean of three individual plants, and three samples were analyzed for each.

### 3.2.13 Thylakoid isolation and D1 protein immunoblotting

Leaf discs of different tobacco lines were dark-adapted for 12 h to $F_v/F_m$ around 8.4 for all of the WT, SL (BCH-sense lines) and ASL (BCH-antisense lines), and then incubated in 2 mmol lincomycin (Sigma) for 2 h under dim light (PFD<5 $\mu mol.m^{-2}.s^{-1}$). After exposure to strong light (PFD: 1600-1750 $\mu mol.m^{-2}.s^{-1}$) for 0-, 0.5-, 1.0-, 1.5-, 2.0-, and 3.0 h, the leaf discs were transferred to low light (PFD: 20-30 $\mu mol.m^{-2}.s^{-1}$) for 6 h, frozen in liquid nitrogen and stored at –80°C until isolation of the thylakoid membranes. Three replicates were taken for each of the treatments.

Thylakoid membranes were isolated according to Rintamaki *et al.* [45]. Thylakoid polypeptides were separated by SDS-PAGE using a 12% (w/v) polyacrylamide gel containing 6 M urea according to Yamamoto and Sotah [46]. Two micrograms of chlorophyll was loaded per well. The polypeptides were transferred to a Hybond-C extra nitrocellulose membrane (Amersham-Pharmacia Biotech) and the D1 protein was detected with the primary D1 antibody using an enhanced chemiluminescence (ECL) western blotting analysis system (Amersham-Pharmacia Biotech). The D1 antibody was obtained from Y. Yamamoto, and is described in Yamamoto and Sotah [46]. Each D1 protein band on the x-ray film was scanned and converted to total gray using the AlphaEase software. Protein intensities were normalized relative to chlorophyll *a* (assayed spectrophotometerically according to Lichtenthaler, 1986 [41]). Following the different treatments the relative abundance of the D1 protein was normalized relative to the dark-adapted, 0 h light-illuminated samples.

## 3.3 RESULTS

### 3.3.1 Isolation and sequence analysis of the *Vitis vinifera* BCH gene

Construction and screening of two sub-genomic libraries (*Eco*RV and *Pst*I) lead to the isolation of two clones that collectively contained the entire BCH encoding gene, as well as the putative promoter and downstream flanking sequences. The 5.0 kb *Pst*I and

5.6 kb *Eco*RV genomic fragments overlap by approximately 1.6 kb, giving a genomic sequence that spans 4.5 kb upstream of the putative ATG, and 3.5 kb downstream of the putative stop codon of the BCH gene. The BCH genomic sequence is 1.7 kb (from the putative ATG to the stop codon) and contains seven exons (and, therefore, six introns). The translated genomic BCH sequence was aligned to protein sequences in the NCBI database using the BLASTX algorithm [47], and the grapevine BCH showed stretches of high homology to other plant BCHs in the database. The genomic sequence was further submitted to the CBS NetPlantGene server for intron-exon splice site prediction. Six intron-exon splice sites were predicted (with at least 96% confidence) that also corresponded to the gaps generated by the BLASTX alignments. These intron-exon junctions were confirmed by aligning the BCH genomic sequence to the BCH cDNA sequence obtained. Southern hybridizations of genomic DNA digested with a range of restriction enzymes showed that the BCH gene is present as a single-copy in the grapevine genome (Fig. 3.2).

The CBS TMHMM server predicted four transmembrane helices in the theoretical translated BCH sequence that corresponds to the highly conserved transmembrane helices found in other plant BCHs, as reported by several authors [15;48] (Fig. 3.4), and suggests that the BCH enzyme is membrane-associated.

A putative chloroplast transit peptide was predicted in the BCH amino acid sequence (by the CBS TargetP server), and the the subcellular localization is, therefore, most likely the chloroplast. This is to be expected from carotenoid biosynthetic genes that are nuclear-encoded but functional in the chloroplast.

ClustalX alignments of the predicted BCH protein sequence (obtained by translating the cDNA sequence) to all complete plant BCH protein sequences in the NCBI database, showed the homology of the grapevine BCH to be between 65% (to the *Tagetes erecta* BCH) and 69% (to the *Lycopersicon esculentum* BCH) (Fig. 3.3). If the predicted transit peptides are omitted, however, the percentage homology increases to 75% and 77% for *T. erecta* and *L. esculentum*, respectively (data not shown).

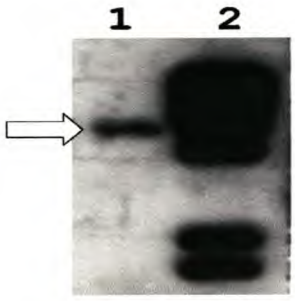


Figure 3.2. Southern hybridization of *Vitis vinifera* L. cv. Pinotage genomic DNA digested with *Eco*RV and separated in an agarose gel. The DNA was transferred to nylon membranes and probed with the DIG-labelled β-carotene hydroxylase (BCH) gene. Lane 1, genomic DNA; lane 2, DNA molecular weight marker (λ DNA digested with *Bst*EII). The open arrow indicates the single copy BCH gene of 5.6 kb.

```
Lycopersicon    MAAAARISASSTSRTFYFRHSPFLGPKPTSTTSHVSPISPFSLNLGPILRSRRKPSFTVC 60
Capsicum        --MAAEISISASSRAICLQRNPFPAPKYFATAPPLLFFSPLTCNLDAILRSRRKPRLAAC 58
Tagetes         --MAAAIAVPCSSRPFGLGRMRLLGHKPTTITCHFPFSFSIKS-FTPIVRGRR---CTVC 54
Arabidopsis     --MAAGLSTIAVTLKP-LNRSSFSANHP---ISTAVFP-PSLRFNG----FRRRKILTVC 49
Vitis           --MATGISASLNSMSRRLGRNSFTATGPSSVISLSSFLTPVTHLKGNIFPLQRRRSLKVC 58

Lycopersicon    FVLEDEKLKPQFDDEAEDFEKK--------IEEQILATRLAEKLARKKSERFTYLVAAIM 112
Capsicum        FVLKDDKLYTAQSGKQSDTEAIGDEIEVETNEEKSLAVRLAEKFARKKSERFTYLVAAVM 118
Tagetes         FVAGGDSNSNSNNNSDSNSNNPGLDLN---PAVMNRNRLVEEKMERKKSERFTYLVAAIM 111
Arabidopsis     FVVEERKQSSPMDDDNKPESTTS-------SSEILMTSRLLKKAEKKKSERFTYLIAAVM 102
Vitis           LVLEKKIEDGIEIEDDSPESSNR-------ASERLAR---------KKAERYTYLVAAMM 102

Lycopersicon    SSFGITSMAVMAVYYRFSWQMEGGEVPVTEMLGTFALSVGAAVGMEFWARWAHKALWHAS 172
Capsicum        SSLGITSMAVISVYYRFSWQMEGGEMPFSEMFCTFALAFGAAIGMEYWARWAHRALWHAS 178
Tagetes         STFGITSMAVMAVYYRFSWQMEGGEIPYVEMFGTFALSVGAAVGMEYWARWAHEALWHAS 171
Arabidopsis     SSFGITSMAIMAVYYRFSWQMKGGEVSVLEMFGTFALSVGAAVGMEFWARWAHRALWHDS 162
Vitis           SSLGITSMAIVAVYYRFSWQMEGGEIPVLEMLGTFALSVGAAVGMEFWARWAHKALWHAS 162

Lycopersicon    LWHMHESHHKPREGPFELNDVFAITNAVPAIALLNYGFFHKGLIAGLCFGAGLGITVFGM 232
Capsicum        LWHMHESHHRPREGPFELNDIFAIINAVPAIAFFSFGFNHKGLIPGICFGAGLGITVFGM 238
Tagetes         LWHMHESHHKPREGPFELNDVFAITNAVPAIALLSYGFFHKGIIPGLCFGAGLGITVFGM 231
Arabidopsis     LWNMHESHHKPREGAFELNDVFAITNAVPAIGLLYYGFLNKGLVPGLCFGAGLGITMFGM 222
Vitis           LWHMHESHHRPREGPFELNDVFAIINAVPAISLLSYGLFNKGLVPGLCFGAGLGITVFGM 222

Lycopersicon    AYMFVHDGLVHKRFPVGPVANVPYLRKVAAAHSLHHSEKFNGVPYGLFFGPKELEEVGGT 292
Capsicum        AYMFVHDGLVHKRFPVGPIAKVPYFQRVAAAHQLHHSDKFDGVPYGLFLGPKELEEVGVI 298
Tagetes         AYMFVHDGLVHRRFQVGPIANVPYLRRVAAAHQLHHTEKFNGVPYGLFLGPKELEEVGGT 291
Arabidopsis     AYMFVHDGLVHKRFPVGPIANVPYLRKVAAAHQLHHTDKFKGVPYGLFLGPKEVEEVGGK 282
Vitis           AYMFVHDGLVHRRFPVGPIANVPYLRKVASAHQLHHSDKFNGVPYGLFLGPMELEEVGGM 282

Lycopersicon    EELEKEVIRRTRLSKGS---- 309
Capsicum        EELEKEVNRRIKSLKRL---- 315
Tagetes         EELDKEIQRRIKLYNNTK--- 309
Arabidopsis     EELEKEISRRIKLYNKGSSTS 303
Vitis           EELEKEINRRIKSSD--SS-- 299
```

Figure 3.3. Multiple alignment of the predicted amino acid sequence of the isolated *Vitis vinifera* β-carotene hydroxylase (BCH) gene to the BCH protein sequences of *Lycopersicon esculentum* (CAB55625), *Capsicum annuum* (CAA70427), *Tagetes erecta* (AAG10430), and *Arabidopsis thaliana* (NP_200070). (*), indicates identical amino acid residues; (:) indicates similar amino acid residues.

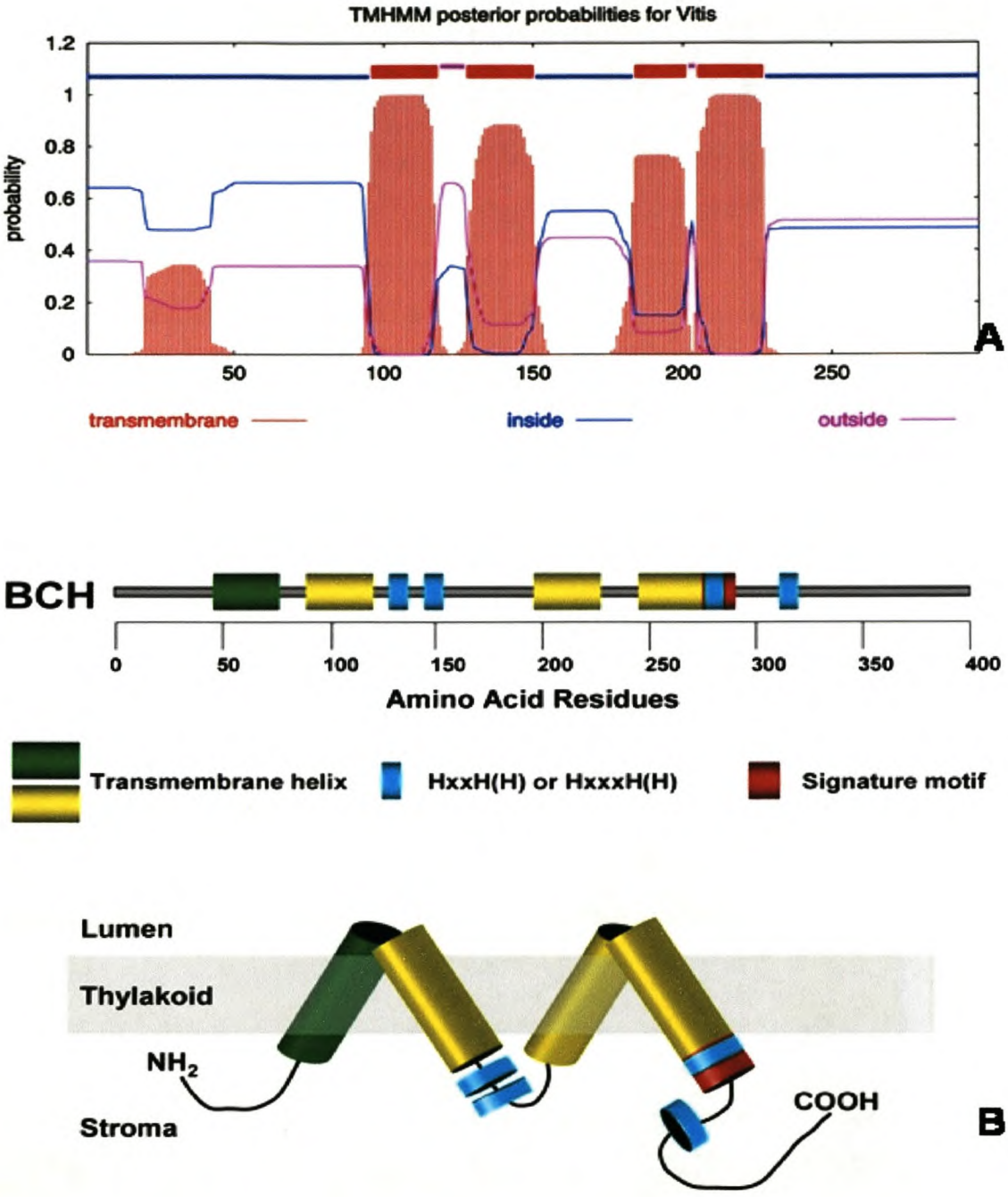


Figure 3.4. (A) Hydropathy plot for the predicted *Vitis vinifera* β-carotene hydroxylase (BCH) protein sequence. (B) The putative folding in the thylakoid membrane can be deduced from the predicted transmembrane helices. The dark green stretch represents a transmembrane helix that occurs only in plants, the yellow stretches represent transmembrane spanning regions found in all carotene hydroxylases (bacteria, fungi, algae and plants). The light blue stretches are histidine repeats that are crucial for the functioning of the enzyme. The red area is a highly conserved stretch of amino acids found in all β-carotene hydroxylases (adapted from Cunningham and Gantt [15]).

### 3.3.2 RT-PCR mediated amplification of a full-length cDNA copy of the BCH-encoding gene from grapevine

RT-PCR primers used were designed using the predicted coding sequence (i.e. the ATG and STOP codon positions) in the BCH genomic sequence. RT-PCR from Pinotage cDNA yielded a 957 bp fragment that corresponded in size to the predicted full-length cDNA copy of the gene. This product was isolated, cloned and sequenced. Alignments of the BCH genomic- and sequenced cDNA copy confirmed the predicted intron-exon splice sites (from the CBS NetPlantGene server). The *V. vinifera* BCH cDNA sequence was submitted to GenBank (accession number, AF499108).

### 3.3.3 Expression analysis of the grapevine BCH

Northern blot analysis of BCH expression using total RNA from different grapevine organs was unsuccessful, possibly due to the low levels of the BCH transcript, as has been reported by other authors [14;49]. RT-PCR analysis was used to study the expression of the BCH encoding gene in grapevine. The more sensitive RT-PCR assay detected BCH transcripts in all the grapevine organs tested (flowers, berries, shoot tips, leaves and roots) albeit at very low levels. The highest transcript levels were detected in leaves and the lowest levels in ripening berries (Fig. 3.5). Flowers also yielded high transcript levels (data not shown).

Induction of the BCH transcript levels was also analyzed during wounding. Detached field-grown leaves were wounded (using a pincer) and the relative expression of the BCH gene was measured by RT-PCR. There was an observable upregulation of the gene after one hour (after the treatment), relative to a control leaf, but the expression after 24 hours was similar to the control plant. The two genes that were used for normalization are constitutively expressed, and are used as internal standards for quantitative RT-PCR experiments [50]. Two genes were used as standards in order to provide independent data for the subsequent normalization. As would be expected, the absolute values obtained from the cDNA pools tested for the expression of these two genes differed. The relative amounts of the two genes were however similar, and the subsequent normalized trends were also in close agreement (Fig. 3.5).

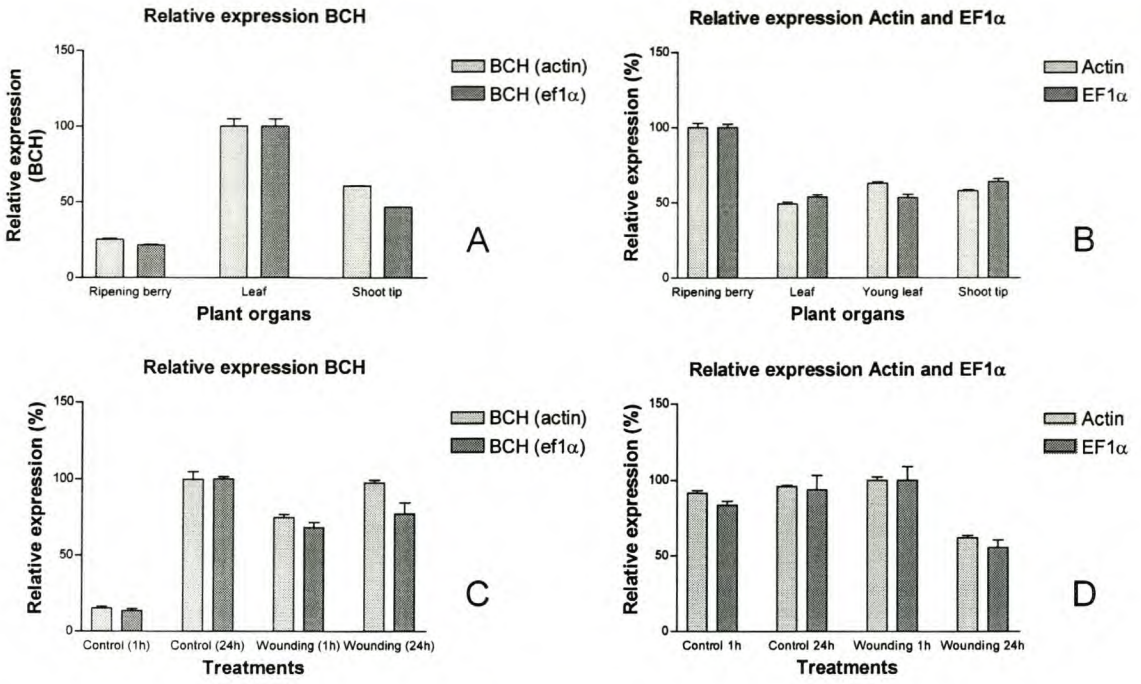


Figure 3.5. RT-PCR analysis of the relative expression of the β-carotene hydroxylase (BCH) encoding gene of *Vitis vinifera* in (A) ripening berries, fully-expanded leaves and shoot tips; and (C) leaves 1 h and 24 h after a wounding treatment. The data for (A) and (C) were normalized against the constitutively expressed actin gene, as well as the elongation factor (ef)-1α gene. (B) and (D) show the expression levels of the actin and ef1α gene in the different cDNA pools used for the analyses. Data are represented as a percentage with the 0% corresponding to 0.0, and 100% corresponding to the expression with the highest value. Each data set represents the mean of three values.

### 3.3.4 Heterologous functional complementation in *Escherichia coli*

The expression vector, pET-BCH was co-transformed with the carotenoid-accumulating plasmid, pAC-BETA into *E. coli* to confirm the functionality of the grapevine BCH. The expressed BCH gene converted β-carotene to zeaxanthin (via the intermediate, β-cryptoxanthin) as shown by TLC and confirmed by HPLC (data not shown).

### 3.3.5 Transient promoter analysis

The expression of the BCH transcript is very low in grapevine and can only be detected by RT-PCR. This result was further supported by the apparent inability of the putative promoter fragments to drive GUS expression in transient reporter gene expression assays. *N. tabacum* and *V. vinifera* leaves, as well as the fruits of *V. vinifera*, *L. esculentum*, and *C. annuum* (both the flesh and the skin, separately) were

bombarded with the different promoter constructs, yet no GUS activity was detected in any of the analyzed tissue after histochemical staining (following both 24 and 72 hours of incubation). The expression of the GUS gene by the constitutive (strong) CaMV 35S promoter served as a positive control, and consistently yielded GUS-producing blue spots. Likewise, the promoterless negative control showed no blue spots.

### 3.3.6 Plant transformations

After *Agrobacterium*-mediated transformation and selection of putative transformants under selective conditions, integration of the BCH gene was verified in 23 primary transformant ($T_o$) lines by Southern blot analysis. Copy number varied between one and three copies (data not shown). Of these 23 primary transformants, only three of the sense lines (10.6S, 10.17S, and 10.18S) and two antisense lines (8.3A, 8.6A), expressed the heterologous BCH gene as shown by northern hybridizations (Fig. 3.6). The $T_1$-progeny seeds from the selfed $T_0$-plants were harvested from these five primary transformant lines.

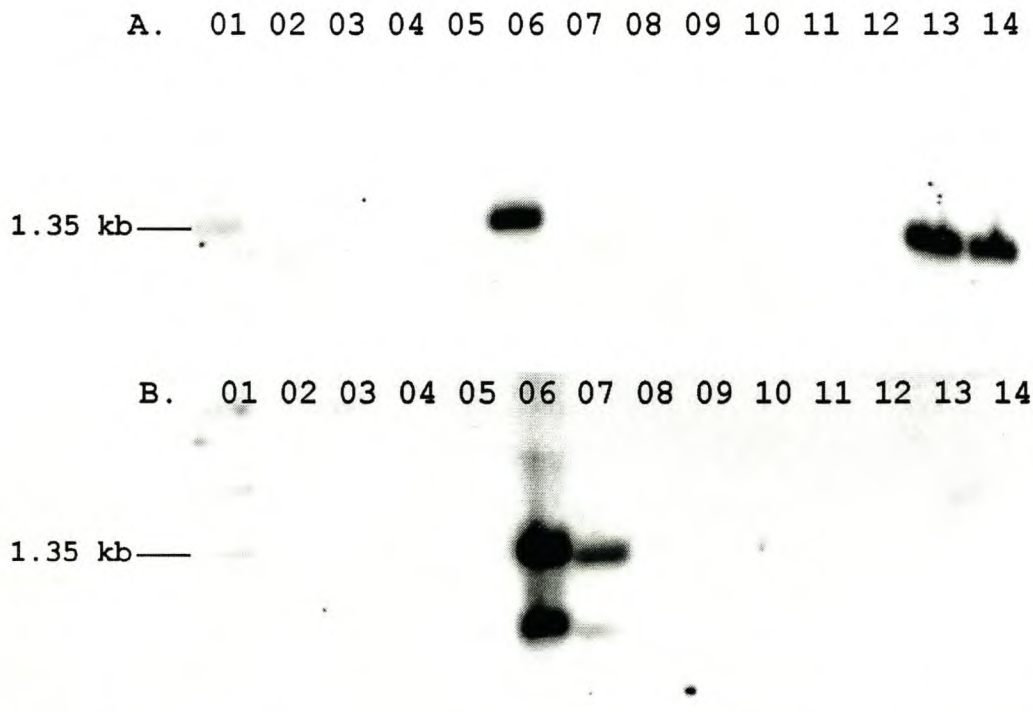


Figure 3.6. Expression of the *Vitis vinifera* β-carotene hydroxylase (BCH) gene in (A) the sense orientation and, (B) the antisense orientation in transgenic *Nicotiana tabacum* lines (T1-progeny). Lane 1, 0.24-9.5 kb RNA molecular weight marker ; Lane 2, total RNA from wild-type *N. tabacum*; Lanes 3-14, total RNA from putative transgenic T1-plants probed with the DIG-labelled BCH gene.

### 3.3.7 The overexpression of the grapevine BCH gene in tobacco $T_1$-seedlings increases the xanthophyll pigment pool, but the leaf pigment content remains unaltered

HPLC was used to assay the changes in the leaf photosynthetic pigments of the WT-, BCH-SL and BCH-ASL. Three plants of each plant line were assayed. Since the pigment profiles of the three BCH-SL plants were indistinguishable, only one plant line per construct was evaluated. The different tobacco transformants were acclimated to relatively low light conditions, and their ability to cope with a sudden exposure to full sunlight was subsequently evaluated. The tobacco control-, S- and AS-lines were grown under peak PFD of 400 $\mu mol.m^{-2}.s^{-1}$ for 10 weeks and then shifted to natural outdoor light conditions with peak PFD at midday of 1700-1800 $\mu mol.m^{-2}.s^{-1}$ (during winter in Stellenbosch, 20°C) to assay the diurnal pigment changes. The diurnal pigment changes revealed that the overexpression of the grapevine BCH in tobacco alters the xanthophyll pool without significantly altering the β-carotenoids (mainly β-carotene) and α-carotenoids (mainly lutein) content in leaves (Fig. 3.7 and data not shown). The xanthophyll pool size in the leaves of the BCH-SL increased by approximately 15-20% after illumination with sunlight (compared to the WT), while the BCH-ASL xanthophyll pool decreased by 5-15%. No significant differences in any of the other pigments were observed between the different plant lines (data not shown).

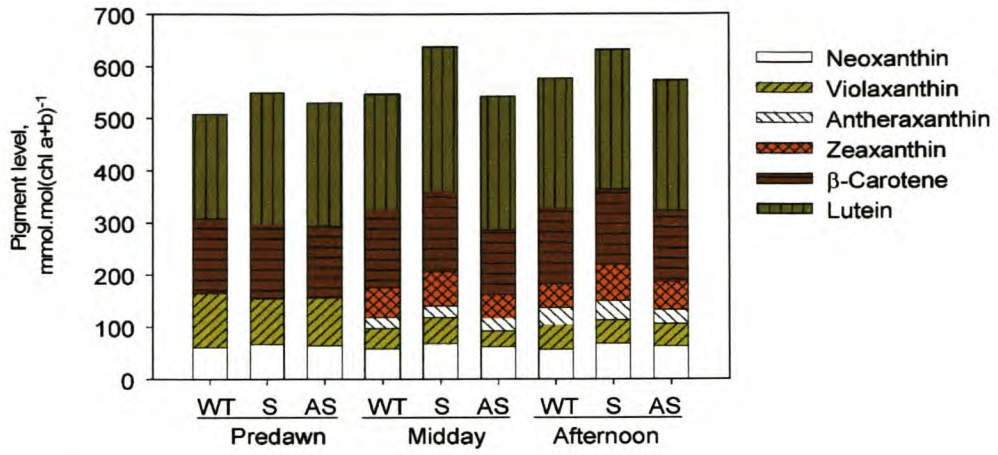


Figure 3.7. Diurnal changes in the pigment levels of tobacco lines transformed with the *Vitis vinifera* β-carotene hydroxylase (BCH) gene. The BCH sense (S), antisense (AS), and wild-type (WT) plant lines were grown in a greenhouse under low light intensity (peak PFD of 200-400 $\mu mol.m^{-2}.s^{-1}$) for six weeks, and then transferred to natural light conditions (peak PFD of 1750 $\mu mol.m^{-2}.s^{-1}$) for one day. Six leaf discs (11 mm in diameter), with three replicates of the 4$^{th}$, 5$^{th}$ and 6$^{th}$ fully-expanded leaves were cut at predawn (06h00), noon (12h00), and afternoon (16h00). The leaf discs were frozen in liquid nitrogen, pigments were extracted under dim light and detected at 450 nm. Each value represents the mean of three individual plants, and three samples were analyzed for each.

### 3.3.8 Expression of a grapevine BCH alters the photosynthetic characteristics in transgenic tobacco

Photosynthetic parameters were determined by using a fluorometer and gas exchange system. In Fig. 3.8 the photochemical quenching coefficient (qP) and electron transport rate (ETR) distribution is illustrated. Relative to the WT, both the net assimilation rate and stomatal conductance were altered in the BCH transformants. The qP coefficient reflects the proportion of excitations captured by open traps being converted to chemical energy in the PSII reaction center [16], alternatively it indicates the proportion of open PSII reaction centers [36]. At low light intensity (100 $\mu mol.m^{-2}.s^{-1}$), there were no observable differences in the open PSII reaction centers of the three tobacco lines (data not shown). Illumination with high light (2500 $\mu mol.m^{-2}.s^{-1}$), however, caused an increase in both the qP and ETR of the BCH-SL (relative to both the WT and BCH-ASL) (Fig. 3.8). After prolonged illumination (>5 min) the qP and ETR values of the BCH-ASL dropped below that of the WT.

The saturation PFD for all three tobacco lines was approximately 250 μmol.m$^{-2}$.s$^{-1}$. The net assimilation rates of the BCH-SL and the WT remained relatively stable from 250- to 2000 μmol.m$^{-2}$.s$^{-1}$, while a decrease was observed in the BCH-ASL. Stomatal conductance showed a double-sigmoidal increase with an increase in the PFD in both the BCH-SL and WT tobacco, and an as yet unexplainable linear decrease in the ASL.

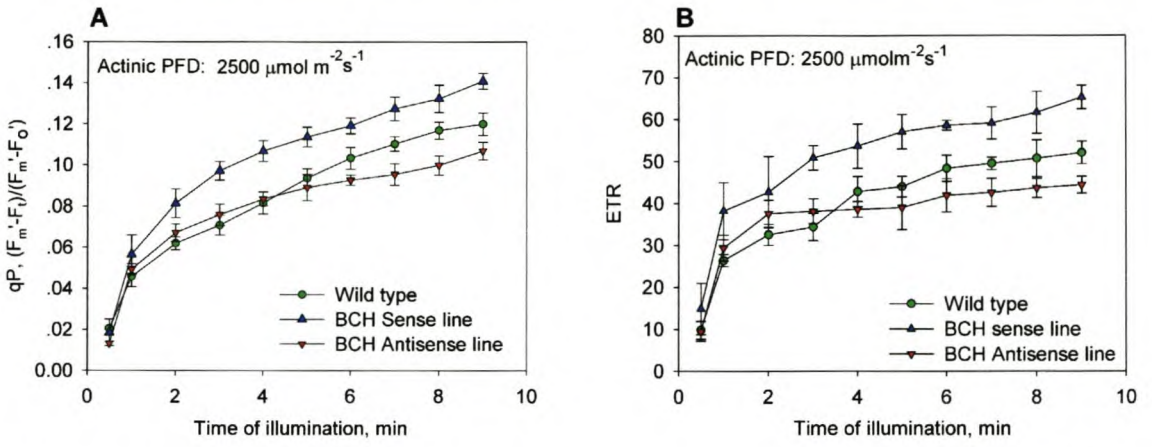


Figure 3.8. Chlorophyll *a* fluorescence time response curves of tobacco lines transformed with the *Vitis vinifera* β-carotene hydroxylase (BCH) gene. The different tobacco lines include the BCH -sense [S], -antisense [AS], and wild-type [WT] lines. Tobacco leaves from 6 and 10 week old plants were dark adapted for 2 h before fluorescence measurements. The initial fluorescence ($F_o$) was measured with a modulated dim red light. The maximal fluorescence level ($F_m$) was obtained with a saturating pulse (duration of 800 ms) of 6000 μmol.m$^{-2}$.s$^{-1}$. After 45 s, an actinic light (2500 μmol.m$^{-2}$.s$^{-1}$) was switched on and the steady-state fluorescence ($F_s$) and the maximum fluorescence in the light ($F_m$') were collected at regular intervals before and after the saturating light pulse. A, photochemical quenching (qP) and B, electron transport rate (ETR) were recorded and the mean value was calculated from three independent assays of different plants.

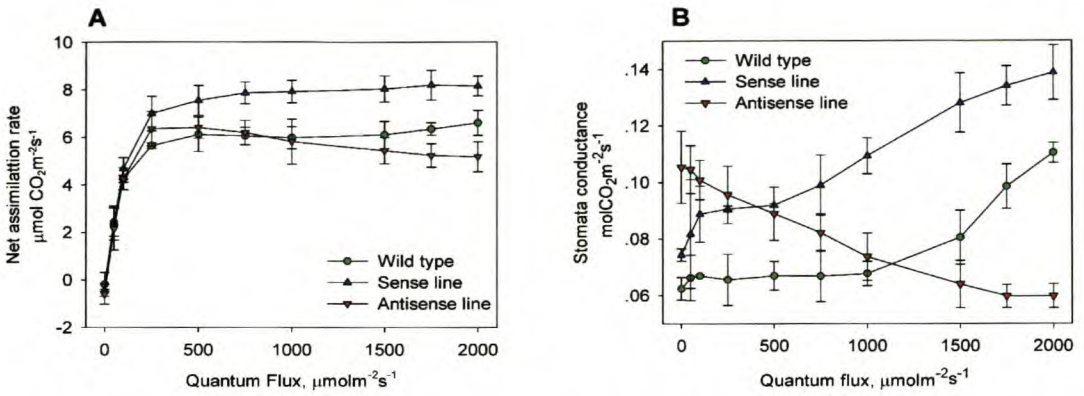


Figure 3.9. Photosynthetic parameters of tobacco lines transformed with the *Vitis vinifera* β-carotene hydroxylase (BCH) gene. The different tobacco lines include the BCH -sense [S], -antisense [AS], and wild-type [WT] lines. Greenhouse grown tobacco (6 and 10 week old) was assayed with a portable $CO_2/H_2O$ open gas-exchange system. The gas exchange measurements were conducted on the first five fully-expanded leaves in a 6 $cm^2$ leaf chamber (at constant leaf temperature of 22°C and reference $CO_2$ at 380 μmol.mol (air)$^{-1}$. After the water vapour pressure and $CO_2$ concentration stabilized, the net assimilation rate and stomatal conductance of the leaves of three independent plants were measured in triplicate.

### 3.3.9 Tobacco overexpressing BCH are more resistant to excess high light induced photoinhibition

Fig. 3.8 and 3.10 illustrates the main results of the chlorophyll *a* fluorescence parameters gained from the dark recovery process of the high light/short time illuminated tobacco leaves (at both vegetative- and flowering stages). After 5 minutes of high light illumination (2500 μmol photons.$m^{-2}$.$s^{-1}$), both the photochemical quenching (qP) and the electron transport rate (ETR) of the BSH-SL was significantly higher than the wild-type plants, which was in turn higher than the BCH-ASL plants. This trend was not seen with low light illumination (up to 1000 μmol photons.$m^{-2}$.$s^{-1}$), where the measurements of the different plant lines were indiscernible. The BCH-SL and -ASL differed in both the PSII reaction center recovery rate (Fig. 3.10a,b) and the long term NPQ relaxing (Figure 3.10c,d). With the BCH-SL tobacco plants recovering at a faster rate than the untransformed control plants

### 3.3.10 D1 protein damage and turnover

The D1 protein is one of the core proteins in the PSII reaction center, and has an unusually high light-dependent turnover rate due to its susceptibility to photodamage. The photosynthetic apparatus can only regain functionality by the *de novo* synthesis and

replacement of the D1 protein in the photosynthetic reaction center [51;52]. Fig. 3.11 represents the degradation of the D1 protein in tobacco leaf discs treated with full sunlight (1650-1700 μmol.m$^{-2}$.s$^{-1}$) and lincomycin. When the D1 protein synthesis and reassembly was blocked by lincomycin,however, the levels of the D1 protein in the BCH-SL was higher than both the WT and the BCH-ASL.

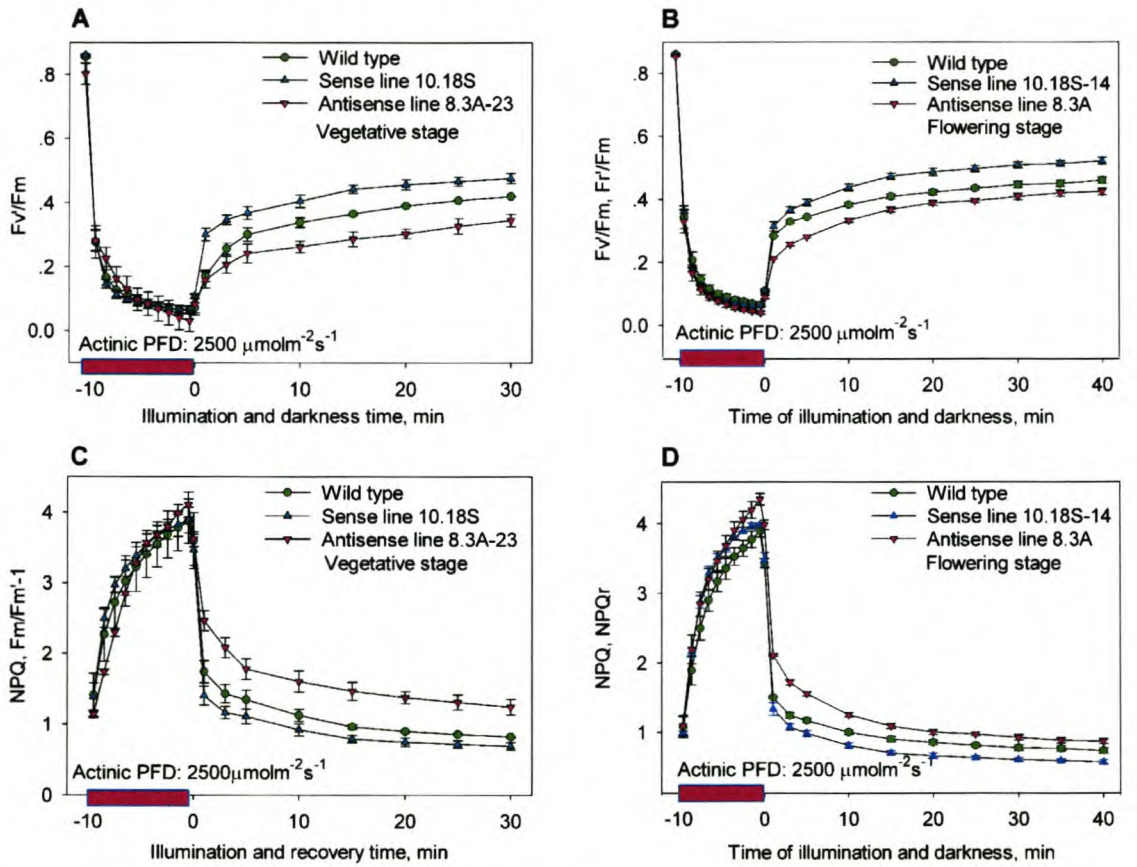


Figure 3.10. Long term dark recovery of the active photosynthetic reaction centers (Fr'/Fm') and the slow relaxing of NPQ of tobacco lines transformed with the *Vitis vinifera* β-carotene hydroxylase (BCH) gene. The different tobacco lines are the BCH-sense [S], -antisense [AS], and wild-type [WT] lines at different developmental stages (A and C, vegetative; B and D, flowering). The measurements and the pretreatments of the leaves were the same as in Fig. 3.8. After illumination, the actinic light was turned off and a 2 s pulse of far-red light was used to calculate the minimum fluorescence in the light (Fo'). Following this the saturating light pulse was applied at regular intervals and the maximum fluorescence in the dark (Fmr) was detected. A and B, the recovery of the active photosynthetic centers calculated as Fr/Fm=(Fmr-Fo')/Fm; C and D, the slow relaxing NPQ was calculated as NPQs=(Fm-Frm)/Frm. All the chlorophyll fluorescence parameters were measured on the 5$^{th}$ and 6$^{th}$ fully-expanded leaves in triplicate at room temperature (22°C).

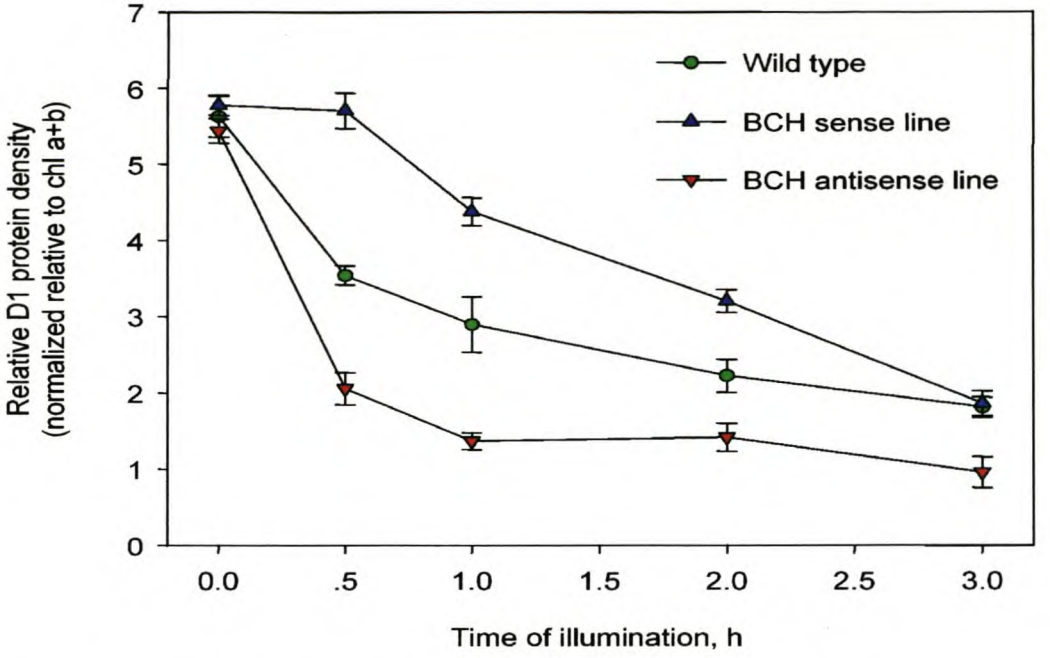


Figure 3.11. D1 protein damage and turnover of tobacco lines transformed with the *Vitis vinifera* β-carotene hydroxylase (BCH) gene. The different tobacco lines include the BCH -sense [S], -antisense [AS], and wild-type [WT] lines. Leaf discs of the different tobacco lines were dark-adapted for 12 h (until a Fv/Fm ratio of 8.4 was obtained) before incubation in 2 mmol lincomycin for 2 h under dim light (PFD < 5 μmol $m^{-2}$ $s^{-1}$). After exposure to strong light (PFD = 1600-1750 μmol.$m^{-2}$.$s^{-1}$) for 0, 0.5, 1, 1.5, 2, and 3 h, the leaf discs were transferred to low light (PFD: 20-30 μmol.$m^{-2}$.$s^{-1}$) for 6 h, and frozen in liquid nitrogen until isolation of the thylakoid membranes. The equivalent of 2 μg of total chlorophyll was loaded onto a 6 M urea-SDS PAGE (12%) for electrophoretic separation of the proteins. Immunoblotting of the D1 protein with the primary D1 antibody and an enhanced chemiluminescence (ECL) western blotting analysis system was used to determine the mature D1 protein. The resultant D1 protein bands from the x-ray film were scanned, and digitally converted into total optical density. The final data was normalized using the total chlorophylls loaded. Each data point represents the mean of 3 replicates.

## 3.4 DISCUSSION

The BCH gene has been isolated from *V. vinifera* L. Pinotage. The *V. vinifera* genome contains only a single copy of the BCH gene, unlike *Arabidopsis* where two functionally redundant copies occur (Fig. 3.2) [14].

Determining the expression patterns of the BCH gene in *V. vinifera* proved to be problematic. The levels of the BCH transcript were not detectable using northern blot analyses of RNA from different grapevine tissue and during different developmental

stages. The more sensitive RT-PCR method proved more successful and the BCH transcripts were detected in all tissues and stages tested. The normalization of the RT-PCR products relative to the constitutively expressed actin and EF1α genes, although useful for identifying general trends in expression, is not sufficient for absolute quantitation. The trends showed that the *V. vinifera BCH* gene has the highest levels of expression in leaves and the lowest level in the berries. It is possible that the level of expression is correlated to the photosynthetic potential of the organs tested (Fig. 3.5). These observed trends will have to be reassessed using a quantitative approach and including additional biological repeats into the experiment. Analysis of the BCH promoter also suggested that the transcriptional levels of the BCH gene are low (i.e. below the level of the GUS histochemical detection threshold). It is possible that the 2.0 kb 5'-flanking sequence tested does not contain the entire promoter, and is therefore not capable of driving transcription of the reporter gene. Although upregulation of the BCH transcript levels have been shown, this is only during the transition from chloroplasts to chromoplasts in *Capsicum annuum* [49]; or from etioplasts to chloroplasts in *N. tabacum* [53]. It is possible that the BCH gene is not transcriptionally regulated in leaves, and that regulation then occurs at either the translational and/or post-translational level [7]. Additional protein and enzyme work will be required to address this issue.

The predicted protein sequence of the BCH gene (deduced from the cDNA sequence), has all the characteristics expected of a carotene hydroxylase. The predicted transit peptide localizes the enzyme to the chloroplast, and the four predicted transmembrane helices (that are conserved in all plant BCHs), indicate that the enzyme is membrane-associated (most likely the thylakoid). A conserved protein domain ("carotene hydroxylase"), as the name indicates, is common to all carotene hydroxylases and is detected in the amino acid sequence (Fig. 3.3 and 3.4).

Light harvesting systems are structurally flexible and are able to alternate between two functional states - light harvesting under photosynthetically favourable conditions, and dissipation of excess light energy (as heat) under unfavourable conditions. PSII is particularly vulnerable to light-induced damage, and the first sign of stress to a plant is typically damage to PSII. The ability of the different transgenic tobacco lines (expressing BCH) to cope with high light stress was evaluated by chlorophyll *a*

fluorescence measurements. Differences between the different transgenic lines could not be seen under low (or limiting) light conditions (i.e. up to 1000 $\mu mol.m^{-2}.s^{-1}$), under high light conditions (up to 2300 $\mu mol.m^{-2}.s^{-1}$), however, the BCH-SL performed better photosynthetically.

The proportion of PSII reaction centers that are open is reflected by the fluorescence parameter, qP. The BCH-SL showed a higher qP value than both the wild-type and the BCH-ASL (Fig. 3.8a). The linear electron transport rate (ETR) showed the same trend with the BCH-SL performing better (Fig. 3.8b). This seems to indicate that under high light stress conditions the BCH-SL had more oxidized $Q_A$, and the BCH-ASL had more reduced $Q_A$ (relative to the WT, respectively). The capacity for active electron transport in the BCH-SL was therefore increased under high light stress conditions. The qP and ETR fluorescence parameters were substantiated by both $CO_2$ assimilation and stomatal conductance experiments (Fig. 3.9a and b). The BCH-ASL displayed an unexpected sharp linear decrease in stomatal conductance that can not be explained. Alterations in the BCH-ASLs levels of abscisic acid might be responsible for this observation, but will require further investigation before a conclusion can be drawn.

Cumulatively, these measurements illustrate that the BCH-SL plants are photosynthetically active under conditions that caused photoinhibition in both the wild-type and BCH-ASL. Zeaxanthin plays an important role in quenching excited chlorophyll and reactive oxygen species that are formed under high light conditions when the absorbed energy is in excess of that which can be used by photosynthesis. Violaxanthin de-epoxidase (VDE) is activated by the resultant trans-thylakoid $\Delta pH$ gradient, which then facilitates the rapid conversion of violaxanthin to zeaxanthin [54]. The BCH-SL plants possess a functional xanthophyll cycle (that will convert violaxanthin to zeaxanthin when VDE is activated), as well as the additional zeaxanthin formed by the overexpression of the BCH gene. It would, therefore, seem as if this additional zeaxanthin provides additional protection to the tobacco plants under high light stress conditions. The conversion of $\beta$-carotene to zeaxanthin by BCH, seems to occur in the wild-type as well, since the photosynthetic activity of the BCH-ASL plant lines was lower than both the BCH-SL and the wild-type plants, and this suggests that it is not exclusively the activity of VDE that provides the zeaxanthin required for photoprotection but, to a lesser degree, also BCH.

The changes in pigment levels observed in the BCH-SL were consistent with the results obtained from tobacco transformed with a bacterial BCH gene [55], but differed from the observations in *A. thaliana* overexpressing the native BCH (*chy*B) gene, where the xanthophyll pool was effectively doubled [21]. Even the observed relatively small changes in the pigment levels of the BCH-SL, and –ASL had a significant effect on the plants photosynthetic capacity under high-light stress conditions (Fig. 3.7). It is important to note that the xanthophyll cycle carotenoids are flexible and constantly adjust in response to light conditions. These responses can occur daily and/or seasonally and, furthermore, can vary between sun- and shade leaves [5]. These trends could be seen in the pigment profiles of the different plant lines measured at different times of the day (corresponding to different light intensities), and compounded the analysis of carotenoid changes in the transgenic plants evaluated in this study (Fig. 3.7).

Under high light conditions, light energy is absorbed by the light harvesting pigment-protein complexes (LHCs). Some of this absorbed light energy is utilized to drive the photochemical reaction (photochemical quenching, qP), the excess light energy is typically re-emitted as chlorophyll fluorescence, and needs to be dissipated by a thermal release process (e.g. NPQ). NPQ consists of at least three parts: (i) energy-dependent quenching (qE), (ii) state transition (qT), and (iii) photoinhibition (qI) [16;56]. Although qE is the major component of NPQ under most conditions; decreases in PSII fluorescence due to both qT and qI may also contribute to what is measured as NPQ. These different quenching processes have different relaxation times, ranging from a few minutes to several hours. The kinetics of the relaxation of these processes is used to distinguish these components from each other [16;36;56]. The BCH-SL and -ASL differed in both their long term NPQ relaxing, and the PSII reaction center recovery rate. This indicates that the additional BCH (and, therefore, the additional zeaxanthin) assists the plants existing photoprotective system under saturating light conditions. The kinetics of the relaxation of qI and the efficiency of PSII recovery (Fv/Fm) can be correlated to the damage to PSII reaction center [57]. These data suggests that the degree of damage to the PSII reaction center (due to photoinhibition under light stress condiions) is significantly altered in the transgenic plant lines. Since the kinetics of the relaxation of qI and the efficiency of PSII recovery (Fv/Fm) can be correlated to the damage to PSII

reaction center, the reaction centers of the BCH-SL plants were less damaged (and therefore more photosynthetically active) than both the wild-type and BCH-ASL [57].

Damage to the PSII protein complex requires the degradation and replacement of the D1 protein (as well as other PSII proteins) in order to re-establish photosynthetic function [4]. This photo-oxidative damage is caused by the short-lived singlet oxygen ($^1O_2$) molecule, and is confined to PSII, and specifically targets the D1 protein for degradation. Photo-oxidative damage, especially to PSII, appears to be an unavoidable consequence of the photosynthetic activity and is one of the major factors affecting photosynthetic efficiency. Western blots of the transgenic tobacco lines indicated that the rate of degradation of the D1 protein in the BCH-SL was much lower than the wild-type plants (and conversely that this loss was accelerated in the BCH-ASL) (Fig. 3.11). It appears as if the additional BCH (and therefore zeaxanthin) in the BCH-SL, has a protective effect on the photosynthetic apparatus. The reason for this observation is not known. In a similar study, Davison *et al.* overexpressed the native BCH in *Arabidopsis* which lead to a two-fold increase in xanthophyll pigment levels [21]. The resultant transgenic plants were more resistant to elevated temperature (40°C) and high light-induced (1000 μmol photons.$m^{-2}$.$s^{-1}$) stress than the wild-type plants. The investigators showed that the transgenic plants formed less anthocyanins (as an indicator of stress) and also displayed less lipid peroxidation than the wild-type. It is clear that zeaxanthin serves a protective function in preventing peroxidation of the membrane lipids by reactive oxygen species [21]. The degree of damage to the thylakoid membrane of the different tobacco plant lines expressing the *V. vinifera* BCH was not determined in this study. It would be interesting to see if the additional zeaxanthin had any effect on the degree of lipid peroxidation under high light conditions.

In the BCH-SL the increased BCH activity (and therefore the additional available zeaxanthin) assisted the transgenic tobacco plants in coping with excess light and maintaining active photosynthetic apparatus. The mechanism by which this has occurred is, however, not clear. It has been reported that elevated zeaxanthin levels can reduce the light-induced inactivation of PSII by quenching damaging triplet excited chlorophyll, as well as preventing damage to the D1 protein [58]. Under high light stress the D1 protein turnover in the BCH-SL tobacco was not only much lower, but the degree of damage to the D1 protein was also significantly less. The availability of the additional

functional BCH for the SL tobacco under high light stress further enabled the plants to maintain active photosynthetic centres, resulting in an improved photosynthetic ability in these plants.

In conclusion we report the isolation and characterization of a functional BCH encoding gene from *V. vinifera* and show that overexpression of this gene in tobacco assists the transgenic plants in maintaining photosynthesis under saturating light conditions.

## 3.5 LITERATURE CITED


[1] Ma,Y.Z., Holt,N.E., Li,X.P., Niyogi,K.K., & Fleming,G.R. (2003) Evidence for direct carotenoid involvement in the regulation of photosynthetic light harvesting. *Proc Natl Acad Sci USA*, **100,** 4377-4382.

[2] Depka,B., Jahns,P., & Trebst,A. (1998) β-carotene to zeaxanthin conversion in the rapid turnover of the D1 protein of photosystem II. *FEBS Lett*, **424,** 267-270.

[3] Keren,N., Berg,A., van Kan,P.J., Levanon,H., & Ohad,I., I (1997) Mechanism of photosystem II photoinactivation and D1 protein degradation at low light: The role of back electron flow. *Proc Natl Acad Sci USA*, **94,** 1579-1584.

[4] Rintamaki,E., Salo,R., Lehtonen,E., & Aro,E.M. (1995) Regulation of D1-protein degradation during photoinhibition of photosystem II *in vivo*: phosphorylation of the D1 protein in various plant groups. *Planta*, **195,** 379-386.

[5] Demmig-Adams,B. & Adams,W.W., III (1992) Photoprotection and other responses of plants to high light stress. *Annu Rev Plant Physiol Plant Mol Biol*, **43,** 599-626.

[6] Demmig-Adams,B. & Adams,W.W., III (1996) The role of xanthophyll cycle carotenoids in the protection of photosynthesis. *Trends Plant Sci*, **1,** 21-26.

[7] Pogson,B.J. & Rissler,H.M. (2000) Genetic manipulation of carotenoid biosynthesis and photoprotection. *Philos Trans R Soc Lond B: Biol Sci*, **355,** 1395-1403.

[8] Sarry,J.E., Montillet,J.L., Sauvaire,Y., & Havaux,M. (1994) The protective function of the xanthophyll cycle in photosynthesis. *FEBS Lett*, **353,** 147-150.

[9] Bugos,R.C., Hieber,A.D., & Yamamoto,H.Y. (1998) Xanthophyll cycle enzymes are members of the lipocalin family, the first identified from plants. *J Biol Chem*, **273,** 15321-15324.

[10] Bugos,R.C., Chang,S.H., & Yamamoto,H.Y. (1999) Developmental expression of violaxanthin de-epoxidase in leaves of tobacco growing under high and low light. *Plant Physiol*, **121,** 207-213.

[11] Faria,T., GarciaPlazaola,J.I., Abadia,A., Cerasoli,S., Pereira,J.S., & Chaves,M.M. (1996) Diurnal changes in photoprotective mechanisms in leaves of cork oak (*Quercus suber*) during summer. *Tree Physiol*, **16,** 115-123.

[12] Muller-Moule,P., Conklin,P.L., & Niyogi,K.K. (2002) Ascorbate deficiency can limit violaxanthin de-epoxidase activity *in vivo*. *Plant Physiol*, **128,** 970-977.

[13] Sun,Z., Gantt,E., & Cunningham,F.X., Jr. (1996) Cloning and functional analysis of the β-carotene hydroxylase of *Arabidopsis thaliana*. *J Biol Chem*, **271,** 24349-24352.

[14] Tian,L., Magallanes-Lundback,M., Musetti,V., & DellaPenna,D. (2003) Functional analysis of β- and ε-ring carotenoid hydroxylases in *Arabidopsis*. *Plant Cell*, **15,** 1320-1332.

[15] Cunningham,F.X., Jr. & Gantt,E. (1998) Genes and enzymes of carotenoid biosynthesis in plants. *Annu Rev Plant Physiol Plant Mol Biol*, **49,** 557-583.

[16] Krause,G.H. & Weis,E. (1991) Chlorophyll fluorescence and photosynthesis: The basics. *Annu Rev Plant Physiol Plant Mol Biol*, **42,** 313-349.

[17] Havaux,M. & Niyogi,K.K. (1999) The violaxanthin cycle protects plants from photooxidative damage by more than one mechanism. *Proc Natl Acad Sci USA*, **96,** 8762-8767.

[18] Niyogi,K.K., Grossman,A.R., & Björkman,O. (1998) *Arabidopsis* mutants define a central role for the xanthophyll cycle in the regulation of photosynthetic energy conversion. *Plant Cell*, **10,** 1121-1134.

[19] Niyogi,K.K. (1999) Photoprotection revisited: Genetic and molecular approaches. *Annu Rev Plant Physiol Plant Mol Biol*, **50,** 333-359.

[20] Wentworth,M., Ruban,A.V., & Horton,P. (2000) Chlorophyll fluorescence quenching in isolated light harvesting complexes induced by zeaxanthin. *FEBS Lett*, **471,** 71-74.

[21] Davison,P.A., Hunter,C.N., & Horton,P. (2002) Overexpression of β-carotene hydroxylase enhances stress tolerance in *Arabidopsis*. *Nature*, **418,** 203-206.

[22] Verhoeven,A.S., Bugos,R.C., & Yamamoto,H.Y. (2001) Transgenic tobacco with suppressed zeaxanthin formation is susceptible to stress-induced photoinhibition. *Photosynth Res*, **67,** 27-39.

[23] Cunningham,F.X., Jr., Chamovitz,D., Misawa,N., Gantt,E., & Hirschberg,J. (1993) Cloning and functional expression in *Escherichia coli* of a cyanobacterial gene for lycopene cyclase, the enzyme that catalyzes the biosynthesis of β-carotene. *FEBS Lett*, **328,** 130-138.

[24] Cunningham,F.X., Jr., Sun,Z., Chamovitz,D., Hirschberg,J., & Gantt,E. (1994) Molecular structure and enzymatic function of lycopene cyclase from the cyanobacterium *Synechococcus* sp. strain PCC7942. *Plant Cell*, **6,** 1107-1121.

[25] Hood,E.E., Helmer,G.L., Fraley,R.T., & Chilton,M.D. (1986) The hypervirulence of *Agrobacterium tumefaciens* A281 is encoded in a region of pTiBo542 outside of T-DNA. *J Bacteriol*, **168,** 1291-1301.

[26] Steenkamp,J.A., Wiid,I., Lourens,A., & van Helden,P. (2003) Improved method for DNA extraction from *Vitis vinifera*. *Am J Enol Vitic*, **45,** 102-106.

[27] Davies,C. & Robinson,S.P. (1996) Sugar accumulation in grape berries. Cloning of two putative vacuolar invertase cDNAs and their expression in grapevine tissues. *Plant Physiol*, **111,** 275-283.

[28] Chomczynski,P. & Sacchi,N. (1987) Single-step method of RNA isolation by acid guanidinium thiocyanate-phenol-chloroform extraction. *Anal Biochem*, **162,** 156-159.

[29] Sambrook,J., Fritsch,E.F., & Maniatis,T. (1989) *Molecular cloning: a laboratory manual*, 2nd edn. Cold Spring Harbor Laboratory Press, Cold Spring Harbor, N.Y. (USA).

[30] Gleave,A.P. (1992) A versatile binary vector system with a T-DNA organisational structure conducive to efficient integration of cloned DNA into the plant genome. *Plant Mol Biol*, **20,** 1203-1207.

[31] Jefferson,R.A., Kavanagh,T.A., & Bevan,M.W. (1987) GUS fusions: β-glucuronidase as a sensitive and versatile gene fusion marker in higher plants. *EMBO J*, **6,** 3901-3907.

[32] Emanuelsson,O. & von Heijne,G. (2001) Prediction of organellar targeting signals. *Biochim Biophys Acta*, **1541,** 114-119.

[33] Thompson,J.D., Gibson,T.J., Plewniak,F., Jeanmougin,F., & Higgins,D.G. (1997) The CLUSTAL_X windows interface: flexible strategies for multiple sequence alignment aided by quality analysis tools. *Nucleic Acids Res*, **25,** 4876-4882.

[34] Gallois,P. & Marinho,P. (1995) Leaf disk transformation using *Agrobacterium tumefaciens* – expression of heterologous genes in tobacco. *Methods Mol Biol*, **49,** 39-48.

[35] Van Kooten,O. & Snel,J.F.H. (1990) The use of chlorophyll fluorescence nomenclature in plant stress physiology. *Photosynth Res*, **25,** 147-150.

[36] Maxwell,K. & Johnson,G.N. (2000) Chlorophyll fluorescence - a practical guide. *J Exp Bot*, **51,** 659-668.

[37] Peterson,R.B. & Havir,E.A. (2000) A nonphotochemical-quenching-deficient mutant of *Arabidopsis thaliana* possessing normal pigment composition and xanthophyll-cycle activity. *Planta*, **210,** 205-214.

[38] Britton,G. (1985) General carotenoid methods. In *Methods in enzymology* (Law,J.H. & Rilling,H.C., eds), pp. 113-149. Academic Press, Orlando.

[39] Rock,C.D. & Zeevaart,J.A. (1991) The *aba* mutant of *Arabidopsis thaliana* is impaired in epoxy-carotenoid biosynthesis. *Proc Natl Acad Sci USA*, **88,** 7496-7499.

[40] Schwartz,S.H., Tan,B.C., Gage,D.A., Zeevaart,J.A., & McCarty,D.R. (1997) Specific oxidative cleavage of carotenoids by VP14 of maize. *Science*, **276,** 1872-1874.

[41] Lichtenthaler,H.K. (1987) Chlorophylls and carotenoids: Pigments of photosynthetic biomembranes. In *Methods in Enzymology* (Packer,L. & Douce,R., eds), pp. 350-382.

[42] Thayer,S.S. & Björkman,O. (1990) Leaf xanthophyll content and composition in sun and shade determined by HPLC. *Photosynth Res*, **23,** 331-343.

[43] Park,H., Kreunen,S.S., Cuttriss,A.J., DellaPenna,D., & Pogson,B.J. (2002) Identification of the carotenoid isomerase provides insight into carotenoid biosynthesis, prolamellar body formation, and photomorphogenesis. *Plant Cell*, **14,** 321-332.

[44] Schoefs,B., Bertrand,M., & Lemoine,Y. (1995) Separation of photosynthetic pigments and their precursors by reversed-phase high-performance liquid-chromatography using a photodiode-array detector. *J Chromatogr A*, **692,** 239-245.

[45] Rintamaki,E., Kettunen,R., & Aro,E.M. (1996) Differential D1 dephosphorylation in functional and photodamaged photosystem II centers. Dephosphorylation is a prerequisite for degradation of damaged D1. *J Biol Chem*, **271,** 14870-14875.

[46] Yamamoto,Y. & Satoh,K. (1998) Processing of precursor D1 protein in the PSII membrane by CtpA over-expressed in *E. coli.* An analysis using an antibody which specifically recognizes the cleavage product. In *Photosynthesis: Mechanisms and Effects* (Garab,G., ed), pp. 3131-3134. Kluwer Academic Publishers, Netherlands.

[47] Altschul,S.F., Madden,T.L., Schaffer,A.A., Zhang,J., Zhang,Z., Miller,W., & Lipman,D.J. (1997) Gapped BLAST and PSI-BLAST: a new generation of protein database search programs. *Nucleic Acids Res*, **25,** 3389-3402.

[48] Cunningham,F.X., Jr., Pogson,B., Sun,Z., McDonald,K.A., DellaPenna,D., & Gantt,E. (1996) Functional analysis of the β– and ε–lycopene cyclase enzymes of *Arabidopsis* reveals a mechanism for control of cyclic carotenoid formation. *Plant Cell*, **8,** 1613-1626.

[49] Bouvier,F., Keller,Y., d'Harlingue,A., & Camara,B. (1998) Xanthophyll biosynthesis: Molecular and functional characterization of carotenoid hydroxylases from pepper fruits (*Capsicum annuum* L.). *Biochim Biophys Acta*, **1391,** 320-328.

[50] Vandesompele,J., De Preter,K., Pattyn,F., Poppe,B., Van Roy,N., De Paepe,A., & Speleman,F. (2002) Accurate normalization of real-time quantitative RT-PCR data by geometric averaging of multiple internal control genes. *Genome Biol*, **3,** 1-12.

[51] Aro,E.M., Virgin,I., & Andersson,B. (1993) Photoinhibition of photosystem II. Inactivation, protein damage and turnover. *Biochim Biophys Acta*, **1143,** 113-134.

[52] Flanigan,Y.S. & Critchley,C. (1996) Light response of D1 turnover and photosystem II efficiency in the seagrass *Zostera capricorni. Planta*, **198,** 319-323.

[53] Woitsch,S. & Romer,S. (2003) Expression of xanthophyll biosynthetic genes during light-dependent chloroplast differentiation. *Plant Physiol*, **132,** 1508-1517.

[54] Horton,P. (2000) Prospects for crop improvement through the genetic manipulation of photosynthesis: morphological and biochemical aspects of light capture. *J Exp Bot*, **51,** 475-485.

[55] Gotz,T., Sandmann,G &. Romer, S. (2002) Expression of a bacterial carotene hydroxylase gene (crtZ) enhances UV tolerance in tobacco. *Plant Mol Biol*, **50,** 129-142.

[56] Muller,P., Li,X.P., & Niyogi,K.K. (2001) Non-photochemical quenching. A response to excess light energy. *Plant Physiol*, **125,** 1558-1566.

[57] Schansker,G., Rensen,J.J.S., & van Rensen,J.J.S. (1999) Performance of active photosystem II centers in photoinhibited pea leaves. *Photosynth Res*, **62,** 175-184.

[58] Jahns,P., Depka,B., & Trebst,A. (2000) Xanthophyll cycle mutants from *Chlamydomonas reinhardtii* indicate a role for zeaxanthin in the D1 protein turnover. *Plant Physiol Biochem*, **38,** 371-376.

# CHAPTER 4

# RESEARCH RESULTS

## Isolation and characterization of candidate genes in the isoprenoid and carotenoid biosynthetic pathways of *Vitis vinifera* L. I

This manuscript will be submitted for publication in ***Plant Molecular Biology***

# Isolation and characterization of candidate genes in the isoprenoid- and carotenoid biosynthetic pathways of *Vitis vinifera* L. I

Philip R. Young[1], Kerry L. Taylor[1], Isak S. Pretorius[2] and Melané A. Vivier[1*]

[1]Institute for Wine Biotechnology, Department of Viticulture and Oenology, Stellenbosch University, Stellenbosch, South Africa, 7600; [2]Australian Wine Research Institute, Adelaide, Australia

## ABSTRACT

Carotenoids represent one of a large heterogeneous group of plant isoprenoids that are essential for photosynthesis by assisting in light-harvesting, and by fulfilling a protective function in photosynthetic membranes. Carotenoids are also precursors of the plant growth regulator, abscisic acid. Five genes have been isolated that encode for enzymes that are either directly, or indirectly, involved in the carotenoid biosynthetic pathway of *Vitis vinifera*: 1-deoxy-D-xylulose 5-phosphate synthase (DXS), lycopene β-cyclase (LBCY), 9-*cis* epoxy carotenoid dioxygenase (NCED), phytoene synthase (PSY), and zeaxanthin epoxidase (ZEP) genes. Both the cDNA- and genomic copies of the genes have been isolated, cloned and sequenced. Southern hybridizations showed that the DXS, PSY, and ZEP genes are present as single copies in the *V. vinifera* genome. LBCY and NCED, on the other hand, contain two- and three copies, respectively. Analysis of the isolated nucleotide sequences has enabled the prediction of the putative proteins and the sub-cellular localization of these proteins. These predictions, together with the identification of conserved domains have provided additional information regarding the *in vivo* role of these enzymes. The putative promoters of all the genes have been isolated and subsequent transient reporter gene assays of the promoter fragments fused to the β-glucuronidase (GUS) reporter gene, however, did not show any transcriptional activity. RT-PCR analyses were used to establish expression profiles of the isolated genes in different organs, during different developmental stages, and following treatments with abscisic acid, NaCl and wounding. The functionality of LBCY and PSY was confirmed in a heterologous bacterial complementation assay. The isolation and characterization of these five genes from *V. vinifera* Pinotage are discussed in the context of carotenoid biosynthesis.

*Corresponding author: Institute for Wine Biotechnology, Department of Viticulture and Oenology, Stellenbosch University, Private Bag X1, Matieland, ZA7602, South Africa. Tel: +27 21 8083773; Fax: +27 21 8083771; Email: mav@sun.ac.za

## 4.1 INTRODUCTION

Carotenoids are one of a diverse group of naturally occurring isoprenoids that are present in all photosynthetic organisms. Carotenoids are one of the most abundant and widely distributed classes of pigments that perform a variety of essential biological functions in plants [1]. Plant carotenoids are synthesized and accumulated in plastids, and the genes encoding the enzymes of carotenoid biosynthesis are nuclear-encoded, but post-translationally targeted to the plastids. Although most of the genes encoding these enzymes have been cloned from higher plants (i.e. the protein and nucleotide sequence information is available), the mechanisms regulating these genes are still not fully understood [2-4].

All isoprenoids are synthesized from two $C_5$ precursors: isopentenyl diphosphate (IPP) and its isomer dimethylallyl diphosphate (DMAPP). Two distinct pathways are utilized by plants for the biosynthesis of IPP: (i) the classical acetate/mevalonate pathway that operates in the cytosol and is responsible for the formation of, amongst others, sterols and certain sesquiterpenes; and (ii) the novel mevalonate-independent route, the 1-deoxy-D-xylulose 5-phosphate (DOXP)/2-C-methyl-D-erythritol 4-phosphate (MEP) pathway that forms the plastidic isoprenoids (e.g. isoprene, phytol and carotenoids) [1;5;6]. The carotenoid biosynthetic pathway is well characterized and has been comprehensively reviewed (Fig. 4.1) [2;3].

The isolation of carotenoid biosynthetic genes has been accelerated in the last few years due to the availability of a heterologous functional complementation assay [7]. This complementation system has not only enabled the isolation of carotenoid biosynthetic genes, but also genes indirectly involved in carotenoid biosynthesis (i.e. genes encoding isoprenoid precursors) [8;9].

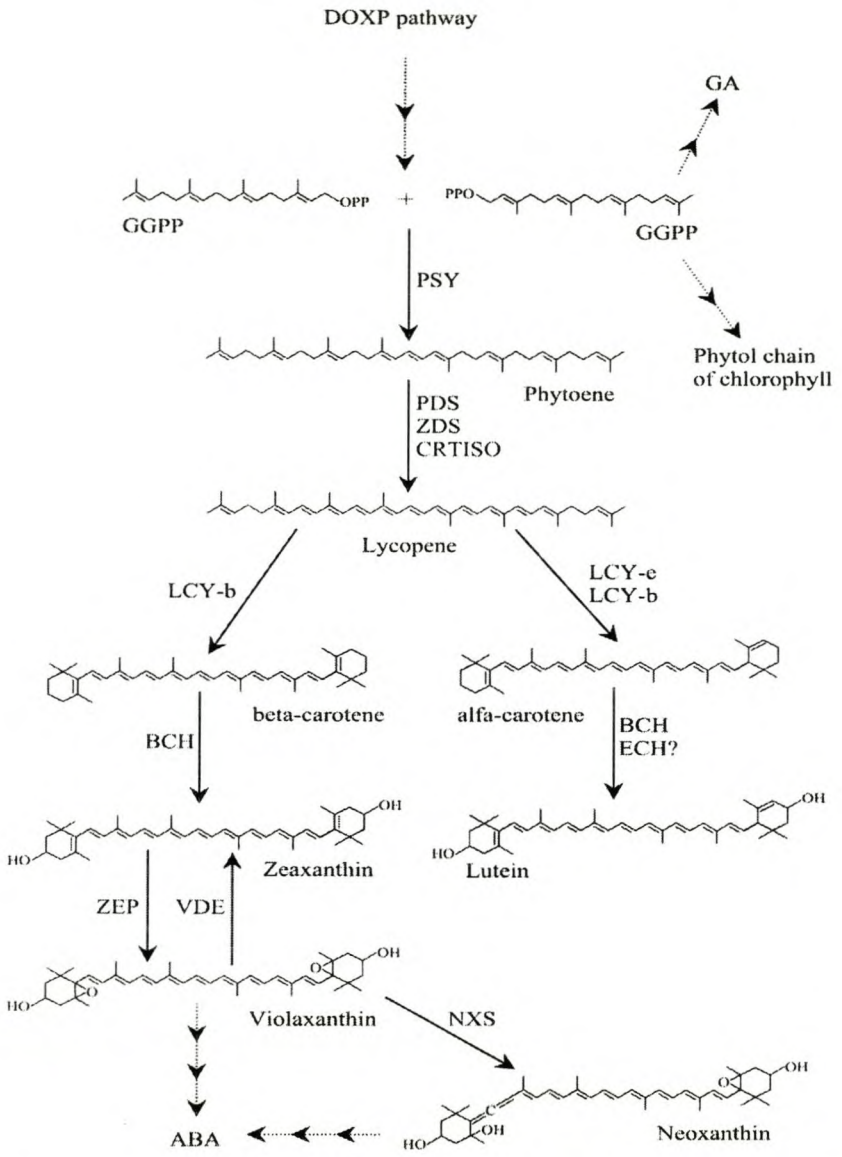


Figure 4.1. A brief overview of carotenoid biosynthesis in plastids. DOXP, 1-deoxy-D-xylulose 5-phosphate; GGPP, geranylgeranyl diphosphate; GA, gibberellic acid; PSY, phytoene synthase; PDS, phytoene desaturase; ZDS, ζ-carotene desaturase; CRTISO, carotene isomerase; LCY-b, lycopene β-cyclase; LCY-e, lycopene ε-cyclase; BCH, β-carotene hydroxylase; ECH, ε-carotene hydroxylase; ZEP, zeaxanthin epoxidase; VDE, violaxanthin de-epoxidase; NXS, neoxanthin synthase; ABA, abscisic acid. The steps indicated by broken arrows have been omitted for simplification [10].

Carotenoids have received much attention in the last decade for two reasons: (i) β-carotene (pro-Vitiamin A) is required in the human diet as a precursor for Vitamin A production; and (ii) the oxygenated carotenoids (xanthophylls) are integral pigments of

the photosynthetic apparatus and are required for light-harvesting and photoprotection [11;12]. The ability to successfully manipulate the carotenoid levels in a crop plant (like grapevine) will have several potentially positive outcomes. Firstly, increasing the β-carotene levels in the fruit will concomitantly improve the nutritional value of the product (grape berries). Secondly, carotenoids are thought to be precursors of β-damascenone, vitispirane and other $C_{13}$-norisoprenoids compounds that are associated with grape- and wine quality [13]. Increasing the flux into the carotenoid pathway could lead to an increase in these compounds. Thirdly, recent studies in *Arabidopsis* have reported increased photoprotection in transgenic plants overexpressing xanthophyll biosynthetic enzymes. Relative to the control plants, these plants were less affected by high light and high temperature induced photo-oxidative stresses [14]. The carotenoid biosynthetic pathway is therefore proving to be a promising target for genetic manipulation to produce stress tolerant plants.

As the first step in gaining insight into the carotenoid biosynthetic pathway in *Vitis vinifera*, we have isolated five genes that are either directly, or indirectly, involved in carotenoid biosynthesis: (i) DXS (the DOXP/MEP pathway); (ii, iii and iv) PSY, LBCY, and ZEP (the carotenoid biosynthetic pathway); and (v) NCED (the ABA biosynthetic pathway). The genomic copies of LBCY, NCED, PSY and ZEP have been isolated and sequenced from *V. vinifera* genomic DNA. The obtained genomic sequences were analyzed and used to design primers for the isolation of the cDNA copies of the respective genes. Furthermore, the potential of the putative promoters of these genes to drive transcription of a reporter gene was assessed in a transient assay. The cloned cDNA copies of LBCY and PSY were shown to be functional in a heterologous bacterial complementation system. The expression of the LBCY, PSY and ZEP genes in different plant organs, during different developmental stages, and following different inductions were also determined by RT-PCR analysis. Preliminary results have provided useful insights into both the genomic organisation and the expression of these genes in *V. vinifera*.

## 4.2 MATERIALS AND METHODS

### 4.2.1 Plant Material

*Vitis vinifera* L. cv. Pinotage leaves were collected in the field and flash frozen in liquid nitrogen. Berries were collected throughout the growth season (October, 2001 through to February, 2002) in one-week intervals. The frozen tissue was ground in liquid nitrogen and, if not used immediately, stored at -80ºC.

Field-grown leaf tissue was used for induction experiments and subsequent RT-PCR analyses. The petioles of detached leaves were placed in (i) sterile water (control treatment), (ii) 100 μM abscisic acid, (iii) without water (i.e. dehydration), (iv) 300 mM NaCl, or (iv) wounding the leaf blades with a pincer. Leaf tissue was collected 1 h and 24 h after the induction, frozen in liquid nitrogen, and stored at -80°C until RNA was extracted.

### 4.2.2 Plasmids, bacterial strains and growth conditions

*Escherichia coli* DH5α cultures were grown in LB media, and transformed bacterial cultures were grown in LB media supplemented with the appropriate antibiotic(s) [15]. Unless otherwise stated, all cultures were grown at 37ºC. The plasmids pAC-85b, pAC-LYC, pAC-BETA, and pAC-ZEAX for the functional complementation assay were obtained from F. X. Cunningham and are described in Cunningham et al. [7;16].

### 4.2.3 Isolation and manipulation of nucleic acids

All DNA fragments for cloning were separated on 1.0% (w/v) TAE agarose gels and the fragments of interest were isolated using the QIAquick Gel Extraction Kit as instructed by the supplier (Qiagen GmbH, Hilden, Germany). The pGEM-T Easy vector system was used to clone all PCR-generated fragments, according to the specifications of the supplier (Promega, Madison, WI). High molecular weight genomic DNA was isolated from fully expanded *V. vinifera* leaves as described by Steenkamp et al. [17]. Total RNA from different grapevine tissues was extracted according to the methods described by Davies and Robinson [18]. Unless otherwise stated, all standard methods for plasmid DNA isolation, manipulations and cloning of DNA fragments, and agarose gel electrophoresis were used as described by Sambrook et al. [15].

### 4.2.4 Construction of vectors

The PCR primers used to amplify partial- and full-length carotenoid biosynthetic genes (CBGs) are listed in Table 4.2. The PCR reactions were performed using 10-50 ng of Pinotage genomic DNA as template. PCR amplifications were performed in a BioRad PCR thermal cycler (BioRad, Hercules, CA) using the following program: initial denaturation at 94°C for 5 min; subsequent denaturations at 94°C for 35 s; annealing at 55°C for 35 s; extension at 72°C for 1 min per kb (refer to Table 4.2); and a final elongation at 72°C for 10 min. Amplifications were performed for 30 cycles.

A genomics approach was used to isolate full-length CBGs and their associated flanking sequences (i.e. the complete coding sequence as well as the 5'- and 3'-flanking sequences). This entailed the search and retrieval of representative protein sequences for DXS, LBCY, NCED, PSY and ZEP from Genbank and the alignment of the retrieved amino acid sequences (Table 4.4). Areas showing a high degree of homology were identified in the resultant multiple alignments of the protein sequences (using ClustalX), and the nucleotide sequences corresponding to these areas were retrieved (from Genbank) and aligned (Figure 4.3-4.7). The areas with the highest degree of homology (or least degeneracy) in the nucleotide sequence alignments were further analyzed for the final primer design (Table 4.2). The degenerate primers were used to amplify partial fragments of the CBGs from *V. vinifera* genomic DNA. The PCR amplification products for DXS, LBCY, NCED, PSY and ZEP were isolated and cloned to yield pGEM-DXS, pGEM-LBCY, pGEM-NCED, pGEM-PSY and pGEM–ZEP, respectively. These constructs were sequenced by the Central Analytical Facility, Stellenbosch University, using an ABI Prism 3100 Genetic Analyzer, and were further used as templates to PCR label probes for the screening of the constructed sub-genomic libraries.

In order to isolate the full-length genomic sequences and the corresponding flanking sequences it was necessary to construct and screen a number of customized sub-genomic libraries. Southern blot analyses were used to determine which subgenomic libraries needed to be constructed for each of the specific CBGs (i.e. for DXS, LBCY, NCED, PSY and ZEP). This was done by digesting ten micrograms of Pinotage genomic DNA with a range of restriction endonucleases, separating the fragments in a 0.8% (w/v) TBE agarose gel, and transferring to Hybond-N nylon membranes. The membranes were cross-linked and probed with the DIG-labeled partial

CBGs (from pGEM-DXS, pGEM-LBCY, pGEM-NCED, pGEM-PSY and pGEM-ZEP). The hybridization signals from the Southern blots identified a number of potential restriction endonucleases for subsequent library construction. In order to construct these sub-genomic libraries, genomic DNA fractions corresponding to the size of the hybridization signals obtained from the Southern blots were isolated, gel-purified and cloned into the corresponding sites of pBluescript II SK(+) or pGEM-7zf+ (Table 4.2). The ligation mixtures were transformed into competent DH5α *E. coli* cells, amplified by growing the cells at 37°C for 16-20 h. The resultant sub-genomic libraries were PCR screened to identify the cloned genomic fragments containing the gene(s) of interest (Table 4.1).

In total eleven sub-genomic libraries were constructed from Pinotage genomic DNA, and they are designated Pinotage genomic library (PGL-), followed by the restriction endonuclease(s) used for the genomic DNA digestions. A number after the endonuclease is used to differentiate between PGLs made with the same restriction endonuclease (but differing in the size of the fragments they contain). The construction of the eleven PGLs was as follows:

(i) and (ii). *V. vinifera* genomic DNA fragments (ranging in size from 4300-8000 bp) from an *Eco*RV digest were cloned into the *Eco*RV site of pBluescript II SK+. The resultant sub-genomic library (PGL-*Eco*RV-1) was screened for DXS, LBCY and ZEP. Similarly, the sub-genomic library, PGL-*Eco*RV-2 was constructed by cloning *Eco*RV digested genomic fragments (ranging in size from 2300-4300 bp) into the corresponding site of pBluescript II SK+. PGL-*Eco*RV-2 was screened for DXS, LBCY, NCED and PSY.

(iii). In order to screen for DXS, the PGL-*Eco*RI/*Hin*DIII sub-genomic library was constructed by cloning *Eco*RI/*Hin*DIII digested genomic DNA fragments (of approximately 4000 bp in size) into the *Eco*RI/*Hin*DIII sites of pBluescript II SK+.

(iv). PGL-*Pst*I/*Spe*I was constructed by cloning *Pst*I/*Spe*I digested genomic DNA fragments (of approximately 3600 bp in size) into the *Nsi*I/*Xba*I sites of pGEM7zf+. PGL-*Pst*I/*Spe*I was screened for PSY.

(v) and (vi). Two sub-genomic libraries, PGL-*Kpn*I-1 and PGL-*Kpn*I-2, were constructed by cloning *Kpn*I digested genomic DNA fragments (approximately 5600 bp

and 2300 bp in size, respectively) into the *Kpn*I site of pBluescript II SK+. The PGL-*Kpn*I-1 sub-genomic library was screened for ZEP, and PGL-*Kpn*I-2 for NCED.

(vii) PGL-*Pst*I was constructed for the screening of NCED, by cloning the *Pst*I digested genomic DNA fragments (approximately 1700 bp in size) into the *Pst*I site of pBluescript II SK+.

(viii), (ix) and (x). Three PGL-*Hin*DIII sub-genomic libraries were constructed (PGL-*Hin*DIII-1,-2, and -3) by cloning *Hin*DIII digested genomic DNA (approximately 6000 bp, 3400 bp and 1500 bp in size, respectively) into the *Hin*DIII site of pBluescript II SK+. These sub-genomic libraries were screened for NCED, PSY and DXS, respectively.

(ix) The PGL-*Bam*HI/*Pst*I sub-genomic library was constructed by cloning *Bam*HI/*Pst*I digested genomic DNA (approximately 3600 bp) into the *Bam*HI/*Nsi*I site of pBluescript II SK+. The resultant sub-genomic library was screened for LBCY.

Table 4.1

| SUB-GENOMIC LIBRARY | GENE(S) | DESCRIPTION |
|---|---|---|
| PGL-*Eco*RV-1 | DXS[1], LBCY[2], ZEP[3] | Genomic DNA[4] was digested with the RE[5] *Eco*RV and the ~4300-8400 bp size fragments were cloned into the *Eco*RV site of pBS[6] |
| PGL-*Eco*RV-2 | DXS, LBCY, NCED[7], PSY[8] | Genomic DNA was digested with the RE *Eco*RV and the ~2300-4300 bp size fragments were cloned into the *Eco*RV site of pBS |
| PGL-*Eco*RI/*Hin*DIII | DXS | Genomic DNA was digested with the RE *Eco*RI/*Hin*DIII and the ~4000 bp size fragments were cloned into the *Eco*RI/*Hin*DIII site of pBS |
| PGL-*Pst*I/*Spe*I | PSY | Genomic DNA was digested with the REs *Pst*I/*Spe*I and the ~3600 bp size fragments were cloned into the *Nsi*I/*Xba*I site of pGEM7[9] |
| PGL-*Kpn*I-1 | ZEP | Genomic DNA was digested with the RE *Kpn*I and the ~5600 bp size fragments were cloned into the *Kpn*I site of pBS |
| PGL-*Kpn*I-2 | NCED | Genomic DNA was digested with the RE *Kpn*I and the 2300 bp size fragments were cloned into the *Kpn*I site of pBS |
| PGL-*Pst*I | NCED | Genomic DNA was digested with the RE *Pst*I and the ~1700 bp size fragments were cloned into the *Pst*I site of pBS |
| PGL-*Hin*dIII-1 | NCED | Genomic DNA was digested with the RE *Hin*DIII and the ~6000 bp size fragments were cloned into the *Hin*DIII site of pBS |
| PGL-*Hin*dIII-2 | PSY | Genomic DNA was digested with the RE *Hin*DIII and the ~3400 bp size fragments were cloned into the *Hin*DIII site of pBS |
| PGL-*Hin*dIII-3 | DXS | Genomic DNA was digested with the RE *Hin*DIII and the ~1500 bp size fragments were cloned into the *Hin*DIII site of pBS |
| PGL-*Bam*HI/*Pst*I | LBCY | Genomic DNA was digested with the REs *Bam*HI/*Pst*I and the ~3600 bp size fragments were cloned into the *Bam*HI/*Nsi*I site of pBS |

[1]The gene encoding 1-deoxy-D-xylulose 5-phosphate synthase from *V. vinifera*. [2]The gene encoding lycopene β-cyclase from *Vitis vinifera*. [3]The gene encoding zeaxanthin epoxidase from *V. vinifera*. [4]Genomic DNA from *V. vinifera* L. cv. Pinotage. [5]Restriction endonuclease(s). [6]The cloning vector, pBluescript II SK+ (Stratagene). [7] The gene encoding 9-*cis*-epoxy carotenoid dioxygenase from *V. vinifera*. [8]The gene encoding phytoene synthase from *V. vinifera*. [9]The cloning vector, pGEM-7zf+ (Promega)

The Cauliflower mosaic virus 35S-promoter ($CaMV35S_P$), β-glucuronidase (GUS) reporter gene and the nopaline synthase terminator ($NOS_T$) was isolated as a *Pst*I/*Eco*RI cassette from pBI221 (Clontech Laboratories, Palo Alto, CA), and cloned into the *Pst*I/*Eco*RI-site of pBluescript II SK(+) (Stratagene, La Jolla, CA). This plasmid was subsequently designated pBS-[CaMV-GUS]. The different putative promoter fragments

were PCR-amplified from Pinotage genomic DNA and cloned into pGEM-T Easy vector. The putative promoter fragments were isolated from pGEM-T Easy vector by digestion with *Not*I/*Bam*HI and cloned into the *Not*I/*Bam*HI-site of pBS-[CaMV-GUS]. This replaces the entire CaMV35S$_P$ of pBS-[CaMVp-GUS] with the putative promoter of interest, and gave rise to pBS-DXSp-GUS, pBS-LBCYp-GUS, pBS-NCEDp-GUS, pBS-PSYp-GUS, and pBS-ZEPp-GUS, containing 800-, 2000-, 4300-, 859-, and 1300 bp promoter fragments, respectively, in front of the GUS reporter gene (Table 4.3).

The full-length (i.e. from the putative ATG to the stop codon) cDNA copies of the CBGs were PCR-amplified from cDNA. The resultant PCR products were cloned into the pGEM-T Easy vector and sequenced by the Central Analytical Facility, Stellenbosch University, using an ABI Prism 3100 Genetic Analyzer. The resultant CBG cDNA constructs were designated pGEM-cDXS, pGEM-cLBCY, pGEM-cNCED, pGEM-cPSY and pGEM–cZEP (Table 4.3).

The cloned cDNA copies of the CBGs were excised from the relevant pGEM-T Easy constructs, and cloned into pART7 [19] using the restriction endonuclease sites listed in Table 4.3. The resultant CaMV35S$_P$-[CBG]-NOS$_T$ cassettes were isolated from pART7 as *Not*I-fragments, and cloned into the dephosphorylated *Not*I-site of the binary vector, pART27 [19] to generate pART27-cDXS, pART27-cLBCY, pART27-cNCED, pART27-cPSY and pART27-cZEP constructs (Table 4.3). These plasmids were constructed for plant transformations (data pending), but were also the constructs used to confirm the functionality of the expressed CBGs in a bacterial complementation assay.

Table 4.2

| Primer | Sequence (5' to 3') | Product description |
|---|---|---|
| DXS5' | TCC RTG RTC AAT GTA HCK RTC WGG AAG | Degenerate primers amplifying an internal 662 bp DXS[1] fragment from genomic DNA[2]. |
| DXS3' | GTM ATG GCT CCY TCY GAY GAA RGC | |
| DXS5'-ATG | CTC GAG GAA ATG GCT ATC TGT ACG CTC TCA | Amplifies the full-length[3] DXS gene from cDNA (2151 bp) and genomic DNA (6000 bp). |
| DXS3'-STOP | CTA TGA CAT GAA TCT CCA GGG CC | |
| DXS5'-PROM | TAA AGG GTA TAG CCG TGT GGG AG | Amplifies the 5'-upstream flanking[4] sequence (from position -1 to -800 bp). |
| DXS3'-PROM | ACT AGT ATT TGA ATG ATC CAA AAC CAA A | |
| LBCY5' | TAT GGW GTT TGG GTK GAT GAR TTT GA | Degenerate primers amplifying an internal 450 bp LBCY fragment from genomic DNA. |
| LBCY3' | AGR ATA TCC ATW CCR AAR CAR AAG AAC TC | |
| LBCY5'-ATG | ATG GAT ACT TTA CTC AAG ACT CAT AAT AAG C | Amplifies the full-length LBCY gene from cDNA (1515 bp) and genomic DNA (1515 bp). |
| LBCY3'-STOP | GTT CCA TCA TCT TAA TCC TTG TCC TG | |
| LBCY5'-PROM | GAG AGG GAG CGT CAT CTA GTG AT | Amplifies the 5'-upstream flanking sequence (from position -1 to -2000 bp). |
| LBCY3'-PROM | GGA TCC GAA ATT CAA ACA AGG GTT TCC C | |
| NCED5' | CCA MGC RTT CCA SAG MTG GAA MCA A | Degenerate primers amplifying an internal 740 bp NCED fragment from genomic DNA. |
| NCED3' | CAC CAY YTC TTC GAY GGM GAC GG | |
| NCED5'-ATG | GTCGACATGGCTTCTCCTGCAGCTGC | Amplifies the full-length NCED gene from cDNA (1833 bp) and genomic DNA (1833 bp). |
| NCED3'-STOP | CAA TCT GAC ACC AAG CAG CCA TG | |
| NCED5'-PROM | GTG GGC TCG AAT TTA GGT AGA GA | Amplifies the 5'-upstream flanking sequence (from position -1 to -4300 bp). |
| NCED3'-PROM | GGA TCC GTT TCC CTA TTG TAT TAA AAG AGA GAG | |
| PSY5' | CCA TTY MKR GAY ATG RTY GAA GGR ATG | Degenerate primers amplifying an internal 185 bp PSY fragment from genomic DNA. |
| PSY3' | GCC AAR GCA GCR YTR TAD ACR CTY TC | |
| PSY5'-ATG | ATG TCT GTT GCT CTG TTG TGG ATT G | Amplifies the full-length PSY gene from cDNA (1317 bp) and genomic DNA (3973 bp). |
| PSY3'-STOP | CTC GAG GAT GTC CAT TCA TGC CTT GAC T | |
| PSY5'-PROM | GAA GGT AGA AGG GCT AGA GAG CAG A | Amplifies the 5'-upstream flanking sequence (from position -1 to -859 bp). |
| PSY3'-PROM | GGA TCC GCT GAG ATC TCT TGG GAT ATC CCA | |
| ZEP5' | CAC AAA CAR TAC TTY GTT TCT TCR GAT GT | Degenerate primers amplifying an internal 2100 bp ZEP fragment from genomic DNA. |
| ZEP3' | CCA CCA ACT CTT CCW GGA TGT GGT S | |
| ZEP5'-ATG | GTC GAC ATG GCT TCA GCA GTG TTT TAT AG | Amplifies the full-length ZEP gene from cDNA (1977 bp) and genomic DNA (6500 bp). |
| ZEP3'-STOP | TCA AAC CGC CTG GAA GAG CT | |
| ZEP5'-PROM | GGT ACC CTC AGT ACC AGA ACC TG | Amplifies the 5'-upstream flanking sequence (from position -1 to -1300 bp). |
| ZEP3'-PROM | GGA TCC TCT TGT GTG GAG AAA ATG ATG AA | |
| Oligo-$dT_{16}$ | TTTTTTTTTTTTTTTN | Binds to poly-A tail of mRNA, and primes the first-strand synthesis of reverse transcription. |
| ACTIN5' | GATACTGAAGATATCCAGCCCCTCG | Amplifies a partial fragment of the actin[9] gene from cDNA (521 bp). |

| | | |
|---|---|---|
| ACTIN3' | GCATGGGGAAGTGCATAACCTT | |
| EF1α5' | CACATCAACATTGTCGTCATTGGC | Amplifies a partial fragment of the ef1α[10] gene from cDNA (557 bp). |
| EF1α3' | GGGACAAATGGAATCTTATCAGGG | |

[1]The gene encoding 1-deoxy-D-xylulose 5-phosphate synthase from *Vitis vinifera* . [2]Genomic DNA from *V. vinifera* L. cv Pinotage. [3]The full-length sequence, i.e. from the putative ATG (position +1) to the putative stop codon. [4]The 5'-flanking sequence, i.e. the sequence immediately upstream of the putative ATG. [5]The gene encoding lycopene β-cyclase from *V. vinifera*. [6] he gene encoding 9-*cis*-epoxy carotenoid dioxygenase from *V. vinifera*. [7]The gene encoding phytoene synthase from *V. vinifera*. [8]The gene encoding zeaxanthin epoxidase from *V. vinifera*. [9]The gene encoding actin from *V. vinifera*. [10]The gene encoding elongation factor 1-α from *V. vinifera*.

Table 4.3

| CONSTRUCT | DESCRIPTION |
|---|---|
| pGEM-DXS | A partial 662 bp DXS[1] fragment was PCR-amplified from genomic DNA[2] (using the primers DXS-5' and DXS-3') and cloned into pGEM-T[3] |
| pGEM-LBCY | A partial 450 bp LBCY[4] fragment was PCR-amplified from genomic DNA (using the primers LBCY-5' and LBCY-3') and cloned into pGEM-T |
| pGEM-NCED | A partial 740 bp NCED[5] fragment was PCR-amplified from genomic DNA (using the primers NCED-5' and NCED-3') and cloned into pGEM-T |
| pGEM-PSY | Partial 185 bp PSY[6] fragment was PCR-amplified from genomic DNA (using the primers PSY-5' and PSY-3') and cloned into pGEM-T |
| pGEM-ZEP | The 2100 bp partial ZEP[7] fragment was PCR-amplified from genomic DNA (using the primers ZEP-5' and ZEP-3') and cloned into pGEM-T |
| pGEM-DXSp | The 800 bp putative DXS promoter was PCR-amplified from genomic DNA (using DXS5'-PROM and DXS3'-PROM) and cloned into pGEM-T |
| pGEM-LBCYp | The 2000 bp putative LBCY promoter was PCR amplified from genomic DNA (using LBCY5'-PROM and LBCY3'-PROM) and cloned into pGEM-T |
| pGEM-NCEDp | The 4300 bp putative NCED promoter was PCR-amplified from genomic DNA (using NCED5'-PROM and NCED3'-PROM) and cloned into pGEM-T |
| pGEM-PSYp | The 859 bp putative PSY promoter was PCR amplified from genomic DNA (using PSY5'-PROM and PSY3'-PROM) and cloned into pGEM-T |
| pGEM-ZEPp | The 1300 bp putative ZEP promoter was PCR-amplified from genomic DNA (using ZEP5'-PROM and ZEP3'-PROM) and cloned into pGEM-T |
| pBS-GUS | A 2200 bp *Bam*HI/*Eco*RI fragment containing the GUS[8] gene and $NOS_T$[9] was isolated from pBI221[10] and cloned into the corresponding sites of pBS[11] |
| pBS-CaMV-GUS | A 3000 bp *Pst*I/*Eco*RI fragment containing the $CaMV35S_P$[12], the GUS gene and $NOS_T$ was isolated from pBI221 and cloned into the corresponding sites of pBS |
| pBS-DXSp-GUS | The 800 bp putative DXS promoter was excised from from pGEM-DXSp as a *Not*I/*Bam*HI fragment and cloned into the corresponding sites in pBS-[CaMV-GUS] |
| pBS-LBCYp-GUS | The putative 2000 bp LBCY promoter was excised from from pGEM-LBCYp as a *Not*I/*Bam*HI fragment and cloned into the corresponding sites in pBS-[CaMV-GUS] |
| pBS-NCEDp-GUS | The putative 4300 bp NCED promoter was excised from from pGEM-NCEDp as a *Not*I/*Bam*HI fragment and cloned into the corresponding sites in pBS-[CaMV-GUS] |
| pBS-PSYp-GUS | The 859 bp putative PSY promoter was excised from pGEM-PSYp as a *Not*I/*Bam*HI fragment and cloned into the corresponding sites in pBS-[CaMV-GUS] |
| pBS-ZEPp-GUS | The putative ZEP promoter was excised from from pGEM-ZEPp as a *Not*I/*Bam*HI fragment and cloned into the corresponding sites in pBS-[CaMV-GUS] |
| pGEM-cDXS | The 2151 bp full-length DXS was PCR-amplified from cDNA (using the primers DXS5'-ATG and DXS3'-STOP) and cloned into pGEM-T |
| pGEM-cLBCY | The 1515 bp full-length LBCY was PCR-amplified from cDNA (using the primers LBCY5'-ATG and LBCY3'-STOP) and cloned into pGEM-T |
| pGEM-cNCED | The 1833 bp full-length NCED was PCR-amplified from cDNA (using the primers NCED5'-ATG and NCED3'-STOP) and cloned into pGEM-T |
| pGEM-cPSY | The 1317 bp full-length PSY was PCR-amplified from cDNA (using the primers PSY5'-ATG and PSY3'-STOP) and cloned into pGEM-T |
| pGEM-cZEP | The 1977 bp full-length ZEP was PCR-amplified from cDNA (using the primers ZEP5'-ATG and ZEP3'-STOP) and cloned into pGEM-T |
| pART7-cDXS | The 2151 bp full-length DXS was excised from pGEM-cDXS as a *Xho*I/*Spe*I fragment and cloned into the *Eco*RI/*Xba*I sites of pART7[13] |
| pART7-cLBCY | The 1515 bp full-length LBCY was excised from pGEM-cLBCY as an *Eco*RI/*Spe*I fragment and cloned into the *Eco*RI/*Xba*I sites of pART7[13] |
| pART7-cNCED | The 1833 bp full-length NCED was excised from pGEM-cNCED as a *Sal*I/*Kpn*I fragment and cloned into the *Xho*I/*Kpn*I sites of pART7 |
| pART7-cPSY | The 1317 bp full-length PSY was excised from pGEM-cPSY as an *Eco*RI/*Spe*I |

| | |
|---|---|
| | fragment and cloned into the *Eco*RI/*Xba*I sites of pART7 |
| pART7-cZEP | The 1977 bp full-length ZEP was excised from pGEM-cZEP as a *Xho*I/*Spe*I fragment and cloned into the *Xho*I/Xba*I sites of pART7 |
| pART27-cDXS | Cassette containing DXS under the control of the CaMV35S$_P$ and OCS$_T$[14] was excised from pART7-cLBCY as a 3715 bp *Not*I fragment and cloned into the corresponding site of pART27[13] |
| pART27-cLBCY | Cassette containing LBCY under the control of the CaMV35S$_P$ and OCS$_T$[14] was excised from pART7-cLBCY as a 3715 bp *Not*I fragment and cloned into the corresponding site of pART27[13] |
| pART27-cNCED | Cassette containing NCED under the control of the CaMV35S$_P$ and OCS$_T$ was excised from pART7-cNCED as a 4033 bp *Not*I fragment and cloned into the corresponding site of pART27 |
| pART27-cPSY | Cassette containing PSY under the control of the CaMV35S$_P$ and OCS$_T$ was excised from pART7-cPSY as a 3517 bp *Not*I fragment and cloned into the corresponding site of pART27 |
| pART27-cZEP | Cassette containing ZEP under the control of the CaMV35S$_P$ and OCS$_T$ was excised from pART7-cZEP as a 4177 bp *Not*I fragment and cloned into the corresponding site of pART27 |

[1]The gene encoding 1-deoxy-D-xylulose 5-phosphate synthase. [2]Genomic DNA from *Vitis vinifera* L. cv. Pinotage. [3]pGEM-T Easy vector (Promega). [4]The gene encoding lycopene β-cyclase. [5]The gene encoding 9-*cis*-epoxy carotenoid dioxygenase. [6]The gene encoding phytoene synthase. [7]The gene encoding zeaxanthin epoxidase. [8]The gene encoding β-glucuronidase. [9]The nopaline synthase terminator. [10]The cloning vector, pBI221 (Clontech). [11]The cloning vector, pBluescript II SK(+) (Stratagene). [12]The cauliflower mosaic virus 35S promoter. [13]The cloning vevtor, pART7 and the plant binary vector, pART27 [19]

### 4.2.5 Southern and northern hybridizations

For Southern blot analyses 10 μg of Pinotage genomic DNA was digested and separated in a 0.8% TBE (w/v) agarose gel and transferred to a positively charged Hybond-N nylon membrane as described by the supplier (Amersham-Pharmacia Biotech, Buckinghamshire, UK).

For northern blot analyses 10 μg of total RNA was separated in a 1.2% (w/v) formaldehyde-agarose gel, and transferred to a positively charged Hybond-N nylon membrane as described by the supplier.

Labelling, hybridization of probes, and DIG detection were performed using the DIG non-radioactive nucleic acid labelling and detection system according to the specifications of the supplier (Roche Diagnostics, Mannheim, Germany).

### 4.2.6 RT-PCR

The reverse transcriptase, *C. therm.* polymerase- (from *Carboxydothermus hydrogenoformans*), the supplied buffer and the "two-step" protocol of the supplier (Roche Diagnostics) was used to synthesize cDNA. The first strand reactions were

performed at 45°C with 0.5-1.0 μg total RNA as template, and using an oligo-$dT_{16}$ primer (Table 4.2). The subsequent RT-PCR program was the same as described for the genomic DNA amplification, but using 1% (v/v) of the first strand reaction as template and the primers designated "5'-ATG" and "3'-STOP" in Table 4.2 for the respective full-length CBGs. The levels of the CBG cDNAs amplified from the various tissues were compared relative to the expression of the constitutively expressed actin and elongation factor 1-α (EF1 α) genes. Partial internal fragments of the actin and EF1α genes were PCR-amplified and separated in a 1% (w/v) agarose gel. The resultant ethidium bromide stained actin and EF1α products were quantified densitometrically. The obtained RT-PCR products of the respective CBGs were also quantified densitometrically and subsequently normalized relative to the expression of both the actin and EF1α gene.

### 4.2.7 Functional complementation, pigment extraction and analysis

*E. coli* cultures containing the plasmids expressing CBGs from *Erwinia herbicola* were used for the functional complementation assay as previously described [7]. For functional complementation of LBCY, an *E. coli* culture containing pAC-LYC was transformed with pART27-cLBCY. For PSY an *E. coli* culture containing pAC-85b was transformed with pART27-cPSY. These cultures were also used to isolate pigments for TLC and HPLC analysis to confirm the functionality of the carotenoid genes isolated. Care was taken to avoid light exposure to the cells or isolated pigments. Pigments were extracted from 2-5 ml of culture by harvesting the cells by centrifugation (4000×g for 5 min at room temperature). The media was decanted and the cells were resuspended in sterile water in order to remove residual media components, and recovered by centrifugation (as above). The cells were vortexed to loosen the pellet, and resuspended in 1 ml acetone. The extraction was placed at 65°C for 10 min with subsequent centrifugation at 13000×g for 10 min, and the supernatant (containing the pigments) was aspirated into a clean 2 ml microcentrifuge tube. The extracted pigments were concentrated by centrifugation in a DNA110 Speed vac (Savant). The recovered pigments were resuspended in hexane:acetone (98:2, v/v) and separated on TLC plastic sheets (silica gel 60, Merck) with hexane:acetone (98:2, v/v) as the mobile phase. Reverse phase high performance liquid chromatography (HPLC) will be used to confirm the identity of the carotenoids formed in the functional complementation assay (data pending).

### 4.2.8 Biolistic bombardments and the analysis of the transient expression of the β-glucuronidase reporter gene

The potential promoter activity of the 5'-flanking regions of the isolated CBGs was determined by assessing the transcription of the β-glucuronidase (GUS) reporter gene in a transient assay system. The following constructs were used for the transient reporter gene expression assay: pBS-DXSp-GUS, pBS-LBCYp-GUS, pBS-NCEDp-GUS, pBS-PSYp-GUS, and pBS-ZEPp-GUS, containing 800-, 2000-, 4300-, 859-, and 1300 bp promoter fragments, respectively (Table 4.3). Five micrograms of plasmid DNA (respective promoter constructs) was coated onto 1 μm gold particles and biolistically bombarded into *V. vinifera* and *N. tabacum* leaves (from *in vitro* tissue). After the bombardments, the leaves were transferred to: (i) 1% (w/v) agarose, (ii) 1% (w/v) agarose containing 100 μm abscisic acid, (iii) 1% (w/v) agarose containing 300 mM NaCl, or (iv) dry filter paper (i.e. dehydration) and incubated at 23°C (16 h light-8 h dark cycle) for 24-72 h before analysis. These different conditions were chosen to complement the native expression data obtained by RT-PCR. The pBS-[CaMV-GUS] plasmid was used as a positive control, and the promoterless pBS-GUS was used as a negative control. Leaves of *in vitro* plant tissue was bombarded using the Biolistic PDS-1000/He particle delivery system (BioRad) with 1100 p.s.i. rupture discs and the application of 80 kPa vacuum in the chamber. The microcarrier preparation and subsequent DNA-coating was performed as described by the supplier (BioRad). For the bombardments the macrocarrier was spaced 6 mm from the stopping screen and the samples were placed 9 cm from the macrocarrier, and each construct was bombarded in triplicate. The experiment was repeated to verify the obtained results.

Histochemical GUS-staining was performed 24 h and 72 h after bombardment according to Jefferson et al. [20]. The GUS-staining solution contained 0.1 M sodium phosphate buffer (pH 7.0), 1 mM 5-bromo-4-chloro-3-indolyl-ß-D-glucuronic acid, 10 mM EDTA, 0.5 mM $K_3Fe(CN)_6$, 0.5 mM $K_4Fe(CN)_6$ and 0.1% (v/v) Triton X-100. Samples were submerged in this solution and incubated at 37°C in the dark.

### 4.2.9 Computer analyses

The National Center for Biotechnology Information (NCBI) Entrez search and retrieval system was used to obtain nucleotide and protein sequences from the Genbank databases (http://www.ncbi.nlm.nih.gov/Entrez/). Alignments to sequences in the Genbank databases were executed using the relevant Blast algorithm (http://www.ncbi.nlm.nih.gov/BLAST/). Both amino acid- and nucleotide sequences were aligned using ClustalX [21].

Intron- and exon splice sites in the genomic sequences were predicted using the NetPlantGene server of the Center for Biological Sequence (CBS) Analysis (http://www.cbs.dtu.dk/services/NetPGene/) [22]. The putative localization of protein sequences were predicted using ProtComp (http://www.softberry.com/berry.phtml). The predicted amino acid sequences of the CBGs were submitted to the NCBI Conserved Domain Database (CDD), in order to identify homology to existing conserved protein domains (http://www.ncbi.nlm.nih.gov/Structure/cdd/wrpsb.cgi) [23;24].

*V. vinifera* expressed sequence tags (ESTs) were retrieved from The Institute for Genomic Research (TIGR) Grape Gene Index (http://www.tigr.org/tdb/tgi/vvgi/).

The putative promoter sequences were analyzed for homology to nucleotide sequence motifs commonly found in plant *cis*-acting regulatory DNA elements using the PLACE database (http://www.dna.affrc.go.jp/htdocs/PLACE/) [25].

The intensity of the bands on autoradiograms and ethidium bromide stained gels, were quantified using a digital camera (AlphaImager 1220; Alpha Innotech Corporation, San Leandro, CA) and the AlphaEase v5.5 densitometry software (Alpha Innotech Corporation).

All statistical analyses of data were processed using the Graphpad Prism v3.02 software (Graphpad Software, San Diego, USA).

## 4.3 RESULTS

### 4.3.1 Isolation of carotenoid biosynthetic genes and putative promoters from *Vitis vinifera* genomic DNA

The partial genomic fragments of DXS, LBCY, NCED, PSY and ZEP were PCR-amplified from *V. vinifera* L cv Pinotage genomic DNA using the corresponding degenerate primers listed in Table 4.2. The amplified PCR products were isolated and cloned into pGEM-T Easy to yield pGEM-DXS (662 bp insert), pGEM-LBCY (450 bp insert), pGEM-NCED (740 bp insert), pGEM-PSY (185 bp insert) and pGEM-ZEP (2100 bp insert). The cloned fragments were sequenced, and the resultant DNA sequences were aligned to existing protein sequences in the NCBI database using the BLASTX algorithm.

*V. vinifera* L cv Pinotage genomic DNA was subsequently digested with a range of restriction endonucleases (REs) (both single- and double digests) separated in an agarose gel. Southern hybridizations using the DIG-labeled partial genes (from pGEM-DXS, pGEM-LBCY, pGEM-NCED, pGEM-PSY and pGEM-ZEP, respectively) as probes enabled the identification of the REs that gave hybridization signals of a size that we expected would contain the entire genomic copy of the genes of interest, as well as the 5'- and 3'-flanking sequences (Table 4.1). The size of these identified fragments varied between 1.5- and 8.5 kb. In order to achieve these goals it was necessary to construct and screen more than one sub-genomic library for each of the CBGs. Fragments of the identified sizes were subsequently isolated and cloned to yield the sub-genomic libraries listed in Table 4.1. Screening of these libraries resulted in the isolation of the full-length genes (i.e. from the predicted putative ATG to the stop codon) for DXS, LBCY, NCED, PSY and ZEP. In addition, the putative promoters (i.e. any sequences upstream of the ATG) for all five genes were also obtained.

Of the four sub-genomic libraries constructed and screened for DXS (PGL-*Eco*RV1, -2, PGL-*Eco*RI/*Hin*DIII, and PGL-*Hin*DIII-3), only PGL-*Eco*RV-2, PGL-*Eco*RI/*Hin*DIII, and PGL-*Hin*DIII-3 were required for the entire DXS genomic context (i.e. full-length genomic copy of the gene, as well as the 5'- and 3'-flanking sequences). Similarly, three sub-genomic libraries were constructed and screened for LBCY (i.e. PGL-*Eco*RV-1, -2 and PGL-*Bam*HI/*Pst*I), but only the latter two were

required for the complete genomic context of LBCY. NCED required four sub-genomic libraries to be constructed and screened: PGL-*Eco*RV-2, PGL-*Kpn*I-1, -2, and PGL-*Hin*DIII-1. Three sub-genomic libraries were required for PSY: PGL-*Eco*RV-2, PGL-*Pst*I/*Spe*I and PGL-*Hin*DIII-2. Lastly, the PGL-*Eco*RV-1 and PGL-*Kpn*I-1 sub-genomic libraries were constructed and screened for ZEP.

Table 4.5 lists the sizes of the full-length genomic copies of the respective CBGs as well as the lengths of the 5'-flanking sequences (i.e. the putative promoters) isolated.

Table 4.4. Accession numbers of the amino acid and nucleotide sequences used for alignments and the plant species they were obtained from.

| Gene | Plant species | GenBank accession number | | % Homology to predicted *Vitis vinifera* protein |
|---|---|---|---|---|
| | | **Protein** | **Nucleotide** | |
| DXS[1] | *Lycopersicon esculentum* | AAD38941 | AF143812 | 86% |
| | *Nicotiana tabacum* | CAC17468 | AJ291721 | ND |
| LBCY[2] | *L. esculentum* | CAA60170 | X86452 | 85% |
| | *N. tabacum* | CAA57386 | X81787 | 83% |
| | *Narcissus pseudonarcissus* | CAA67331 | X98796 | 78% |
| | *Arabidopsis thaliana* | AAB53337 | U50739 | 79% |
| NCED[3] | *L. esculentum* | CAB10168 | Z97215 | 72% |
| | *Phaseolus vulgaris* | AAF26356 | AF190462 | 71% |
| | *Zea mays* (maize) | AAB62181 | U95953 | 62% |
| PSY[4] | *N. pseudonarcissus* | CAA55391 | X78814 | 66% |
| | *Capsicum annuum* | CAA48155 | X68017 | 76% |
| | *A. thaliana* | AAB65697 | AF009954 | 65% |
| | *Oryza sativa* | AAK07735 | AY024351 | 56% |
| | *L. esculentum* | CAA42969 | X60441 | 72% |
| ZEP[5] | *L. esculentum* | CAB06084 | Z83835 | 74% |
| | *Nicotiana plumbaginifolia* | CAA65048 | X95732 | 74% |
| | *C. annuum* | CAA62795 | X91491 | 71% |
| | *Prunus armeniaca* | AAC24582 | AF071888 | 75% |
| | *A. thaliana* | AAG17703 | AF281655 | 70% |

[1] The gene encoding 1-deoxy-D-xylulose 5-phosphate synthase from *Vitis vinifera*. [2] The gene encoding lycopene β-cyclase. [3] The gene encoding 9-*cis*-epoxy carotenoid dioxygenase from *V. vinifera*. [4]. The gene encoding phytoene synthase from *V. vinifera*. [5] The gene encoding zeaxanthin epoxidase from *V. vinifera*. [6] ND, not determined due to the fact that the protein sequence (CAC17468) is not full-length.

The genomic sequences of LBCY, NCED, PSY and ZEP were analyzed for putative intron-exon splice sites using the Netplantgene server from CBS. The DXS genomic sequence is approximately 6000 bp in length and has not been completely sequenced yet.

The BlastX algorithm (from NCBI) was used to align the translated genomic sequences (in all six frames) against the Genbank protein database. This, together with the CBS intron splice site predictions, enabled the identification of potential exons and introns in the genomic sequences (Table 4.5). From these analyses it can be deduced that LBCY and NCED have no introns (i.e. only one exon), whereas six exons (i.e. five introns) and sixteen exons (fifteen introns) were predicted in the genomic sequences of PSY and ZEP, respectively. These results were confirmed by aligning the subsequently isolated cDNA sequences to the genomic sequences (data not shown).

The copy number of the different CBGs in the grapevine genome was determined by Southern hybridizations. Probing of the digested genomic DNA with the DIG-labeled partial genes revealed that DXS, PSY and ZEP are single-copy genes in the genome of *V. vinifera*. LBCY, on the other hand, has two copies, and NCED has at least three copies (Fig. 4.2).

Table 4.5. Analysis of genomic sequences of the carotenoid biosynthetic genes.

| Gene | Genomic copy (ATG to STOP) | Putative promoter (5'-flanking sequence) | Exons |
|---|---|---|---|
| DXS[1] | 6000 bp | 740 bp | n/d[6] |
| LBCY[2] | 1515 bp | 2000 bp | One |
| NCED[3] | 1833 bp | 4300 bp | One |
| PSY[4] | 3973 bp | 800 bp | Six |
| ZEP[5] | 6500 bp | 1300 bp | Sixteen |

[1]The gene encoding 1-deoxy-D-xylulose 5-phosphate synthase from *Vitis vinifera*. [2]The gene encoding lycopene β-cyclase from *V. vinifera*. [3]The gene encoding 9-cis-epoxy carotenoid dioxygenase from *V. vinifera*. [4]The gene encoding phytoene synthase from *V. vinifera*. [5]The gene encoding zeaxanthin epoxidase from *V. vinifera*. [6]Not determined.

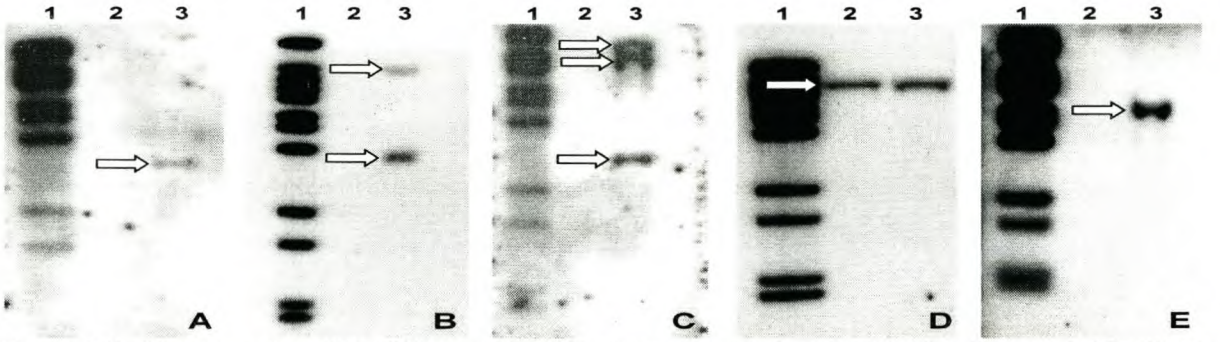


Figure 4.2. Copy number of the CBGs in the *Vitis* genome as determined by Southern hybridizations: A, DXS; B, LBCY; C, NCED; D, PSY; and E; ZEP. In A, B, C and E, lane 3 contains *V. vinifera* L. cv. Pinotage genomic DNA digested with the restriction endonuclease *Eco*RV. In D, lane 2 contains *Bam*HI- and lane 3 *Bam*HI/*Pst*I-digested genomic DNA. The digested genomic DNA was separated in an agarose gel, transferred to nylon membranes and probed with the respective DIG-labeled partial CBGs. A DNA size marker (λ DNA digested with the restriction endonuclease, *Bst*EII) is loaded in lane 1 of A–E. Lane 2 was left open for A, B, C and E. Open white arrows indicate the hybridization signals obtained from the Southern blot: DXS, 3.3 kb; LBCY, 8.0- and 3.5 kb; NCED, 9.0-, 8.0- and 3.0 kb; PSY, 7.0 kb; and ZEP, 5.0 kb.


Figure 4.3. Clustal alignment of the predicted amino acid sequence of the isolated *Vitis vinifera* 1-deoxy-D-xylulose 5-phosphate synthase (DXS) gene to the DXS protein sequence of *Lycopersicon esculentum* (AAD3894). (*), indicates an identical amino acid residue; (:) indicates a similar amino acid residue.

```
Lycopersicon    MDTLLKTPNNLEFLNP-HHGFAVKASTFRSEKHHN----FGSRKFCETLGRSVCVKGSSS 55
Nicotiana       MDTLLKTPNKLEFLHP-VHGFSVKASSFNSVKPHK----FGSRKICENWGKGVCVKAKSS 55
Vitis           MDTLLKTHNKLEFLHP-LHGFAEKLGNLTFPKLQNQEFRFGPKKSNLKWGRNGCVKASSS 59
Arabidopsis     MDTLLKTPNKLDFFIPQFHGFERLCSNNPYHSRVR----LGVKKRAIKIVSS--VVSGSA 54
Narcissus       MDTLLRTHNRLELLYP-LHELAKRHFLSPSPNPQNPNFKFFSRKPYQKKCRNGYIGVSSN 59
                *****:* *.*::: *  * :          . .    : :*   .  . :   *

Lycopersicon    ALLELVPETKKENLDFELPMYDPSKGVVVDLAVVGGGPAGLAVAQQVSEAGLSVCSIDPN 115
Nicotiana       ALLELVPETKKENLDFELPMYDPSKGLVVDLAVVGGGPAGLAVAQQVSEAGLSVVSIDPS 115
Vitis           ALLELVPETKKENLEFELPMYDPSKGLVVDLAVVGGGPAGLAVAQQVSEAGLSVCSIDPS 119
Arabidopsis     ALLDLVPETKKENLDFELPLYDTSKSQVVDLAIVGGGPAGLAVAQQVSEAGLSVCSIDPS 114
Narcissus       QLLDLVPEIKKEHLEFDLPLYDPSKALTLDLAVVGGGPLARSCSTSLG-GGLSVVSIDPN 118
                 **:**** ***:*:*:**:**.**. .:***:***** . : : .:. .**** ****.

Lycopersicon    PKLIWPNNYGVWVDEFEAMDLLDCLDATWSGAAVYIDDNTAKDLHRPYGRVNRKQLKSKM 175
Nicotiana       PKLIWPNNYGVWVDEFEAMDLLDCLDATWSGTVVYIDDNTTKDLDRPYGRVNRKQLKSKM 175
Vitis           PKLIWPNNYGVWVDEFEAMDLLDCLDTTWSGAVVFIDDHSKKDLGRPYARVNRKQLKSKM 179
Arabidopsis     PKLIWPNNYGVWVDEFEAMDLLDCLDTTWSGAVVYVDEGVKKDLSRPYGRVNRKQLKSKM 174
Narcissus       PKLIWPNNYGVWVDEFEDMDLLDCLDATWSGAIVYVDDRSTKNLSRPYARVNRKNLKSKM 178
                ***************** ********:****: *:::*:   *:* ***.*****:*****

Lycopersicon    MQKCIMNGVKFHQAKVIKVIHEESKSMLICNDGITIQATVVLDATGFSRSLVQYDKPYNP 235
Nicotiana       MQKCILNGVKFHHAKVIKVIHEEAKSMLICNDGVTIQATVVLDATGFSRCLVQYDKPYKP 235
Vitis           MQKCILNGVKFHQAKVIKVIHEESKSLLICNDGVTIQAAVVLDATGFSRCLVQYDKPYNP 239
Arabidopsis     LQKCITNGVKFHQSKVTNVVHEEANSTVVCSDGVKIQASVVLDATGFSRCLVQYDKPYNP 234
Narcissus       MKKCVSNGVRFHQATVVKAMHEEEKSYLICSDGVTIDARVVLDATGFSRCLVQYDKPYNP 238
                ::**: ***:**::.* :.:*** :* ::*.**:.*:* **********.********:*

Lycopersicon    GYQVAYGILAEVEEHPFDVNKMVFMDWRDSHLKNNTDLKERNSRIPTFLYAMPFSSNRIF 295
Nicotiana       GYQVAYGILAEVEEHPFDTSKMVLMDWRDSHLGNNMELKERNRKVPTFLYAMPFSSNKIF 295
Vitis           GYQVAYGILAEVEEHPFDVDKMVFMDWRDSHLNNNMELKNRNGRIPTFLYAMPFSSNRIF 299
Arabidopsis     GYQVAYGIVAEVDGHPFDVDKMVFMDWRDKHLDSYPELKERNSKIPTFLYAMPFSSNRIF 294
Narcissus       GYQVAYGILAEVEEHPFDVDKMVFMDWRDSHLNGKAELNERNAKIPTFLYAMPFSSNRIF 298
                ********:***: ****..***:*****.** .  :*::** ::*************:**

Lycopersicon    LEETSLVARPGLRIDDIQERMVARLNHLGIKVKSIEEDEHCLIPMGGPLPVLPQRVVGIG 355
Nicotiana       LEETSLVARPGLRMDDIQERMVARLNHLGIKVKSIEEDEHCVIPMGGSLPVIPQRVVGTG 355
Vitis           LEETSLVARPGVPMEDIQERMVARLRHLGIKVKSIEEDERCIIPMGGPLPVLPQRVVGIG 359
Arabidopsis     LEETSLVARPGLRMEDIQERMAARLKHLGINVKRIEEDERCVIPMGGPLPVLPQRVVGIG 354
Narcissus       LEETSLVARPGLKMEDIQERMVARLNHLGIRIKSIEEDERCVIPMGGPLPVIPQRVVGIG 358
                ***********: ::******.***.****.:* *****:*:*****.***:****** *

Lycopersicon    GTAGMVHPSTGYMVARTLAAAPVVANAIIQYLGS--ERSHSGNELSTAVWKDLWPIERRR 413
Nicotiana       GTAGLVHPSTGYMVARTLAAAPVVANAIIHYLGS--EKDLLGNELSAAVWKDLWPIERRR 413
Vitis           GTAGMVHPSTGYTVARTLAAAPIVANSIVQYLGS--DRSFFGNELSSEVWRDLWPIERRR 417
Arabidopsis     GTAGMVHPSTGYMVARTLAAAPIVANAIVRYLGSPSSNSLRGDQLSAEVWRDLWPIERRR 414
Narcissus       GTAGMVHPSTGYMVARTLAAAPIVANSIVQYLVS--DSGLSGNDLSADVWKDLWPIERRR 416
                ****:******** *********:***:*::** *  . .  *::**: **:********** 

Lycopersicon    QREFFCFGMDILLKLDLPATRRFFDAFFDLEPRYWHGFLSSRLFLPELIVFGLSLFSHAS 473
Nicotiana       QREFFCFGMDILLKLDLPATRRFFDAFFDLEPRYWHGFLSSRLYLPELIFFGLSLFSRAS 473
Vitis           QREFFCFGMDILLKLDLQGTRRFFDAFFDLEPRYWHGFLSSRLFLPELIFFGLSLFSHAS 477
Arabidopsis     QREFFCFGMDILLKLDLDATRRFFDAFFDLQPHYWHGFLSSRLFLPELLVFGLSLFSHAS 474
Narcissus       QREFFCFGMDILLKLDLEGTRRFFDAFFDLEPRYWHGFLSSRLFLPELVPFGLSLFSHAS 476
                ***************** .*********:*:**********:****: *******:**

Lycopersicon    NTSRFEIMTKGTVPLVNMINNLLQDKE 500
Nicotiana       NTSRIEIMTKGTLPLVNMINNLLQDTE 500
Vitis           NTSRIEIMAKGTLPLINMINNLIQDKD 504
Arabidopsis     NTSRLEIMTKGTVPLAKMINNLVQDRD 501
Narcissus       NTCKLEIMAKGTLPLVNMINNLVQDRD 503
                **.::***:***:** :*****:** :
```

Figure 4.4. Clustal alignment of the predicted amino acid sequence of the isolated *Vitis vinifera* lycopene β-cyclase (LBCY) gene to the LBCY protein sequences of *Lycopersicon esculentum* (CAA60170), *Nicotiana tabacum* (CAA57386), *Narcissus pseudonarcissus* (CAA67331), *Arabidopsis thaliana* (AAB53337). (*), indicates an identical amino acid residue; (:) indicates a similar amino acid residue.


Figure 4.5. Clustal alignment of the predicted amino acid sequence of the isolated *Vitis vinifera* 9-*cis* epoxy carotenoid dioxygenase (NCED) gene to the NCED protein sequences of *Lycopersicon esculentum* (CAB10168), *Phaseolus vulgaris* (AAF26356), *Zea mays* (AAB62181). (*), indicates an identical amino acid residue; (:) indicates a similar amino acid residue.

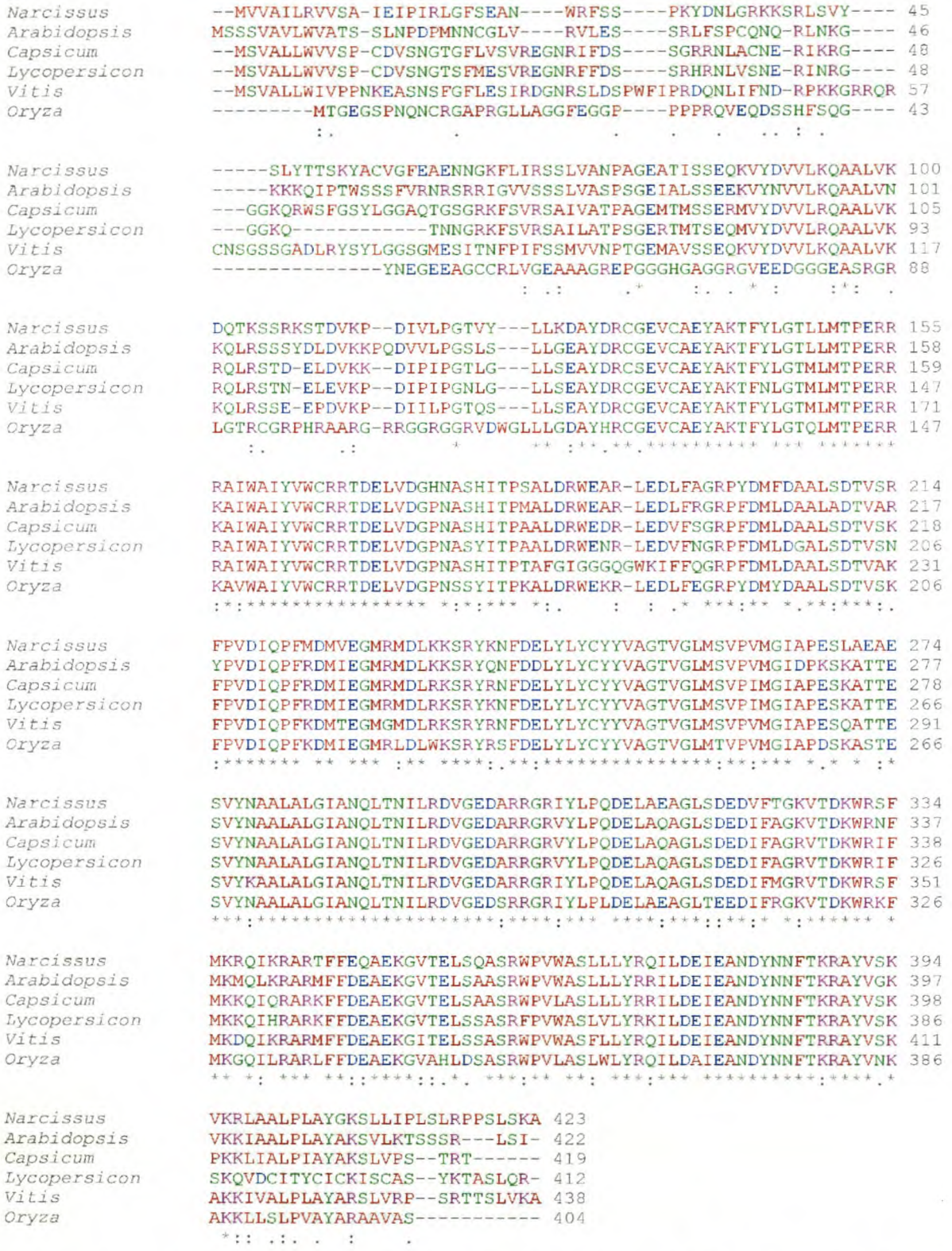


Figure 4.6. Clustal alignment of the predicted amino acid sequence of the isolated *Vitis vinifera* phytoene synthase (PSY) gene to the PSY protein sequences of *Narcissus pseudonarcissus* (CAA55391), *Capsicum annuum* (CAA48155), *Arabidopsis thaliana* (AAB65697), *Oryza sativa* (AAK07735) and *Lycopersicon esculentum* (CAA60170). (*), indicates an identical amino acid residue; (:) indicates a similar amino acid residue.


Figure 4.7. Clustal alignment of the predicted amino acid sequence of the isolated *Vitis vinifera* zeaxanthin epoxidase (ZEP) gene to the ZEP protein sequences of *Lycopersicon esculentum* (CAB06084), *Nicotiana plumbaginifolia* (CAA65048), *Capsicum annuum* (CAA62795), *Prunus armeniaca* (AAC24582), *Arabidopsis thaliana* (AAG17703). (*), indicates an identical amino acid residue; (:) indicates a similar amino acid residue.

### 4.3.2 Isolation of the full-length cDNA clones encoding carotenoid biosynthetic genes

Based on the predicted intron-exon splice sites in the genomic sequences of the CBGs, the ATG and stop codons were putatively identified, and primers subsequently designed to amplify the full-length coding sequences (i.e. from the predicted putative ATG to the stop codon) (Table 4.2). These primers were used to amplify the cDNA copies of the respective genes. Full-length cDNA copies of all five genes targeted for isolation (i.e. DXS, LBCY, NCED, PSY and ZEP), have been isolated. The respective PCR products (from cDNA) were subsequently cloned and their identity verified by sequencing.

The protein sequences of the CBGs were predicted by translating the obtained cDNA sequences. These predicted protein sequences were aligned to protein sequences in the GenBank database (using the BlastP algorithm) and to selected sequences using ClustalX. Fig. 4.3-4.7 displays the alignments of the predicted amino acid sequences of the CBGs DXS, LBCY, NCED, PSY and ZEP to the protein sequences listed in Table 4.4. The ProtComp server was used to predict the sub-cellular localization of the DXS, LBCY, NCED, PSY and ZEP proteins. The results of the ProtComp predictions suggest that the proteins of all the *V. vinifera* CBGs were localized in the chloroplast.

The predicted protein sequences of the isolated CBGs (i.e. DXS, LBCY, NCED, PSY and ZEP) were further submitted to the Conserved Domain Database (CDD) to identify any potential homology to conserved domains. This database does not rely on direct sequence homology, but rather on domain profiles or domain architecture. Domain architecture can be defined as the sequential order of conserved domains in protein sequences [26]. The CDD search using the DXS protein sequences detected two domains with a similar domain architecture: a transketolase N-terminal subunit (COG3959), and a transketolase C-terminal subunit (COG3958). DXS is a transketolase. The LBCY showed homology to the crtY domain, which is present in LBCYs, lycopene e-cyclases (LECY), neoxanthin synthases (NSY) and capsanthin capsorubin synthases (CCS). The CCSs, however contain a FAD-binding domain that LBCY, LECY and NSY do not contain. The NCED protein shares homology with β, β-carotene dioxygenases (retinal pigment epithelial membrane proteins) (KOG1285). The PSY protein detects a PSY domain (KOG1459), and similarly the

ZEP protein detects a ZEP domain (KOG2614), but also a Forkhead associated (FHA) domain (CD00060), that is thought to be a nuclear signalling domain [27].

Alignments to the EST databases of TIGR and NCBI provided additional sequence information and helped to identify untranslated regions (UTRs) in the CBGs cDNA sequences (Table 4.6). These analyses identified UTRs in the 3'-flanking sequences of DXS (178 bp), LBCY (148 bp), NCED (430 bp), PSY (204 bp), and ZEP (304 bp). 5'-UTRs were not available for all the genes investigated and were, therefore, omitted from this study.

Table 4.6. Analysis of the cDNA sequences of the carotenoid biosynthetic genes.

| Gene | cDNA (ATG to stop) | Untranslated regions (UTRs) | Predicted protein (aa) |
|---|---|---|---|
| DXS[1] | 2151 bp | 3'-UTR (178 bp) | 717 |
| LBCY[2] | 1512 bp | 3'-UTR (148 bp) | 504 |
| NCED[3] | 1830 bp | 3'-UTR (430 bp) | 610 |
| PSY[4] | 1314 bp | 3'-UTR (204 bp) | 438 |
| ZEP[5] | 1974 bp | 3'-UTR (304 bp) | 658 |

[1]The gene encoding 1-deoxy-D-xylulose 5-phosphate synthase from *Vitis vinifera*. [2]The gene encoding lycopene β-cyclase from *V. vinifera*. [3]The gene encoding 9-*cis*-epoxy carotenoid dioxygenase from *V. vinifera*. [4]The gene encoding phytoene synthase from *V. vinifera*. [5]The gene encoding zeaxanthin epoxidase from *V. vinifera*.

### 4.3.3 Functional complementation and pigment analysis

The isolation of carotenoid biosynthetic genes has been accelerated in the past decade due to a functional complementation system that utilises *E. coli* strains genetically engineered to synthesise carotenoids due to the introduction of CBGs of *Erwinia herbicola* [7;16]. Although this assay was not used for the isolation of the genes in this study, it was (where possible) used to confirm the functionality of the CBGs from *V. vinifera*. Typically, a colony colour change corresponding to the pigment formed (following complementation in the relevant *E.coli* strain), confirms the functionality of the expressed gene. DXS, LBCY, PSY were tested using this assay, but only LBCY and PSY were functional in this bacterial system. Functional complementation of NCED and ZEP was not possible in our test system due to the fact that we could not differentiate between violaxanthin and xanthoxin for NCED, and zeaxanthin and violaxanthin for ZEP. HPLC with authentic carotenoid pigments as standards will address this issue.

The pigments that accumulated in the transformed *E. coli* cells of the functional complementation assay were analyzed by thin layer chromatography (TLC), and

confirmed that lycopene is actively converted to β-carotene by pART27-cLBCY; and similarly, that GGPP is converted to β-carotene by pART27-cPSY (data not shown). HPLC using authentic carotenoid standards is required to verify the carotenoids formed.

### 4.3.4 Expression analysis of the carotenoid biosynthetic genes in *Vitis vinifera*

RT-PCR analysis was used to determine the relative expression of DXS, LBCY, PSY, NCED and ZEP in different organs and different developmental stages of *V. vinifera.* cDNA was synthesized from ripening berries (véraison), fully-expanded leaves and shoot tips and RT-PCR reactions were performed. Only the data obtained from LBCY, PSY and ZEP showed time-dependent differences and will be discussed further. The data indicate that the expression of LBCY, PSY and ZEP are consistently higher in leaves and shoot tips, and lowest in berries (Fig. 4.8). The expression of the CBG genes was also determined following different treatments on detached field-grown leaves. The treatments were chosen based on the occurrence of these genes in existing public EST databases for *V. vinivfera* (i.e. TIGR and NCBI). EST database searches for the occurrence of DXS, LBCY, NCED, PSY and ZEP identified ABA, NaCl and wounding as potential induction treatments. The different treatments selected were, therefore, 100 μM ABA, 300 mM NaCl, or wounding. Samples were taken after 1 h and 24 h after the induction of the treatment.

Both the ABA and NaCl treatments resulted in a time-dependent increase in the relative expression of PSY. ZEP, on the other hand, showed a time-dependent decrease in expression (Fig. 4.9).

The wounded leaves however showed a different pattern: LBCY and PSY were unaffected by the treatment, whereas ZEP showed an inverse pattern to the control plant, with an increase in expression after 1 h (relative to an unwounded leaf), but a decrease after 24 h.

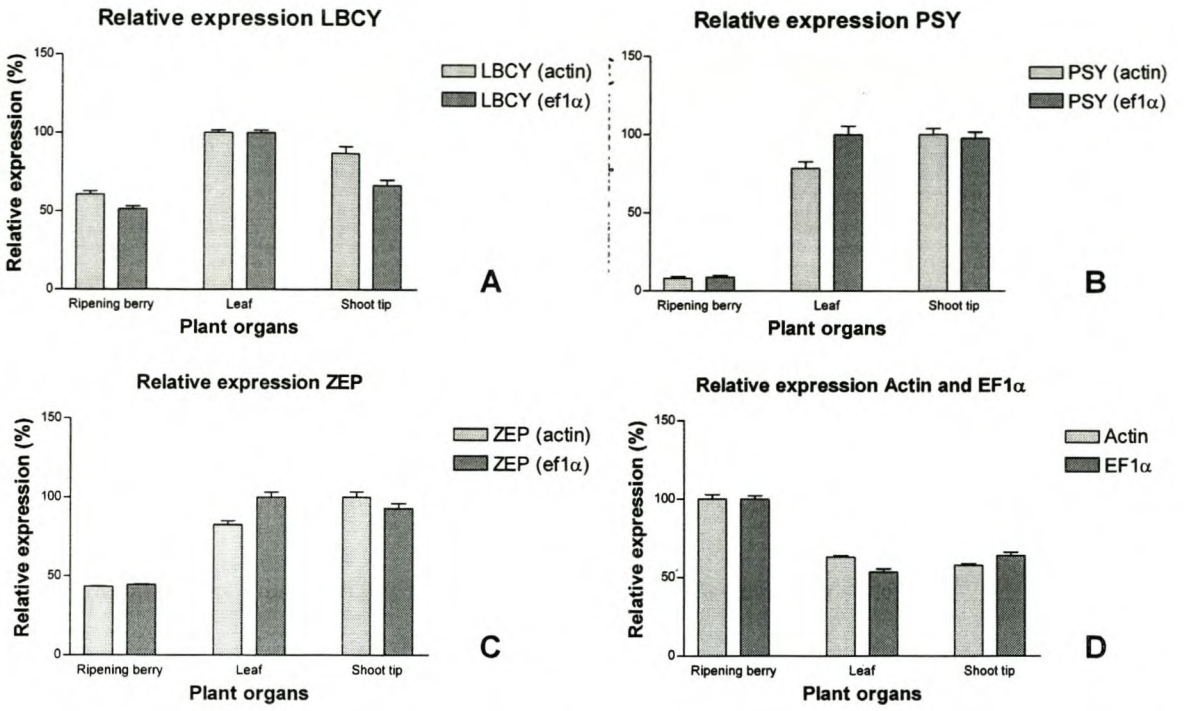


Figure 4.8. Normalized expression of the (A) lycopene β-cyclase (LBCY), (B) phytoene synthase (PSY) and (C) zeaxanthin epoxidase (ZEP) genes in ripening berries, fully-expanded leaves and shoot tips of *Vitis vinifera* L. cv. Pinotage. The expression of LBCY, PSY and ZEP was normalized relative to the expression of two independent constitutively expressed genes: actin (light grey blocks) and elongation factor 1-α (EF1α) (dark grey blocks) encoding genes. Data are represented as a percentage with the 0% corresponding to 0.0 on the Y-axis, and 100% corresponding to the expression with the highest value. Each data set represents the mean of three values.

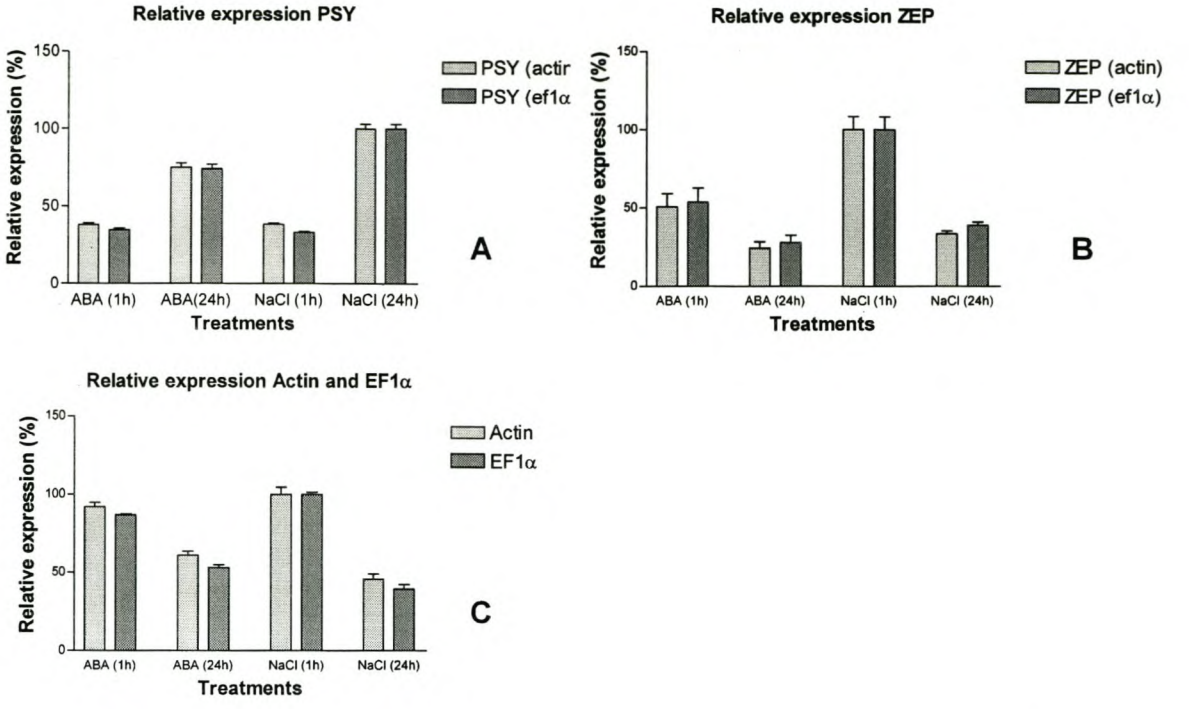


Figure 4.9. Time course analysis of the expression of (A) phytoene synthase (PSY) and (B) zeaxanthin epoxidase (ZEP) genes in detached leaves of *Vitis vinifera* L. cv. Pinotage determined after 1 h and 24 h of treatment with 100 μM abscisic acid (ABA) or 300 mM NaCl. The expression of PSY and ZEP was normalized relative to (C), the expression of both the constitutively expressed genes: actin (light grey blocks) and elongation factor 1-α (EF1α) (dark grey blocks) encoding genes. Data are represented as a percentage with the 0% corresponding to 0.0 on the y-axis, and 100% corresponding to the expression with the highest value. Each data set represents the mean of three values.

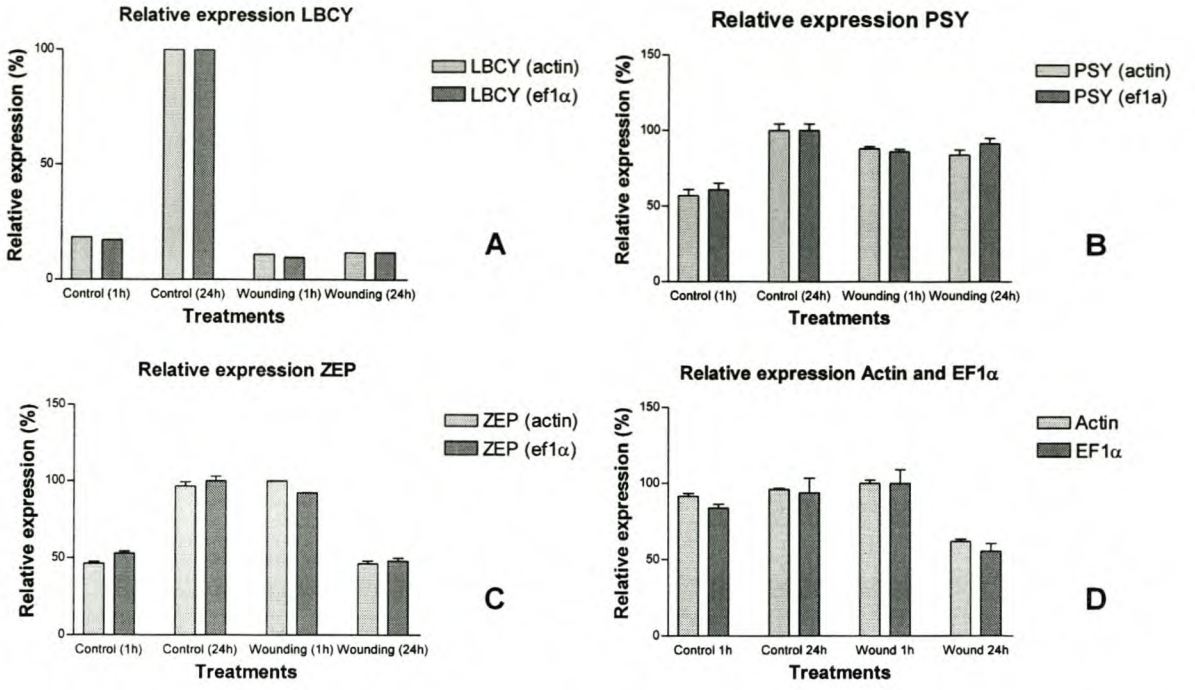


Figure 4.10. Time course analysis of the expression of (A) lycopene β-cyclase (LBCY), (B) phytoene synthase (PSY), (C), zeaxanthin epoxidase (ZEP) genes in detached leaves of *Vitis vinifera* L. cv. Pinotage determined 1 h and 24 h after wounding the leaves (relative to a control treatment). The expression of LBCY, PSY and ZEP was normalized relative to (D), the expression of both the constitutively expressed genes: actin (light grey blocks) and elongation factor 1-α (EF1α) (dark grey blocks) encoding genes. Data are represented as a percentage with the 0% corresponding to 0.0 on the Y-axis, and 100% corresponding to the expression with the highest value. Each data set represents the mean of three values, except (A) where only one measurement was taken.

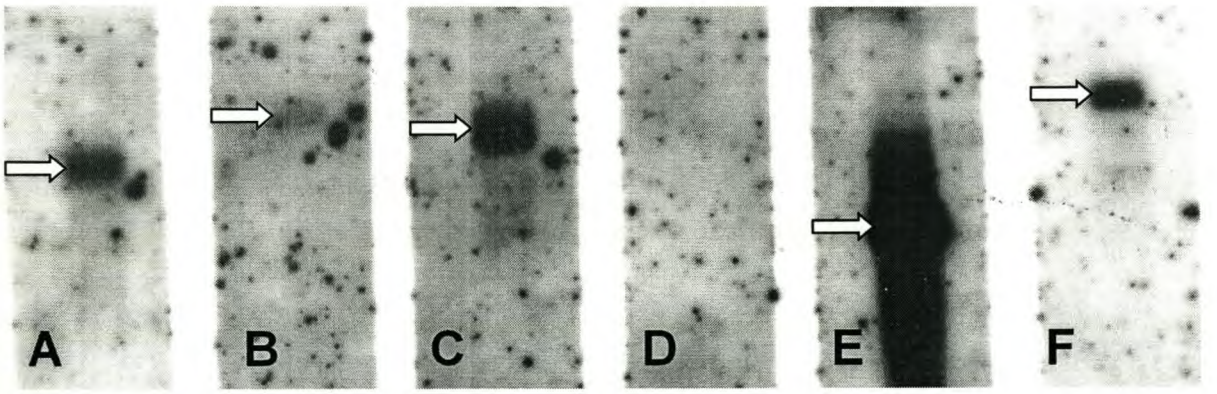


Figure 4.11. Northern blot analyses of the expression of the (A) phytoene synthase- (1317 bp), (B) 9-*cis*-epoxy dioxygenase- (1833 bp), (C) lycopene β-cyclase (1515 bp), (D) 1-deoxy-D-xylulose 5-phosphate synthase- (2157 bp) (E) D1 protein- (1077 bp), and (F) zeaxanthin epoxidase- (1977 bp) encoding genes in field-grown fully-expanded leaves of *Vitis vinifera* L. cv. Pinotage. Total RNA was

separated on a formaldehyde agarose gel, transferred to nylon membranes, and probed with the respective partial CBGs. The hybridization signals are indicated with open arrows.

### 4.3.5 Transient promoter analysis

None of the putative CBG promoter constructs (i.e. pBS-DXSp-, LBCYp-, NCEDp-, PSYp-, ZEPp-GUS) tested showed any promoter activity in any of the tissue analyzed, or on any of the media used (i.e. 100 μM ABA, 300 mM NaCl or dehydration). The positive control, pBS-[CaMV-GUS] consistently showed positive GUS activity (the presence of blue spots) in the subsequent stainings. Conversely, the negative control, pBS-GUS, showed no GUS activity.

## 4.4 DISCUSSION

Five genes (DXS, LBCY, NCED, PSY and ZEP) that are either directly or indirectly involved in the carotenoid biosynthetic pathway have been isolated from *V. vinifera* L. cv Pinotage. The intron-exon splice sites predicted in the genomic sequences using the CBS server were confirmed by alignments of the genomic- and cDNA sequences, thereby verifying the usefulness of the prediction server for these analyses in *V. vinifera*. The copy number of the isolated genes was determined by Southern hybridization and DXS, PSY and ZEP are present as single-copy genes in the *V. vinifera* genome, whereas LBCY and NCED have two and three copies, respectively (Fig. 4.2). Future work will focus on isolating the additional copies of LBCY and NCED. In most plant species studied, NCED comprises a gene family consisting of several members. Nine hypothetical genes in the *Arabidopsis* genome encode for NCED, of which four (*AtNCED2, -3, -6,* and *-9*) have been shown to catalyze the cleavage reaction in ABA synthesis. It is thought that the different NCED-encoding genes in *Arabidopsis* are expressed in different tissues and at different developmental stages, and it can be assumed that a similar scenario exists in *V. vinifera* [28].

Analyses of the predicted protein sequences provided additional structural information regarding the isolated genes. The ProtComp server was used to predict the sub-cellular localization of these proteins in the cell. This server combines several prediction methods (neural network-based prediction, sequence alignments, and prediction of certain functional peptide sequences) in order to putatively localize the proteins sub-cellularly. The accuracy of the prediction is reported as being

between 80- and 90% [29]. Since the CBGs are known to be nuclear-encoded, but functional in the chloroplast – it is expected that these amino acids will contain chloroplast transit peptides (cTPs). In order to determine the validity of the prediction program (ProtComp), the sequences of the proteins used for the initial alignments were analyzed (Table 4.4). The predictions indicated that the proteins were membrane-bound and localized in the chloroplast. The sub-cellular targeting of the hypothetical proteins of DXS, LBCY, NCED, PSY and ZEP from *V. vinifera* were subsequently predicted using the ProtComp server. Although NCED is discussed in the carotenoid biosynthetic pathway, it is strictly speaking not a carotenoid biosynthetic gene, but rather an abscisic acid biosynthetic gene by catalyzing the first committed step in ABA biosynthesis by converting violaxanthin and neoxanthin to xanthoxin (in the chloroplast). The results of the ProtComp predictions confirmed that the proteins of all the *V. vinifera* CBGs were localized in the chloroplast. As expected, the preproteins of the carotenoid enzymes are nuclear-encoded, and post-translationally targeted to the plastids and processed. Regulation can, therefore, potentially take place transcriptionally, post-transcriptionally, or translationally.

The predicted protein sequences of the isolated CBGs (i.e. DXS, LBCY, NCED, PSY and ZEP) were submitted to the Conserved Domain Database (CDD) to identify any potential conserved domain profiles. Domains can be regarded as the structural and functional building blocks of proteins that divide the primary and tertiary structure of an amino acid chain into distinct units. In addition to analyzing the full-length protein sequences (e.g. by protein alignments), it is also useful to analyze the proteins as collections of domains [23;24]. The identified domains proved particularly useful in identifying areas in the gene sequences that are necessary for function and are usually highly conserved between species. Since the homologies are based on functional domains and domain profiles, these predictions also provided additional *in silico* confirmation of the function of the analyzed proteins.

Although the 3'-UTRs of DXS, LBCY, PSY and ZEP showed no homology with any other CBGs (or any other genes in the NCBI databases), the sequence of 3'-UTR of the isolated NCED gene, however, contained two stretches that are conserved in the UTRs of other NCEDs. It would be interesting to test the role of this conserved "element(s)" on the expression and regulation of the NCED gene (Fig. 4.6).

Only LBCY and PSY were shown to be functional in the heterologous functional complementation assay. This only indicates that DXS, NCED and ZEP are not functional in the assay they were tested in, and it is possible that the transit peptides are not processed and their presence in the mature peptide interferes with the functioning of the enzyme in the bacterial system. For example, the chloroplast transit peptide of NCED is predicted to be 70 amino acids (i.e. 210 bp) in length, and it is quite plausible that the presence of this additional amino acid stretch interferes with the enzymes functioning in *E. coli*.

Although RT-PCR proved more sensitive than northern hybridizations for determining the relative expression levels of the LBCY, PSY and ZEP genes, it was not possible to quantify the absolute expression levels. Trends in the relative expression levels could, however, be determined. Since the experiments were repeated in triplicate from the same batch of cDNA (i.e. technical repeats), the observed trends would be strengthened by repeating the experiment using independently synthesized cDNA batches (i.e. biological repeats). For LBCY, PSY and ZEP the expression levels were higher in leaves and shoot tips than ripening berries. This could be due to the fact that the leaves and shoot tips are still photosynthetically active, whereas the ripening berries (véraison) are not (Fig. 4.8). ABA and NaCl showed a similar expression profile for PSY and caused a time-dependent up-regulation. Similarly, ABA and NaCl showed a similar profile for ZEP, but unlike PSY causing a time-dependent down-regulation (Fig. 4.9). The wounding response in LBCY, PSY, and ZEP was less clear. The wounding treatment showed no significant effect in LBCY or PSY, but the ZEP expression was down-regulated. The interpretation of the data from the wounding treatments becomes problematic when analyzing the control RT-PCR reactions. The control represents detached leaves that were placed in water. These leaves showed the highest "induction" in LBCY, and slight induction in both PSY and ZEP. The reason for this is unclear. The treatment of the leaves before the inductions was identical, and any diurnal pattern should not be detectable since the samples were taken 24 h apart. Additional experiments need to be conducted to address these questions (Fig. 4.10).

Since transcript levels of all the CBGs tested (except DXS) were detected by northern hybridization (LBCY, NCED, PSY, and ZEP) and/or RT-PCR analysis (DXS, LBCY, NCED, PSY, and ZEP), it stands to reason that the promoters of the isolated

genes are transcriptionally active (Fig. 4.11). The apparent inability of the cloned promoter fragments of the CBGs to drive the expression of the GUS gene could be due to the lack of sensitivity of the assay used for the detection of the reporter gene (i.e. histochemical staining), or alternatively due to low transcriptional levels of the CBG genes. Another option is that the promoter fragments isolated and cloned are too short and, therefore, do not contain a functional promoter to drive the expression of the reporter gene. Isolation of larger promoter fragments of the CBGs, in combination with stable integration of the putative promoter constructs into model plants (i.e. *Arabidopsis* or *Nicotiana*) should address these potential problems and provide information on the expression of these genes.

The DXS, LBCY, NCED, PSY and ZEP-encoding genes isolated in this study have been cloned into the plant binary vector, pART27, and transformed via *A. tumefaciens* into both *A. thaliana* and *N. tabacum*. The plants are currently being evaluated and the future analyses of these transgenic plants overexpressing the respective CBGs should provide useful information into the *in vivo* role(s) of these enzymes in plants and, in particular, their contribution to photosynthesis.

## 4.5 LITERATURE CITED

[1] Lange,B.M., Rujan,T., Martin,W., & Croteau,R. (2000) Isoprenoid biosynthesis: The evolution of two ancient and distinct pathways across genomes. *Proc Natl Acad Sci USA*, **97,** 13172-13177.

[2] Cunningham,F.X., Jr. & Gantt,E. (1998) Genes and enzymes of carotenoid biosynthesis in plants. *Annu Rev Plant Physiol Plant Mol Biol*, **49,** 557-583.

[3] Hirschberg,J. (2001) Carotenoid biosynthesis in flowering plants. *Curr Opin Plant Biol*, **4,** 210-218.

[4] Demmig-Adams,B., Gilmore,A.M., & Adams,W.W., III (1996) Carotenoids 3: *In vivo* function of carotenoids in higher plants. *FASEB J*, **10,** 403-412.

[5] Eisenreich,W., Rohdich,F., & Bacher,A. (2001) Deoxyxylulose phosphate pathway to terpenoids. *Trends Plant Sci*, **6,** 78-84.

[6] Rohdich,F., Zepeck,F., Adam,P., Hecht,S., Kaiser,J., Laupitz,R., Grawert,T., Amslinger,S., Eisenreich,W., Bacher,A., & Arigoni,D. (2003) The deoxyxylulose phosphate pathway of isoprenoid biosynthesis: studies on the mechanisms of the reactions catalyzed by IspG and IspH protein. *Proc Natl Acad Sci USA*, **100,** 1586-1591.

[7] Cunningham,F.X., Jr., Sun,Z., Chamovitz,D., Hirschberg,J., & Gantt,E. (1994) Molecular structure and enzymatic function of lycopene cyclase from the cyanobacterium *Synechococcus* sp strain PCC7942. *Plant Cell*, **6,** 1107-1121.

[8] Harker,M. & Bramley,P.M. (1999) Expression of prokaryotic 1-deoxy-D-xylulose-5-phosphatases in *Escherichia coli* increases carotenoid and ubiquinone biosynthesis. *FEBS Lett*, **448,** 115-119.

[9] Cunningham,F.X., Jr., Lafond,T.P., & Gantt,E. (2000) Evidence of a role for LytB in the nonmevalonate pathway of isoprenoid biosynthesis. *J Bacteriol*, **182,** 5841-5848.

[10] Lindgren,L.O., Stalberg,K.G., & Hoglund,A.S. (2003) Seed-specific overexpression of an endogenous *Arabidopsis* phytoene synthase gene results in delayed germination and increased levels of carotenoids, chlorophyll, and abscisic acid. *Plant Physiol*, **132,** 779-785.

[11] Bendich,A. (1989) Symposium conclusions: Biological actions of carotenoids. *J Nutr*, **119,** 135-136.

[12] Britton,G. (1995) Structure and properties of carotenoids in relation to function. *FASEB J*, **9,** 1551-1558.

[13] Steel,C.C. & Keller,M. (2000) Influence of UV-B irradiation on the carotenoid content of *Vitis vinifera* tissues. *Biochem Soc Trans*, **28,** 883-885.

[14] Davison,P.A., Hunter,C.N., & Horton,P. (2002) Overexpression of β-carotene hydroxylase enhances stress tolerance in *Arabidopsis*. *Nature*, **418,** 203-206.

[15] Sambrook,J., Fritsch,E.F., & Maniatis,T. (1989) *Molecular cloning: a laboratory manual*, 2nd edn. Cold Spring Harbor Laboratory Press, Cold Spring Harbor, N.Y. (USA).

[16] Cunningham,F.X., Jr., Chamovitz,D., Misawa,N., Gantt,E., & Hirschberg,J. (1993) Cloning and functional expression in *Escherichia coli* of a cyanobacterial gene for lycopene cyclase, the enzyme that catalyzes the biosynthesis of β-carotene. *FEBS Lett*, **328,** 130-138.

[17] Steenkamp,J.A., Wiid,I., Lourens,A., & van Helden,P. (2003) Improved method for DNA extraction from *Vitis vinifera*. *Am J Enol Vitic*, **45,** 102-106.

[18] Davies,C. & Robinson,S.P. (1996) Sugar accumulation in grape berries. Cloning of two putative vacuolar invertase cDNAs and their expression in grapevine tissues. *Plant Physiol*, **111,** 275-283.

[19] Gleave,A.P. (1992) A versatile binary vector system with a T-DNA organisational structure conducive to efficient integration of cloned DNA into the plant genome. *Plant Mol Biol*, **20,** 1203-1207.

[20] Jefferson,R.A., Kavanagh,T.A., & Bevan,M.W. (1987) GUS fusions: β-glucuronidase as a sensitive and versatile gene fusion marker in higher plants. *EMBO J*, **6,** 3901-3907.

[21] Thompson,J.D., Gibson,T.J., Plewniak,F., Jeanmougin,F., & Higgins,D.G. (1997) The CLUSTAL_X windows interface: flexible strategies for multiple sequence alignment aided by quality analysis tools. *Nucleic Acids Res*, **25,** 4876-4882.

[22] Hebsgaard,S.M., Korning,P.G., Tolstrup,N., Engelbrecht,J., Rouze,P., & Brunak,S. (1996) Splice site prediction in *Arabidopsis thaliana* pre-mRNA by combining local and global sequence information. *Nucleic Acids Res*, **24,** 3439-3452.

[23] Marchler-Bauer,A., Panchenko,A.R., Shoemaker,B.A., Thiessen,P.A., Geer,L.Y., & Bryant,S.H. (2002) CDD: a database of conserved domain alignments with links to domain three-dimensional structure. *Nucleic Acids Res*, **30,** 281-283.

[24] Marchler-Bauer,A., Anderson,J.B., DeWeese-Scott,C., Fedorova,N.D., Geer,L.Y., He,S., Hurwitz,D.I., Jackson,J.D., Jacobs,A.R., Lanczycki,C.J., Liebert,C.A., Liu,C., Madej,T., Marchler,G.H., Mazumder,R., Nikolskaya,A.N., Panchenko,A.R., Rao,B.S., Shoemaker,B.A., Simonyan,V., Song,J.S., Thiessen,P.A., Vasudevan,S., Wang,Y., Yamashita,R.A., Yin,J.J., & Bryant,S.H. (2003) CDD: a curated Entrez database of conserved domain alignments. *Nucleic Acids Res*, **31,** 383-387.

[25] Higo,K., Ugawa,Y., Iwamoto,M., & Korenaga,T. (1999) Plant *cis*-acting regulatory DNA elements (PLACE) database: 1999. *Nucleic Acids Res*, **27,** 297-300.

[26] Geer,L.Y., Domrachev,M., Lipman,D.J., & Bryant,S.H. (2002) CDART: Protein homology by domain architecture. *Genome Res.*, **12,** 1619-1623.

[27] Durocher,D. & Jackson,S.P. (2002) The FHA domain. *FEBS Letters*, **513,** 58-66.

[28] Iuchi,S., Kobayashi,M., Yamaguchi-Shinozaki,K., & Shinozaki,K. (2000) A stress-inducible gene for 9-*cis*-epoxycarotenoid dioxygenase involved in abscisic acid biosynthesis under water stress in drought-tolerant cowpea. *Plant Physiol*, **123,** 553-562.

[29] Buckingham,S. (2003) Bioinformatics: programmed for success. *Nature*, **425,** 209-215.

# CHAPTER 5

# RESEARCH RESULTS

## Isolation and characterization of candidate genes in the isoprenoid and carotenoid biosynthetic pathways of *Vitis vinifera* L. II

This manuscript will be submitted for publication in ***Plant Molecular Biology***

# Isolation and characterization of candidate genes in the isoprenoid and carotenoid biosynthetic pathways of *Vitis vinifera* L. II

Philip R. Young[1], Isak S. Pretorius[2] and Melané A. Vivier[1*]

[1]Institute for Wine Biotechnology, Department of Viticulture and Oenology, Stellenbosch University, Stellenbosch, South Africa, 7600; [2]Australian Wine Research Institute, Adelaide, Australia

## ABSTRACT

All isoprenoids are synthesized from only two $C_5$ precursors: isopentenyl diphosphate (IPP) and dimethyllallyl diphosphate (DMAPP). In plants, two pathways are involved in the biosynthesis of IPP and DMAPP: the mitochondrial/cytosolic mevalonate pathway and the plastidic 1-deoxy-D-xylulose 5-phosphate [(DOXP)/2-C-methyl-D-erythritol 4-phosphate (MEP) pathway (or mevalonate independent)] pathway. Searches of the publicly available expressed sequence tag (EST) databases of the National Center for Biotechnology Information (NCBI) and The Institute for Genomic Research (TIGR) provided sufficient sequence information that facilitated the isolation of five full-length genes encoding for: farnesyl diphosphate synthase (FPS), IPP isomerase (IPI), 3-hydroxy-3-methylglutaryl coenzyme A synthase (HMGS), 4-hydroxy-3-methylbut-2-enyl diphosphate reductase (lytB/ispH), geranylgeranyl diphosphate synthase (GGPS); as well as eight partial genes encoding for: 1-deoxy-D-xylulose 5-phosphate reductase (DXR), hydroxymethylbutenyl diphosphate synthase (gcpE/ispG), ζ-carotene desaturase (ZDS), carotenoid isomerase (CISO), lycopene ε-cyclase (LECY), violaxanthin de-epoxidase (VDE), xanthine dehydrogenase (XDH) and a short chain dehydrogenase/reductase (SCD). These genes were identified by their homology to related genes from other species, and selected based on their involvement in either the mevalonate pathway or the DOXP/MEP pathway to IPP and DMAPP; the carotenoid biosynthetic pathway; or the abscisic acid biosynthetic pathway. The cDNA copies of the respective full-length- and partial genes have been isolated, cloned and sequenced. The isolation and *in silico* analyses of the obtained nucleotide sequences and their predicted protein sequences from *V. vinifera* are discussed in the context of isoprenoid biosynthesis.

*Corresponding author: Institute for Wine Biotechnology, Department of Viticulture and Oenology, Stellenbosch University, Private Bag X1, Matieland, ZA7602, South Africa. Tel: +27 21 8083773; Fax: +27 21 8083771; Email: mav@sun.ac.za

## 5.1 INTRODUCTION

Plant isoprenoids are diverse in both their structure and function, yet all isoprenoids are formed from only two $C_5$-molecules: isopentenyl diphosphate (IPP) and its isomer dimethylallyl diphosphate (DMAPP) [1]. Plant isoprenoids include chlorophylls and carotenoids (photosynthetic pigments), ubiquinone and plastoquinone (electron carriers), and abscisic acid, cytokinins and gibberellins (growth regulators). In higher plants IPP is formed from two independent pathways that are functional in different sub-cellular compartments: the cytosolic mevalonate pathway and the plastidic 1-deoxy-D-xylulose 5-phosphate (DOXP)/2-C-methyl-D-erythritol 4-phosphate (MEP) pathway [2]. The cytosolic pathway requires acetyl coenzyme A and proceeds via mevalonate to produce the precursors for sterols and ubiquinone. The alternative plastidic MEP pathway, on the other hand, requires the condensation of pyruvate and glyceraldehyde-3-phosphate and proceeds via 1-deoxy-D-xylulose 5-phosphate to form isoprene, carotenoids, abscisic acid, and the side chains of chlorophylls and plastoquinone [2]. These two pathways have received much attention in the last few years and comprehensive reviews are available (Fig. 5.1) [3;4]. Similarly, the subsequent reactions of the carotenoid- and the abscisic acid biosynthetic pathways have also been well reviewed (Fig. 5.1) [5-9].

In 2000, Ye *et al.* reported the successful engineering of the carotenoid biosynthetic pathway in rice. This "Golden rice" accumulated β-carotene (proVitamin A) in the normally carotenoid-free endosperm of rice [10]. The significance of increasing the carotenoid levels in a crop plant is of particular importance due to the prevalence of Vitamin A deficiency in poor and developing countries [11]. Similarly, transgenic *Arabidopsis* plants with higher xanthophyll levels were shown to be more tolerant to high light and high temperature induced stress [12]. The ability to successfully manipulate the carotenoid levels in a crop plant (like grapevine) will have several potential applications. Apart from the increased stress tolerance of the plant under adverse conditions; increasing the carotenoid levels in the grape berry will also improve the nutritional value of the fruit. Furthermore, carotenoids are regarded as the precursors of β-damascenone, vitispirane and other $C_{13}$-norisoprenoids compounds that are associated with grape- and wine quality [13]. Increasing the flux into the carotenoid pathway could lead to an increase in these quality-associated compounds. The

carotenoid biosynthetic pathway is therefore proving to be a promising target for genetic manipulation.

The international sequencing projects that are currently underway in a wide variety of plant species (including *V. vinifera*) have resulted in a huge amount of sequence data being deposited in the publicly accessible sequence repositories. The availability of vast amounts of genome sequence information has had a dramatic effect on the experimental scale and strategies for conducting research. This genetic resource has accelerated the isolation and study of genes in a wide range of biosynthetic organisms across species [14;15]. Using the available expressed sequence databases, we have isolated five full-length genes (i.e. from the putative ATG to the STOP codon) encoding: farnesyl diphosphate (FPS), isopentenyl diphosphate isomerase (IPI), 3-hydroxy-3-methylglutaryl coenzyme A synthase (HMGS), 4-hydroxy-3-methylbut-2-enyl diphosphate reductase (lytB), geranylgeranyl diphosphate synthase (GGPS); and eight partial genes encoding for: 1-deoxy-D-xylulose 5-phosphate reductase (DXR), hydroxymethylbutenyl diphosphate synthase (gcpE), ζ-carotene desaturase (ZDS), carotenoid isomerase (CISO), lycopene ε-cyclase (LECY), violaxanthin de-epoxidase (VDE), xanthine dehydrogenase (XDH) and a short chain dehydrogenase/reductase (SCD). The isolation of the partial genes are reported, but only the full-length sequences of FPS, IPI, HMGS, lytB and GGPS are anayzed and discussed. The degree of homology that exists between the obtained predicted protein sequences to selected protein sequences available in the public databases are shown. The presence of any conserved domains in the protein sequences are reported, and the sub-cellular localization of the proteins are, furthermore, predicted and the isolated genes discussed in relation to isoprenoid biosynthesis.

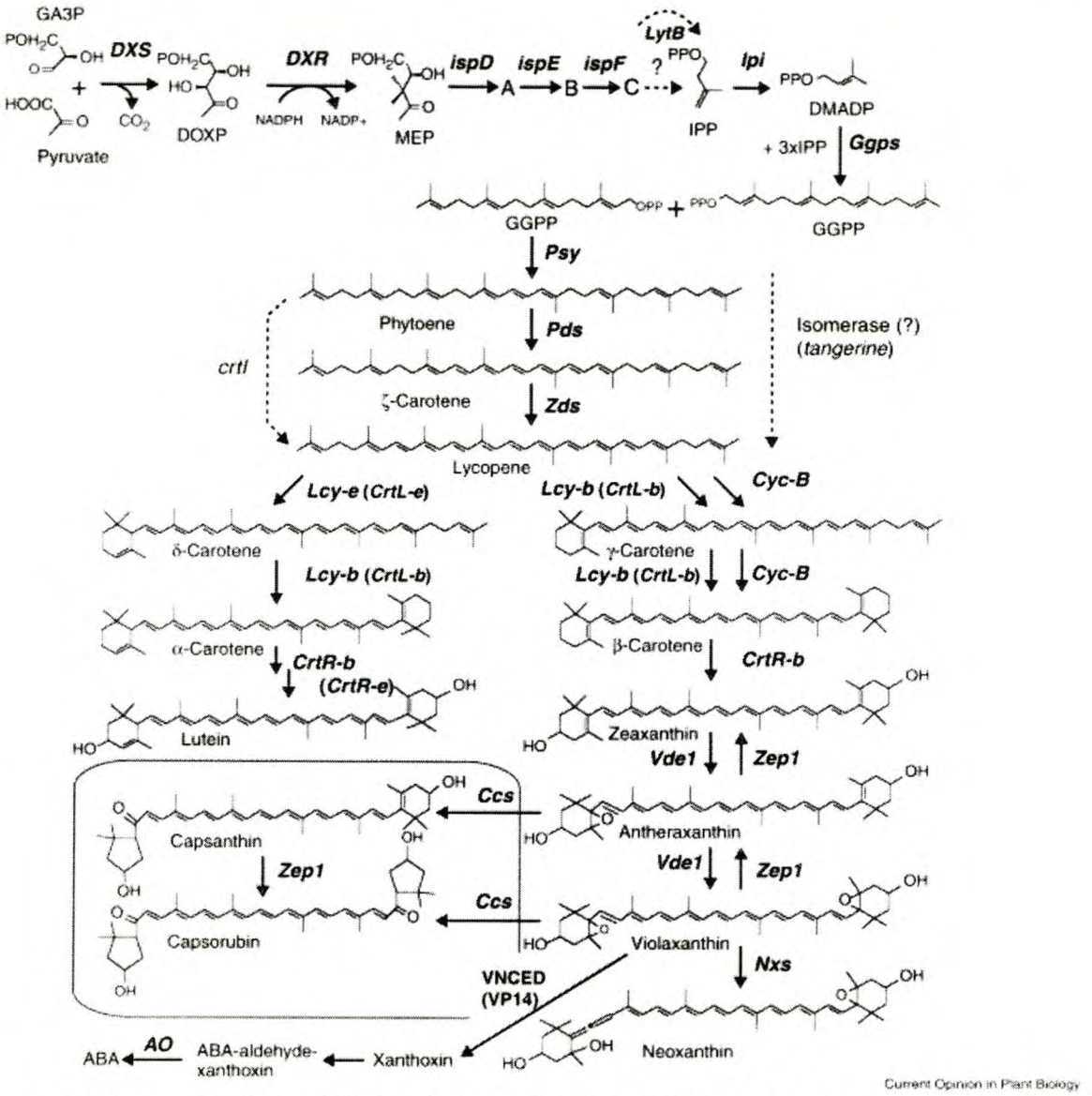


Figure 5.1. The 2-*C*-methyl-D-erythritol 4-phosphate (MEP) pathway from glyceraldehyde-3-phosphate (GA3P) and pyruvate to isopentenyl diphosphate (IPP) and dimethylallyl diphosphate (DMADP) and the subsequent reactions of the carotenoid- and abscisic acid biosynthetic pathways. Only the abbreviations with relevance to this study will be defined: *DXR*, 1-deoxy-D-xyxlulose 5-phosphate reductase; *lytB*, 4-hydroxy-3-methylbut-2-enyl diphosphate reductase; *Ipi*, isopentenyl diphosphate isomerase; *Ggps*; geranylgeranyl diphosphate (GGPP) synthase; *Zds*, ζ-carotene desaturase; carotenoid isomerase (*tangerine* represents a mutation in this gene that has been identified in tomato [16]); *Lcy-e (CrtL-e)*; lycopene ε-cyclase; VNCED, 9-*cis* epoxy carotenoid dioxygenase (VP14 represents an NCED mutation that has been identified in maize [17]) [6].

## 5.2 MATERIALS AND METHODS

### 5.2.1 Plant material

*Vitis vinifera* L. cv. Pinotage leaves were collected in the field and flash frozen in liquid nitrogen. Berries were collected throughout the growth season (October, 2001 through to February, 2002) in one-week intervals. The frozen tissue was ground in liquid nitrogen and, if not used immediately, stored at -80°C.

### 5.2.2 Plasmids, bacterial strains and growth conditions

*Escherichia coli* DH5α cultures were grown in LB media, and transformed bacterial cultures were grown in LB media supplemented with the appropriate antibiotic(s). Unless otherwise stated, all cultures were grown at 37°C.

### 5.2.3 Isolation and manipulation of nucleic acids

All DNA fragments for cloning were separated in 1.0% (w/v) TAE agarose gels and the fragments of interest were isolated using the QIAquick Gel Extraction Kit as instructed by the supplier (Qiagen GmbH, Hilden, Germany). The pGEM-T Easy vector system was used to clone all PCR-generated fragments, according to the specifications of the supplier (Promega, Madison, WI). High molecular weight genomic DNA was isolated from fully expanded *V. vinifera* leaves as described by Steenkamp *et al.* [18]. Total RNA from different grapevine tissues was extracted according to the methods described by Davies and Robinson [19]. Unless otherwise stated, all standard methods for plasmid DNA isolation, manipulations and cloning of DNA fragments, and agarose gel electrophoresis were used as described in Sambrook *et al.* [20].

### 5.2.4 RNA isolation and cDNA construction

The integrity of total RNA isolated from different grapevine tissues was evaluated visually by formaldehyde-agarose gel electrophoresis and ethidium bromide staining. First strand cDNA synthesis was performed at 45°C (for two hours) using 1 μg of total RNA as template, an oligo $dT_{16}$ reverse primer and *Carboxydothermus hydrogenoformans* (*C. therm*) reverse transcriptase and buffers as described by the supplier (Roche Diagnostics). The genes were subsequently PCR-amplified from the synthesized cDNAs using the respective primers listed in Table 5.1.

### 5.2.5 Construction of vectors

Homology searches of the TIGR Grape Gene Index (VvGI) and NCBI EST (dbEST) databases using available *Arabidopsis thaliana* sequences of FPS, IPI, lytB, HMGS and GGPS yielded the accession numbers listed in Table 5.1. For the NCBI dbEST searches the query was limited to Viridiplantae and only queries containing the word "*Vitis*" were retrieved. These nucleotide sequences were aligned to the available protein sequences in the NCBI database using the BLASTX algorithm (i.e. the nucleotide sequence is translated into all six frames and the resultant hypothetical protein sequences are aligned to sequences available in the NCBI protein databases). These alignments enabled the identification of the putative ATG and STOP codons. PCR primers were designed in these regions in order to amplify the full-length sequences from *V. vinifera* cDNA. Similarly the partial gene sequences of DXR, gcpE, ZDS, CISO, LECY, VDE, XDH, SCD were PCR amplified from cDNA, but they lacked either the putative ATG (gcpE, and SCD) or the STOP (DXR, ZDS, VDE and XDH) codon. CISO and LECY are internal fragments and as such do not contain a putative ATG or STOP codon.

The PCR primers used to amplify the genes of interest are listed in Table 5.1. The PCR reactions were performed using Takara BioTaq DNA polymerase and buffer and 10-50 ng of Pinotage genomic DNA, or 10 ng cDNA as template. PCR amplifications were performed in a BioRad PCR thermal cycler (BioRad, Hercules, CA) using the following program: initial denaturation at 98°C for 5ºmin; subsequent denaturations at 98°C for 15 s; annealing at 55ºC for 35 s; extension at 72°C for 1 min per kb (refer to Table 5.1); and a final elongation at 72°C for 10 min. Amplifications were performed for 40 cycles. The resultant PCR products were separated on a 1% (w/v) agarose gel, isolated and cloned into the pGEM-T Easy vector to form pGEM-FPS, -IPI, -HMGS, -lytB, -GGPS, -DXR, -gcpE, -ZDS, -CISO, -LECY, -VDE, -XDH and -SCD (Table 5.2). These constructs were sequenced at the Central Analytical Facility, Stellenbosch University, using an ABI Prism 3100 Genetic Analyzer.

The full-length genes (FPS, IPI, HMGS, lytB and GGPS) were isolated from the respective pGEM-T Easy clones as *Xho*I/*Spe*I (Vv-FPS and Vv-IPI), *Xho*I/*Xba*I (Vv-lytB), *Sal*I/*Spe*I (Vv-HMGS) and *Eco*RI/*Spe*I (Vv-GGPS) fragments and cloned into the *Xho*I/*Xba*I (Vv-FPS, Vv-IPI, Vv-lytB, and Vv-HMGS) or the *Eco*RI/*Xba*I (Vv-GGPS) sites

of pART7 to form pART7-FPS, -IPI, -HMGS, -lytB, and -GGPS [21]. The cassettes containing the respective genes of interest under the control of the strong constitutive cauliflower mosaic virus (CaMV) 35S promoter and octopine synthase (OCS) terminator were excised from pART7 as *Not*I fragments and cloned into the corresponding sites of the plant binary vector, pART27 to form pART27-FPS, -IPI, -HMGS, -lytB, and -GGPS [21].

### 5.2.6 Computer analyses

The National Center for Biotechnology Information (NCBI) Entrez search and retrieval system was used to obtain nucleotide and protein sequences from the Genbank databases (http://www.ncbi.nlm.nih.gov/Entrez/). Alignments to sequences in the Genbank databases were executed using the relevant Blast algorithm (http://www.ncbi.nlm.nih.gov/BLAST/). Pairwise amino acid- and nucleotide sequences were aligned using ClustalX [22].

The putative localization of the protein sequences were predicted using ProtComp (http://www.softberry.com/berry.phtml). Protein domains or conserved protein regions in the predicted amino acid sequences of the isolated genes were identified by searching the Protein families (Pfam) database of alignments and HMMs (http://pfam.wustl.edu/cgi-bin/hmmsearch) or the NCBI Conserved Domain Database (CDD) (http://www.ncbi.nlm.nih.gov/Structure/cdd/wrpsb.cgi) [23].

*V. vinifera* expressed sequence tags (ESTs) were retrieved from The Institute for Genomic Research (TIGR) Grape Gene Index (http://www.tigr.org/tdb/tgi/vvgi/) and NCBI Entrez.

The intensity of the bands on autoradiograms and ethidium bromide stained gels were quantified using a digital camera (AlphaImager 1220; Alpha Innotech Corporation, San Leandro, CA) and the AlphaEase densitometry software v5.5 (Alpha Innotech Corporation).

All statistical analyses of data were processed using the Graphpad Prism v3.02 software (Graphpad Software, San Diego, USA).

## 5.3 RESULTS AND DISCUSSION

### 5.3.1 Isolation of candidate genes involved in the isoprenoid-, carotenoid-, and abscisic acid biosynthetic pathways

Nucleotide homology searches of the TIGR and NCBI databases identified full-length genes encoding FPS, GGPS, HMGS, IPI and lytB and partial genes encoding DXR, gcpE, ZDS, CISO, LECY, VDE, XDH and SCD from *V. vinifera*. These genes and gene fragments have been isolated, cloned and sequenced.

FPS catalyzes the synthesis of farnesyl diphosphate (FPP) from IPP and DMAPP. FPP is central to several branched pathways leading to the synthesis of a variety of isoprenoid compounds that include: phytosterols, dolichols, ubiquinones, abscisic acid, and sesquiterpenoid phytoalexins. FPP is essential for protein prenylation, a mechanism that promotes membrane interactions and biological activities of cellular proteins involved in signal transduction, membrane biogenesis, and cellular growth control [25]. The *V. vinifera* FPS encoding gene is 1023 bp in length and the predicted protein is 341 amino acids with a theoretical molecular weight of 51 kDa and pI of 5.9. The protein shares 79.3% identity (87% similarity) to the *A. thaliana* FPS (Table 5.1, 5.2 and Figure 5.2).

GGPS catalyzes the linear addition of three IPP molecules to DMAPP to form the 20-carbon molecule geranylgeranyl diphosphate (GGPP). GGPP is a precursor for gibberellins, carotenoids, chlorophylls, isoprenoid quinones, and geranylgeranylated proteins in plants [30]. The *V. vinifera* GGPS encoding gene is 1107 bp in length and the predicted protein is 368 amino acids with a theoretical molecular weight of 51 kDa and pI of 5.9. The protein shares 68.4% identity (80.2% similarity) to the *A. thaliana* GGPS (Table 5.1, 5.2 and Fig. 5.3).

The first reaction of the mevalonate pathway is the formation of the $C_6$-compound 3-hydroxy-3-methylglutaryl coenzyme A (HMG-CoA) by the fusion of three molecules of acetyl coenzyme A, which is catalyzed by HMGS. HMGS represents the only gene isolated in this study that encodes for an enzyme in the mevalonate pathway. This pathway operates in both the cytosol and mitochondria and is required for, amongst others, the synthesis of sterols and ubiquinones [24]. The *V. vinifera* HMGS encoding gene is 1395 bp in length and the predicted protein is 464 amino acids with a theoretical

molecular weight of 51 kDa and pI of 5.9. The protein shares 80.7% identity (88.8% similarity) to the *A. thaliana* HMGS (Table 5.1, 5.2 and Fig. 5.4).

IPI and lytB catalyze reactions in the non-mevalonate DOXP/MEP pathway. LytB (ispH) catalyzes the reaction of 1-hydroxy-2-methyl-2-(E)-butenyl 4-diphosphate to IPP and DMAPP and has been shown to affect the ratio of IPP and DMAPP that is formed [26;27]. IPI catalyzes the reversible isomerization of IPP to the more reactive DMAPP molecule. Additional IPP molecules can subsequently be added to DMAPP by sequential head-to-tail condensation reactions [28;29]. The *V. vinifera* IPI encoding gene is 876 bp in length and the predicted protein is 293 amino acids with a theoretical molecular weight of 51 kDa and pI of 5.9. The protein shares 74.4% identity (80.9% similarity) to the *A. thaliana* IPI (Table 5.1, 5.2 and Fig. 5.5).

The *V. vinifera* lytB encoding gene is 1401 bp in length and the predicted protein is 465 amino acids with a theoretical molecular weight of 51 kDa and pI of 5.9. The predicted *V. vinifera* lytB protein is 466 amino acids in length, with a theoretical molecular weight of 52.6 kDa and pI of 5.3. The protein shares 77.9% identity (85% similarity) to the *A. thaliana* lytB (Table 5.1, 5.2 and Fig. 5.6).

### 5.3.2 Sub-cellular localization of the isolated genes

The nucleotide sequences of FPS, IPI, lytB, HMGS and GGPS were translated, and the resultant predicted protein sequences were analyzed for the presence of transit peptides using the ProtComp prediction server. The FPS and lytB protein sequences are predicted to be targeted to the cytoplasm, whereas IPI and GGPS are likely to be localized to the chloroplast. The prediction server predicted both the chloroplast and the cytoplasm for the localization of HMGS, with equivalent scores (data not shown). The *Arabidopsis* FPS, IPI, lytB, HMGS and GGPS proteins that showed the highest degree of global homology to the predicted *V. vinifera* proteins, were also analyzed using the ProtComp server. The same results were obtained for FPS, lytB, GGPS and HMGS, but IPI was localized to either the cytoplasm or the peroxisome.

Table 5.1

| | GENE | PRIMER NAME | PRIMER SEQUENCE[1] | PREDICTED SIZE (a/a)[2] | SIZE (bp)[3] | ACCESSION NUMBER[4] |
|---|---|---|---|---|---|---|
| FULL-LENGTH GENES | Vv-FPS | VvFPS-5' (ATG)<br>VvFPS-3' (STOP) | 5'-ctcgag***ATG***AGCGAGACGAAGTCCAA<br>5'-CTGCTGAAAACCCTACTTCTGTC | 342 | 1023 | TC33247 |
| | Vv-IPI | VvIPI-5' (ATG)<br>VvIPI-3' (STOP) | 5'-ctcgag***ATG***ACTCTGTCTTCTCGCTTATATACT<br>5'-CCTTCAAGTCAACTTGTGAATGG | 284 | 876 | TC32368 |
| | Vv-lytB | VvlytB-5' (ATG)<br>VvlytB-3' (STOP) | 5'-ctcgag***ATG***GCGATGTCTCTGCAACTCT<br>5'-tctagaGCTTCACTTCTACACTTATTATGCC | 466 | 1401 | TC32365 |
| | Vv-HMGS | VvHMGS-5' (ATG)<br>VvHMGS-3' (STOP) | 5'-gtcgacGAAA***ATG***ACGAAAAATGTGGGAA<br>5'-GTTATCAGTGACCATTGGCCAGTG | 461 | 1395 | TC31953 |
| | Vv-GGPS | VvGGPS-5' (ATG)<br>VvGGPS-3' (STOP) | 5'-ctcgag***ATG***AATACTGTGAATCTGGGC<br>5'-CAACTGGTCAGACCATTGAGACAAC | 371 | 1107 | TC27066 |
| | Vv-DXR | VvDXR-5'<br>VvDXR-3' (STOP) | 5'-GTCACGGTTGACTCAGCTACCCTTTT<br>5'-GGAGAAGCTGTTTATCCATGCTGGAACA | 477 | 590 | TC33818 |
| PARTIAL GENES | Vv-gcpE | VvgcpE-5' (ATG)<br>VvgcpE-3' | 5'-***ATG***GCGACTGGATCTGTTCCGA<br>5'-TCACTTCCAAGAGCCACATTCCC | 740 | 299 | TC34134 |
| | Vv-ZDS | VvZDS-5'<br>VvZDS-3' (STOP) | 5'-GTGCCAGTGTCACAGTGCAACTT<br>5'-GGTGTGAGGTGTCAGACAAGACTC | 558 | 616 | TC34441 |
| | Vv-Ciso | VvCiso-5'<br>VvCiso-3' | 5'-GGGTAGGGACACCAAAAACAC<br>5'-CACAGTTACATCCAAGGAGTCTAGAC | 595 | 547 | TC30535 |
| | Vv-LECY | VvLECY-5'<br>VvLECY-3' | 5'-GTGGTCCCAGGGTTTCTGTCCA<br>5'-GGTAAGGATCCACCAACAGGGA | 524 | 334 | TC35429 |
| | Vv-VDE | VvVDE-5'<br>VvVDE-3' (STOP) | 5'-CGGTGTACTAGCTTGCACAATGTT<br>5'-CAGGAATTAAACTGGGGTTTCAGG | 462 | 1130 | TC33779<br>CA817814 |
| | Vv-XDH | VvXDH-5'<br>VvXDH-3' (STOP) | 5'-GATTGGAAGACTGGCAAAGGGA<br>5'-CAGCAGCAACCAGTGGATTAAAC | 1359 | 595 | TC34024 |
| | Vv-SCD | VvSCD-5' (ATG)<br>VvSCD-3' | 5'-***ATG***GTTAGCAGCTCATTGCTTTCA<br>5'-GTGTTACAATGGTGACACCACCAT | 285 | 787 | TC27156 |

[1]Sequences of the designed primers (5'-3') with incorporated restriction endonuclease recognition sites in lower case, and putative ATGs in bold italics. [2]Predicted size of the amino acid sequence of the corresponding gene in *Arabidopsis thaliana*. [3]The size (in bp) of the products obtained using the respective primer pairs. [4]The accession numbers of the relevant sequence(s) in the TIGR- (TC-prefix) or the NCBI (CA-prefix) databases. The abbreviations are as used in the text.

The *in silico* analyses of the predicted protein sequences of FPS, IPI, lytB, HMGS and GGPS provided additional structural information regarding the isolated full-length genes. Apart from HMGS, the sub-cellular localization predictions for FPS, IPI, lytB and the GGPS protein sequences were as expected. The mevalonate pathway to IPP/DMAPP is found in both the mitochondria and the cytoplasm and proteins involved in the pathway will usually have a defined transit peptide (i.e. for the mitochondria or the cytoplasm, not both) [31]. Although it is possible (and was predicted), that the HMGS protein is targeted to both the mitochondria and the cytoplasm, this phenomenon has not previously been reported and will require additional experimental evidence to verify. The *Arabidopsis* HMGS was similarly localized to both the cytosol and the mitochondria.

Since the DOXP/MEP pathway to IPP is functional in the chloroplast, it is expected that the enzymes required for this pathway will contain chloroplast transit peptides. The ProtComp prediction verified this assumption for the *V. vinifera* lytB.

Five dedicated GGPS isoforms are found in *Arabidopsis* that are expressed in three different compartments (the endoplasmic reticulum, the cytoplasm and the chloroplast) [30]. Based on the chloroplast transit peptide prediction and the assumption that a similar scenario exists in *V. vinifera*, then the *V. vinifera* GGPS isolated represents the chloroplastic isoform of this gene.

Similarly, in *N. tabacum*, two distinct IPI isoforms are found, one localized to the cytosol and the other to the chloroplast [29]. The localization prediction of the *V. vinifera* IPI indicates that the isolated gene encodes for the chloroplastic isoform. Since the homology in the N-terminal end of the *V. vinifera* IPI and the *Arabidopsis* IPI is very low, it is expected that the predictions will differ (Table 5.5). It is possible that the *V. vinifera* IPI and *Arabidopsis* IPI proteins that were aligned, represent different isoforms of the same gene and are therefore localized in different sub-cellular compartments.

Table 5.2. *In silico* characterization of predicted protein

| GENE | PREDICTED PROTEIN (a/a)[1] | SUB-CELLULAR LOCATION[2] | %IDENTITY[3] | %SIMILARITY[4] | pI[5] | MW (kDa)[6] |
|---|---|---|---|---|---|---|
| Vv-FPS | 341 | Cytoplasmic | 79.3 | 87.2 | 5.5 | 39.1 |
| Vv-IPI | 293 | Chloroplastic | 74.4 | 80.9 | 6.2 | 33.6 |
| Vv-lytB | 465 | Cytoplasmic | 77.9 | 85 | 5.3 | 52.6 |
| Vv-HMGS | 464 | Mitochondrial/ Cytoplasmic | 80.7 | 88.8 | 5.9 | 51.0 |
| Vv-GGPS | 368 | Chloroplastic | 68.4 | 80.2 | 5.9 | 39.8 |

[1]Size of the predicted protein (in amino acids) obtained by translating the nucleotide sequence of the *Vitis vinifera* gene. [2]The sub-cellular localization of the putative proteins as determined by the ProtComp prediction server. [3]The percentage homology obtained by pairwise alignment of the *V. vinifera* protein to the corresponding *Arabidopsis thaliana* protein. [4]The percentage similarity obtained by a pairwise alignment of the *V. vinifera* protein to the corresponding *A. thaliana* protein. [5]The theroretical pI of the predicted putative *V. vinifera* protein. [6]The theoretical molecular weight (MW) in kDa of the predicted putative *V. vinifera* protein. The abbreviations are as described in the text.

### 5.3.3 Functional complementation of IPI and GGPS

The functionality of lytB, IPI, FPS, HMGS and GGPS isolated from *V. vinifera* were tested in an available bacterial complementation system. For GGPS, the plasmid, pAC-94N was co-transformed with pART27-GGPS. Relative to the control strain, the transformed colonies appeared yellow (due to β-carotene accumulation) (data not shown). The GGPS is therefore functional in a bacterial complementation system. The ability of a lytB (from *Synechoccus*) and IPI (from *E. coli*) to increase the production of lycopene in a bacterial complementation system has previously been reported [32;33]. Co-transformation of pAC-LYC with pART-27-IPI lead to increased lycopene production (i.e. colonies appeared darker pink than the control strain containing only pAC-LYC). The functional complementation of lytB, FPS and HMGS showed no phenotypical differences relative to the control strain containing only pAC-LYC (data not shown). Although TLC was used to tentatively identify the pigments, HPLC will be needed to accurately quantify and qualify the resultant pigments relative to authentic standards. The inability of lytB to increase the production of lycopene (as reported for *Synechoccus*), could be due to the presence of the chloroplast transit in the plant lytB. It is possible that the unprocessed transit peptide interferes with the functioning of the mature protein in bacteria.

### 5.3.4 Identification of conserved protein domains in the predicted protein sequences of the isolated genes

The predicted protein sequences of the isolated genes (i.e. lytB, IPI, HMGS, FPS and GGPS) were submitted to the Conserved Domain Database (CDD) to identify any potential homology to conserved domains. This database relies on domain profiles or domain architecture rather than direct sequence homology. Domain architecture can be defined as the sequential order of conserved domains in protein sequences [34]. The CDD search using the lytB protein sequences detected an ispH/lytB domain (PFAM02401). The IPI protein contained an IPI domain (KOG0142). Similarly, the HMGS protein contains a HMGS domain (PFAM01154). The GGPS protein shares homology with a FPS domain (KOG0776). The only domain that requires discussion is the GGPS protein that contains a domain that is also found in FPS. This is possibly due to the fact that both of these enzymes act on IPP and will therefore be expected to share homology in their domain profiles. Since the domains detected in all the analyzed proteins are based on functional domains and domain profiles, these predictions serve as additional *in silico* confirmation of the identity of the isolated proteins.

The availability of genomic- and cDNA sequences, as well as homology-based search programs have accelerated the isolation of genes across a wide range of species. This has been illustrated in this study by the isolation and *in silico* characterization of five genes involved in isoprenoid biosynthetic pathways.

```
CLUSTAL W (1.82) multiple sequence alignment

Vv-FPS          M-SETKSKFLEVYSVLKSELLNDPAFEFTDDSRQWVERMLDYNVPGGKLNRGLSVVDSYK 59
Hb-FPS          MA-DLKSTFLKVYSVLKQELLEDPAFEWTPDSRQWVERMLDYNVPGGKLNRGLSVIDSYK 59
At-FPS          METDLKSTFLNVYSVLKSDLLHDPSFEFTNESRLWVDRMLDYNVRGGKLNRGLSVVDSFK 60
                *  : **.**:******.:**.**:**:* :** **:******* **********:**:*

Vv-FPS          LLQ-GRQLTDDEVFLACVLGWCIEWLQAYFLVLDDIMDNSHTRRGQPCWFRVPKVGMIAA 118
Hb-FPS          LLKEGQELTEEEIFLASALGWCIEWLQAYFLVLDDIMDSSHTRRGQPCWFRVPKVGLIAA 119
At-FPS          LLKQGNDLTEQEVFLSCALGWCIEWLQAYFLVLDDIMDNSVTRRGQPCWFRVPQVGMVAI 120
                **: *.:**::*:**:..********************.* ***********:**::*

Vv-FPS          NDGVILRNQIPRILKNHFKGKPYYVDLLDLFNEVEFQTASGQMIDLITTIEGEKDLSKYS 178
Hb-FPS          NDGILLRNHIPRILKKHFRGKAYYVDLLDLFNEVEFQTASGQMIDLITTLEGEKDLSKYT 179
At-FPS          NDGILLRNHIHRILKKHFRDKPYYVDLVDLFNEVELQTACGQMIDLITTFEGEKDLSKYS 180
                ***::***:* ****:**:.*.*****:*******:***.*********:*********:

Vv-FPS          LPLHRRIVQYKTAYYSFYLPVACALLMAGENLDNHTSVKDILVQMGIYFQVQDDYLDCFG 238
Hb-FPS          LSLHRRIVQYKTAYYSFYLPVACALLIAGENLDNHIVVKDILVQMGIYFQVQDDYLDCFG 239
At-FPS          LSIHRRIVQHKTAYYSFYLPVACALLMAGENLENHIDVKNVLVDMGIYFQVQDDYLDCFA 240
                *.:******:*****************:*****:**  **::**:***************.

Vv-FPS          DPQVIGKIGTDIEDFKCSWLVVKALEICNEEQKKTLYGNYGKADPANVAKVKALYKDLDL 298
Hb-FPS          DPETIGKIGTDIEDFKCSWLVVKALELCNEEQKKVLYEHYGKADPASVAKVKVLYNELKL 299
At-FPS          DPETLGKIGTDIEDFKCSWLVVKALERCSEEQTKILYENYGKTDPSNVAKVKDLYKELDL 300
                **:.:********************** *.***.* ** :***:**:.***** **::*.*

Vv-FPS          QGVFLEYESKSYETLVSSIEAHPSKAVQAVLKSFLGKIYKRQK 341
Hb-FPS          QGVFTEYENESYKKLVTSIEAHPSKPVQAVLKSFLAKIYKRQK 342
At-FPS          EGVFMEYESKSYEKLTGAIEGHQSKAIQAVLKSFLAKIYKRQK 343
                :*** ***.:**:.*. :**.* **.:********.*******
```

Figure 5.2. Alignment of the predicted *Vitis vinifera* (Vv-) farnesyl diphosphate synthase (FPS) protein sequence to the FPS protein sequences of *Hevea brasiliensis* (Hb-) (S71454) and *Arabidopsis thaliana* (At-) (CAA53433). (*), indicates an identical amino acid residue; (:), indicates a similar amino acid residue.

```
CLUSTAL W (1.82) multiple sequence alignment

Vv-GGPS         MNTVNLGTWVHTSYVFNHG--GRLKSPVLSRMLHPLKNPSFPMLSQRSGRPMS-LAAVLT 57
Hb-GGPS         MSSVNLGSWVHTSYVLNQATRSRSKSKSFSLPFNPLKSLAISFAYRKSERPISSVSAIIT 60
At-GGPS         MASVTLGSWIVVHHHNHHHP-SSILTKSRSRSCPITLTKPISFR---SKRTVSSSSSIVS 56
                * :*.**:*: . :  ::   .   :  *       . .:.:    * *.:*  :::::

Vv-GGPS         KEEMVRGGDTPEEEKPAFNFNAYILDKANSVNKALDDAVPIREPVKVHESMRYSLLAGGK 117
Hb-GGPS         KEEETLQ-EEQNNPPPSFDFKSYMLQKGNSINQALEAAIPLQEPAKIHESMRYSLLAGGK 119
At-GGPS         SSVVTKEDNLRQSEPSSFDFMSYIITKAELVNKALDSAVPLREPLKIHEAMRYSLLAGGK 116
                ..  .   :  :.  .:*:* :*:: *.: :*:**: *:*::** *:**:********** 

Vv-GGPS         RVRPVLCIAACELVGGDEATAMPAACAVEMIHTMSLMHDDLPCMDNDDLRRGKPTNHKVF 177
Hb-GGPS         RVRPALCLAACELVGGNDSMAMPAACAVEMIHTMSLIHDDLPCMDNDDLRRGKPTNHIVF 179
At-GGPS         RVRPVLCIAACELVGGEESTAMPAACAVEMIHTMSLIHDDLPCMDNDDLRRGKPTNHKVF 176
                ****.**:******** ::: ****************:****************** **

Vv-GGPS         GENVAILAGDALLAFAFEHMATATVG--VPPGWIVRAVGELAKSIGSEGLVAGQVVDICS 235
Hb-GGPS         GEDVAVLAGDALLAFAFEHIAVSTLN--VSSARIVRAVGELAKAIGAEGLVAGQVVDINS 237
At-GGPS         GEDVAVLAGDALLSFAFEHLASATSSDVVSPVRVVRAVGELAKAIGTEGLVAGQVVDISS 236
                **:**:*******:*****:* :* .  *..  :*********:**:********** * 

Vv-GGPS         EGL--KDVGLEHLEYIHVHKTAALLEGAVVLGAILGGGSNEEIEKLRKFARCIGLLFQVV 293
Hb-GGPS         EGS--SEVDLEKLEFIHIHKTAKLLEGAVVLGAILGGGTDEEVEKLRKYARDIGLLFQVV 295
At-GGPS         EGLDLNDVGLEHLEFIHLHKTAALLEASAVLGAIVGGGSDDEIERLRKFARCIGLLFQVV 296
                **   .:*.**:**:**:**** ***.:.*****:***::::*:*:***:** ******** 

Vv-GGPS         DDILDVTKSSQELGKTAGKDLVADKLTYPKLLGIEKSRELAEQLNKDAKDQLSGFDPDKA 353
Hb-GGPS         DDILDVTKSSQELGKTAGKDLVADKVTYPKLLGIEKSREFAEKLNKEAQEQLAGFDPEKA 355
At-GGPS         DDILDVTKSSKELGKTAGKDLIADKLTYPKIMGLEKSREFAEKLNREARDQLLGFDSDKV 356
                **********:**********:***:****::*:*****:**:**::*::** ***.:*.

Vv-GGPS         APLIALSNYIAYRQN 368
Hb-GGPS         APLIALANYIAHRQN 370
At-GGPS         APLLALANYIAYRQN 371
                ***:**:****:***
```

Figure 5.3. Alignment of the predicted *Vitis vinifera* (Vv-) geranylgeranyl diphosphate synthase (GGPS) protein sequence to the GGPS protein sequences of *Hevea brasiliensis* (Hb-) (BAB60678) and *Arabidopsis thaliana* (At-) (CAB16803). (*), indicates an identical amino acid residue; (:), indicates a similar amino acid residue.

```
CLUSTAL W (1.82) multiple sequence alignment

Vv-HMGS         MTKNVGILAMDIYFPPTCVQQEALEVHDGASKGKYTIGLGQDCMAFCSEVEDVISMSLTV 60
Hb-HMGS         MAKNVGILAVDIYFPPTFVQQEALEAHDGASKGKYTIGLGQDCMAFCTEVEDVISMSLTA 60
At-HMGS         MAKNVGILAMDIYFPPTCVQQEALEAHDGASKGKYTIGLGQDCLAFCTELEDVISMSFNA 60
                *:*******:******* *******.*****************:***:*:********:..

Vv-HMGS         VTSLLEKYGIDPKQIGRLEVGSETVIDKSKSIKTFLMQIFEECGNNDIEGVDSSNACYGG 120
Hb-HMGS         VTSLLDKYNIDPKQIGRLEVGSETVIDKSKSIKTFLMQIFEKFGNTDIEGVDSTNACYGG 120
At-HMGS         VTSLFEKYKIDPNQIGRLEVGSETVIDKSKSIKTFLMQLFEKCGNTDVEGVDSTNACYGG 120
                ****::** ***:*************************:**: **.*:******:******

Vv-HMGS         TAALFNCVNWVESSSWDGRYGLVVCTDSAVYAEGPARPTGGAAAIAMLVGPDAPIAFESK 180
Hb-HMGS         TAALFNCVNWVESSSWDGRYGLVVCTDSAVYAEGPARPTGGAAAIAILVGPDAPIAFESK 180
At-HMGS         TAALLNCVNWVESNSWDGRYGLVICTDSAVYAEGPARPTGGAAAIAMLIGPDAPIVFESK 180
                ****:********.*********:************************:*:******.****

Vv-HMGS         LRGSHMSHAYDFYKPNLASEYPVVDGKLSQTCYLMALDSCYKLLCSKYEKLEGKQFSIAD 240
Hb-HMGS         FRGSHMSHAYDFYKPNLASEYPVVDGKLSQTCYLMALDSCYKHFCAKYEKFEGKQFSISD 240
At-HMGS         LRASHMAHVYDFYKPNLASEYPVVDGKLSQTCYLMALDSCYKHLCNKFEKIEGKEFSIND 240
                :*.***:*.********************************** :* *:**:***:*** *

Vv-HMGS         ADYFVFHSPYNKLVQKSFARLVFNDVVRNASSVDEAGKQKLEPFSSLSGDESYQNRDLEK 300
Hb-HMGS         AEYFVFHSPYNKLVQKSFARLVFNDFVRNASSIDETAKEKLAPFSNLSGDESYQNRDLEK 300
At-HMGS         ADYIVFHSPYNKLVQKSFARLLYNDFLRNASSIDEAAKEKFTPYSSLTLDESYQSRDLEK 300
                *:*:*******************::**.:*****:**:.*:*: *:*.*: ******.*****

Vv-HMGS         ASQQVAKPLYDAKVQPSTLLPKQVGNMYTASLYAAFVSVLHNKHSELSGKRVVMFSYGSG 360
Hb-HMGS         VSQQVAKPLYDAKVKPTTLIPKQVGNMYTASLYAAFASLLHSKHTELAGKRVTLFSYGSG 360
At-HMGS         VSQQISKPFYDAKVQPTTLIPKEVGNMYTASLYAAFASLIHNKHNDLAGKRVVMFSYGSG 360
                .***::**:*****:*:**:**:*************.*::*.**.:*:****.:******

Vv-HMGS         LTATMFSFQLRDGQHPFSLSNIATVMDVAGKLKARHEFPPEKFVEILKLMEHRYGAKDFV 420
Hb-HMGS         LTATMFSLRLHEGQHPFSLSNIASVMNVAGKLKARHELPPEKFVDIMKLMEHRYGAKDFV 420
At-HMGS         STATMFSLRLNDNKPPFSISNIASVMDVGGKLKARHEYAPEKFVETMKLMEHRYGAKDFV 420
                 ******::*.:.: ***:****:**:*.******** .*****: :**************

Vv-HMGS         TSKD--CSLLPPGTHYLTEVDSMYRRFYSKKAGSCTCENGSLANGH 464
Hb-HMGS         TSKD--CSLLASGTYYLTEVDSLYRRFYAQKAVGNTVENGLLANGH 464
At-HMGS         TTKEGIIDLLAPGTYYLKEVDSLYRRFYGKKG-----EDGSVANGH 461
                *:*:   .**..**:**.****:*****.:*.     *:* :****
```

Figure 5.4. Alignment of the predicted *Vitis vinifera* (Vv-) 3-hydroxy-3-methylglutaryl synthase (HMGS) protein sequence to the HMGS protein sequences of *Hevea brasiliensis* (Hb-) (AAL18930) and *Arabidopsis thaliana* (At-) (CAA58763). (*), indicates an identical amino acid residue; (:), indicates a similar amino acid residue.

```
CLUSTAL W (1.82) multiple sequence alignment

Vv-IPI          MTLSSRLYTFASPKLPKHCARPQISPSFPLKYPPILTRSLPFASHFRRASLSFSTRSTAM 60
Cb-IPI          MSLTSRLYKLRLSSLHSFGSLPILPP--PLRSSRIAA---PLSLRVSLSTRSIAT-SIAM 54
At-IPI          MSASS-LFNLPLIRLRSLALSSSFSS-FRFAHRPLSS----ISPRKLPNFRAFSG--TAM 52
                *: :* *:.:    * .    . :..   :    : :    :: :      :::    **

Vv-IPI          GDAVDAGMDAVQRRLMFEDECILVDENDRIVGHDTKYNCHLMEKIESENLLHRAFSVFLF 120
Cb-IPI          GEAADAGMDAVQRRLMFDDECILVDEVDRVVGHESKYNCHMWEKIESGNMLHRAFSVFLF 114
At-IPI          TDTKDAGMDAVQRRLMFEDECILVDETDRVVGHDSKYNCHLMENIEAKNLLHRAFSVFLF 112
                 :: ************:******** **:***::*****: *:**: *:**********

Vv-IPI          NSKFELLLQQRSATKVTFPLVWTNTCCSHPLYRESELIDENALGVRNAAQRKLLDELGIP 180
Cb-IPI          NSKFELLLQQRSATKVTFPLVWTNTCCSHPLYRESELIDENNLGVRNAAQRKLLDELGIP 174
At-IPI          NSKYELLLQQRSNTKVTFPLVWTNTCCSHPLYRESELIQDNALGVRNAAQRKLLDELGIV 172
                ***:******** **************************::* ****************

Vv-IPI          AEDAPVDQFTPLGRMLYKAPSDGKWGEHELDYLLFIVRDVNVNPNPDEVADVKYVSRNDL 240
Cb-IPI          AEDVPVDEFTPLSRMLYKAPSDGKWGEHELDYLLFIVRDVAVHPNPDEVAEIKYVNREQL 234
At-IPI          AEDVPVDEFTPLGRMLYKAPSDGKWGEHELDYLLFIVRDVKVQPNPDEVAEIKYVSREEL 232
                ***.***:****.*************************** *:*******::***.*::*

Vv-IPI          KELLRKADAGEEGLKLSPWFRLVVDNFLFKWWDHVEKGTLLEAADMKTIHKLT 293
Cb-IPI          KELLKKADAGEEGLKLSPWFRLVVDNFLPKWWDHVEKGTLSEAVDMKSIHKL- 286
At-IPI          KELVKKADAGEEGLKLSPWFRLVVDNFLMKWWDHVEKGTLVEAIDMKTIHKL- 284
                ***::************************ ********** ** ***:****
```

Figure 5.5. Alignment of the predicted *Vitis vinifera* (Vv-) isopentenyl diphosphate isomerase (IPI) protein sequence to the IPI protein sequences of *Clarkia breweri* (Cb-) (Q39471) and *Arabidopsis thaliana* (At-) (Q42553). (*), indicates an identical amino acid residue; (:), indicates a similar amino acid residue.

```
CLUSTAL W (1.82) multiple sequence alignment

Vv-lytB         MAMSLQLCRFSTFSDRSLPEAFAG-IGVFRCRKPLSVRCSGESESSSSSSVAVDSDFDAK 59
Ap-lytB         MATSLQFCRFSTPSDLSFPETRSS-TRLYRSKKPFSVRCHSEG-PSGSSSTAVESEFDAK 58
At-lytB         MAVALQFSRLCVRPDTFVRENHLSGSGSLRRRKALSVRCSSGDENAPSPSVVMDSDFDAK 60
                ** :**:.*:.. .*  . *   .     * :*.:**** . .  : *.*..::*:**** 

Vv-lytB         VFRHNLTRSKNYNRKGFGHKDETLELMNREYTSDIIKTLKENGNEYKWGNVTVKLAEAYG 119
Ap-lytB         SFRHNLTRSKNYNRRGFGHKDETLELMNSEYTSDVIKKLKENGNEYSWGPVTVKLAESYG 118
At-lytB         VFRKNLTRSDNYNRKGFGHKEETLKLMNREYTSDILETLKTNGYTYSWGDVTVKLAKAYG 120
                 **:*****.****:*****:***:*** *****:::.** **  *.** ******::** 

Vv-lytB         FCWGVERAVQIAYEARKQFPEEKIWITNEIIHNPTVNQRYAEMEVKDIPIDDGQKQFEVV 179
Ap-lytB         FCWGVERAVQIAYEARKQFPDEKIWITNEIIHNPTVNKRLEEMEVKEIPVGDGKKHFDVV 178
At-lytB         FCWGVERAVQIAYEARKQFPEERLWITNEIIHNPTVNKRLEDMDVKIIPVEDSKKQFDVV 180
                ********************:*::*************:*  :*:** **: *.:*:*:** 

Vv-lytB         DKGDVVILPAFGAAVDEMLTLSNKNVQIVDTTCPWVSKVWNIVEKHKKGEYTSIIHGKYS 239
Ap-lytB         AKGDVVILPAFGAAVSEMLTLSEKNVQIVDTTCPWVSKVWNSVEKHKKGEYTSIIHGKYS 238
At-lytB         EKDDVVILPAFGAGVDEMYVLNDKKVQIVDTTCPWVTKVWNTVEKHKKGEYTSVIHGKYN 240
                 *.**********.*.** .*.:*:***********:**** **********:*****. 

Vv-lytB         HEETIATASFAGKYIIVKNMAEAMYVCDYILGGELDGSSSTREEFFEKFKFAISEGFDPD 299
Ap-lytB         HEETIATASFAGKYIIVKNMDEAMYVCDYILGGELNGSSSDKQALLEKFKYAISEGFDPD 298
At-lytB         HEETIATASFAGKYIIVKNMKEANYVCDYILGGQYDGSSSTKEEFMEKFKYAISKGFDPD 300
                ****************** ** *********: :**** :: ::****:***:***** 

Vv-lytB         IDLSKVGIANQTTMLKGETEEIGKLVERTMMRKYGVENVNNHFISFNTICDATQERQDAM 359
Ap-lytB         TDLIKTGIANQTTMLKGETEDIGKLLEKTMMRKYGVENINDHFISFNTICDATQERQDAM 358
At-lytB         NDLVKVGIANQTTMLKGETEEIGRLLETTMMRKYGVENVSGHFISFNTICDATQERQDAI 360
                 ** *.**************:**:*:* **********:..****************:

Vv-lytB         YKLVEEKLDVMLVVGGWNSSNTSHLQEIAEDRGIPSYWIDXEKRIGPGNRISHKLMHGEL 419
Ap-lytB         FKLVEEKVDLILVVGGWNSSNTSHLQEISELRGIPSYWIDSETRIGPGNKISHKLNHGEL 418
At-lytB         YELVEEKIDLMLVVGGWNSSNTSHLQEISEARGIPSYWIDSEKRIGPGNKIAYKLHYGEL 420
                ::*****:*::*****************:* ********* *.******:*::** :***

Vv-lytB         VEKENWLPEGPITIGVTSGASTPDKIVEDVLIKVFDIKRXEALQLA 465
Ap-lytB         VETENWLPEGPVTIGVTSGASTPDKAVEDALVKVFDIKREQLLQLA 464
At-lytB         VEKENFLPKGPITIGVTSGASTPDKVVEDALVKVFDIKREELLQLA 466
                **.**:**:**:************* ***.*:******* : **** 
```

Figure 5.6. Alignment of the predicted *Vitis vinifera* (Vv-) 4-hydroxy-3-methylbut-2-enyl diphosphate reductase (lytB) protein sequence to the lytB protein sequences of *Adonis palaestina* (Ap-) (AAG21984 ) and *Arabidopsis thaliana* (At-) (AAN87171). (*), indicates an identical amino acid residue; (:), indicates a similar amino acid residue.

## 5.5 LITERATURE CITED


[1] Hoeffler,J.F., Hemmerlin,A., Grosdemange-Billiard,C., Bach,T.J., & Rohmer,M. (2002) Isoprenoid biosynthesis in higher plants and in Escherichia coli: on the branching in the methylerythritol phosphate pathway and the independent biosynthesis of isopentenyl diphosphate and dimethylallyl diphosphate. *Biochem J*, **366,** 573-583.

[2] Laule,O., Furholz,A., Chang,H.S., Zhu,T., Wang,X., Heifetz,P.B., Gruissem,W., & Lange,M. (2003) Crosstalk between cytosolic and plastidial pathways of isoprenoid biosynthesis in *Arabidopsis thaliana*. *Proc Natl Acad Sci USA*, **100,** 6866-6871.

[3] Lichtenthaler,H.K. (2000) Non-mevalonate isoprenoid biosynthesis: Enzymes, genes and inhibitors. *Biochem Soc Trans*, **28,** 785-789.

[4] Rohdich,F., Kis,K., Bacher,A., & Eisenreich,W. (2001) The non-mevalonate pathway of isoprenoids: genes, enzymes and intermediates. *Curr Opin Chem Biol*, **5,** 535-540.

[5] Cunningham,F.X., Jr. & Gantt,E. (1998) Genes and enzymes of carotenoid biosynthesis in plants. *Annu Rev Plant Physiol Plant Mol Biol*, **49,** 557-583.

[6] Hirschberg,J. (2001) Carotenoid biosynthesis in flowering plants. *Curr Opin Plant Biol*, **4,** 210-218.

[7] Bartley,G.E., Scolnik,P.A., & Giuliano,G. (1994) Molecular biology of carotenoid biosynthesis in plants. *Annu Rev Plant Physiol Plant Mol Biol*, **45,** 287-301.

[8] Cutler,A.J. & Krochko,J.E. (1999) Formation and breakdown of ABA. *Trends Plant Sci*, **4,** 472-478.

[9] Giraudat,J., Parcy,F., Bertauche,N., Gosti,F., Leung,J., Morris,P.C., Bouvier-Durand,M., & Vartanian,N. (1994) Current advances in abscisic acid action and signalling. *Plant Mol Biol*, **26,** 1557-1577.

[10] Ye,X., Al Babili,S., Kloti,A., Zhang,J., Lucca,P., Beyer,P., & Potrykus,I. (2000) Engineering the provitamin A (β-carotene) biosynthetic pathway into (carotenoid-free) rice endosperm. *Science*, **287,** 303-305.

[11] Castenmiller,J.J.M. & West,C.E. (1998) Bioavailability and bioconversion of carotenoids. *Annu Rev Nutr*, **18,** 19-38.

[12] Davison,P.A., Hunter,C.N., & Horton,P. (2002) Overexpression of β-carotene hydroxylase enhances stress tolerance in *Arabidopsis*. *Nature*, **418,** 203-206.

[13] Steel,C.C. & Keller,M. (2000) Influence of UV-B irradiation on the carotenoid content of *Vitis vinifera* tissues. *Biochem Soc Trans*, **28,** 883-885.

[14] Saier,M.H., Jr. (1998) Genome sequencing and informatics: New tools for biochemical discoveries. *Plant Physiol*, **117,** 1129-1133.

[15] Stormo,G.D. (2000) Gene-finding approaches for eukaryotes. *Genome Res*, **10,** 394-397.

[16] Isaacson,T., Ronen,G., Zamir,D., & Hirschberg,J. (2002) Cloning of tangerine from tomato reveals a carotenoid isomerase essential for the production of β–carotene and xanthophylls in plants. *Plant Cell*, **14,** 333-342.

[17] Schwartz,S.H., Tan,B.C., Gage,D.A., Zeevaart,J.A., & McCarty,D.R. (1997) Specific oxidative cleavage of carotenoids by VP14 of maize. *Science*, **276,** 1872-1874.

[18] Steenkamp,J.A., Wiid,I., Lourens,A., & van Helden,P. (2003) Improved method for DNA extraction from *Vitis vinifera*. *Am J Enol Vitic*, **45,** 102-106.

[19] Davies,C. & Robinson,S.P. (1996) Sugar accumulation in grape berries. Cloning of two putative vacuolar invertase cDNAs and their expression in grapevine tissues. *Plant Physiol*, **111,** 275-283.

[20] Sambrook,J., Fritsch,E.F., & Maniatis,T. (1989) *Molecular cloning: a laboratory manual*, 2nd edn. Cold Spring Harbor Laboratory Press, Cold Spring Harbor, N.Y. (USA).

[21] Gleave,A.P. (1992) A versatile binary vector system with a T-DNA organisational structure conducive to efficient integration of cloned DNA into the plant genome. *Plant Mol Biol*, **20,** 1203-1207.

[22] Thompson,J.D., Gibson,T.J., Plewniak,F., Jeanmougin,F., & Higgins,D.G. (1997) The CLUSTAL_X windows interface: flexible strategies for multiple sequence alignment aided by quality analysis tools. *Nucleic Acids Res*, **25,** 4876-4882.

[23] Marchler-Bauer,A., Anderson,J.B., DeWeese-Scott,C., Fedorova,N.D., Geer,L.Y., He,S., Hurwitz,D.I., Jackson,J.D., Jacobs,A.R., Lanczycki,C.J., Liebert,C.A., Liu,C., Madej,T., Marchler,G.H., Mazumder,R., Nikolskaya,A.N., Panchenko,A.R., Rao,B.S., Shoemaker,B.A., Simonyan,V., Song,J.S., Thiessen,P.A., Vasudevan,S., Wang,Y., Yamashita,R.A., Yin,J.J., & Bryant,S.H. (2003) CDD: a curated Entrez database of conserved domain alignments. *Nucleic Acids Res*, **31,** 383-387.

[24] Disch,A. & Rohmer,M. (1998) On the absence of the glyceraldehyde 3-phosphate/pyruvate pathway for isoprenoid biosynthesis in fungi and yeasts. *FEMS Microbiol Lett*, **168,** 201-208.

[25] Liang,P., Ko,T. & Wang,A. (2002) Structure, mechanism and function of prenyltransferases. *Eur J Biochem*, **269,** 3339-3354.

[26] Altincicek,B., Kollas,A.K., Sanderbrand,S., Wiesner,J., Hintz,M., Beck,E., & Jomaa,H. (2001) GcpE is involved in the 2-C-methyl-D-erythritol 4-phosphate pathway of isoprenoid biosynthesis in *Escherichia coli*. *J Bacteriol*, **183,** 2411-2416.

[27] Rohdich,F., Hecht,S., Gartner,K., Adam,P., Krieger,C., Amslinger,S., Arigoni,D., Bacher,A., & Eisenreich,W. (2002) Studies on the nonmevalonate terpene biosynthetic pathway: metabolic role of IspH (LytB) protein. *Proc Natl Acad Sci USA*, **99,** 1158-1163.

[28] Cunningham,F.X., Jr. & Gantt,E. (2000) Identification of multi-gene families encoding isopentenyl diphosphate isomerase in plants by heterologous complementation in *Escherichia coli*. *Plant Cell Physiol*, **41,** 119-123.

[29] Nakamura,A., Shimada,H., Masuda,T., Ohta,H., & Takamiya,K. (2001) Two distinct isopentenyl diphosphate isomerases in cytosol and plastid are differentially induced by environmental stresses in tobacco. *FEBS Lett*, **506,** 61-64.

[30] Okada,K., Saito,T., Nakagawa,T., Kawamukai,M., & Kamiya,Y. (2000) Five geranylgeranyl diphosphate synthases expressed in different organs are localized into three subcellular compartments in *Arabidopsis*. *Plant Physiol*, **122,** 1045-1056.

[31] Eisenreich,W., Rohdich,F., & Bacher,A. (2001) Deoxyxylulose phosphate pathway to terpenoids. *Trends Plant Sci*, **6,** 78-84.

[32] Cunningham,F.X., Jr., Lafond,T.P., & Gantt,E. (2000) Evidence of a role for LytB in the nonmevalonate pathway of isoprenoid biosynthesis. *J Bacteriol*, **182,** 5841-5848.

[33] Kim,S.W. & Keasling,J.D. (2001) Metabolic engineering of the nonmevalonate isopentenyl diphosphate synthesis pathway in *Escherichia coli* enhances lycopene production. *Biotechnol Bioeng*, **72,** 408-415.

[34] Geer,L.Y., Domrachev,M., Lipman,D.J., & Bryant,S.H. (2002) CDART: Protein homology by domain architecture. *Genome Res.*, **12,** 1619-1623.

# CHAPTER 6

# GENERAL DISCUSSION AND CONCLUSION

## 6.1 GENERAL DISCUSSION AND CONCLUSION

In essence, the light reactions of the photosynthetic process absorb energy from the sun, use the energy obtained from these photons for electron transport reactions, and consequently release oxygen into the atmosphere. When light conditions are not saturating to the photosynthetic process, all the absorbed light energy is quenched by the photochemical electron transfer reactions. This scenario changes as soon as light becomes saturating. Both light intensities that are too high and photosynthetic rates that are too low will cause a blockage in the electron transfer reactions. Under these conditions highly reactive photo-oxidative intermediates are formed that cause damage to the photosynthetic apparatus. Any damage to the photosynthetic apparatus will result in photoinhibition, and eventually photodamage [1;2]. Both these processes will result in a decrease in the photosynthetic capacity of plants.

Extreme environmental conditions are cited as one of the principal reasons for reductions in global crop yield; it is therefore becoming increasingly important to generate crops that can withstand these conditions [3]. Since plants are faced with fluctuating, and sometimes extreme, environmental conditions on a daily and seasonal basis, they must have systems in place to cope with the associated stresses. Due to their ability to quench reactive oxygen species that are formed during these stress conditions, carotenoids represent one such photoprotective mechanism. Apart from their photoprotective role, carotenoids are also integral components of the photosynthetic apparatus and are responsible for the assembly and stability of the pigment-protein complexes, as well as assisting in light-harvesting during photosynthesis [4]. Genetic manipulation of carotenoids (especially the xanthophylls) has been identified as a promising target for the production of transgenic plants with enhanced stress tolerance, and as proof of this, plants with elevated xanthophyll levels have already been shown to be less susceptible to high light and high temperature induced oxidative damage [5].

In light of the above, the decision to focus on the manipulation of the carotenoid biosynthetic pathway in grapevine was taken based on the following anticipated benefits: (i) to increase the nutritional content (and associated value) of the grape; (ii) to increase the stress tolerance of the field grown grapevine to environmental stresses;

and (iii) to increase the production of certain quality-associated $C_{13}$-norisoprenoid compounds in the grape berry.

The last decade has seen the completion of the genome sequencing projects of *Homo sapiens, Drosophila melanogaster, Saccharomyces cerevisiae*, and eight plant genomes that include: *Arabidopsis thaliana*, *Lycopersicon esculentum* and *Oryza sativa* (http://www.ncbi.nlm.nih.gov/genomes/static/euk_g.html). These sequencing projects have resulted in a huge amount of sequence data being deposited in the publicly accessible sequence repositories (e.g. the National Center for Biotechnology Information [NCBI] and The Institute for Genomic Research [TIGR]). The availability of genome sequence information has dramatically altered both the experimental scale and strategies for conducting research [6].

The isolation of carotenoid biosynthetic genes (CBGs) has been accelerated in the last few years due to heterologous functional complementation assays [7]. These systems have lead to the isolation of numerous CBGs from bacteria, algae and plants based on the reactions that their encoded products catalyse [8;9]. Several of the CBGs can be functionally complemented using this system: geranylgeranyl diphosphate synthase (GGPS), phytoene synthase (PSY), phytoene desaturase (PDS), lycopene ε-cyclase (LECY), lycopene β-cyclase (LBCY), and β-carotene hydroxylase (BCH). This system can also be used to isolate genes involved in isopentenyl diphosphate (IPP) biosynthesis (as precursors of carotenoids), since it causes an increase in the carotenoid accumulation of the bacterial strains (e.g. IPP isomerase [IPI], 1-deoxy-D-xylulose 5-phosphate [DOXP] synthase [DXS], and 4-hydroxy-3-methylbut-2-enyl diphosphate reductase [lytB]). The limitation of this assay is that it can only isolate genes encoding enzymes that cause a colour change in the respective *E. coli* colonies (due to the formation of a different carotenoid, or the formation of more carotenoids). To overcome this problem we decided to use the high degree of conservation that exists in the genes encoding for enzymes involved in the carotenoid- and related biosynthetic pathways, and the data available on the publicly accessible sequence databases to isolate genes that are either directly, or indirectly involved in carotenoid biosynthesis. Two approaches were used, and relied on the following:

(i) if *V. vinifera* sequence information was available (genomic or cDNA), the sequence was analysed and primers designed that would amplify the gene of interest (or if not full-length, as large as possible);

(ii) if *V. vinifera* sequence information was not available, representative protein sequences were aligned to identify any potential conserved areas, and degenerate PCR primers were designed to amplify the gene of interest (or if not full-length, as large as possible);

(iii) the CBGs were PCR-amplified from genomic- and/or cDNA, and the resultant product was cloned and sequenced;

(iv) the isolated CBGs were labeled and used to probe digested genomic DNA in subsequent Southern hybridisations;

(v) the genomic fragments identified in (iv) were isolated and sub-genomic libraries were constructed;

(vi) the constructed sub-genomic libraries were screened for the CBGs of interest;

(vii) positive clones were subcloned and sequenced; and

(viii) if not full-length, the process from step (iv) was repeated but using different restriction endonucleases.

This facilitated the isolation of eleven full-length- and eight partial genes from *V. vinifera*. These genes can be grouped into the following pathways:

(i) The DOXP/2-C-methyl-D-erythritol 4-phosphate (MEP) pathway (i.e. the plastidic IPP biosynthetic pathway): DXS, DOXP reductase (DXR), hydroxymethylbutenyl diphosphate synthase (gcpE/ispG), lytB and IPI;

(ii) the mevalonate pathway (i.e. the cytosolic/mitochondrial IPP biosynthetic pathway): 3-hydroxy-3-methylglutaryl coenzyme A synthase (HMGS);

(iii) the carotenoid biosynthetic pathway: PSY, ζ-carotene desaturase (ZDS), LECY, LBCY, carotenoid isomerase (CISO), BCH, ZEP, and violaxanthin de-epoxidase (VDE);

(iv) the abscisic acid biosynthetic pathway (as a degradation product of carotenoids): 9-*cis*-epoxy carotenoid dioxygenase (NCED), xanthine dehydrogenase (XDH), and a short chain dehydrogenase (SCD);

(v) and general isoprenoid precursors: farnesyl diphosphate synthase (FPS) and GGPS.

Only the full-length genes were subjected to further *in silico* analyses (as discussed in Chapters 3, 4 and 5).

Chapter 3 describes the isolation and characterisation of the BCH-encoding gene from *V. vinifera*. In 1996 a study by Sun *et al.* reported the cloning of the first BCH-encoding gene from a plant (*A. thaliana*), and identified highly conserved regions in the BCH encoding gene that corresponded to transmembrane helices in the predicted protein sequence [10]. These transmembrane helices were shown to be crucial for enzymatic functioning and are conserved between bacterial and plant BCHs [11]. These regions were used to design primers that were subsequently used to PCR-amplify and isolate the *V. vinifera* BCH, based purely on the degree of conservation of the BCH genes in different plant species. The methods used for the cloning and characterisation of the BCH gene served as a model for the isolation of the genes discussed in Chapter 4.

Web-based prediction servers are routinely used to analyse genomic sequences. For this study the correct prediction of introns and exons in genomic DNA was essential when designing primers from genomic sequences for RT-PCR (Chapter 4). The isolation of both the genomic- and cDNA copies of the BCH gene provided empirical data regarding the intron-exon splice sites in *V. vinifera*. This sequence information was used to validate the effectiveness of the prediction servers used to identify putative splice sites sites in genomic DNA. The prediction of the intron-exon splice sites in the BCH genomic sequence was in complete agreement with the gaps generated by aligning the BCH genomic- and cDNA sequences. This provides us with a degree of confidence when using the prediction server for subsequent genomic analyses (Chapter 4). The isolation and subsequent analyses of the genomic- and cDNA copies of the PSY and ZEP encoding genes has further verified this finding.

The overall (or global) degree of homology of the protein sequences to homologous protein sequences in the public databases were determined, and the sequences were further analysed for the presence of putative transit peptides that would give some indication as to the sub-cellular localisation of the isolated proteins. Since the biosynthetic pathways are functional in defined compartments, the mature peptides should be targeted to these locations in order to perform their respective functions. Problems arise, however, when more than one isozyme exists. For example, *Arabidopsis* has five GGPS encoding genes that are targeted to three different sub-cellular locations: the endoplasmic reticulum, the cytosol and the chloroplast [12]. Each isozyme would therefore require a different transit peptide, and although the genes encoding the different isozymes would catalyse the same enzymatic reaction, they would differ in their N-terminal sequences due to the different transit peptides. DXS, IPI, GGPS, PSY, LBCY, BCH, ZEP and NCED were all localised to the chloroplast (where the DOXP/MEP- and carotenoid biosynthetic pathways are functional). The predicted proteins of lytB and FPS were localised to the cytoplasm; and HMGS to both the cytoplasm and the mitochondria. Although unexpected, both these compartments require the mevalonate pathway, and it is therefore plausible that the isolated HMGS protein has a "dual-function" transit peptide. In this study we evaluated different transit peptide prediction servers, and quite often obtained conflicting results. The isolation and analysis of these genes has underlined the need for experimental data to validate *in silico* biological predictions. Although not part of the mature peptide, the transit peptides represent a genetic resource of their own. This study focused on the function of the mature peptides (encoded by the CBGs), yet the transit peptides would prove useful for future grapevine transformations. Fusion of a functional transit peptide to candidate genes would facilitate the targeted expression of the engineered product. Targeted expression would ensure that the gene products are channeled to the sub-cellular location of interest.

The putative promoters of six of the isolated genes (i.e. BCH, DXS, LBCY, NCED, PSY and ZEP) were isolated and cloned. The ability of the putative promoters to drive the transcription of a reporter gene was analysed in a transient reporter gene assay. None of the putative promoters could, however, be shown to have any transcriptional activity in a range of different tissues, and following different inductions. There are a

number of possible explanations for this: (i) the promoter fragments isolated are too small to contain the core promoter; (ii) transcription of the reporter gene occurs, but the detection system is not sensitive enough; (iii) the promoters are not active in the conditions tested; or (iv) the promoters are not active. The promoter fragments isolated ranged from 800 bp (DXS) to 4300 bp (NCED). The possibility that all these fragments were too small to contain the functional promoter, although probable, is highly unlikely. Since BCH, DXS and PSY are single copy genes in the grapevine genome and encode for crucial enzymes in central biosynthetic pathways, it is not possible that the promoters of these genes are transcriptionally inactive. The most likely problem is that the histochemical staining and subsequent microscopical analysis of the reporter gene was not optimal and fluorometric measurements would prove more sensitive and quantitative. One way of addressing these problems is to transform the promoter-reporter gene fusions into model plants and subsequently analyse the promoter activity in the stable transformants.

The RT-PCR technique used in this study proved only useful for determining trends in the relative expression of the genes. The semi-quantitative RT-PCR method has provided promising trends in the expression profiles that require further investigation. The only feasible high-throughput technique available to absolutely quantify the expression levels of these genes relative to each other is real-time PCR. All nineteen *Vitis* genes isolated in this study (both full-length and partial) can be monitored using this technique. These data would provide comprehensive insights into the transcriptional regulation of the genes of the isoprenoid biosynthetic pathways.

In order to assign a functional physiological role for the isolated genes, it is necessary to express the genes in model plants and evaluate the resultant transgenic plants phenotypically. Due to the logistical implications involved in overexpressing, maintaining and analyzing all the full-length genes isolated from this study in transgenic plants, it was decided to continue with only one gene of the isolated genes, BCH. The *V. vinifera* BCH gene was constitutively overexpressed in tobacco plants, in both the sense and the antisense orientation (Chapter 3). Previous studies in *Arabidopsis* have shown that zeaxanthin is essential for photoprotection under saturating light conditions [5]. Our results support this finding, and suggest that the additional zeaxanthin formed due to the constitutively expressed BCH gene, enables the transgenic plants to maintain

photosynthesis under conditions that typically caused a decrease in the untransformed control plants. How the additional zeaxanthin facilitates this photoprotection is thus far not known. Chlorophyll fluorescence measurements indicated that the nonphotochemical quenching ability of the transgenic plants increases with an increase in zeaxanthin levels. It is possible that under saturating light conditions, the additional zeaxanthin formed due to the overexpressed *V. vinifera* BCH, supplements the zeaxanthin pool formed via violaxanthin by the xanthophyll cycle. Under stress conditions, the additional available zeaxanthin can fulfill its photoprotective function by preventing oxidative damage to the photosynthetic apparatus. Conversely, the antisense plants showed that decreased zeaxanthin levels provided less photoprotection to the plant under light stress conditions. Since the photoprotection of the antisense plants was even lower than the untransformed control plants, it suggests that the zeaxanthin formed via β-carotene does have a role to play in photoprotection. It is interesting to note that under conditions where light is not saturating (i.e. low light); the altered zeaxanthin levels of both the sense- and antisense plants had no observable effect on the plants' photosynthetic ability.

The D1 protein is an integral protein of the reaction center of photosystem II, and due to its susceptibility to photodamage it requires an exceptionally high light-dependent turnover rate. Once damaged, the photosynthetic apparatus can only regain functionality by the *de novo* synthesis and replacement of the D1 protein in the photosynthetic reaction center [13]. The transgenic tobacco plants overexpressing the *V. vinifera* BCH showed distinct differences in the level of their D1 protein under high light conditions (relative to the untransformed control plants). It seems that the observed photoprotection under saturating light conditions involves protection of the proteins of the photosynthetic apparatus (including the D1 protein). Since carotenoids are capable of directly, and indirectly quenching reactive oxygen species, it is clear that additional carotenoids in the photosynthetic apparatus would have a protective effect [14]. Conversely, less zeaxanthin will result in a decrease in the levels of D1 protein, as was the case with the BCH antisense plant lines.

Collectively these results confirm the role of zeaxanthin in photoprotection, and although the exact mechanism was not determined in this study, the effect of the additional zeaxanthin on photosynthesis in the transgenic plants was clear. The

chlorophyll fluorescence measurements and the trends in the D1 protein levels showed that the additional zeaxanthin protects the photosynthetic apparatus under conditions that illicit a stress response in the untransformed control plants.

For the future transformation of HMGS, DXS, IPI, lytB, HMGS, FPS, GGPS, PSY, LBCY, NCED and ZEP genes, it would be useful to consider using the model plant, *A. thaliana*. From a genetic point of view, the *Arabidopsis* genome is completely sequenced, and even more importantly, a number of plant lines are available with mutations in carotenoid biosynthetic genes [15]. These null mutants are well-characterised and will complement the overexpression studies to provide the necessary experimental data to elucidate the *in planta* role of these pigments in photosynthesis. The main advantage of doing the analyses in *Arabidopsis* is the availability of DNA microarray technology for monitoring genome-wide gene expression and so doing provide transcript profiles for genes of interest.

This isolation of candidate genes from the isoprenoid-, carotenoid- and abscisic acid biosynthetic pathways has provided us with a genetic resource that needs to be exploited. The analyses of these genes has contributed to our understanding of the genomic organisation, regulation and possible function(s) of these genes in *V. vinifera* and plants in general. The expression of these genes in model plants will provide additional information regarding the physiological function of specific carotenoids in plants, and if successful, represent the first step towards the generation of future transgenic grapevines with improved nutritional content or enhanced stress tolerance.

## 6.2 LITERATURE CITED

[1] Demmig-Adams,B. & Adams,W.W., III (1992) Photoprotection and other responses of plants to high light stress. *Annu Rev Plant Physiol Plant Mol Biol*, **43,** 599-626.

[2] Arora,A., Sairam,R.K., & Srivastava,G.C. (2002) Oxidative stress and antioxidative system in plants. *Curr Sci*, **82,** 1227-1238.

[3] Moffat,A.S. (2002) Plant genetics. Finding new ways to protect drought-stricken plants. *Science*, **296,** 1226-1229.

[4] Pogson,B.J. & Rissler,H.M. (2000) Genetic manipulation of carotenoid biosynthesis and photoprotection. *Philos Trans R Soc Lond B: Biol Sci*, **355,** 1395-1403.

[5] Davison,P.A., Hunter,C.N., & Horton,P. (2002) Overexpression of β-carotene hydroxylase enhances stress tolerance in *Arabidopsis*. *Nature*, **418,** 203-206.

[6] Wu,S.H., Ramonell,K., Gollub,J., & Somerville,S. (2001) Plant gene expression profiling with DNA microarrays. *Plant Physiol Biochem*, **39,** 917-926.

[7] Cunningham,F.X., Jr., Sun,Z., Chamovitz,D., Hirschberg,J., & Gantt,E. (1994) Molecular structure and enzymatic function of lycopene cyclase from the cyanobacterium *Synechococcus* sp strain PCC7942. *Plant Cell*, **6,** 1107-1121.

[8] Harker,M. & Bramley,P.M. (1999) Expression of prokaryotic 1-deoxy-D-xylulose-5-phosphatases in *Escherichia coli* increases carotenoid and ubiquinone biosynthesis. *FEBS Lett*, **448,** 115-119.

[9] Cunningham,F.X., Jr., Lafond,T.P., & Gantt,E. (2000) Evidence of a role for LytB in the nonmevalonate pathway of isoprenoid biosynthesis. *J Bacteriol*, **182,** 5841-5848.

[10] Sun,Z., Gantt,E., & Cunningham,F.X., Jr. (1996) Cloning and functional analysis of the β-carotene hydroxylase of *Arabidopsis thaliana*. *J Biol Chem*, **271,** 24349-24352.

[11] Bouvier,F., Keller,Y., d'Harlingue,A., & Camara,B. (1998) Xanthophyll biosynthesis: Molecular and functional characterization of carotenoid hydroxylases from pepper fruits (*Capsicum annuum* L.). *Biochim Biophys Acta*, **1391,** 320-328.

[12] Okada,K., Saito,T., Nakagawa,T., Kawamukai,M., & Kamiya,Y. (2000) Five geranylgeranyl diphosphate synthases expressed in different organs are localized into three subcellular compartments in *Arabidopsis*. *Plant Physiol*, **122,** 1045-1056.

[13] Aro,E.M., Virgin,I., & Andersson,B. (1993) Photoinhibition of photosystem II. Inactivation, protein damage and turnover. *Biochim Biophys Acta*, **1143,** 113-134.

[14] Ma,Y.Z., Holt,N.E., Li,X.P., Niyogi,K.K., & Fleming,G.R. (2003) Evidence for direct carotenoid involvement in the regulation of photosynthetic light harvesting. *Proc Natl Acad Sci USA*, **100,** 4377-4382.

[15] Niyogi,K.K., Grossman,A.R., & Björkman,O. (1998) *Arabidopsis* mutants define a central role for the xanthophyll cycle in the regulation of photosynthetic energy conversion. *Plant Cell*, **10,** 1121-1134.